

12-2017

Characterization and Mechanisms of Anthocyanin Degradation and Stabilization

Nathan Blaine Stebbins
University of Arkansas, Fayetteville

Follow this and additional works at: <https://scholarworks.uark.edu/etd>



Part of the [Food Biotechnology Commons](#), and the [Food Chemistry Commons](#)

Citation

Stebbins, N. B. (2017). Characterization and Mechanisms of Anthocyanin Degradation and Stabilization. *Graduate Theses and Dissertations* Retrieved from <https://scholarworks.uark.edu/etd/2618>

This Dissertation is brought to you for free and open access by ScholarWorks@UARK. It has been accepted for inclusion in Graduate Theses and Dissertations by an authorized administrator of ScholarWorks@UARK. For more information, please contact uarepos@uark.edu.

Characterization and Mechanisms of Anthocyanin Degradation and Stabilization

A dissertation submitted in partial fulfillment
of the requirements for the degree of
Doctor of Philosophy in Food Science

by

Nathan B. Stebbins
University of Scranton
Bachelor of Science in Biology and Environmental Science, 2011
University of Scranton
Master of Arts in Biochemistry, 2013

December 2017
University of Arkansas

This dissertation is approved for recommendation to the Graduate Council.

Dr. Luke Howard
Dissertation Director

Dr. Andy Proctor
Committee Member

Dr. Ronald Prior
Committee Member

Dr. Jackson Lay
Committee Member

Dr. Matt McIntosh
Committee Member

Abstract

Anthocyanins (ACYs) are polyphenol compounds found in nature, which contribute vivid colors to many fruits and vegetables, while also possessing significant health benefits. These pigments range in color from orange-red to blue-violet and could serve as natural colorants to replace artificial additives. There is a great demand from consumers to have fewer artificial compounds in their foods. However, the relatively instability of ACYs must be further understood in order to limit color degradation before they can completely replace synthetic colorants.

ACYs slowly degrade over time, but there is a knowledge gap on their fate and mechanisms causing degradation. In order to understand the mechanistic changes, different techniques were employed to understand ACY transformations over storage. Various types of solid phase extraction, high-pressure liquid chromatography columns, and gel electrophoresis analyses were used in an attempt to separate anthocyanin-tannin polymers by degree of polymerization. These compounds were detected using mass spectrometry, but separation by chromatographic techniques was not possible.

Ascorbic acid accelerates ACY degradation, but the mechanism was controversial. Model systems of a pure ACY, cyanidin-3-glucoside (C3G), and blackberry juice supplemented with ascorbic acid were prepared and hydroxyl radicals formed via the Haber-Weiss reaction. Hydroxyl radicals are highly unstable and reacted with C3G forming 6-hydroxy-C3G, which degrades faster than C3G. The combination of identifying the hydroxylated ACY using tandem mass spectrometry and detection the hydroxyl radicals via electron spin resonance verified the reaction mechanism of ascorbic acid catalyzed degradation of ACYs. Next, blackberry juice was supplemented with various additives to understand ACY stabilization mechanisms. Glutathione

significantly improved anthocyanin retention over storage, so combinations of glutathione with lipoic and ascorbic acids were added to assess a potential antioxidant recycling mechanism. The combination was not more effective at stabilizing ACYs than glutathione alone. Finally, novel ACY compounds were created from radishes through a reaction originally found in wine fermentation. Using acetaldehyde as a polymerization agent, radish ACYs reacted with catechin to form stable pigments that were identified by mass spectrometry. This research furthers the understanding of anthocyanin reactions and degradation mechanisms, which improves their use as natural colorants in the food and beverage industry.

Acknowledgements

I would like to sincerely thank my advisor, Dr. Luke Howard, for your guidance, encouragement, and expertise in food science. Through the ups and downs, you have been inspiring, understanding, and everything I could ever ask for in an advisor. In addition, I would like to acknowledge and thank my dissertation committee Drs. Andy Proctor, Ron Prior, Jackson Lay, and Matt McIntosh. Fulfillment of this research would not have been possible without your support, patience, and wealth of knowledge. Thank you for all of your instruction, mentorship, and counsel while I grow as a scientist. Cindi Brownmiller deserves the utmost thanks for your infinite knowledge, unending patience, and all around support. I would like to express my gratitude to the faculty and staff over the course of my higher education, including Drs. Rohana Liyanage, Ya-Jang Wang, Renee Threlfall, Andy Mauromoustakos and Joe Vinson for always being helpful. Next, I would like to thank my fellow graduate students for listening during the stressful times and the laughs during the entertaining spells. Last but not least, I extend my heartfelt gratitude to my family and friends who have loved and supported me unconditionally during my education. I would not have made it this far without the support all these people.

Table of contents

CHAPTER 1. Introduction	1
CHAPTER 2. Literature Review	5
Anthocyanins	5
Fruit processing	8
Color and copigmentation	9
Health benefits and bioavailability	11
Proanthocyanidins and polymeric pigments	13
Degradation products and mechanisms	15
Anthocyanin model systems	21
Acetaldehyde effect on wine color	23
Analytical techniques	26
References	28
Tables and figures	35
CHAPTER 3. Assessment of methods to separate polymeric pigments	
Abstract	50
Introduction	51
Materials and methods	55
Results and discussion	63
References	80
Figures	83
CHAPTER 4. Ascorbic acid-catalyzed degradation of cyanidin-3-glucoside: Proposed mechanism and identification of a novel hydroxylated product	
Abstract	112
Introduction	113
Materials and methods	115
Results and discussion	118
References	124
Figures	128
CHAPTER 5. Stabilization of anthocyanins in blackberry juice by glutathione fortification	
Abstract	136
Introduction	137
Materials and methods	138
Results and discussion	143
References	152
Tables and figures	157
Appendix	170

CHAPTER 6. Formation, mass spectrometric identification, and color stability of acetaldehyde-catalyzed condensation of red radish (*Raphanus sativus*) anthocyanins and (+) catechin

Abstract	186
Introduction	187
Materials and methods	188
Results and discussion	193
References	202
Tables and figures	205
CHAPTER 7. Conclusion	218

List of publications

Published:

Chapter 4:

Stebbins, N.B.; Howard, L.R.; Prior, R.L.; Brownmiller, C.; Liyanage, R.; Lay, J.O.; Yang, X.; Qian, S.Y. Ascorbic acid-catalyzed degradation of cyanidin-3-*O*- β -glucoside: Proposed mechanism and identification of a novel hydroxylated product. *J. Berry Res.* **2016**, *6*, 175-187.

Chapter 5:

Stebbins, N.B., Howard, L.R.; Prior, R.L.; Brownmiller, C.; Mauromoustakos, A. Stabilization of anthocyanins in blackberry juice by glutathione fortification. *Food Funct.* **2017**, *8*, 3459-3468.

Collaborative Publications:

Lestario, L.N.; Howard, L.R.; Brownmiller, C.; **Stebbins, N.B.**; Liyanage, R.; Lay, J.O. Changes in polyphenolics during maturation of Java plum (*Syzygium cumini* Lam.). *Food Res. Intl.* **2017**, doi.org/10.1016/j.foodres.2017.04.02.

CHAPTER 1. Introduction

Eating a rainbow of different colored fruits and vegetables provides an appealing plate as well as offering health benefits from the array of phytochemicals in the food. Some of those vivid colors are provided by anthocyanins (ACYs), which are water-soluble compounds with antioxidant and anti-inflammatory properties as well as other potential health benefits. An individual's diet can have a profound effect on their health status, including modulation of a variety of chronic diseases. Foods with benefits beyond their direct nutritional value are termed functional foods and are a growing market trend with vibrant foods gathering plenty of attention. Replacing artificial colorants with natural alternatives, like ACYs, allows a consumer reading the product's label to perceive an ingredient instead of an additive.

Much of the ACY research has been performed on wine, but these compounds are frequently found in nature from apples to berries to purple potatoes (Wu, Prior 2005, Giusti 2003). Throughout nature, there are six main ACY forms: cyanidin, malvidin, pelargonidin, peonidin, petunidin, and pelargonidin. These polyphenol compounds fall into the category of flavonoids, which also contains tannins, flavonols, and isoflavonoids. Structurally, ACYs are interesting compounds because of the unique flavylium ion that is unlike any other flavonoid. The flavylium ion encompasses a positively charged oxygen atom, which negatively affects the stability of the molecule. This ion allows conjugation through the fused rings and that conjugation is the reason for the vibrant colors. The array of colors that ACYs contribute to juices is appealing; however, the concentration of ACYs in chokeberry juice stored for 6 months degrades to 25% of the levels in 1 month stored juice (Wilkes 2014). This instability is concerning since the health attributes of the compound clearly cannot be exerted on the body if the concentration has dissipated. The identity of some breakdown products has been elucidated,

but this does not account for all of the original ACY content. Along with this decline, the color of the chokeberry juice remains as vibrant as ever, which is puzzling.

ACYs and other flavonoids are degraded as a result of processing, while tannins/procyanidins can change in their relative degree of polymerization (Wilkes et al. 2014). Perhaps most intriguing of all the changes is the tendency toward the formation of polymeric pigments (PPs), also called anthocyanin-tannin polymers. These pigments can be produced by a condensation reaction between an ACY and either flavan-3-ols or their polymeric counterpart, procyanidins (Singleton and Trousdale 1992). This is a compelling lead in determining the fate of ACYs, but the difficulty arises in the measurement of PPs. Currently, PPs are determined as a ratio to ACY content by means of a percent polymeric color assay (Giusti and Wrolstad 2001). Qualitative data can be obtained using matrix assisted laser desorption ionization-time of flight-mass spectrometry (MALDI-TOF-MS), but this type of mass spectrometer does not permit quantification (Reed et al. 2005).

Other than PPs as a source of a natural colorant in the food industry, ACY extracts from root vegetables are potential candidates. Root vegetables have larger ACYs than those in berries due to acylation and multiple glycosidic moieties. Radishes, black carrots, and purple potatoes all produce acylated ACYs and exhibit excellent color stability at low pH values (Giusti 2003, Cevallos 2004). ACYs are not stable at neutral and elevated pH values. In order for a natural colorant to compete with current synthetic colorants, the cost of production must be economical. Radishes are an inexpensive source of acylated ACYs and closely match the hue of FD&C Red No. 40/E129 (Giusti 2003). Using a reaction originally discovered in wine, this research applied the fermentation reaction to non-grape sources for the first time. Radish extracts were combined with catechin using acetaldehyde as a polymerization agent. The resulting compounds formed a

violet solution that had a stable hue over six months of storage. The colored compounds were identified using liquid chromatography-mass spectrometry. These purple pigments could serve as the next generation of natural colorants and replace both FD&C Red No. 40 and Blue No. 1 in purple beverages.

This doctoral dissertation explores ACY degradation and stabilization mechanisms. The objectives were:

1. Create a new HPLC method to separate and quantify PPs in order to resolve their changes during storage.
2. Clarify the degradation mechanism of ACYs in the presence of ascorbic acid.
3. Identify transformation products of ACYs from degradation reactions.
4. Determine the effect of potential additives on ACY stabilization.
5. Develop a novel and stable ACY-based colorant for the food and beverage industry.

References

- Wilkes, K.; Howard, L.R.; Brownmiller, C.; Prior, R.L. Changes in chokeberry (*Aronia melanocarpa* L.) polyphenols during juice processing and storage. *J. Agric. Food Chem.* **2014**, dx.doi.org/10.1021/jf404281n.
- Singleton, V.L.; Trousdale, E.K. Anthocyanin-tannin interactions explaining differences in polymeric phenols between white and red wines. *Am. J. Enol. Vitic.* **1992**, *43*, 63-70.
- Giusti, M.; Wrolstad, R.E. Characterization and measurement of anthocyanins with UV-visible spectroscopy. In *Current Protocols in Food Analytical Chemistry*; Wrolstad, R.E., Ed.; Wiley: New York, 2001; pp. F1.2.1-F1.2.13
- Reed, J.D.; Kreuger, C.G.; Vestling, M.M. MALDI-TOF mass spectrometry of oligomeric food polyphenols. *Phytochem.* **2005**, *66*, 2248-2263.
- Giusti, M.M.; Wrolstad, R.E. Acylated anthocyanins from edible sources and their applications in food systems. *Biochem. Eng. J.* **2003**, *14*, 217-225.
- Cevallos-Casals, B.A.; Cisneros-Zevallos, L. Stability of anthocyanin-based aqueous extracts of Andean purple corn and red-fleshed sweet potato compared to synthetic and natural colorants. *Food Chem.* **2004**, *86*, 69-77.

CHAPTER 2. Literature Review

Anthocyanins

Many fruits, vegetables, and flowers owe their vibrant colors to ACYs. The beautiful color change of the leaves in autumn is due to chlorophyll degradation and ACY content emerging (Field, Lee, Holbrook 2001). The aglycone structures, called anthocyanidins, appear in nature in six common forms, while there are other less common anthocyanidins with different substituents. Figure 1 depicts the six main anthocyanidins and their respective substituents on the B ring. Their antioxidant potential is affected by the hydroxylation and methoxylation patterns on the B ring (Wang et al. 1997). Increasing the number of hydroxyl groups increases the antioxidant potential, but increasing the number of methoxy groups does not function as efficiently as hydroxyl substituents. The relative abundance of ACYs in a wide variety fruits and vegetables is shown in Table 1 (Simmons 2012).

Flavonoids are a class of polyphenols and possess a C₆-C₃-C₆ multi-ring skeleton containing a central heterocyclic oxygen ring. ACYs fall into the broader class of flavonoids and contain a unique heterocyclic oxygen ring with a positive charge, called a flavylium ion. The cation is electron-deficient, which makes it more vulnerable to nucleophilic attack from ascorbic acid, water or peroxides (Jackman 1987). The nucleophilic addition removes the conjugation around the central ring, therefore removing the vibrant color. The newly formed hydrate is often called a carbinol pseudobase that is colorless, but actually has absorption near 330 nm (Brouillard & Delaporte 1977). Approximately 90% of all ACYs have a glucosyl moiety attached to the skeleton (Andersen and Markham 2006) and a glucosyl unit bonded to carbon 3 is 2.5 times as common as diglucosides on carbons 3 and 5, with cyanidin-3-glucoside as the most frequently found anthocyanin in nature (Kong et al. 2003). Many researchers cleave the

glycosidic bonds using acid hydrolysis in order to quantify the aglycones due to the vast number of possible arrangements of sugar moieties (Cho et al. 2004).

A plant's production of ACYs is based on the available soil nutrients, UV radiation, temperature fluctuations, predatory interactions and other factors (Harbone & Williams 2000, Gould & Lee 2002, Simmonds 2003). Within plant cells, the ACYs are located in the vacuoles and sometimes found attached to the cell wall (Vowinkel 1975). This is very important in the extraction of ACYs since the time, temperature, and solvents are based on the location of the analyte and its surroundings. Pectinases are used in juice processing in order to release more of these compounds from the cell walls and increase juice yield (Skrede 1996). The biosynthetic pathways in plants involves multiple enzymes, including flavanone hydroxylase, flavonol synthase, and anthocyanidin synthase, to create the unique stereochemistry and substituent positioning of polyphenols (Turnbull et al. 2004).

The majority of purchasable ACYs are extracted from plant material in a tedious process resulting in high cost per unit mass. Many of the publications about synthetic means of producing ACYs were published a few decades ago and few breakthroughs have been produced since. The two basic routes of synthesis involve starting materials that are closely related in structure, like flavonols and other flavonoids, or else starting with much smaller reagents and building the molecule through Diels-Alder, Grignard, or other synthesis techniques (Iacobucci and Sweeny 1983, Andersen & Markham 2006). One interesting manner in generating isotopically labeled polyphenols comes from developing the plants in a growth chamber filled with $^{13}\text{CO}_2$, therefore limiting the plant to produce solely isotopically labeled molecules (Gleichenhagen et al. 2013). This research did not use plants that produced notable quantities of ACYs, but the process should be transferrable for many varieties of plants.

Figure 1 displays the structures of the major ACYs, which affects their color based on B ring substituents. Greater methoxylation increases the red and blue hues to reach purple colors and this can be seen in the flowers where the ACYs get their respective names. Meanwhile, Figure 2 shows the variability of the ACY structure with varying pH and temperature. The proton transfer, hydration, and tautomeric reactions are all endothermic, so any increase in temperature will result in the chalcone structure being favored (Brouillard & Delaporte 1977). Hydrating carbon 2 with a hydroxyl group removes the conjugation that is present in the flavylium ion, which brings the λ_{\max} to near 330 nm. Water will always be present in a juice system, so this reaction is a constant threat to the long-term color stability.

Red radishes are fast growing vegetables with vibrant and stable pigmentation providing ideal natural colorant potential. Red radish ACYs were first identified in the 1960's (Harborne 1963, Fuleki 1969) with predominantly pelargonidin forms, while purple radishes are composed mainly of cyanidin derivatives (Hanlon 2011). The two major ACYs in red radish are pelargonidin-3-sophoroside-5-glucoside (P) with malonic acid and either ferulic (PFM) or *p*-coumaric acid (PCM) moieties, while the two secondary ACYs are P with either ferulic (PF) or *p*-coumaric acid (PC) (Giusti 1996). These ACYs were characterized on a divinylbenzene HPLC column with mass spectrometric detection. The phenolic acids provide unique spectrometric profiles that aid in identification of the acylated ACYs with a shoulder near 440 nm (Giusti 1996). Pigments were quantified and compared based on variety, harvest time, and location with differences between each criterion. Spring varieties had red skin with white flesh and a total ACY content ranging from 39.3-185 mg ACY/100g skin, while the winter cultivars had red flesh and contained 12.2-53 mg ACY/100g root (Giusti 1998). This would allow a pigment yield of 1.3-14 kg/ha and an ideal substrate for red colored product development.

Maraschino cherries were colored with radish extract, evaluated for color characteristics similar to FD&C Red No. 40, and tested exceptionally close to the original red color over six months of storage. There was no significant difference in color among the L*, a*, or b* between FD&C Red No. 40 (200 ppm) and red radish extract at either 600 or 1200 mg/L. The half-lives of radish ACYs were 29 and 33 weeks for the 600 and 1200 mg/L, respectively. The remarkable ACY stability is attributed to the phenolic acids bound to the glycosidic moieties. The sugar groups can act as hinges allowing the acyl groups to protect the flavylium cation from hydrolysis by stacking around the pyrylium ring (Brouillard 1981).

Another example of red radish colorants used in a model juice product by Rodriguez-Saona et al., which also compared red-fleshed potato extract to FD&C Red No. 40. Half-lives of ACYs at ambient temperature were 22 weeks for red radish, while just 10 weeks for red potato juice concentrate and this difference could be caused by the monoacylation of red potatoes compared to the diacylation of red radishes (Rodriguez-Saona et al. 1999). The percent polymeric color assay measured at the start of storage for the potato and radish juices were 20% and 8%, ending with near 60% and 40%, respectively for 35 weeks. Typically ACY degradation follows first order kinetics (Daravingas et al. 1968); however, the red radish and potato ACYs in the model juices fit a quadratic model, which agrees with the nonlinear degradation of other acylated ACYs potentially caused by the flexible moieties protecting the flavylium ion (Rodriguez-Saona et al. 1999, Baublis et al. 1994).

Fruit processing

Berries are one of the most popular sources of ACYs and a high value crop. The growing season for berry fruit is short and the shelf life is limited due to mold growth, so berries can be

made into juices, jams, jellies, or wines for preservation. Nearly 75% of the sugars in berry fruits are glucose and fructose, which are excellent substrates for mold growth. Hence, almost all commercial berry products are pasteurized even though the process greatly decreases the ACY content (Mikulic-Petkvssek et al. 2012, Wilkes et al. 2014). There are several organic acids, including citric, malic, tartaric, and shikimic acids, found in blueberries, blackberries, raspberries, strawberries, currants, elderberries, and chokeberries (Mikulic-Petkvssek et al. 2012). Fumaric acid is found in each of these berries, except for blueberries and chokeberries, and the heat applied in certain stages of processing potentially encourages each organic acid to react with other constituents, including ACYs. Processing of berries illustrated in Figure 3 and involves applying heat to the fruit, separation of liquid and solid materials, which affect extraction efficiencies, and pasteurization. The fruit is treated with enzymes, such as pectinases, to disrupt the cell walls to release beneficial compounds, including ACYs, while all enzymes should be deactivated through pasteurization (Skrede 1996). ACYs degrade over storage of these products, which affects quality. In order to maintain high quality and vivid color, this research examines the mechanistic causes of ACY degradation over storage.

Color and copigmentation

Color is in the eye of the beholder; however, this reworded cliché is not completely true. Depending if you are reading this on a computer or mobile phone screen or on printed-paper, the origin of color is slightly different. Screens produce color from combinations of red-green-blue pixels, since those are the three colors the human eye detects through its cones. The visible spectrum can be broken into individual nanometer segments, each with a different wavelength from 450-700 nm; however, the eye cannot detect all of these wavelengths. The cones perceive

colors through the mixtures of different wavelengths that activate either the red, green, or blue or combinations of them. Color originating from a fruit in your hand is caused by subtractive color, which means the fruit absorbs all the wavelengths of visible light, except for the color that is seen. Much of this research is centered on color and the fate of the pigmented molecules. Color can be divided into three categories: hue (color), lightness, and saturation (vividness). A colorimeter can detect each of these parameters and display the units in the CIELAB format, which is closely related to the L*C*h color space (Konica Minolta 2007).

An important characteristic in the pigmentation of colored juices is copigmentation, which is the shift in color due to intra- or intermolecular interactions. Metal complexation, hydrophobic interactions, and π - π stacking are some of the mechanisms behind copigmentation (Mazza & Brouillard 1990). The various sugar and acid moieties attached to the ACY can greatly affect the coloration (Andersen & Markham 2006). Solubility, stability, and hydrogen bonding increase with an increasing number of these moieties (Giusti & Wrolstad 2003). The phenyl rings of the substituent acids and sugars can provide steric protection from nucleophilic attack, thus limiting the formation of colorless compounds and preserving pigment (Brouillard 1981, Mazza & Brouillard 1990). A high degree of intramolecular copigmentation from several acyl moieties causes a greater efficiency in stabilizing ACY color compared to high ratios of intermolecular copigmentation from aromatic acids (Dangles et al. 1993). The sugar substituents function as joints allowing the acyl moieties to bend around and shield the flavylum ion. This has been described as a sandwich effect where the aromatic rings wrap around and stack on top of each other to protect carbon 2 from hydration (Berke & de Freitas 2005). Figure 4 illustrates the sandwich effect with two caffeoyl esters surrounding the ACY (Mistry et al. 1991). This

effect can increase with increasing levels of acylation and glycosylation. Common sources of acylated ACYs are radishes, red cabbage, purple potatoes, and black carrots.

On the other hand, there is a phenomenon called anti-copigmentation where the colored compounds are encapsulated inside a β -cyclodextrin cavity (Dangles et al. 1992a). The typical copigmentation effect results in a bathochromic shift, while this anti-copigmentation produces a dampened absorbance. Dangles et al. (1992a) reports “a macrocycle to callistephin ratio of 50, the absorbance drops to less than half of its initial value in the absence of cyclodextrin.” The color reduction is favored with nonplanar structures, such as the chalcone and hemiacetal configurations as opposed to the planar flavylum ion (Dangles et al. 1992b). The interaction with cyclodextrin decreased with an increasing number of substituents on the B ring of the ACY (Dangles et al. 1992a). This illustrates the complicated process and multitude of interactions that can affect color.

Comparing a sandwich structure to a polymeric structure, researchers found the sandwich structure much more likely to form since it will have a very low activation energy compared to the high energy of the polymer formation. Creating a polymer involves the breaking of two C-H bonds, which cause the high energy of activation, followed by the formation of a more stable C-C bond (Kunsagi-Mate et al. 2011). Elevated temperatures above 20 °C cause copigmentation complexes to decay and increase the rate of polymerization (Kunsagi-Mate et al. 2011).

Health benefits and bioavailability

ACYs have long been thought to have a low bioavailability because of the instability of the flavylum ion in the physiological pH of 7.4; however, there are many metabolites and smaller degradation products along with the ACYs that appear in human serum, urine, fecal, and

breath. The primary metabolic pathways for the intact ACY are glucuronidated, sulfated, or methylated conjugates (Hackett 1986). It is possible for one ACY to become methylated and therefore be classified as a different ACY. There is evidence of cyanidin methylation *in vivo* and changing into peonidin (Wu et al. 2002).

Humans are very different from each other so there is quite often a high standard error for human studies. The variation is even greater when the subjects are both male and female, so for this reason, studies are frequently conducted on a single gender. Fortunately, the excretion time of many medications is slightly longer on average for men than women due to their larger size (Schwartz 2003). One study fed blueberries or elderberry extract to four elderly women and found cyanidin-3-sambubioside, cyanidin-3-glucoside, peonidin-3-glucoside, peonidin-3-sambubioside, peonidin monoglucuronide, cyanidin-3-glucoside monoglucuronide in their urine (Wu et al. 2002). The mean intake of those metabolites, as a percent of the intake volume, is $0.077 \pm 0.013\%$, which was collected between 0-4 hours after consuming elderberry extract. This is measured solely from urine, so much of the intake volume could likely be found in fecal material, breath, serum/blood, or even stored in organs for extended time periods. One of the great difficulties in measuring bioavailability of molecules or plant extracts is the timing for collection. Many studies record samples at various time points, often ceasing within 48 hours, and from multiple avenues of excretion in order to capture as much initial ingested volume as possible.

In a groundbreaking study, Czank et al. used stable carbon isotopes to synthesize C3G that contained five ^{13}C atoms in the 6, 8, 10, 3', and 5' positions so there were three ^{13}C atoms on the A ring, along with two on the B ring. The isotopically labeled C3G was used to investigate the absorption, distribution, metabolism, and elimination of ACYs in humans. Eight male

subjects were provided with 500 mg of the sample, and then urine, breath, fecal, and blood samples were acquired over 48 hours. Intact C3G was found in the serum and urine over the course of 48 hours with recoveries of 9.99 ± 3.90 and 36.47 ± 20.27 ng, respectively. This is believed to be the first published evidence of ACY-derived carbon to be found in the breath. The C_{\max} in breath occurred at 24 hours and maintained levels $^{13}\text{CO}_2$ over 48 hours, which might be caused by continued absorption of small molecules from fecal material. The other significant findings from this research are the comparable relative bioavailability of C3G ($12.38 \pm 1.38\%$), and presumably other ACYs, to flavan-3-ols (2.5%) and flavones (18.5%) (Czank et al. 2013, Williamson & Manach 2005).

Proanthocyanidins and polymeric pigments

Also called condensed tannins, proanthocyanidins (PACs) are important for a myriad of health benefits, but also for their interactions with ACYs in forming polymers, which will be discussed in the next section. (Jurd 1969, Somers 1971). PACs are a category of flavonoids that includes the likes of procyanidins, prodelfinidins, propelargonidins, and others. They are named as such because the procyanidins compounds can be hydrolyzed, under either acidic or alkaline conditions, into cyanidin. Proanthocyanidins have an estimated daily intake volume of 57.7 mg/person and the major sources in the American diet are apples, chocolate, and grapes (Gu et al. 2004). Upon incubation with human microbiota, A-type and B-type procyanidins are digested by the microbes into benzoic, 2-phenylacetic, 3-phenylpropionic, and other small phenyl acids (Ou et al. 2014). This is beneficial to human health because smaller molecular weight molecules are more readily absorbed into the body than the large polymeric procyanidins.

Free radical reactions, including Fenton and Haber-Weiss, are catalyzed by iron and copper ions in a solution (Cos et al. 2004). The Fenton reaction can produce hydroxyl radicals that will react with most any organic compound and negatively impact their stability. Procyanidins can form strong complexes with iron and copper with stoichiometric binding ratios of 2:1 for Fe^{2+} :procyanidin and 4:1 for Cu^{2+} :procyanidin (Facino et al. 1996). The strength of the procyanidin binding to the iron is five orders of magnitude lower than the binding strength of iron to EDTA, as assessed by the stability constant values of $\log K$ equaling 9.35 and 14.4, respectively (Facino et al. 1996). There is certainly a large difference between those binding strengths, but it does indicate the metal binding potency of the procyanidin. Also interesting to note is the longer the procyanidin chain, the greater the stability between the metal and the PAC complex (Yoneda et al. 1998). A similar trend is shown with *o*-dihydroxyphenyl groups, also called catechol groups. Therefore, the metal ion will complex with the PAC and not be reactive with other parts of the system. This protective effect can be found in food systems as well as biological systems. Superoxide radicals are more efficiently scavenged with metal-flavonoid complexes than the flavonoid alone, which infers a cytoprotective function (Moridani et al. 2003).

Analysis of procyanidins is often accomplished using HPLC with fluorescence detection because UV detection at 280 nm reveals many other phenolic compounds and is not as sensitive or selective as fluorescence (Lazarus et al. 1999). As illustrated in Figure 5, procyanidins often have a linear order to their polymerization, with bonds between carbons 4 and 8, which is a B-type procyanidin; however, there is a less common form of B-type that is branched with bonds between carbons 4 and 6, shown with a dashed bond in Figure 5. The A-type procyanidins have

an ether bond from carbon 2 to the A or B ring hydroxyl group as well as a carbon-carbon bond (Kelm et al. 2005). The ether bond in Figure 5 is shown as a dashed bond to the B ring.

Due to the similarity between units of the polymer and the many combinations of potential bonding patterns between the oligomers and polymers, separation via HPLC can be very difficult. HILIC phase HPLC using a diol column can be used to cleanly separate procyanidins up to decamers; however, normal phase has better separation within the same number of monomeric units of one PAC, as seen in Figure 6 (Khanal et al. 2009). Notice how the chromatogram elutes the larger polymers as one, large peak. Further research is needed to better resolve polymers with $DP > 10$, while remaining intact. Thiolysis treatment breaks PACs using benzyl mercaptan or toluene α -thiol to measure the average degree of polymerization by detecting the number of terminal units (Gu et al. 2002). A-type PACs, often found in cranberries, contain an ether bond and another carbon-carbon bond, as seen in the dashed bonds in Figure 5, that severely limit thiolysis from occurring (Kerchesy and Hemingway 1986).

PACs can combine with ACYs to form polymeric pigments (PPs), which are colored polymers. PPs might be the source of long-term color in aged juices and wines, but currently there is no method to separate and quantify PPs to determine if this is true. Methodology needs to be developed to separate PACs from PPs and PPs by degree of polymerization.

Degradation products and mechanisms

The purpose of this research is to discover novel degradation products of ACYs, and to determine their mechanism of formation, impact on color, and stability over time. Each of these poses unique problems for identification and analysis. In particular, the mechanisms are mostly theoretical functions based in fundamental organic chemistry. ACYs follow the breakdown

pattern shown in Fig. 2, from the quinodal base to the flavylum ion to the carbinol pseudobase to the chalcone, the last of which is thermolabile and quickly cleaved (Sadilova et al. 2007).

Cyanidin produces two primary degradation products: phloroglucinaldehyde and protocatechuic acid, as seen in Figure 7 (Sadilova et al. 2007). Thermal degradation pathways are different at pH 1 and pH 3.5, with pH 3.5 prolonging the life of cyanidin-3-galactoside-xyloside-glucoside. The xyloside is believed to function in ring stacking/ sandwich stabilizing effect shown in Figure 4. Protocatechuic acid and phloroglucinaldehyde account for most of the carbons in cyanidin; however, the red-colored carbon in Figure 7 is not included in these products and may form carbon dioxide. Polymeric pigments, which were discussed previously, are technically not a degradation product, but a reaction product, and a likely source of the persisting red color during storage.

It is possible for hydrogen peroxide to form in solution as a product of oxidation in the presence of metal ions (Bradshaw 2011). The catechol group depicted in Figure 8 is found in cyanidin, C3G, and other polyphenols and frequently produces hydrogen peroxide in combination with the metal ions naturally found in fruit juices. The catechol group reacts to form a quinone and hydrogen peroxide in the presence of metal ions and oxygen (Danilewicz 2003). Once the radical is generated from peroxide breakdown, a vast array of reactions can take place and model systems will be used to isolate and identify the degradation products. Predicting the pattern of reactions that will follow the radical relies on knowing which forms of compounds are present at the pH, temperature, storage time, and other factors, which makes the process extremely difficult.

Building on the reactivity of radicals in solution, Lopes et al. found a novel degradation product of malvidin 3-*O*-glucoside in a model wine system. Proposing a Baeyer-Villiger

oxidation, hydrogen peroxide attacks carbon 2 and the peroxy group initiates rearrangement to become a seven-membered ring with carbon 2 as a carbocation, along with the loss of water. The resulting malvone is cleaved, similar to a chalcone breakdown, into anthocyanone A and syringic acid, which would be protocatechuic acid if the starting reagent was cyanidin (Lopes et al. 2007).

Ascorbic acid (Vitamin C) is a highly reducing compound that is found in many fruits, as well as berry juice and wine. Many model systems are prepared with ascorbic acid, yet there are many other model system elements that affect reactions, such as pH, buffer solutions, temperature, metal ions, different metal oxidation states, and oxygen availability, among others. The multitude of variants makes direct comparisons difficult, but some conclusions can be drawn. The most reactive components of ascorbic acid are the enediol between carbons 3 and 4, and the hydroxyl groups on carbons 6 and 7. The first proton to be removed from ascorbic acid is quite acidic with a pKa of 4.25 and assists in its antioxidant properties (Bradshaw 2011). After several hydrogen transfers, ascorbic acid becomes dehydroascorbic acid (DHA) with two ketones replacing the enediol. Both ascorbic acid and DHA have vitamin C activity and each are measured to determine total vitamin C content on nutrition labels. (Nielsen 2010). As seen in Figure 9, the two carbonyl carbons can undergo hydration reactions to become the hydrated dehydroascorbic acid. Each of these structures has a different mass, which must be accounted for in mass spectrometric analysis of the degradation products of model systems.

The chelating property of ascorbic acid with different metals and organic compounds is a common topic and the resonance surrounding the enediol is a key component. The enediol is located between carbons 2 and 3, with a ketone on carbon 4; however, the oxygen in the heterocyclic ring provides the electron density to stabilize the ketone at carbon 2. As previously

mentioned, the first hydrogen is quickly removed to form mono-anionic ascorbic acid (HA^-), with a hydroxyl group at carbon 3. The hydroxyl group can form a hydrogen bond with either the anionic oxygen or the carbonyl oxygen, allowing the metal to form a connection with carbon 3 and the non-hydrogen bonded atom. Whether copper or iron, the positions of the chelation remain the same and result in the production of dehydroascorbic acid (Martell 1982). Chelation is important to the mechanism of oxidation and reduction of ascorbic acid. A lack of dissolved oxygen (DO) with a metal chelate causes a slower oxidation of ascorbic acid than DO in combination a metal (Dekker et al. 1940). Figure 10 illustrates several of the aforementioned reactions and resonance structures, focusing on diatomic oxygen becoming hydrogen peroxide. This highlights the importance of water purity along with metal removal and other contaminants for model systems. One experiment that will be accomplished with this research is monitoring ACY content in the presence and absence of ascorbic acid using model systems. Also, EDTA will be used to determine the effect of metals on ACYs and the degradation products resulting from their degradation.

There are numerous studies published on ascorbic acid degradation and there are nearly as many breakdown products, depending on the reaction conditions. Although ACY-rich juices are the focus of the research, many publications concentrate on ethanolic systems, such as red wine. Most fruit juices and wines have a pH of approximately 3.5, which affects the degradation pathways of ascorbic acid (Hsu et al. 2012). A general breakdown pathway of ascorbic acid can be seen in Figure 11: DHA opens its ring to become 2,3-diketogulonic acid and has a carboxyl group removed as carbon dioxide to create xylosone (Kimoto et al. 1993). Xylosone (XLS) can further degrade into several compounds, the most common of which are 3-hydroxy-2-pyrone (3H2P) and 2-furoic acid (FA). An entire breakdown schematic, including the intermediates

between XLS and 3H2P and FA, can be seen in Figure 11. The compounds 3-hydroxy-2-pyrone and 2-furoic acid have the same empirical formula and mass, but differ in their structure, λ_{max} , and LC retention time. 2-furoic acid elutes after 3-hydroxy-2-pyrone, as well as the former being electrochemically inactive (Kimoto et al 1993). While 3-hydroxy-2-pyrone has a λ_{max} at 295 nm, 2-furoic acid has its λ_{max} at 245 nm at pH 7 and 255 nm in acidic conditions (Kimoto et al 1993). This difference in absorbance is understandable with knowledge of UV/visible spectral absorption patterns. Each carbon in 3-hydroxy-2-pyrone has some π characteristic, which delocalizes the electron density and thus lowers the energy needed for absorption. The lower energy related to the absorbance of a molecule produces a longer wavelength for the λ_{max} , which is why 3-hydroxy-2-pyrone strongly absorbs at 295 nm. There is less delocalization in 2-furoic acid around its ring and therefore results in a slightly lower lambda max. Detection of each of the degradation products of ascorbic acid, as well as their potential conjugates with ACYs can be difficult, but necessary to determine the fate of ACYs in the presence of ascorbic acid.

Besides ascorbic acid and hydrogen peroxide altering ACY structures, some phenolic acids can bind to ACYs to form pyranoanthocyanins. These compounds have a secondary pyran ring between carbon 4 and the hydroxyl moiety on carbon 5. Pyranoanthocyanins possess an orange hue and retain much more color than ACYs when the pH is raised from 1 to 5 (Mazza and Miniati 1993). Blocking the nucleophilic hydration to carbon 4 with the newly formed pyran ring likely causes this increased stability. The mechanism between malvidin-3-glucoside and caffeic acid (Fig. 12) involves an initial loss of conjugation with carbocation formation, then loss of carbon dioxide, 2 hydrogen atoms, and 2 electrons and ultimately conjugation returns, and thus the color (Rentzsch 2007). Pyranoanthocyanins are not affected by bisulfite bleaching due to the pyran ring protecting carbon 4 (He et al. 2010).

A subdivision of pyranoanthocyanins, called portisins, have two doubled bonded carbons attached to the carbon adjacent to the oxygen in the pyran ring followed by at least one aromatic ring. First found in Port wines, the aptly named portisins have unique spectral properties with blue hues and λ_{max} near 580 nm (Mateus et al. 2003). Portisins are a secondary degradation product being formed from the primary degradation product of pyranoanthocyanins; likewise, pyranoanthocyanins can form an oligomer (Fig. 13) with acylated or non-acylated flavanols (He et al. 2006). Using flavanol monomers creates a similar molecule to polymeric pigments, so the mass of the pyranoanthocyanin polymer must be monitored upon analysis. Pyranoanthocyanin dimers with single carbon bridge (m/z $[M^+]= 1337$) that encompass one charged ion and a large conjugated system have been detected in wines, lees, and model wine solutions (Oliveira et al. 2010). The majority of the dimers were found in the wine lees likely due to the limited solubility, so the turquoise color at pH 2 ($\lambda_{\text{max}}= 676$ nm) would not contribute much to the overall wine coloration. (Oliveira et al. 2010). The carboxypyranomalvidin-3-glucoside dimer first appeared in the model system “in less than 1 day and attained the maximum formation after 14 days in a much higher quantity (~12 mg; yield of 20%)” (Oliveira et al. 2010). The potential possibilities for long-term color are near limitless with the known variety of different acylation, glycosylation, and monomeric units.

Much of the published research on pyranoanthocyanins has focused on wine, but the chemistry of formation does not restrict their synthesis in berry or other fruit juices. Of course, malvidin 3-glucoside is the most common ACY in wine, so pyranoanthocyanins research has been focused on pyranomalvidin compounds, but pyranocyanidin structures have been discovered in black carrot juice (Schwartz et al. 2004). Stored cherry juices contain 5-carboxypyrananthocyanin: a pyruvic acid adduct of glycosylated cyanidin (Rentzsch et al.

2007). There is little evidence of pyranoanthocyanins in berry juices, but one group added ferulic and sinapic acid, along with 4-vinylsyringol to strawberry and raspberry juices in a 10:1 ratio to ACYs and found pyranoanthocyanins formed from each added reagent (Rein et al. 2005). The pyranoanthocyanins in the strawberry and raspberry juices were purposely formed as means of improving color stability over time, which the pyranoanthocyanins provided. Rein et al. illustrated a mechanism of formation that included a Michael addition of ferulic acid to pelargonidin-3-glucoside along with a loss of carbon dioxide to produce the pyranopelargonidin. There is one type of pyranoanthocyanin without a charged ion and therefore no red hue, but this compound does show a yellowish color. The so-called oxovitisin A was formed from a pyranocyanidin with an acylated sugar moiety on carbon 3, and hydrated at pH 4.5 and 50 °C to remove the conjugation (He et al. 2011). Oxovitisin A is a type of pyranone that has a λ_{max} of 370 nm, was formed in minor quantities at 25 °C, and had a near bell curved shaped production between pH 2.5 to 7, with the mean at pH 4.5 (He et al. 2011).

Anthocyanin model systems

Due to the complex matrix in a fruit juice, model systems are made with only a few components to isolate and identify specific products. The model systems will attempt to determine novel breakdown products of ACYs by combining cyanidin-3-glucoside with various compounds found in berry juices. ACYs will be mixed with ascorbic acid and temperature, pH, color, and time will be monitored as well. There are several analytical techniques to determine the identity of new degradation products, including LC-MS-MS, NMR, and UV/Vis absorbance.

There are many factors dictating the reactivity of an ACY with other products found in juices. The charged flavylum ion is electron deficient and prone to nucleophilic attacks.

Therefore the yellowish, hydrated, hemiketal form is formed with a significant loss of red color due to the loss of conjugation. A few publications have looked at aldehydes reacting with ACYs because aldehydes are more reactive than a carboxylic acid; however, there are more carboxylic acids found in juices.

An interesting approach in a model system to study degradation products is the addition of a free radical generator to initiate the process. Cyanidin 3-*O*- β -D-glucoside was subjected to ten times its concentration of 2,2'-azobis(2,4-dimethylvaleronitrile) in order to facilitate radical reactions (Tsuda 1996). Three main products were formed from C3G: protocatechuic acid and two diastereomers of 4,6-dihydroxy-2-*O*- β -D-glucosyl-3-oxo-2,3-dihydrobenzofuran, with the glucosyl group possessing the choices in stereochemistry. It is unusual that the high concentration of radical generator took over eight hours to breakdown the majority of the cyanidin, based on the absorbance at 530 nm compared to the control (Tsuda 1996). One of the diastereomers rose in concentration faster and reached a higher C_{\max} than the other, which demonstrates the selectivity of the bond reformation during the breakdown of the ACY. Using a radical generator can cause product formation that may not occur during regular storage conditions, so it is unlikely that this type of model system will be used for this research. However, it could be useful to compare a system with and without the radical generator to monitor which types of compounds are formed and hypothesize a mechanism of formation.

Current research has confirmed several degradation products of ACYs using model systems. Phloroglucinaldehyde and protocatechuic acid are formed after heating ACYs from the A and B rings, respectively. Another unique degradation product found using model systems is the trimeric ACY oligomer of malvidin-3-glucoside, which was formed in 20% ethanol with 5 g/L tartaric acid at pH 3.5 (Oliveira et al. 2013). This trimer was also found in grape skin

extract, as well as the young port wine made from those grapes. There are two bonds joining each unit producing an A-type polymeric pigment: a C4-C8 bond and the ether C7-O-C2 bond. With a λ_{max} of 547 nm, it is bathochromically shifted compared to other monomeric ACYs, and this trimer could be one source of the red color of wines over time (Oliveira et al. 2013). Stability of the compound could be measured and compared to the degradation rate of similar molecules for further investigation. Computational studies were performed on the trimer and found the optimized geometry to be in a star shape with each of the B rings and the sugar moieties facing outward (Oliveira et al. 2013).

An important variable to monitor is the oxygen level in the model system. Flushing the system with nitrogen can lead to slightly improved retention of ACY content over 30 days, as seen in Figure 14 (Poei-Langston & Wrolstad 1981). The aforementioned ascorbic acid produces the more noticeable effect in Figure 17, with a dramatic decline in ACY retention over a short time. A similar dichotomy was found in their percent polymeric color results since the ACY had degraded when incorporated with ascorbic acid, the relative amount of polymeric color greatly increased. This would seem to indicate that C4 was blocked by ascorbic acid. This study used 5.96 mg/mL of ascorbic acid combined with 3.73 mg/mL of pelargonidin-3-glucoside.

Acetaldehyde effect on wine color

Acetaldehyde is a small, volatile molecule found in fruits, bread, and wine through microbial growth. It is an oxidized form of ethanol and could be a cause of the hangover feeling (Swift & Davidson 1998). Grassy and apple-like descriptors have been associated with acetaldehyde in beer, cider, and wine (Liu & Pilone 2000). Yeasts excrete acetaldehyde largely during the growth stage (Ribereau-Gayon 1956) with variation in production due to temperature, oxygen, and SO₂ (Ough 1958). Levels can vary from 5-12 mg/L in beer to 90-500 mg/L in

sherry (Liu & Piloni 2000), with measurements conducted chemically, enzymatically, or using GC (Ough 1988).

In the presence of ACYs and flavanols, like catechin or procyanidins, acetaldehyde can act as a polymerization agent by reacting at carbon 8 (Timberlake 1976). The authors found yellow xanthylium ion compounds were formed, but the more significant products were violet. The reaction between malvidin-3-glucoside (M3G), acetaldehyde, and either catechin, epicatechin, procyanidin dimer B2, or procyanidin trimer C1, occurred rapidly and tended toward a violet hue. The optimum pH for the reaction is between 3.75-4.0 according to Timberlake and Bridle (1976). The authors stipulated the monomeric epicatechin was more reactive than the dimeric or trimeric procyanidins. Also, the monoglucoside was more reactive than the diglucoside of malvidin, due to the electron withdrawing power of the 5-glucoside. After seven days of reacting M3G, acetaldehyde, and the phenolics, precipitation occurred. This sedimentation is notable and would be undesired in a formulated product.

This reaction is possible with other aldehydes, including formaldehyde, isobutyraldehyde, isovaleraldehyde, propionaldehyde, and benzaldehyde; however, acetaldehyde reacts faster and more efficiently when using M3G and catechin (Pissarra et al. 2003). Multiple products were identified in the reaction of M3G, acetaldehyde, and procyanidin B2; these include two reddish-blue enantiomers of M3G with an ethyl linkage to B2, along with a red-orange compound thought to contain two flavylium forms: malvidin and pelargonidin (Francia-Aricha 1997). Violet precipitation was also noted in this study.

If excess acetaldehyde is present, oligomeric products are possible by propagation reactions with available monomeric species. Using thiolysis and mass spectrometric techniques, Es-Safi et al. found trimeric and tetrameric compounds, detecting doubly charged molecules

containing two ACY and two flavanol moieties (Es-Safi 1999). One ACY and three epicatechin units were found polymerized with three ethyl-linkages to form a tetramer. In a different experiment in the absence of ACYs, catechin reacted with acetaldehyde to form large polymers measured with gel permeation chromatography with light scattering detection. The average peak mass was near 6000 Da described as a dodecamer peracetate (Saucier 1997). Once again, precipitation occurred and these authors noted the precipitate was ethanol soluble, but not water-soluble.

Garcia-Viguera et al. measured the effect of pH on the polymerization reaction with ACYs and catechin, finding pH 2 having the most rapid production of ethyl-linked dimers compared to pH values of 3, 3.7, 4, and 5 (Garcia-Viguera 1994). Timberlake and Bridle found the most reactivity at pH 3.75-4.00. Other researchers found cyanidin- and peonidin-3-glucoside more reactive than M3G (Dallas et al. 1996).

Acetaldehyde and pyruvic acid can react with ACYs at carbon 4 to produce pyranoanthocyanins (Morata 2007). Acetaldehyde and pyruvic acid together formed fewer pyranoanthocyanins than either reagent individually; acetaldehyde reacted with ACYs more than pyruvic acid (Morata 2007). The by-products of yeast fermentation, aldehydes and carboxylic acids can react with ACYs forming stable pigments with a more reddish-orange color as opposed to the red-purple of young wines (Marquez et al. 2013). There are several possible products in a model system containing standards of ACYs, acetaldehyde, and phenolic compounds, which necessitate high-resolution chromatographic separation. Using fruit and vegetable extracts will further complicate the separation and lead to possible overlapping peaks.

Analytical Techniques

HPLC

High-pressure liquid chromatography is the most common means of separating and characterizing polyphenols. The modern alternative uses ultra high pressure, UPLC, and is more efficient at accomplishing the same degree of separation. The wide ranges of detectors that can be attached to the HPLC allow great quantities of information to be collected about the analyte. The most widespread detector is the photodiode array detector (PDA), which measures light in the UV/Visible range (200-750 nm). Other detectors are fluorescence, refractive index, and electrochemical, and mass spectrometers. Mass spectrometry will be covered in more detail next.

Another vital component of the HPLC is the column and its corresponding solid phase packing material. There are several types of columns that fall under a few main categories: normal phase, reverse phase, HILIC and cation & anion exchange. Normal phase was created prior to reverse phase, hence its name, and uses nonpolar mobile phases with a more polar stationary phase. Clearly reverse phase uses the opposite paradigm and is far more common since its introduction into the chromatography realm. In order to separate the polymeric pigments, a combination of columns may have to be utilized.

Mass spectrometry: MALDI and ESI.

The innovation of mass spectrometry has enabled the detection of a key component in the identification of unknown molecules, their mass. This is the only analytical technique that can obtain the mass of an unknown and there are multiple methods that all use a sample's volatility to create an ion. The ions are quantified by a mass to charge ratio (m/z), so a doubly charged ion will be reported as half the mass of the ion. The two largest divisions of mass spectrometry are hard and soft ionization. Hard ionization produces a greater fractionation pattern by using high-

energy electron impact; meanwhile soft ionization does not fragment the parent molecule to the same degree. The two forms of soft ionization that will be used in this research are electrospray ionization (ESI) and matrix-assisted laser desorption ionization (MALDI).

To discern large amounts of information about the constituents in an unknown sample, liquid chromatography is often coupled with mass spectrometry, known as LC-MS. Engaging a multitude of analytical techniques is an efficient way to gather the data to identify an unknown. The model systems will utilize LC-ESI-MS-MS for a soft ionization of peaks separated on a C18 column. MS-MS fragments each MS peak once more to learn even more about the structure; likewise MS³ can break an ion apart again. Certain reactions occur with consecutive fragmentation, such as retro-Diels Alder (RDA) and dehydration.

UV/Visible Spectrophotometry

The UV/Visible output is often noted by the lambda max of a compound and displays a broad peak and not a single line due to molecular vibrations and rotations. Atomic absorptions are a single line since they do not have as many possible motions. Increasing the conjugation of a molecule increases the λ_{\max} because the electrons are more delocalized around the π system. The increased delocalization of electrons requires less energy for absorption to occur; therefore the lower energy is a longer wavelength. ACY have a heterocyclic ring as well as several hydroxyl or methoxyl moieties, which increases the λ_{\max} into the visible range and produces their attractive colors. The phenolic acids attached to acylated ACYs produces a UV/Visible spectrum with a distinct shoulder depending on the structure of the acid, which aides in identification.

References

- Field, T.S.; Lee, D.W.; Holbrook, N.M. Why leaves turn red in Autumn. The role of anthocyanins in senescing leaves of Red-osier Dogwood. *Plant Physiology*. **2001**, *127*, 566-574.
- Wang, H.; Cao, G.; Prior, R.L. Oxygen radical absorbing capacity of anthocyanins. *J. Agric. Food Chem.* **1997**, *45*, 304-309.
- Simmons, S.T. Commercial applicability of an innovative anthocyanin purification technique, utilizing mixed-mode solid-phase extraction. Thesis, The Ohio State University. **2012**.
- Jackman, R.L. Anthocyanins as food colorants – A review. *J. Food Biochem.* **1987**, *11*, 201-247.
- Brouillard, R.; Delaporte, B. Chemistry of anthocyanin pigments: kinetic and thermodynamic study of proton transfer, hydration, and tautomeric reactions of malvidin 3-glucoside. *J. Am. Chem. Soc.* **1977**, *99*, 8461-8468.
- Andersen, O.M.; Markham, K.R. *Flavonoids: Chemistry, biochemistry, and applications*. Boca Raton, FL: Taylor & Francis Group, LLC. **2006**.
- Kong, J.M.; Chia, L.S.; Goh, N.K.; Chia, T.F., Brouillard, R. Analysis and biological activities of anthocyanins. *Phytochem.* **2003**, *64*, 923-933.
- Cho, M.J.; Howard, L.R.; Prior, R.L.; Clark, J.R. Flavonoid glycosides and antioxidant capacity of various blackberry, blueberry, and red grape genotypes determined by high-performance liquid chromatography/mass spectrometry. *J. Sci. Food Agric.* **2004**, *84*, 1771-1782.
- Harborne, J.B.; Williams, C.A. Advances in flavonoid research since 1992. *Phytochem.* **2000**, *55*, 481-504.
- Gould, K.S.; Lee, D.W. Anthocyanins in leaves. *Advances in Botanical Research*. 37, Academic Press, Amsterdam. **2002**.
- Simmonds, M.S.J. Flavonoid-insect interactions: recent advances in our knowledge. *Phytochemistry*. **2003**, *64*, 21-30.
- Vowinkel, E. Cell wall pigments of peat moss. *Chem. Ber.* **1975**, *108*, 1166-1181.
- Skrede, G. Fruits, in *Freezing effects on food quality*. L.E. Jeremiah, New York: Marcel Dekker, Inc. **1996**, 183-245.
- Turnbull, J.T.; Nakajima, J.; Welford, R.W.D.; Yamazaki, M.; Saito, K.; Schofield, C.J. Mechanistic studies on three 2-oxoglutarate-dependent oxygenases of flavonoid

- biosynthesis: anthocyanidins synthase, flavonols, synthase, and flavone 3 β -hydroxylase. *J. Biol. Chem.* **2004**, *279*, 1206-1216.
- Iacobucci, G.A.; Sweeny, J.G. The chemistry of anthocyanins, anthocyanidins, and related flavylum salts. *Tetrahedron.* **1983**, *39*, 3005-3038.
- Gleichenhagen, M.; Zimmermann, B.F.; Herzig, B.; Janzik, I.; Jahnke, S.; Boner, M.; Stehle, P.; Galensa, R. Intrinsic isotopic ^{13}C labeling of polyphenols. *Food Chem.* **2013**, *141*, 2582-2590.
- Harborne, J.B. . Plant polyphenols IX: the glycosidic pattern of anthocyanin pigments. *Phytochem.* **1963**, *2*, 85-97.
- Fuleki, T. The anthocyanins of strawberry, rhubarb, radish, and onion. *J. Food Sci.* **1969**, *34*, 365-369.
- Hanlon, P.R.; Barnes, D.M. Phytochemical composition and biological activity of 8 varieties of radish (*Raphanus sativus* L.) sprouts and mature taproots. *J. Food Sci.* **2011**, *76*, C185-C192.
- Giusti M.M.; Wrolstad, R.E. Characterization of red radish anthocyanins. *J. Food Sci.* **1996**, *61*, 322-325.
- Giusti, M.M.; Rodriguez-Saona, L.E.; Baggett, J.R.; Reed, G.L.; Durst, R.W.; Wrolstad, R.E. Anthocyanin pigment composition of red radish cultivars as potential food colorants. *J. Food Sci.* **1998**, *63*, 219-224.
- Brouillard, R. Origin of the exceptional colour stability of *Zebrina* anthocyanin. *Phytochem.* **1981**, *20*, 143-145.
- Rodriguez-Saona, L.E.; Giusti, M.M.; Wrolstad, R.E. Color and pigment stability of red radish and red-fleshed potato anthocyanins in juice model systems. *J. Food Sci.* **1999**, *64*, 451-456.
- Daravingas, G.; Cain, R.F. Thermal degradation of black raspberry anthocyanin pigments in model systems. *J. Food Sci.* **1968**, *33*, 138-142.
- Baublis, A.; Spomer, A.; Berber-Jimenez, M.D. Anthocyanin pigments: Comparison of extract stability. *J. Food Sci.* **1994**, *59*, 1219-1223.
- Mikulic-Petkovsek, M.; Schmitzer, V.; Slatnar, A.; Stampar, F.; Veberic, R. Composition of sugars, organic acids, and total phenolics in 25 wild or cultivated berry species. *J. Food Sci.* **2012**, *77*, C1064-C1070.
- Konica Minolta. Color control from perception to instrumentation. Precise Color Communication. Osaka, Japan, Konica Minolta Sensing, Inc. **2007**.

- Mazza, G.; Brouillard, R. Mechanism of co-pigmentation of anthocyanins in aqueous solutions. *Phytochemistry*. **1990**, *29*, 1097-1102.
- Brouillard, R. Origin of the exceptional colour stability of the *Zebrina* anthocyanin. *Phytochemistry*. **1981**, *20*:143-145.
- Dangles, O.; Saito, N.; Brouillard, R. Anthocyanin intramolecular copigment effect. *Phytochemistry*. **1993**, *34*, 119-124.
- Berke, B.; de Freitas, V.A.P. Influence of procyanidins structures on their ability to complex with oenin. *Food Chem.* **2005**, *90*:453-460.
- Mistry, T.V.; Cai, Y.; Lilley, T.H.; Haslam, E. Polyphenol interactions: Part 5: Anthocyanin co-pigmentation. *J. Chem. Soc., Perkin Trans.* **1991**, *8*, 1287-1296.
- Dangles, O.; Wigand, M.C.; Brouillard, R. Anthocyanin anti-copigment effect. *Phytochemistry*. **1992**, *31*, 3811-3812.
- Dangles, O.; Stoeckel, C.; Wigand, M.C.; Brouillard, R. Two very distinct types of anthocyanin complexation: copigmentation and inclusion. *Tetrahedron Letters*. **1992**, *33*, 5227-5230.
- Kunsagi-Mate, S.; May, B.; Tschiersch, C.; Fetzer, D.; Horvath, I.; Killar, L.; Nikfardjam, M. Transformation of stacked π - π -stabilized malvidin-3-*O*- glucoside catechin complexes towards polymeric structures followed by anisotropy decay study. *Food Res. Intl.* **2011**, *44*, 23-27.
- Hackett, A.M. The metabolism of flavonoid compounds in mammals plant flavonoids in biology and medicine: biological, pharmacological, and structure-activity relationships. New York: Alan R. Liss, Inc. **1986**, 177-194.
- Wu, X.L.; Cao, G.H.; Prior, R.L. Absorption and metabolism of anthocyanins in elderly women after consumption of elderberry and blueberry. *J. Nutr.* **2002**, *132*, 1865-1871.
- Schwartz, J.B. The influence of sex on pharmacokinetics. *Clin. Pharmacokinet.* **2003**, *42*, 107-121.
- Czank, C.; Cassidy, A.; Zhang, Q.; Morrison, D.J.; Preston, T.; Kroon, P.A.; Botting, N.P.; Kay, C.D. Human metabolism and elimination of anthocyanin, cyanidin-3-glucoside: a ^{13}C -tracer study. *Am. J. Clin. Nutr.* **2013**, *97*, 995-1003.
- Williamson, G.; Manach, C. Bioavailability and bioefficacy of polyphenols in humans. II Review of 93 intervention studies. *Am. J. Clin. Nutr.* **2005**, *81*(suppl), 243S-255S.
- Jurd, J. Review of polyphenol condensation reactions and their possible occurrence in the aging of wines. *Am. J. Enol. Vitic.* **1969**, *20*, 191-195.

- Somers, T.C. The polymeric nature of wine pigments. *Phytochem.* **1971**, *10*, 2175-2186.
- Gu, L.; Kelm, M.A.; Hammerstone, J.F.; Beecher, G.; Holden, J.; Haytoqitz, D.; Gebhardt, S.; Prior, R.L. Concentrations of proanthocyanidins in common foods and estimations of normal consumption. *J. Nutr.* **2004**, *134*, 613-617.
- Ou, K.; Sarnoski, P.; Schneider, K.R.; Song, K.; Khoo, C.; Gu, L. Microbial catabolism of procyanidins by human gut microbiota. *Mol. Nutr. Food Res.* **2014**, doi: 10.1002/mnfr.201400243.
- Cos, P.; De Bruyne, T.; Hermans, N.; Apers, S. Proanthocyanidins in health care: Current and new trends. *Current Med. Chem.* **2004**, *11*, 1345-1359.
- Facino, R.M.; Carini, M.; Aldini, G.; Berti, F. Procyanidines from *Vitis vinifera* seeds protect rabbit heart from ischemia reperfusion injury: Antioxidant intervention and/or iron and copper sequestering ability. *Planta Medica.* **1996**, *62*, 495-502.
- Yoneda, S.; Nakatsubo, F. Effects of the hydroxylation patterns and degrees of polymerization of condensed tannins on their metal-chelating capacity. *J. Wood Chem. and Tech.* **1998**, *18*, 193-205.
- Moridani, M.Y.; Pourahmad, J.; Bui, H.; Siraki, A.; O'Brien, P.J. Dietary flavonoid iron complexes as cytoprotective superoxide radical scavengers. *Free Rad. Biol. Med.* **2003**, *34*, 243-253.
- Lazarus, S.A.; Adamson, G.E.; Hammerstone, J.F.; Schmitz, H.H. High-performance liquid chromatography/mass spectrometry analysis of proanthocyanidins in foods and beverages. *J. Agric. Food Chem.* **1999**, *47*, 3693-3701.
- Kelm, M.A.; Hammerstone, J.F.; Schmitz, H.H. Identification and quantification of flavonols and proanthocyanidins in foods: How good are the datas? *Clin. Devel. Immun.* **2005**, *12*, 35-41.
- Khanal, R.C.; Howard, L.R.; Prior, R.L. Procyanidin content of grape seed and pomace, and total anthocyanin content of grape pomace as affected by extrusion processing. *J. Food Sci.* **2009**, *74*, H174-H182.
- Gu, L.; Kelm, M.A.; Hammerstone, J.F. Fractionation of polymeric procyanidins from lowbush blueberry and quantification of procyanidins in selected foods with an optimized normal-phase HPLC-MS fluorescent detection method. *J. Agric. Food Chem.* **2002**, *50*, 4852-4860.
- Kerchesy, J.J.; Hemingway, R.W. Condensed tannins: (4 β -8; 2 β -O-7)-linked procyanidins in *Arachis hypogea* L. *J. Agric. Food Chem.* **1986**, *34*, 966-970.
- Sadilova, E.; Carle, R.; Stintzing, F.C. Thermal degradation of anthocyanins and its impact on color and *in vitro* antioxidant capacity. *Mol. Nutr. Food Res.* **2007**, *51*, 1461-1471.

- Bradshaw, M.C.; Barril, C.; Clark, A.C.; Prenzler, P.D.; Scollary, G.R. Ascorbic acid: A review of its chemistry and reactivity in relation to a wine environment. *Crit. Rev. Food Sci. Nutr.* **2011**, *51*:479-498.
- Danilewicz, J.C. Review of reaction mechanisms of oxygen and proposed intermediate reduction products in wine: central role of iron and copper. *Am. J. Enol. Vitic.* **2003**, *54*, 73-85.
- Lopes, P.; Richard, T.; Saucier, C.; Teissedre, P.; Monti, J.; Glories, Y. Anthocyanone A: A quinone derivative resulting from malvidin 3-O-glucoside degradation. *J. Agric. Food Chem.* **2007**, *55*, 2698-2704.
- Nielsen, S. *Food analysis laboratory manual*. Second edition. New York: Springer. **2010**.
- Martell, A.E. Ascorbic acid: chemistry, metabolism, and uses. Ch. 7: Chelates of ascorbic acid. **1982**, 153-178.
- Dekker, A.O.; Dickinson, R.G. Oxidation of ascorbic acid by oxygen with cupric ion as catalyst. *J. Am. Chem. Soc.* **1940**, *62*, 2165-2171.
- Hsu, H.; Tsai, Y.; Fu, C.; Wu, J.S. Degradation of ascorbic acid in ethanolic solutions. *J. Agric. Food Chem.* **2012**, *60*, 10696-10701.
- Kimoto, E.; Tanaka, H.; Ohmoto, T.; Choami, M. Analysis of the transformation products of dehydro-L-ascorbic acid by ion-pairing high performance liquid chromatography. *Anal. Biochem.* **1993**, *214*, 38-44.
- Mazza, G.; Miniati, E. Anthocyanins in fruits, vegetables, and grains. Boca Raton, Fl.:CRC Press. 1993.
- Rentsch, M.; Schwartz, M.; Winterhalter, P. Pyranoanthocyanins- an overview on structures, occurrence, and pathways of formation. *Trends in Food Sci. Tech.* **2007**, *18*, 526-534.
- He, J.; Carvalho, A.R.F.; Mateus, N.; de Freitas, V. Spectral features and stability of oligomeric pyranoanthocyanins-flavanol pigments isolated from red wines. *J. Agric. Food Chem.* **2010**, *58*, 9249-9258.
- Mateus, N.; Silva, A.M.S.; Rivas-Gonzalo, J.C.; Santos-Buelga, C.; de Freitas, V. A new class of blue anthocyanin-derived pigments isolated from red wines. *J. Agric. Food Chem.* **2003**, *51*, 1919-1923.
- He, J.; Santos-Buelga, C.; Mateus, N.; de Freitas, V. Isolation and quantification of oligomeric pyranoanthocyanins-flavanol pigments from red wines by combination of column chromatographic techniques. *J. Chromatography.* **2006**, *1134*, 215-225.

- Oliveira, J.; Azevedo, J.; Silva, A.M.S.; Teixeira, N.; Cruz, L.; Mateus, N.; de Freitas, V. Pyranoanthocyanin dimers: a new family of turquoise blue anthocyanin-derived pigments found in port wine. *J. Agric. Food Chem.* **2010**, *58*, 5154-5159.
- Rentzsch, M.; Quast, P.; Hillebrand, S.; Mehnert, J.; Winterhalter, P. Isolation and identification of 5-carboxy-pyranoanthocyanins in beverages from cherry (*Prunus cerasus* L.). *Innovative Food Science & Emerging Technologies.* **2007**, *8*, 333-338.
- Rein, M.; Ollilainen, V.; Vahermo, M.; Yli-Kauhaluoma, J.; Heinonen, M. Identification of novel pyranoanthocyanins in berry juices. *Eur. Food Res. Technol.* **2005**, *220*, 239-244.
- He, J.; Silva, A.M.S.; Mateus, N.; de Freitas, V. Oxidative formation and structural characterisation of new α -pyranone (lactone) compounds of non-oxonium nature originated from fruit anthocyanins. *Food Chem.* **2011**, *127*, 984-992.
- Tsuda, T.; Ohshima, K.; Kawakishi, S.; Osawa, T. Oxidation products of cyanidin 3-*O*- β -D-glucoside with a free radical initiator. *Lipids.* **1996**, *31*, 1259-1263.
- Oliveira, J.; da Silva, M.A.; Parola, A.J.; Mateus, N.; Bras, N.F.; Ramos, M.J.; de Freitas, V. Structural characterization of a A-type linked trimeric anthocyanin derived pigment occurring in a young Port wine. *Food Chem.* **2013**, *141*, 1987-1996.
- Poei-Langston, M.S.; Wrolstad, R.E. Color Degradation in an ascorbic acid-anthocyanin-flavanol model system. *J. Food Sci.* **1981**, *46*, 1218-1222.
- Swift, R.; Davidson, D. Alcohol hangover: Mechanisms and mediators. *Alcohol Health Res. World.* **1998**, *22*, 54-60.
- Liu, S.; Pilone, G.J. An overview of formation and roles of acetaldehyde in winemaking with emphasis on microbiological implications. *Int'l. Food Sci. Technol.* **2000**, *35*, 49-61.
- Ribereau-Gayon, .; Peynaud, E.; Lafon, M. Investigations on the origin of secondary products of alcoholic fermentation. *Am. Enol. Vitic.* **1956**, *7*, 53-61.
- Ough, C.S.; Amerine, M.A. Studis on aldehyde production under pressure, oxygen, and agitation. *Am. Enol. Vitic.* **1958**, *9*, 111-122.
- Ough, C.S.; Amerine, M.A. *Methods for analysis of musts and wines.* **1988**, 141-148. New York: John Wiley & Sons.
- Timberlake, C.F.; Bridle, P. Interactions between anthocyanins, phenolic compounds, and acetaldehyde and their significance in red wines. *Am. J. Enol. Vitic.* **1976**, *27*, 97-105.
- Pissarra, J.; Mateus, N.; Rivas-Gonzalo, J.; Santos Buelga, C.; De Freitas, V. Reaction between malvidin-3-glucoside and (+)-catechin in model solution containing different aldehydes. *J. Food Sci.* **2003**, *68*, 476-481.

- Francia-Aricha, E.M.; Guerra, M.T.; Rivas-Gonzalo, J.C.; Santos-Buelga, C. New anthocyanin pigments formed after condensation with flavanols. *J. Agric. Food Chem.* **1997**, *45*, 2262-2266.
- Es-Safi, N.; Fulcrand, H.; Cheynier, V.; Moutounet, M. Studies on the acetaldehyde-induced condensation of (-)-epicatechin and malvidin-3-*O*-glucoside in a model solution. *J. Agric. Food Chem.* **1999**, *47*, 2096-2102.
- Saucier, C.; Bourgeois, G.; Vitry, C.; Roux, D.; Glories, Y. Characterization of (+)-catechin-acetaldehyde polymers: a model for colloidal state of wine polyphenols. *J. Agric. Food Chem.* **1997**, *45*, 1045-1049.
- Garcia-Viguera, C.; Bridle, P.; Bakker, J. The effect of pH on the formation of coloured compounds in model solutions containing anthocyanins, catechin and acetaldehyde. *Vitis*. **1994**, *33*, 37-40.
- Dallas, C.; Ricardo-da-Silva, J.M.; Laureano, O. Products formed in model wine solutions involving anthocyanins, procyanidin B2, and acetaldehyde. *J. Agric. Food Chem.* **1996**, *44*, 2402-2407.
- Morata, A.; Calderon, F.; Gonzalez, M.C.; Gomez-Cordoves, M.C.; Suarez, J.A. Formation of the highly stable pyranoanthocyanins (vitisins A and B) in red wines by the addition of pyruvic acid and acetaldehyde. *Food Chem.* **2007**, *100*, 1144-1152.
- Marquez, A.; Serratos, M.P.; Merida, J. Pyranoanthocyanin derived pigments in wine: structure and formation during winemaking. *J. Chem.* **2013**, 1-15.

Tables and figures

Table 1: Anthocyanin frequency and fraction purity, content (---- = not present, + = minimally present, ++ = some present, +++ = highly present, ++++ = vast majority). (Simmons 2012).

Commodity	Anthocyanin Fraction Purity (%)	Mean Anthocyanin Content of Commodity (mg/100g)							Total	Acylated Anthocyanins (% of total)	Approximate Market Price (US \$/lb)
		Cyanidin	Delphinidin	Malvinidin	Pelargonidin	Peonidin	Petunidin				
Blueberry	99.9	++	+++	+++	----	++	++	163.5	0.2 - 8.6	\$0.30-0.98/oz	
Elderberry	99.8	++++	----	----	+	----	----	759.6	0	\$675/kg extract	
Purple corn	99.8	++++	----	----	++	++	-	381.5	35 - 54	?	
Black current	99.7	++	+++	----	+	+	+	272.4	1	\$8.00	
Red cabbage	99.4	++++	+	----	+	----	----	72.98	85	\$0.26-0.40	
Chokeberry	99.4	++++	----	----	+	----	----	437.2	0	\$495/kg extract	
Purple carrot	99.2	++++	----	----	----	----	----	129	76	?	
Bilberry	99.0	+++	+++	++	----	++	++	430.9	0	\$800/kg extract	
Blackberry	97.7	++++	----	----	+	----	----	90.46	100	\$3.56-5.78	
Black raspberry	97.4	++++	----	----	----	+	----	324	0	\$4.17/pt	
Strawberry	94.2	+	+	----	++++	----	+	33.63	9	\$1.50-2.75	
Grape	93.8	++	++	++++	+	++	++	44.86	50	\$0.84-1.42	
Eggplant	93.5	----	++++	----	----	----	----	76.44	\$0.67-1.10	\$0.67-1.10	
Radish	85.6	----	----	----	++++	----	----	25.66	100	\$0.46-0.86	
Blue potato	74.2	----	+	++	++	++++	++	?	99	\$0.64-1.64	

	R ₃ '	R ₅ '
Pelargonidin	H	H
Cyanidin	OH	H
Delphinidin	OH	OH
Peonidin	OCH ₃	H
Petunidin	OCH ₃	OH
Malvidin	OCH ₃	OCH ₃

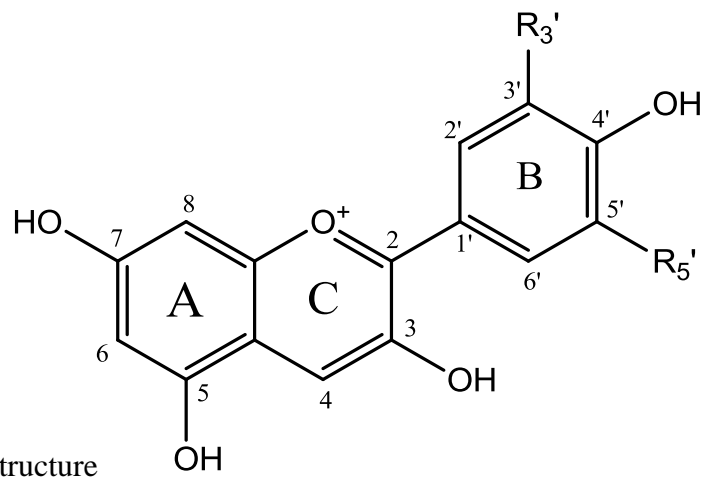


Figure 1: General Anthocyanin Structure

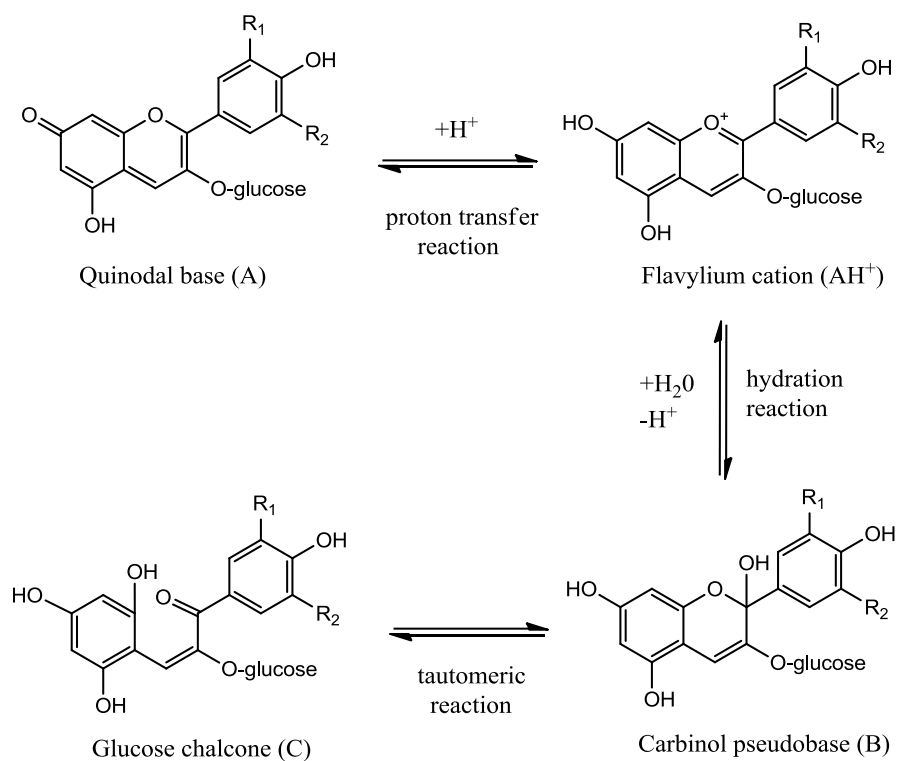


Figure 2: Anthocyanin structure changes with differing pH (adapted from Brouillard, Delaporte 1977)

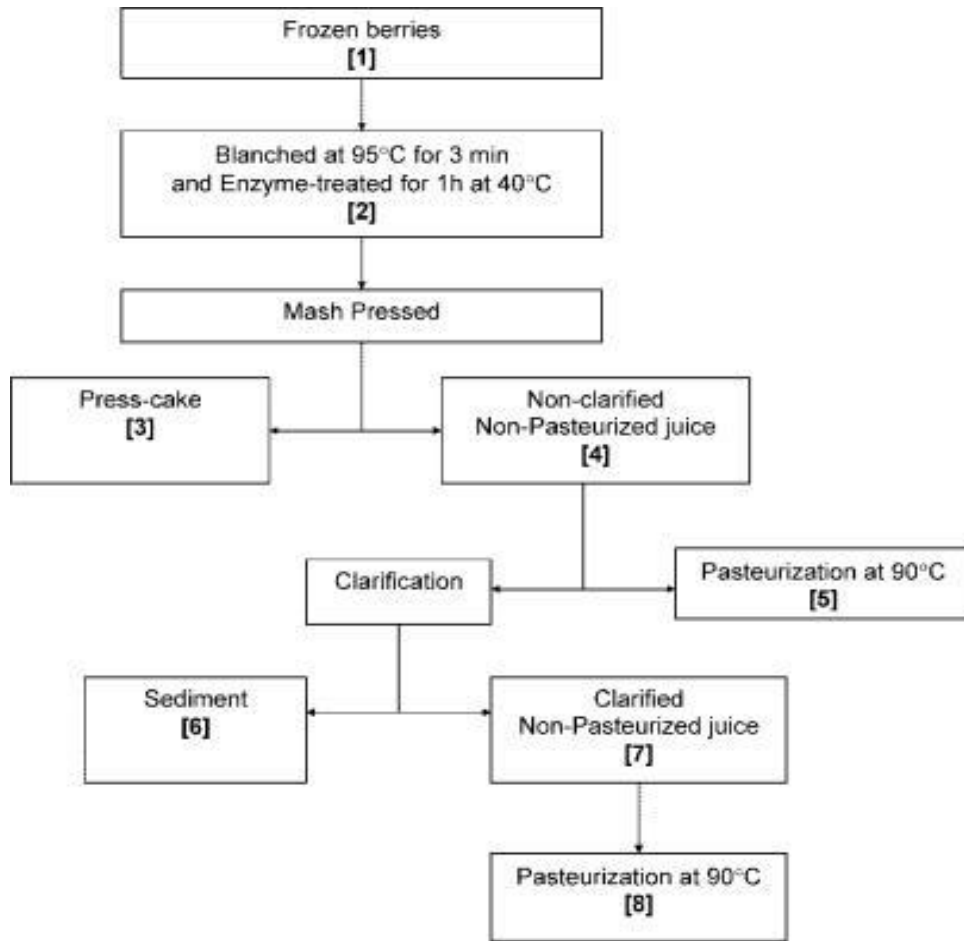


Figure 3: Model juice processing (Hager et al. 2008)

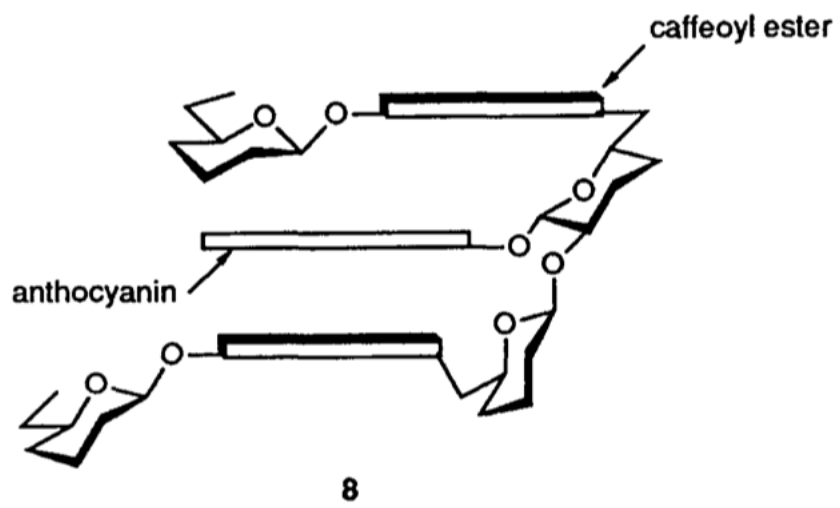


Figure 4: Sandwich effect stabilizing anthocyanin (Mistry et al. 1991)

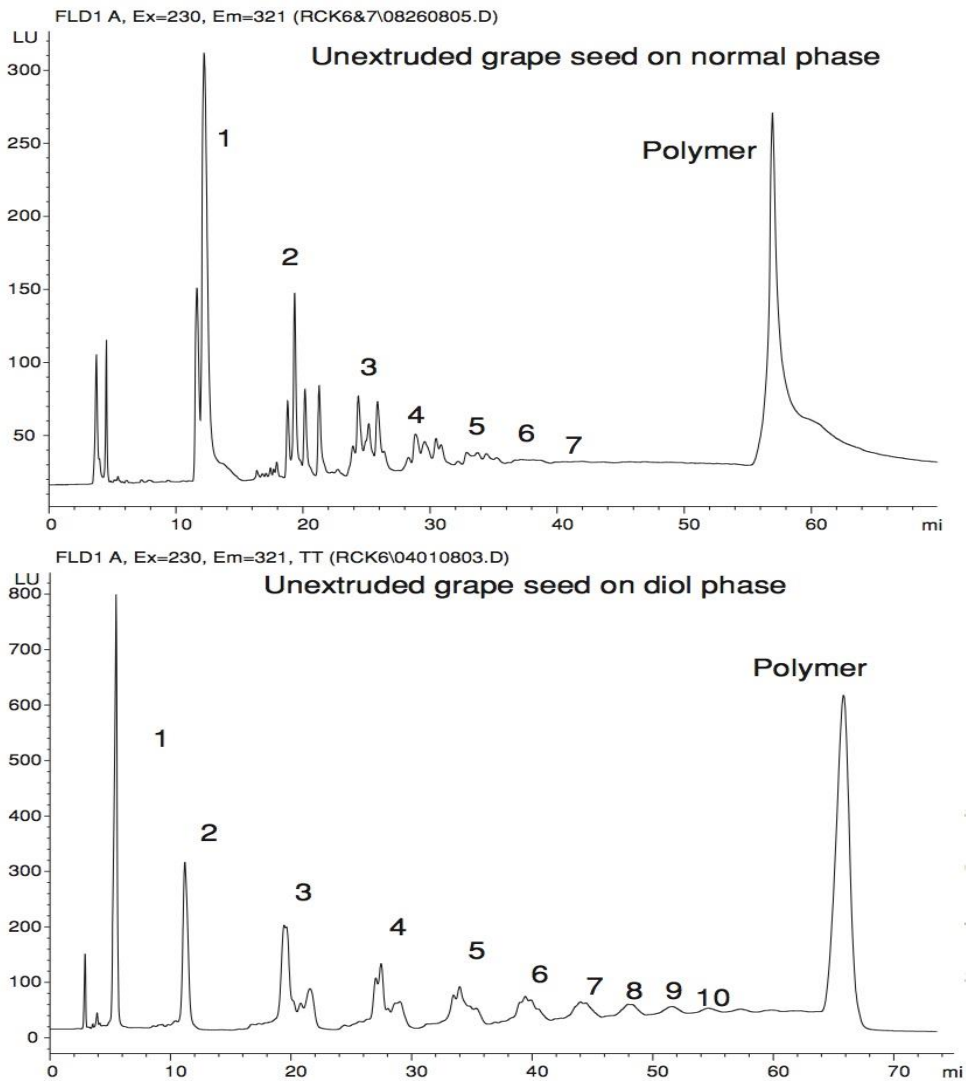


Figure 6: Chromatogram of unextruded grape seed on normal and diol phases (Khanal et al. 2009)

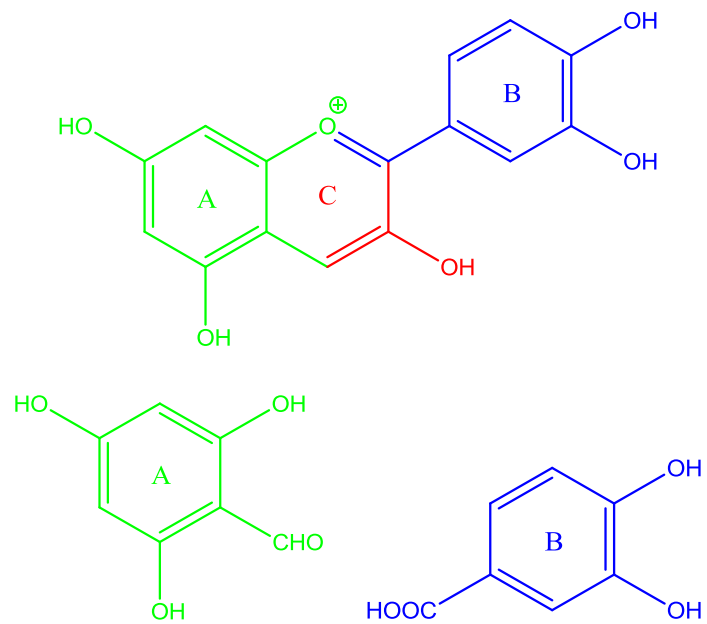


Figure 7: Cyanidin breakdown into phloroglucinaldehyde and protocatechuic acid (Sadilova et al. 2007)

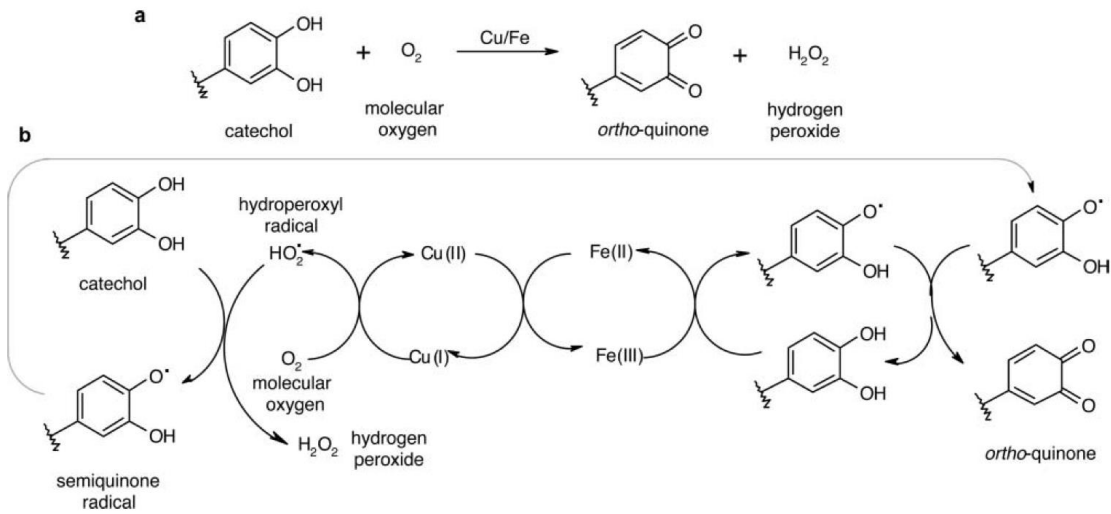


Figure 8: “The a) overall reaction and the b) proposed mechanism for the oxidation of phenolic compounds in wine.” (Bradshaw et al. 2011)

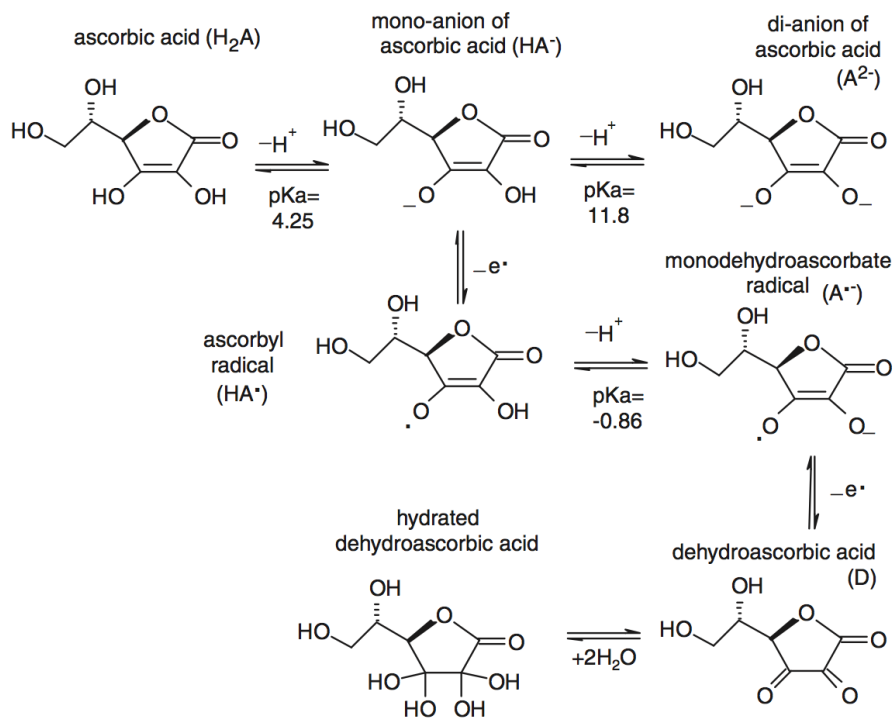


Figure 9: Equilibria of ascorbic acid and some of its breakdown products (Bradshaw 2011)

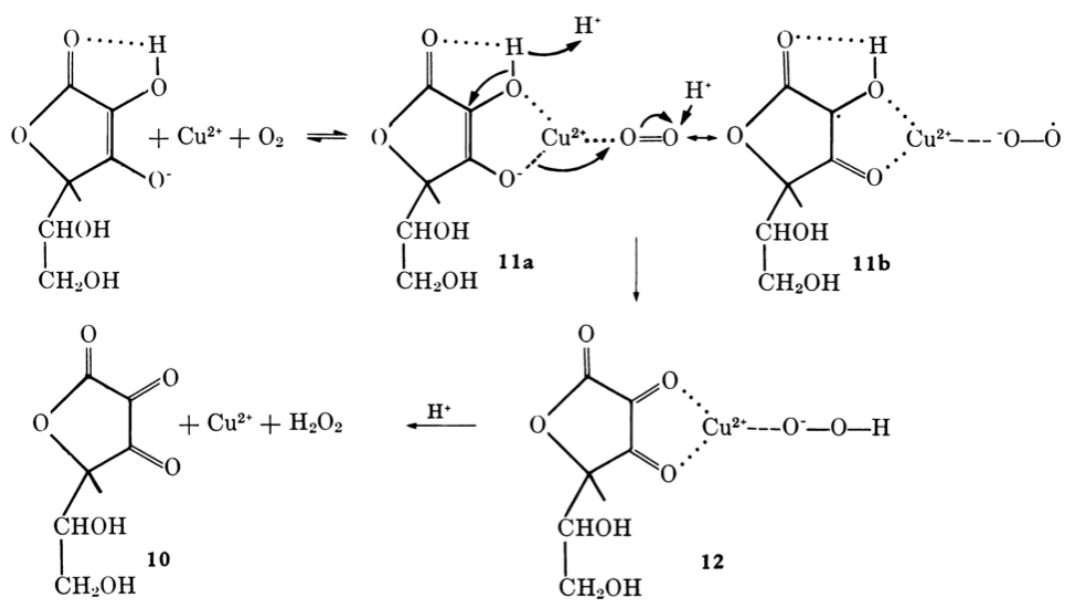


Figure 10: Oxidation of ascorbic acid from copper with the formation of hydrogen peroxide (Martell 1982)

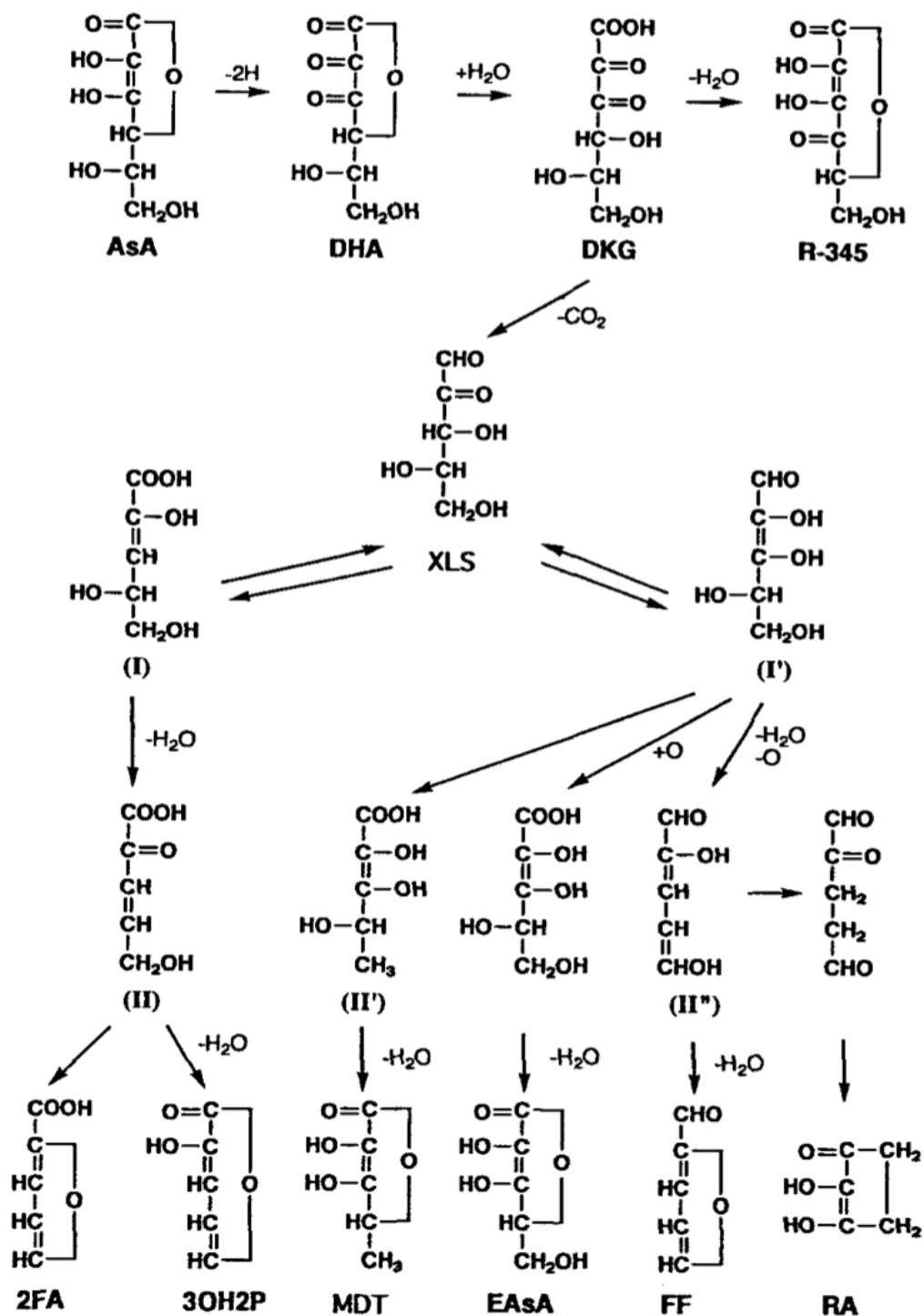


Figure 11: Degradation of ascorbic acid (AsA). DHA=dehydroascorbic acid, DKG= diketogulonic acid, R-345= reducant with λ_{\max} of 345 nm, 2FA=2-furoic acid, 3OH2P=3-hydroxy-2pyrone, MDT= 5-methyl-3,4-dihydroxytetrone, EAsA= erythro-ascorbic acid, FF= furfural, RA= reductic acid (Kimoto et al. 1993)

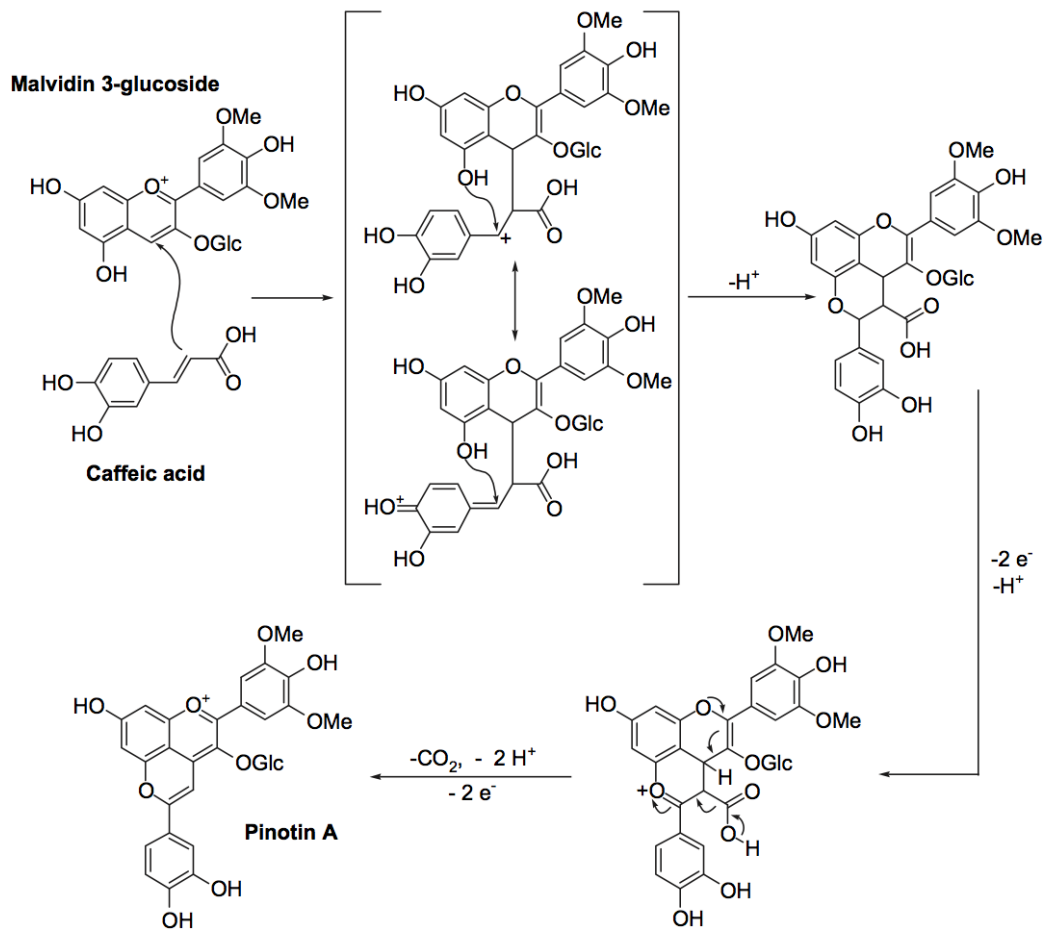


Figure 12: Mechanism of the pyranoanthocyanins: pinotin A (Rentzsch et al. 2007)

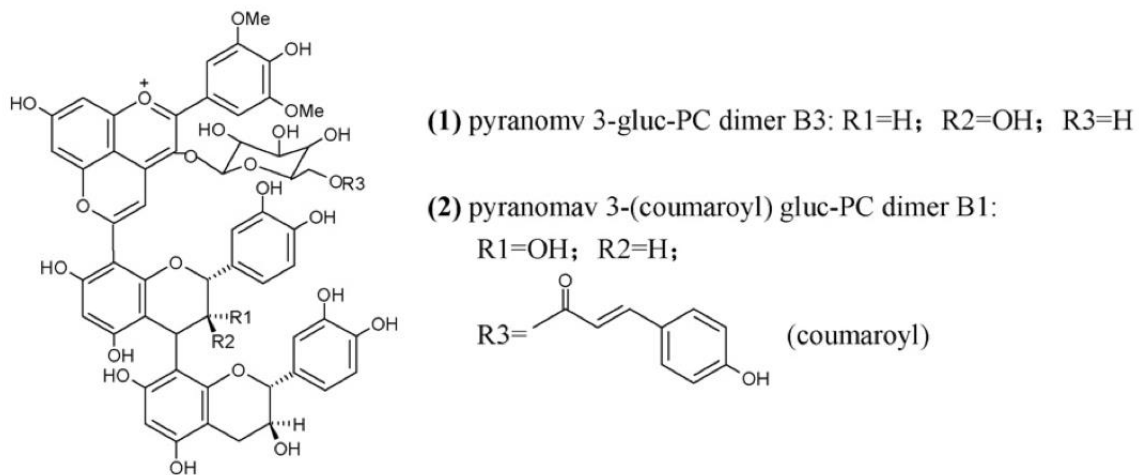


Figure 13: Pyranomalvidin-3-glucoside oligomer (He et al. 2006).

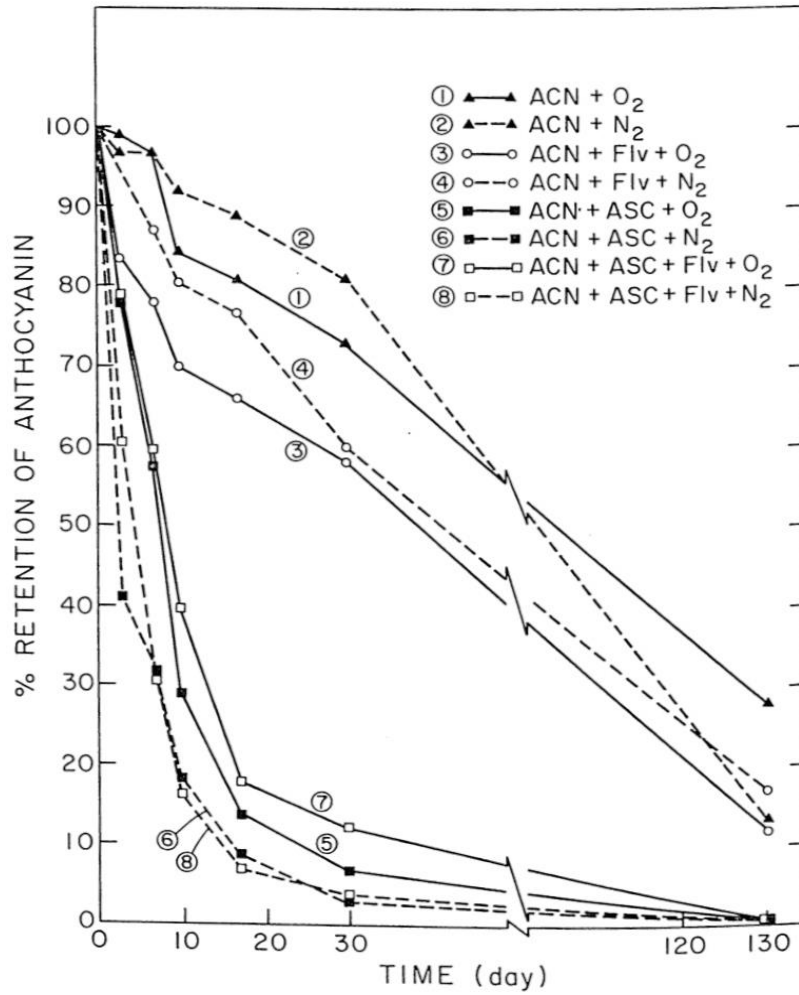


Figure 14: Percent retention of anthocyanin pigment over storage. ACN= anthocyanin; ASC= ascorbic acid; FLV = catechin. (Poei-Langston & Wrolstad 1981)

CHAPTER 3. Assessment of methods to separate polymeric pigments

Abstract

Anthocyanins (ACYs) provide color to many fruit and vegetables, but they decrease in concentration over storage of fruit juices and wines. The juices and wines retain vibrant color even though the ACY concentration is nearly zero over long-term storage and the fate of these molecules is not fully known. The source of long-term color in juices and wines could potentially be due to polymeric pigments (PPs). ACYs can directly bind to a chain of flavanols, called procyanidins (PACs), to form PPs. While it is possible to separate PACs by degree of polymerization (DP) using HPLC techniques, the addition of an ACY to the PAC chain changes the structure such that HPLC separation is no longer possible. Mass spectrometry and UV/visible detectors can differentiate colored PPs from colorless PACs due to structural differences. Creating a method to separate these compounds would be well received by the juice and wine industry and others because it would allow purification and quantification of PPs that could potentially determine the fate of ACYs over storage. Once purified, PPs could also serve as a natural alternative to artificial colorants. The objectives were to develop methods to separate procyanidins from PPs and to separate PPs by DP. Multiple types of chromatographic stationary phases and techniques were evaluated, yet separation was not accomplished. Molecular weight cutoff filters displayed a color gradient for three-year-old chokeberry juice, which indicates the source of long-term color is potentially from PPs as large as 100 kDa. A fresh chokeberry juice did not display the same color gradient due to the increased concentrations of monomeric ACYs compared to the aged juice.

Introduction

The polymerization of PACs with ACYs produces PPs, also called anthocyanin-tannin polymers in either the A-T or T-A⁺ formation as illustrated in Figure 1. A-T type polymers feature glycosylated ACYs in the flavene form since they are bonded to the next monomer on carbon 4 and have yet to be oxidized to flavylum ion; therefore it is a colorless molecule (Hayasaka and Kennedy 2003). The mass of the A-T type will be two Daltons greater than the T-A⁺ type because of this flavene and mass spectrometry can identify this difference. Other researchers refer to these structures as A⁺-F (flavanol), which is the oxidized form of the A-T flavene and the charged ACY possesses color. In some cases, the A⁺-F can undergo dehydration to form xanthylum ions (Figure 2), which develop a fused ring between monomeric units, often have an orange hue, and can be distinguished from the other polymers via mass spectrometry (Duenas et al. 2006). The ACY can attach to the PAC by one of two main mechanisms: direct condensation or an ethyl bridge (Timberlake and Bridle 1976, Jurd 1969, Somers 1971). The formation and breakage of bonds is pH dependent with a preference for low pH between 2.0 and 3.2, but nonexistent above pH 3.8 (Vidal et al. 2002, Salas et al. 2003). Polymer complexity can increase when other compounds replace catechin as the monomeric links in the chain. The linear appearance of the chain can potentially have branches emerging from carbon 6 on the A ring, which greatly complicates the structural analysis of these compounds. The most unique chemical difference between PPs and PACs is the charged flavylum ion in the PP, which also conveys the conjugation that produces color. It is very difficult to separate these two classes of compounds because of structural similarity. However, one clue to separating these compounds is the charge on the PPs, which could be a target for cation exchange chromatography. An ion exchange capsule named ‘Sartobind S’ has been used to fractionate bilberry polyphenols into

ACYs, copigments, and polymers (Juadjur and Winterhalter 2012). Sartobind S uses sulfonic acid groups to retain the charged flavylum ion, which is eluted with 1 M NaCl in methanol; followed by salt removal using XAD-7 (Juadjur and Winterhalter 2012). The copigments that were separated using Sartobind S were phenolic acids and flavonoids. Figure 3 depicts a polymer fraction that was poorly resolved and eluted as the ‘polymer hump,’ which has been described by many researchers.

Using a mixed-mode ion-exchange RP column, one group of researchers separated red wine ACYs in a well ordered manner: anthocyanidin monoglucosides, then acetyl-derivatives, coumaroyl-derivatives, and finally a polymeric peak (Vergara et al. 2010). They also found a 97% correlation between the age of the wine and the area under the polymeric peak, indicating that PPs increase with time. Likewise, the percentage of PPs based on the color-bleaching assay increases with the age of red wines during storage (Somers 1971, Peng et al. 2002). Somers found a nearly linear increase in polymeric pigment content from 2-year-old wines to 10 years old. Wines and berry juices contain many similar ACYs and PACs, but differ in alcohol content, organic acids, sugar content, and other by products of fermentation.

The primary means of measuring PPs is not quantitative, but a relative amount of PP compared to monomeric ACYs via the percent polymeric color assay (Giusti and Wrolstad 2001). The principle of this assay is the loss of conjugation (and color) via sulfate binding to carbon 4 of the ACY. At one point, there was confusion on which carbon was attacked by the sulfate group, but ^1H , ^{13}C , and ^{33}S NMR confirmed that carbon 2 was not attacked due to the steric hindrance of the B ring (Berke et al. 1998). With this evidence, the polymeric color assay lost some credibility because the F-A⁺ polymers would be bleached at the open carbon 4, thus causing an underestimation of PPs. There is a great need for an HPLC method that could

separate PPs by their degree of polymerization. The development of this method is another avenue of this research and would be well received by other scientists working in the field. The HPLC method will allow for the collection of each PP with semi-preparative HPLC, permitting quantification that can describe the changes through processing, aging, and a multitude of other functions. This is a difficult method to produce and could require novel solid phase materials and sensitive detectors. PAC's are currently detected most often by fluorescence, so a combination of fluorescence and UV detection at 510 nm is a probable solution. The PP and proanthocyanidins are very similar in structure and ideally should be separated before HPLC analysis. Countercurrent chromatography (CCC) has been used to pre-fractionate a synthesized F-A⁺ polymer prior to HPLC analysis using *t*-butyl methyl ether, *n*-butanol, acetonitrile, and water in a 2:2:1:5 ratio acidified with 0.1% TFA (Salas et al. 2005a). This 450-minute method produced four fractions with the final fraction containing catechin-catechin-malvidin-glucoside trimer eluting before the dimer, followed by malvidin-3-glucoside (Salas et al. 2005b). Using a Fracto-gel column to fraction pigments from a two-year-old Cabernet Sauvignon, researchers used acidified ethanol and water to elute monomers, then 60:40 acetone/water to elute oligomeric and polymeric compounds. The group further separated the acetone fraction with an iso-amyl alcohol extraction to remove the hump in the HPLC chromatogram, shown in Figure 3 (Remy et al. 2000).

Most of the experimental data about PPs is from mass spectrometry, especially MALDI-TOF-MS due to the fact that “only one molecular ion is formed from each parent molecule, high sensitivity across a broad range of masses [that] allows detection of oligomeric series of compounds, ability to detect compounds of high molecular weight, and interpretation of isotope patterns allows the detection of oligomers with small differences in mass” (Reed et al. 2005).

The common linear PACs bound at C-4 to C-8 are called B-type PACs, while A-type types are bound at those positions and also C-2 to C-7. Mass spectroscopy can discriminate between A- and B-type PPs and PACs based on the two Dalton differences from the loss of two hydrogen atoms with the additional ether bond in A-types. As the mass of each peak increases, the signal decreases, which can be attributed to detector saturation since the smaller molecular masses travel faster, reaching the detector before the heavier masses. The second reason for this phenomenon is the velocity of the ion hitting the detector; the same energy voltage is applied to the entire sample, but the heavier analytes must have a slower velocity based on the kinetic energy equation: $KE=(1/2)mv^2$. Also, smaller molecule weight analytes are more likely to ionize so it is possible that some percentage of the larger polymers do not ionize and therefore cannot be detected. A MALDI-TOF spectrum is shown in Figure 4 displaying the decreasing signal strength with increasing mass. MALDI-TOF typically does not quantify peaks, but some scientists indicate the relative amounts of each mass can be compared. The ions detected by MALDI-TOF are often sodium or potassium adducts, so the resulting m/z must account for those metals added onto the predicted mass of the analyte.

Another possible means for separation lies in the idea of a series of different solid phase extraction materials. Oligomers of pyranoanthocyanins-flavanols from Port wine were separated using Toyopearl gel HW-40S (size exclusion) into two fractions: ACY and pyruvic acid adducts, then oligomeric and polymeric compounds (He et al. 2006). The oligomeric fraction was then passed through a polyamide resin column yielding three fractions via increasing amounts of acidified methanol: non-anthocyanin flavonoids, oligomeric pyranoanthocyanins, and finally other flavonoids (He et al. 2006). The oligomers were isolated and quantified in the range of 0.4-20 mg/L. More research must be accomplished in order to separate, and then quantify PPs.

To date, there is neither a method to separate polymeric pigments from procyanidins, nor a method to separate PPs by degree of polymerization. One method exists to separate ACYs from PPs using a divinylbenzene column with acidified water and acetonitrile as the mobile phase (Peng et al. 2002). The divinylbenzene method will be used to collect the late eluting polymeric pigment peak that also contains procyanidins. This sample will be verified by LC-ESI-MS and MALDI-TOF-MS. Once confirmed, the PP + PAC sample will be attempted to be separated by a battery of tests, including cation exchange mechanisms, diol absorbent, gel electrophoresis and other techniques. A combination of UV/Vis and fluorescence detection is likely the answer for measuring both PACs and PPs.

Materials and methods

Materials

Cyanidin-3-O-glucoside was obtained from Chromadex (Irvine, CA, USA). Chokeberry juice was made by a master's student in our lab and samples were stored frozen before and after juice pasteurization, as well as from stored frozen at one through six months and again at three years of aging at ambient temperature in darkness. HPLC-grade solvents were purchased from EMD Millipore (Billerica, MA, USA) and formic acid from Fischer-Scientific (Fair Lawn, NJ, USA). Other reagents were purchased from Sigma-Aldrich (St. Louis, MO, USA). Strata-X-C solid phase extraction columns were purchased from Phenomenex (Torrance, CA, USA), while sulfoxyethyl cellulose, Sephadex LH-20, Amberlite XAD-16N, Supelco Dowex 50Wx4, CM Sephadex C-25, and alumina were purchased from Sigma-Aldrich. Oasis HLB column were purchased from Waters (Milford, MA, USA). Gel electrophoresis materials were purchased from VWR (Radnor, PA, USA).

HPLC-PDA-FLD analysis

HPLC analysis followed several methods including Peng et al. 2002, Cho et al. 2004, Kelm et al. 2006, and Yanagida et al. 2002. Aged chokeberry juice samples were passed through 0.45 μm nylon syringe filters prior to HPLC injection. A Waters HPLC system (Waters Corp., Milford, MA) comprised of dual 515 pumps, a 717plus autosampler, a 996 photodiode array detector, and a 474 scanning fluorescence detector was used for chromatographic analyses. A Polymer Laboratories PLRP-S divinylbenzene column (250 x 4.6 mm, 5 μm), Waters Symmetry C₁₈ column (250 x 4.6 mm, 5 μm), Develosil Diol column (250 x 4.6 mm, 5 μm), Waters Spherisorb S5 SCX column (100 x 4.6 mm, 5 μm), and Tosoh TSKgel α -3000 column (300 x 7.8 mm, 7 μm) were used for separation. Solvents included acidified water, urea in water, methanol, acetone, acetonitrile, and subsequent mixtures in order to improve separation. Gradients were varied based on attempted separation methodologies. Flow rates were set by each column's pressure limits and adjusted to improve separation. UV-visible spectra were monitored from 250-600 nm and peak areas were integrated at 510 nm. Fluorescence was measured with excitation set to 276 nm and emission at 316 nm.

HPLC-electrospray ionization tandem mass spectrometry (LC-ESI-MS) analysis of polymeric pigments

LC-ESI-MS analysis was conducted using an HP 1000 series HPLC and a Bruker Esquire 2000 quadrupole ion trap mass spectrometer. Samples were separated using columns and solvents as described above. The mass spectrometry analysis was performed in positive ion mode under the following conditions: capillary voltage at 4 kV with polarity [-] for positive ion

mode analysis, nebulizer gas pressure 32 psi, dry gas flow 12 L/min, and skim voltage at 53.7 V. Ions were isolated and fragmented in quadrupole ion trap with excitation amplitude of 1.2 volts.

Phenomenex Strata-X-C solid phase extraction

Triplicate samples of chokeberry juice of various ages were loaded on separate Phenomenex Strata-X-C cartridge columns (5 mL, 600 mg). The cartridges were conditioned with 2 mL of methanol, followed by 2 mL of 1% formic acid in water without allowing the cartridge to dry. Juice samples (1 mL) were loaded and allowed to absorb for 10 minutes. First, the columns were washed with 2 mL of acidified water, then 2 mL of acidified methanol. The pigment was eluted with 6 mL of 5% ammonium hydroxide in methanol. Some pigment remained and was eluted with 4 mL of 1% sodium hydroxide, which was quickly acidified with formic acid. The eluent from the Strata-X-C had an orange-red color. Fractions were dried using a SpeedVac concentrator and suspended in methanol for further analysis.

Sulfoxyethyl cellulose solid phase extraction

Methodology followed Spagna et al. 1992 with some alterations. Triplicate samples of chokeberry juice of various ages and the eluent from LH-20 purification were loaded on separate columns of 5 g sulfoxyethyl cellulose fast flow resin, which were hydrated overnight in 0.02 N hydrochloric acid. Samples (1 mL) were loaded and allowed to absorb for 10 minutes. The first elution appeared with 60 mL of 30% methanol and was pale orange-brown in color. Next, 60 mL of 70% acetone eluted a very faint pink fraction, followed by 40 mL of 2 M ammonium chloride in 50% methanol eluting a pale pink fraction. After that, 60 mL of isopropanol eluted a fraction with a hint of pink color. Finally, 40 mL of 2 N sodium hydroxide caused the bound analytes to

turn from reddish to green-brown with some of the brownish pigment detaching from the column and eluting. This fraction was quickly acidified with hydrochloric acid, which turned the sample a golden hue. All fractions were dried using a SpeedVac concentrator and suspended in methanol for further analysis.

Confocal microscopy

Sulfoxyethyl cellulose fibers and three-year-old chokeberry juice were analyzed using a Leica TCS SP5 confocal microscope. Images were taken using an HyD 4 detector with 15% power on the 561 nm laser and 13% power on the 633 nm laser. Chokeberry juice was applied to a microscope slide and dried in a desiccator. A cover slip was placed over the dried juice and sealed with clear nail polish. Images were false colored to mimic the true sample colors: red for sulfoxyethyl cellulose fibers and purple for dried chokeberry juice.

Sephadex LH-20 solid phase extraction

Methodology followed Kantz et al. 1990 with some alterations. Triplicate samples of chokeberry juice stored for one through six months and also three years were frozen at each time point. Samples were loaded on separate columns of 4 g Sephadex LH-20, which were hydrated overnight in DI water. Samples were loaded onto columns atop the vacuum manifold, allowed to absorb onto the stationary phase, then washed with 30% methanol to remove sugars and small phenolic molecules, which included some monomeric anthocyanins. Next, 70% acetone was used to elute polymeric phenols that were then dried using a SpeedVac concentrator and suspended in 70% acetone for further analysis. LH-20 columns can be reconditioned for

immediate reuse by washing with several bed volumes of 30% methanol, then DI water. No changes in chromatographic properties were observed after 8-10 separation cycles.

Oasis HLB solid phase extraction

Methodology followed Jeffrey et al. 2008 with some alterations. Triplicate samples of chokeberry juice of various ages were loaded on separate Oasis HLB cartridge columns (6 mL, 500 mg). The cartridge was conditioned with 2 mL of methanol, followed by 2 mL of DI water without allowing the cartridge to dry. Each juice sample (1 mL) was loaded onto the column and allowed to completely absorb until the column was dry. The first fraction (F1) was eluted with 40 mL of 95:5 acetonitrile: 0.01 M hydrochloric acid. The second fraction (F2) was eluted with 5 mL of methanol with 0.1% formic acid, while the third fraction (F3) was eluted with 0.3 mL of neat formic acid, then 2.7 mL of 95% methanol. There was color remaining on the column after F3 eluted, so 1 mL of neat formic acid followed by 4 mL of 95% methanol was used to create F4. All fractions were dried using a SpeedVac concentrator and suspended in methanol for further analysis.

Amberlite XAD 16N solid phase extraction

Methodology followed Kammerer et al. 2005 with some alterations. Triplicate samples of chokeberry juice of various ages were loaded on separate columns of 8 g Amberlite XAD 16N, which were hydrated overnight in 90% ethanol. The columns were conditioned with 125 mL of DI water, then 50 mL of 3% formic acid in water. Juice samples (3 mL) were loaded onto the columns and washed with 50 mL of 3% formic acid. Some pigmented eluted in this step, but

most of the color was eluted with 50 mL of 2% formic acid in methanol. All fractions were dried using a SpeedVac concentrator and suspended in methanol for further analysis.

Supelco Dowex 50Wx4 solid phase extraction

This strong cation exchange resin was assessed for its capacity to separate PPs from PACs due to its binding affinity for cations. The resin's structure is divinylbenzene with sulfonic acid moieties attached. Triplicate samples of chokeberry juice of various ages were loaded on separate columns of 4 g Dowex 50Wx4 100-200 mesh, which were hydrated overnight in DI water. Columns were washed with DI water, then loaded with 3 mL of juice. The first fraction was eluted with 30 mL of methanol, which had a pink-peach color. The following eluents did not elute the remaining pigment on the column: 50 mL of 5% formic acid in acetonitrile, 50 mL of 70% acetone, 50 mL of 4 M urea in water (pH 4), 50 mL of 4 M urea in water (pH 11), 20 mL of 2 M sodium hydroxide. The strong basic conditions caused the pigment to turn from red-purple to green-brown. Acidifying the column returned the red hue, but it would not release from the resin. All fractions were dried using a SpeedVac concentrator and suspended in methanol for further analysis.

CM Sephadex C-25 solid phase extraction

This weak cation exchange resin was assessed for its capacity to separate PPs from PACs due to its weak binding affinity for cations. The resin's structure is carboxymethyl cross-linked dextran. Triplicate samples of chokeberry juice of various ages were loaded on separate columns of 4 g CM Sephadex C-25, which were hydrated overnight in DI water. Columns were washed with methanol, then DI water, then loaded with 3 mL of juice. The first fraction was eluted with

30% methanol and had a pale pink color. The second fraction eluted the majority of the remaining pigment using methanol. Organic solvents and salts were applied, but did not elute the slight red pigment stuck on the column. The organic solvents caused the column bed to collapse and shrink to nearly 25% of the initial size. These fractions were not analyzed due to the collapse of the column material and loss of chromatographic integrity.

Alumina solid phase extraction

Methodology followed Lin and Hilton 1980 with some alterations. Columns were prepared with 4 g of alumina (Fisher Scientific) and equilibrated with a 0.1 M sodium citrate buffer. Triplicate samples of chokeberry juice of various ages were loaded onto the columns and allowed to absorb for 10 minutes. The pigment was not well absorbed because most color eluted with 50 mL of citrate buffer. After that, 50 mL of ethanol eluted a slight pink color. All fractions were dried using a SpeedVac concentrator and suspended in methanol for further analysis.

Matrix assisted laser desorption ionization-time of flight (MALDI-TOF) analysis of polymeric pigments

Concentrated samples and a peptide standard were mixed with 1 M dihydroxybenzoic acid (DHB) matrix in methanol in an equal ratio and 1 μ L was spotted onto a stainless steel MALDI plate. Analysis was conducted using a Bruker Reflex III MALDI-TOF-MS (Billerica, MA) equipped with a 337 nm N₂ laser. BrukerDaltonics peptide standard consisting of angiotensin II, angiotensin I, substance P, bombesin, ACTH clip, and somatostatin was used for time of flight calibration. Data was obtained in positive ion reflectron mode with an accelerating voltage of 25 kV and a reflectron voltage of 28 kV. The PPs and PACs were identified as the

molecular ion and potassium and sodium adducts ($[M^+]$, $[M-H+K]^+$ and $[M-H+Na]^+$, respectively). Peaks were statistically evaluated using BrukerClinProTools software.

Molecular weight cutoff filters

Millipore Amicon ultra centrifugal filter devices ranged in cutoff size from 3,000, 10,000, 30,000, 50,000, and 100,000 Daltons. Samples of chokeberry juice of various ages were centrifuged at 10,000 rpm for 30 minutes at 25°C. Filtrates were measured on a spectrophotometer to compare UV/visible absorbance at each molecular cutoff. Filtrates were passed through a 0.45 μ m Nylon filter and injected into the HPLC.

Gel electrophoresis

Bio-rad Mini-Protean Tris-tricine precast acrylamide gels were used to separate chokeberry juice samples of various ages and after molecular weight cutoff filters. A Dual Xtra protein standard was used to compare molecular weights. Samples were mixed (1:1 v/v) with a Tris-tricine loading buffer. Electrophoresis was performed at 150 V for 45 minutes or until the loading buffer reached the end of the gel. These gels were ran in an alkaline environment, so immediately after the electrophoresis reached completion, the gels were soaked in pH 2 DI water to stabilize anthocyanins. Next, gels capable of separation in acidic buffers were created following Saunders and Stites 2012. Briefly, a 15% acrylamide gel was created using 0.9 M acetic acid, 6 M urea, 1 mM sodium toluenesulfinate, 50 μ M diphenyliodonium chloride, and 100 μ M methylene blue. In order for the gel to solidify, it must be placed in direct sunlight for about 10 minutes because ultraviolet light initiates polymerization. The running buffer is made of 0.9 M acetic acid and 0.1 M glycine, while the loading buffer is made of 0.9 M acetic acid, 6 M

urea, and 1% methyl green. Finally, agarose gels were prepared using 1% agarose and required 200 V and three hours to move the analytes approximately half way through the gel. After this time, the anthocyanins did not move any farther, so three hours was used for analysis. A Proteinsimple FluorChem M imaging system (SanJose, CA, USA) was used to scan the gels with a FluoroRGB filter. Pigmented sections of gels were cut and removed, then extracted with 95% acidified methanol overnight. The extracts were quantified and analyzed using MALDI-TOF-MS.

Ultrasonication

A Cole-Parmer Ultrasonic Processor was operated in pulsed mode at 20 °C with 70% amplitude for 15 minutes in trial one, then 80% amplitude for 60 minutes in trial two. Fresh and aged chokeberry juice samples (20 mL each) were compared for the ability to release potentially bound ACYs from soluble complexes. After trials one and two, juice samples were filtered and injected into a Waters HPLC on a Waters Symmetry C₁₈ column as described above. Chromatograms were compared for differences after ultrasonic treatment.

Results and Discussion

Polymeric pigment chromatographic separation

Separation of PPs and PACs is difficult due to their structural similarities, but they can be separated from monomeric ACYs using a divinylbenzene HPLC column (Peng et al. 2002). This publication claimed to separate pigmented polymers from red wine, but failed to show mass spectrometric data for PACs and PPs. Figure 5 shows the chromatogram of an aged chokeberry juice with a large polymer peak near 50 minutes. The mass spectrometric trace does not show a

corresponding peak; however, Fig. 5 (bottom) displays m/z of both PACs and PPs co-eluting in the chromatogram. Both the PP and PAC polymers have units of 288 Da, but PPs have an ACY on the end of the chain and that difference causes the two polymers to have different masses. PP polymers made of cyanidin-3-glucoside have masses of 737, 1025, 1313, 1601, 1889, 2177, 2465, 2753, and 3041 Da for one through 9 catechins attached to the ACY, which yields a dimer to decamer. PAC polymer masses start at 290 for the monomer, then 578, 866, 1154, 1442, 1730, 2018, 2306, 2594, and 2883 Da for masses of a dimer to decamer. A trimeric ACY, made of three malvidin-3-glucosides, has been found in young Port wine (Oliveira et al. 2013), so the potential mass combinations are nearly endless if there are different potential permutations with different ACY structures depending on the source material. The two series of polymers occur evenly distributed and there is no chromatographic retention difference for larger or smaller polymers based on time. Although this is not the goal of this research, it is a start toward separating the molecules. Removing monomeric ACYs and other phenols is progress, so this polymer fraction was collected and pooled to use for further analysis. The pooled fractions were concentrated on a rotary evaporator to remove the organic solvent and then placed in a SpeedVac until dryness. The fraction was pigmented with a vibrant red color after the rotary evaporator, but after removal of all solvent using the SpeedVac it turned a dark brown hue. Upon concentrating, the sample was an oily brown sludge that did not acquire red color after acidification and had poor solubility in organic solvents. The solution to this issue was to remove the organic solvent and some water from the pool of collected fractions using a rotary evaporator and stop concentrating before browning occurs.

The polystyrene divinylbenzene HPLC column's polymer peak can assess whether PACs and PPs have been separated by pre-HPLC solid phase extraction (SPE) techniques. This

chapter will follow the pattern of evaluating different SPE techniques and different samples on HPLC columns for their ability to separate PACs and PPs, while also attempting to separate PPs by degree of polymerization. The first SPE technique to discuss is Phenomenex's Strata-X-C due to its polymeric base comprised of sulfonated styrene divinylbenzene. This is a strong cation exchange resin and should retain the charged PPs while allowing the neutral PACs to elute out of the column. Also, the styrene divinylbenzene polymer base has already been shown to have good retention of both PACs and PPs. Elution of pigment occurred with the addition of 5% ammonium hydroxide, which functions under two mechanisms: the cationic ammonium can replace PPs in the active site of the resin, while the hydroxide can neutralize the charge on the PP. ACYs are unstable at high pH values, so the eluent was quickly acidified with formic acid to stabilize the molecules. Upon addition of ammonium hydroxide, the bound analytes turn a green-brown color, but the red hue returned after acidification. Rinses of acidified water, methanol, or acetonitrile did not elute any pigment. The fractions were concentrated to dryness and dissolved in methanol and then analyzed using LC-ESI-MS. Figure 6 displays a chromatogram and spectrum that greatly resemble that in Fig. 5. This result demonstrates that both PACs and PPs were retained on the Strata-X-C column and eluted together. Perhaps the styrene divinylbenzene was the primary mechanism of retention, so next a similar strong cation exchange was used, composed of a cellulose base.

The aged chokeberry juice was applied to a strong cation exchange columns made of sulfoxyethyl cellulose. This resin does not have the π - π and aromatic binding capabilities of the styrene divinylbenzene resin, but has hydrogen bond interactions to improve retention. Once again a sulfoxyl moiety is attached the resin, which should retain the charged polymers and allow the uncharged PACs to flow through the column. Once the aged chokeberry juice attached to the

resin, 30% methanol eluted a pale brown-orange fraction, followed by 70% acetone eluting a pink-red fraction. Ammonium chloride (2 M) in 50 % methanol was used to displace the ions bound to the sulfoxyethyl cellulose, but only a slightly pink fraction eluted. Diluted sodium hydroxide (0.1 M) was used to alter the positive charge on the PPs, but only changed the bound analytes from red to a dark blue-black color and no detectable color eluted from the column. Isopropanol did not elute any pigment and finally 2 M sodium hydroxide eluted some of the brown color, which was quickly acidified with hydrochloric acid. Upon acidification, eluents usually return to a red hue, but this time the eluent turned golden brown. After all solvents and buffers were applied, there was still pigment on the column that could not be eluted. These fractions were concentrated and analyzed using the divinylbenzene column on the HPLC. The results were disappointing because the chromatograms (not shown) appeared nearly identical to previous analysis, similar to Fig. 5, meaning the sulfoxyethyl cellulose did not separate the PPs and PACs. In order to verify that the polymeric material was able to elute through the cation exchange resin, the aged juice was passed through Sephadex LH-20, which has been used to separate polymeric materials in grapes and wines previously (Kantz et al. 1990). It is composed of hydroxypropylated dextran, which should have comparable retention properties to the sulfoxyethyl cellulose without the cation exchange component. The hydrogen bonding from the polysaccharides and slight hydrophobic interaction due to the ethyl and propyl moieties should work well to elute the polymeric material. The acetone fraction from LH-20 contains both PACs and PPs. This fraction was applied to the sulfoxyethyl cellulose resin and allowed to absorb for 10 minutes. The same series of solvents and buffers were applied to the column, but the result was the same. There were some lightly pigmented fractions, but the majority of the color remained bound to the resin and would not elute.

The column chromatography using strong cation exchange resins did not seem to release the majority of color, but that pigment must be analyzed by some technique. We took the solid pigmented material from the top of the column and analyzed it using a MALDI-TOF mass spectrometer. It is possible to use this technique without extracting the sample in liquid, but it is difficult to obtain meaningful signals. The red colored resin was mixed with the MALDI matrix (dihydroxybenzoic acid) and ground together using a mortar and pestle. A control of unused sulfoxyethyl cellulose resin was used as a comparison. The samples were attached to the MALDI plate using double-sided tape and excess material was shaken off, so it would not come loose inside the instrument. Another application technique was used to limit the potential interferences from the polymers in the double-sided tape. The second application technique was to mix the colored resin with dihydroxybenzoic acid in methanol and place one drop onto the MALDI plate. Another drop of the matrix in methanol was applied over the resin to assist in adherence to the plate. Both application techniques produced signal, but only cellulose units were detected. The control showed the same m/z values and there was no indication that any PPs or PACs were bound to the resin although there was clear red pigment bound to the material. To identify the bound red pigment to the sulfoxyethyl cellulose, a cellulase enzyme was used to degrade the resin and release the bound analytes. The optimum conditions were used and the enzyme was allowed to react with the resin overnight, then the mixture was centrifuged to separate the soluble components. The supernatant was clear and pellet was dried and weighed in order to measure the enzyme degradation to the resin. Unfortunately, the mass was identical to the original mass, so the enzyme was unsuccessful in degrading the resin. This ineffectiveness could be caused by the structural changes to the cellulosic base by modifying it with sulfoxyethyl moieties.

The red pigment could not be removed from sulfoxyethyl cellulose fibers, so microscopy was used to investigate any potential interference that inhibited pigment release. A confocal microscope examined the fibers and found a uniform distribution of color and no particulate matter on the fibers (Fig. 7). Further magnification of the fibers simply revealed the helical nature of the fibrous material. The color of Fig. 7 is not the true color, although the fibers were stained a reddish color after application of chokeberry juice. The three-year-old chokeberry juice was also examined using the confocal microscope. The juice was dried on a microscope slide and sealed under a cover slip with clear nail polish because the slide was inverted in the microscope. The majority of the slide was uniform and transparent with a red-purple hue, but there was a small particulate cluster shown in Fig. 8. A purple hue was applied to false-color the image (Fig. 8) to mimic the juice color on the slide. Figure 8 displays several faint purple spheres in the large cluster and these area likely solids that fell out of solution over storage. They could be starch granules or a mixture of polysaccharides and other previously soluble solids that have precipitated over storage.

Perhaps the strong cation exchange resin SPE did not have enough backpressure to function at its highest capacity, so a Waters S5 SCX HPLC column was evaluated. This column has silica particles bound to propyl sulfonic acid, so the cation exchange should be the primary means of retention. There was limited knowledge in literature about ACY separation on HPLC cation exchange columns because the majority of cation exchange ACY research uses SPE. Using similar approaches to elute the PPs, the aged chokeberry juice was injected into the column and 20 mM ammonium phosphate in methanol was used to elute the pigment. The chromatogram of this elution pattern is shown in Fig. 9 and essentially no compounds were removed from the column that absorbed 510 nm light. This mobile phase was changed to 20 mM

ammonium phosphate in acetonitrile and a small peak eluted near the end of the chromatogram (Fig. 10). In fear of damaging the HPLC column beyond repair, no further injections were made on this column.

Due to the lack of separation of cation exchange materials, we returned to the standard HPLC column material: octadecylsilyl, or C₁₈. To narrow our focus, we used the collected fraction from the divinylbenzene column using the Peng et al. method (2002). The chromatogram of this fraction on a C₁₈ column appeared similar to the divinylbenzene column in that a large, wide peak appeared near the end of the run (Fig. 11). Efforts to elongate this peak by slowing the rate of change between solvents in the gradient did not yield any notable success. Subsequently, a modification of the method used by Kennedy and Waterhouse 2000 could assist the separation by combining an ion pair reagent with the C₁₈ column. Heptanesulfonic acid is the ion pair reagent and can work with the C₁₈ stationary phase in order to temporarily create an ion exchange system. The collected fraction of PPs and PACs was injected into the C₁₈ column along with heptanesulfonic acid and the chromatogram showed no compounds with 510 nm absorption eluted (Fig. 12). The ion pairing was supposed to improve retention on the column and it may have worked too well. Other mobile phases were used to elute the combination of PPs and heptanesulfonic acid, but they were unsuccessful. The complexity of the PPs is proving to be a difficult matter to overcome with current analytical techniques.

Further searching the literature revealed a method published by Jeffery et al. (2008) focusing on solid phase extraction of wine polymers using an Oasis HLB stationary phase. The HLB column has a unique polymeric base that is composed of a hydrophilic portion from a cyclic amide next to a lipophilic portion from a benzyl ring. The PPs have both hydrophilic components from their multiple hydroxyl groups as well as a lipophilic core from the fused rings.

This method produced three fractions with the last fraction requiring neat formic acid to elute the polymers. Using aged chokeberry juice, this method eluted some colored material with neat formic acid and 95% methanol, but color remained on the column. In order to release the bound pigment, another larger volume of neat formic acid was added, followed by 4 mL of 95% methanol. This eluted more pigmented material, but regardless of how many series of formic acid and methanol were applied, there was still pigment bound to the HLB column. The second fraction used acetonitrile to elute some reddish pigment and this fraction was analyzed using a C₁₈ HPLC column. The chromatogram of the second fraction (F2) is shown in Figure 13 and includes two peaks. The early peak is unusual because the pigmented compounds are often retained longer than 15 minutes on the HPLC columns, so MALDI-TOF was used to further analyze the fractions. Figure 14 illustrates the spectra of the second fraction of aged chokeberry juice that eluted from the HLB column. The signal to noise ratio was very poor in this spectrum and none of the small peaks matched the predicted masses of ACYs, PPs, or PACs. The spectrum of the third fraction (Fig. 15) produced a better signal to noise ratio with some matching peaks, but did not separate PACs from PPs. The MALDI spectrum for this sample (Fig. 15) contains PP trimer (m/z 1026), sodiated tetramer (m/z 1336), and sodiated pentamer (m/z 1624). It also shows a PAC sodiated tetramer (m/z 1176) and sodiated pentamer (m/z 1464). Finally, the fourth fraction, which required increased amounts of neat formic acid and methanol, created a clean spectrum with notable peaks representing both PACs and PPs (Fig. 16). The MALDI spectrum for this sample contains a potassiated PAC trimer (m/z 906), PP pentamer (m/z 1603), and a PAC hexamer (m/z 1730). MALDI-TOF has proved to be a capable technique of measuring high molecular masses and should be used to further examine the PPs and PACs.

The two methods to separate PACs by degree of polymerization use normal phase HPLC with a silica column and reverse phase HPLC with a diol column (Kelm et al. 2006). The normal phase method uses dichloromethane, which is potentially harmless to laboratory workers and the environment, so this research will use the reverse phase method to compare the separation of PACs by DP and PPs by DP. The UV/visible signal requires a much higher concentration than fluorescence detection for PACs. This research will use both detectors to provide more information. The PACs will absorb at 280 nm, while the PPs will absorb at 280 and 510 nm. It has been shown in Kelm et al. 2006 and others that PACs can be separated up to decamers with a fluorescence detector. We injected the aged chokeberry juice into the diol column and detected very little signal, so we used some of the LH-20 eluent because it is a concentrated sample containing both PACs and PPs. The chromatogram of LH-20 processed juice is shown in Figure 17. The late peak in this chromatogram was collected, concentrated, and then analyzed using the MALDI-TOF-MS. The resulting spectrum (Fig. 18) shows that peak contained two series of polymers, which relates to the m/z values of PACs and PPs. The PPs in this sample included a sodiated tetramer (m/z 1336), sodiated pentamer (m/z 1624), and sodiated hexamer (m/z 1914), while the PACs included a potassiated trimer (m/z 906), sodiated tetramer (m/z 1178), potassiated pentamer (m/z 1480), sodiated hexamer (m/z 1754), and a sodiated heptamer (m/z 2042). Once again, the desired separation was not achieved. This method did not separate PPs by DP, nor separate PACs from PPs. We also ran the sulfoxyethyl cellulose eluent on the diol column, but the result was an odd chromatogram with very low signal intensity (Fig. 19). Khanal et al. 2009 used a silica column with a mass spectrometer detector to separate PACs and added 10 mM ammonium acetate post-column to facilitate ionization. This author only detected PACs in grape pomace although ACYs and presumably PPs are rich in this waste product. The PPs

may not be detected by the mass spectrometer because they bind so strongly to the inlet of the column and this issue may be the cause of poor detection in our study.

Due to the MALDI-TOF data suggesting the PPs and PACs are large molecular weight compounds and some literature indicating the same idea (Lin and Hilton 1980), we decided to use size exclusion chromatography to measure the changes in molecular composition over storage, as well as potentially separation the PPs by DP. Lin and Hilton (1980) speculated the average mass of grape PPs was approximately 12,000 Daltons through comparisons of chromatographic techniques, diffusion and sedimentation rates, and paper electrophoresis. A Tosoh TSKgel HPLC column α -3000, which has a size limit of approximately 3000 Da, was used because the MALDI-TOF signal intensity decreases above 3,000 Da due to the saturation of the detector with smaller masses. This column has been used in the past to describe large pigments from rose cider before and after fermentation as well as the change in pigment size from grape juice to red wine (Yanagida 2002). This author found the red wine pigments to weigh between 1,150 and 1,400 Da based on a polyethylene oxide standard. The reliability of this standard reference material to the mass of PPs is questionable. Figure 20 shows the signal intensity at 510 nm of chokeberry juice from pasteurization (20A), one month of storage (20B), and six months of storage (20C), while Fig. 20D represents a typical fluorescence detection of these molecules. The lack of fluorescence signal is not new, but confirms the difficulty in detection of PPs. In general, larger molecules elute earlier on a size exclusion column because they are not retained in the particles, while small analytes will be caught in the channels inside the column's particles causing a longer retention. Looking at Fig. 20A-C, it is clear that the first peak in each chromatogram decreases with increasing storage time. It is well known that monomeric ACYs decrease over storage (Wilkes et al. 2014), but it is confusing that the latter

eluting shoulders/peaks are relatively constant over storage. The monomeric ACYs should be the latter eluting peaks. Upon several uses of the TSKgel column, the reproducibility of each run decreased. After several attempts to clean the column using various organic solvents, the pressure and reproducibility were not improving. The inlet cap was removed to check for potential blockages and surprisingly the inlet was bright red (Fig. 21). The cap was replaced and the column was installed on the HPLC with flow moving in the reverse direction from what is specified on the column. Cleaning the column in the reverse direction allowed some of the bound pigments to be removed, but upon further inspection the inlet retained a light pink hue (Fig. 21).

Molecular weight cutoff filters

In order to analyze the size of PPs in a non-chromatographic manner, molecular weight cutoff filters (MWCO) were evaluated. The Millipore Amicon devices are made of regenerated cellulose with different pore sizes to separate a range of molecular weights. Using these filters to separate the pigmented compounds of different ages may lead to an estimation of PP size and the source of long-term color in anthocyanin-rich juices. Comparing filter output of a three year aged chokeberry juice from cutoffs of 3,000, 30,000, 50,000, and 100,000 Da illustrates a color gradient without increasing molecular weight (Fig. 22). The most vibrantly colored fraction comes from the 100,000 Da cutoff meaning the compounds eluting through the filter are smaller than 100,000 Da. This sample has nearly twice the absorbance of the 50,000 Da cutoff eluent and this trend continues in a nearly linear fashion (Fig. 23). Comparing the aged chokeberry juice to a pasteurized juice does not reveal the same trend because of the high concentration of monomeric ACYs in the young juice (Fig. 24). This data indicates that the source of pigment in the aged juice may originate from very large molecules greater than 50,000 Da and potentially

greater than 100,000 Da. In order to get a better understanding of the composition of these MWCO filters, we attempted to identify some of the components using MALDI-TOF-MS because this mass range is much greater than the capacity of LC-ESI-MS. Also, concentration and detector saturation greatly factors into the signal to noise ratio when using MALDI-TOF, so we analyzed the eluents directly, but also passed the eluent through the next cutoff size smaller. This created a narrower range of molecular weights. The mass spectrum of the 30,000-50,000 Da MWCO is shown in Figure 25. This spectrum had the greatest signal to noise ratio compared to all other samples measured and the other MWCO samples had similar spectra. The spectrum had no signal at the high mass ranges related to the cutoff filters and only small peaks below 3000 Da, none of which aligned with PPs, nor PACs. The lack of signal is unlikely to be due to concentration because replicate samples were pooled and concentrated prior to analysis. In a related note, dialysis tubing was tested for its ability to separate PPs by molecular weight and produced a slight correlation with more vibrant color due to increasing molecular weight. However, the dialysis tubing did not correlate as well as the MWCO filters.

Gel electrophoresis

When molecular weight cutoff filters provided a color gradient with increasing color aligning with increasing mass, it probed the question of how to separate very high molecular weight compounds. The most common example of such a technique is gel electrophoresis, which is commonly used to separate large proteins from each other in fine bands along the gel. This method should work well for the PPs because of the electrical charge flowing through the gel should separate the charged PPs. The combination of the cutoff filters and gel electrophoresis may provide more information about PP changes over storage.

Polyacrylamide gels required a pH 8.3 buffer, which turned the red ACYs to a dark grey-green color while electrophoretic separation took place. Figure 26 shows the separation of chokeberry juice of various ages and passed through different MWCO filters in order to detect some differences in electrophoretic separation as well as differences in pigmentation over storage. All samples show a smeared pattern with no defined bands, except for the protein standard. Lane one of Fig. 26 is a pale brown-orange color of straight three-year-old chokeberry juice. Interestingly, lane one was visually not very vibrant at pH 8.3 or acidified in pH 2 DI water, but upon scanning on the Fluoro RGB setting a bright blue spot appeared. This spot aligns with 20 kDa protein standard. The next two lanes are six months old juice passed through 0-50 and 0-100 kDa MWCO filters. There is no significant difference between lanes two and three, which means the compounds producing pigment in the six month chokeberry juice are likely smaller than 50 kDa. The pigmented smears of lanes two and three align with the protein standard representing a range from 2-250 kDa. This is unlikely to truly represent the mass of the PPs because the MWCO filters should elute only molecules smaller than 50 or 100 kDa, respectively. The samples in lanes four and five are six months old juice after two series of MWCO filters to get a narrow mass range: lane four contains 10-30 kDa and lane five has a range of 30-50 kDa. The top two sections of Fig. 26 show little visual difference between lanes four and five, but the Fluoro RGB scan shows more red color in the 30-50 kDa (lane five). Lanes six through nine follow the same pattern as lanes two through five, but use pasteurized chokeberry juice instead of six months old juice. In this instance, lane seven has a stronger red color than lane six, which means there could be PPs between 50 and 100 kDa in the pasteurized juice. PPs are present in fresh chokeberries and pasteurized juice (Wilkes et al. 2014), and this data could indicate a change in average mass between pasteurization and six months of storage.

Lanes eight and nine show the same trend in pasteurized juice as was shown in the six months juice; there is greater pigmentation in the 30-50 kDa range than 10-30 kDa range.

The pigmented areas of the gel were sliced and extracted in 90% methanol, then extracted in 70% acetone. Neither solvent fraction was very strongly pigmented, regardless of the pigment strength in the gel even after concentration from 50 mL to 0.5 mL. The samples were analyzed using MALDI-TOF-MS, but unfortunately did not show any high molecular weight compounds. Also, the low molecular masses did not align with either PPs or PACs.

Next, a different type of polyacrylamide gel was created that is capable of running in an acidic buffer system (Saunders et al. 2012). This gel took on a blue appearance, which made visual ACY identification difficult. Various samples were analyzed using this type of gel and the results were overall similar, with one example shown in Fig. 27. The effect of C₁₈ SepPak purification on unpasteurized, pasteurized, and six months old chokeberry juice was shown in lanes one through six. Generally, the SepPak improved concentration of the pigmented analytes, which allowed for the identification of cyanidin-3-galactoside. This is the predominant ACY in chokeberry juice and decreases quickly over storage. The darkest spot that is pictured approximately half way down the gel in Fig. 27 likely corresponds to cyanidin-3- galactoside. The relatively small molecule should progress faster through the gel than the larger PPs and this spot is hardly visible in lanes four and five because cyanidin-3- galactoside is in the six months old juice in low concentration. The cyanidin-3- galactoside spot aligns with the 20 kDa band in the protein standard, which further indicates that ACYs do not separate in gel electrophoresis according to the same principles as the protein standards. This band and other pigmented regions were cut and extracted with solvent, but the extraction had a poor recovery rate just as the alkaline polyacrylamide gels. The mildly pigmented extracts were concentrated and analyzed

using MALDI-TOF-MS and no expected masses appeared. The MALDI spectra had very little signal.

In order to extract the analytes to learn more about their identity, agarose gels was used instead of polyacrylamide. A 1% agarose solution was poured to make the gel and larger wells had to be created because of the poor visibility of ACYs and PPs in the agarose matrix. The separation produced in the agarose gel was similar to the polyacrylamide gels in that a spot of cyanidin-3-galactoside was visible in unpasteurized juice (Fig. 28 lane one) and decreased in intensity in the pasteurized juice (lane two) and was hardly visible in the six months old chokeberry juice (lane three). The protein standard is in lane five and is nearly invisible in Fig. 28, which illustrates how little visibility there is in agarose gels compared to polyacrylamide gels. Lane eight contains the eluent of a six months old juice after MWCO filtering of 0-100 kDa, which is notably more vibrant than the 0-50 kDa sample in lane seven. This was the same trend in the pasteurized juice in the acrylamide gels; however both the six-month-old juice 0-50 and 0-100 kDa MWCO samples appeared similar in the polyacrylamide gels. Perhaps the agarose gels provide less separation of the larger molecular weight compounds, which makes the bands appear darker or maybe the light reacts differently through the agarose than the polyacrylamide, which makes this sample appear different. Once again, the pigmented regions of the gels were extracted for mass spectrometric analysis, but no notable peaks were detected.

Ultrasonication

It is possible that large molecules, such as polysaccharides, can entangle with each other through π - π or hydrophobic interactions. Therefore it is possible that PPs form complexes with soluble polysaccharides in fruit juices. Potentially, ACYs can be incorporated in these complexes

and applying the proper force could interrupt the complex causing the release of monomeric ACYs. These potential ACYs could be tightly bound to the complex and not be detected during HPLC measurement; however, if they were freed from the complex, HPLC detection would show an increase in ACY peak area. An ultrasonic processor was used due to its ability to exert high shear force and disruptive capabilities.

Both fresh and three-year-old chokeberry juice samples were compared after two separate trials of pulsed ultrasonication of 15 and 60 minutes. Visually there was no color difference between the samples before and after treatment; next the samples were analyzed by HPLC-PDA to detect any change in ACY composition and concentration. Figure 29 shows chromatograms of fresh chokeberry juice ACYs before and after ultrasonication of 60 minutes. These results indicate the ultrasonication treatment did not affect ACY composition or concentration. Chromatograms for the three-year-old juice also appeared the same before and after treatment (data not shown). There was no difference between the 15 and 60 minute treatments. It was postulated that copigmentation, π - π stacking, or hydrophobic interactions might be retaining ACYs in complexes with soluble solid materials, such as polysaccharides or PPs. Using molecular dynamic simulations, it was found that ACY-ACY copigmentation could occur as quickly as ten nanoseconds (Oliveira et al. 2014). This could indicate that ultrasonication could disrupt the copigmentation, but compounds reorganize immediately after treatment terminates. This treatment was a unique approach to PP detection and identifying the source of long-term color in ACY-rich juices.

Conclusion

To recapitulate, many different forms of chromatographic techniques and materials were tested for their ability to separate PPs from PACs and PPs by DP. Both series of polymers can be detected using mass spectrometric techniques (ESI-MS and MALDI-TOF-MS); however, separation of the two polymeric compounds was unsuccessful. Using MWCO filters, a color gradient appeared in aged juices containing very little to no monomeric ACY, which could indicate that the long-term source of color in this juice is due to molecules weighing over 50 or 100 kDa. Attempts to separate the large PPs using gel electrophoresis and identification of bands using mass spectrometry were unsuccessful. Perhaps the current technology is not capable of separating these molecules. This research aids in the advancement of polymeric pigment separation by demonstrating the inefficiencies of numerous methods that do not separate these molecules.

References

- Hayasaka, Y.; Kennedy, J.A. Mass spectrometric evidence for the formation of pigmented polymers in red wine. *Aust. J. Grape Wine Res.* **2003**, *9*, 210-220.
- Duenas, M.; Fulcrand, H.; Cheynier, V. Formation of anthocyanin-flavanol adducts in model solutions. *Analytica Chimica Acta.* **2006**, *563*, 15-25.
- Timberlake, C.F.; Bridle, P. Interactions between anthocyanins, phenolic compounds, and acetaldehyde and their significance in red wines. *Am. J. Enol. Vitic.* **1976**, *27*, 97-105.
- Jurd, L. Review of polyphenol condensation reactions and their possible occurrence in the aging of wines. *Am. J. Enol. Vitic.* **1969**, *20*, 191-195.
- Somers, T.C. The polymeric nature of wine pigments. *Phytochem.* **1971**, *10*, 2175-2186.
- Vidal, S.; Cartalade, D.; Souquet, J.; Fulcrand, H.; Cheynier, V. Changes in proanthocyanidins chain-length in wine-like model solutions. *J. Agric. Food Chem.* **2002**, *50*, 2261-2266.
- Salas, E.; Fulcrand, H.; Meudec, E.; Cheynier, V. Reactions of anthocyanins and tannins in model solutions. *J. Agric. Food Chem.* **2003**, *51*, 7951-7961.
- Juadjur, A.; Winterhalter, P. Development of a novel adsorptive membrane chromatographic method for the fractionation of polyphenols from bilberry. *J. Agric. Food Chem.* **2012**, *60*, 2427-2433.
- Vergara, C.; Mardones, C.; Hermosin-Gutierrez, I.; von Baer, D. Comparison of high performance liquid chromatography separation of red wine anthocyanins on a mixed-mode ion-exchange reversed-phase and on a reversed-phase column. *J. Chromatogr.* **2010**, *1217*, 5710-5717.
- Peng, Z.; Iland, P.G.; Oberholster, A.; Sefton, M.A.; Waters, E.J.; Analysis of pigmented polymers in red wine by reverse phase HPLC. *Aust. J. Grape Wine Res.* **2002**, *8*, 70-75.
- Giusti, M.; Wrolstad, R.E. Characterization and measurement of anthocyanins with UV-visible spectroscopy. In *Current Protocols in Food Analytical Chemistry*; Wrolstad, R.E., Ed.; Wiley: New York, 2001; pp. F1.2.1-F1.2.13
- Berke, B.; Cheze, C.; Vercauteren, J.; Deffieux, G. Bisulfite addition to anthocyanins: revisited structures of colourless adducts. *Tetrahedron Letters.* **1998**, *39*, 5771-5774.
- Salas, E.; Duenas, M.; Schwarz, M.; Winterhalter, P.; Cheynier, V.; Fulcrand, H. Characterization of pigments from different high speed countercurrent chromatography wine fractions. *J. Agric. Food Chem.* **2005**, *53*, 4536-4546.

- Salas, E.; Fulcrand, H.; Poncet-LeGrand, C.; Meudec, E.; Kohler, N.; Winterhalter, P.; Cheynier, V. Isolation of flavanol-anthocyanin adducts by countercurrent chromatography. *J. Chromatogr. Sci.* **2005**, *43*, 488-493.
- Remy, S.; Fulcrand, H.; Labarbe, B.; Cheynier, V.; Moutounet, M. First confirmation in red wine of products resulting from direct anthocyanin-tannin reactions. *J. Sci. Food Agric.* **2000**, *66*, 745-751.
- Reed, J.D.; Kreuger, C.G.; Vestling, M.M. MALDI-TOF mass spectrometry of oligomeric food polyphenols. *Phytochem.* **2005**, *66*, 2248-2263.
- He, J.; Santos-Buelga, C.; Mateus N.; de Freitas, V. Isolation and quantification of oligomeric pyranoanthocyanin-flavanol pigments from red wine by column chromatographic techniques. *J. Chromato. A.* **2006**, *1134*, 215-225.
- Cho, M.J.; Howard, L.R.; Prior, R.L.; Clark, J.R. Flavonoid glycosides and antioxidant capacity of various blackberry, blueberry and red grape genotypes determined by high-performance liquid chromatography/mass spectrometry. *J. Sci. Food Agric.* **2004**, *84*, 1771-1782.
- Kelm, M.A.; Johnson, C.; Robbins, R.J.; Hammerstone, J.F.; Schmitz, H.H. High-performance liquid chromatography separation and purification of cacao (*Theobroma cacao* L.) procyanidins according to degree of polymerization using a diol stationary phase. *J. Agric. Food Chem.* **2006**, *54*, 1571-1576.
- Yanagida, A.; Shoji, T.; Kanda, T. Characterization of polymerized polyphenols by size-exclusion HPLC. *Biosci. Biotechnol., Biochem.* **2002**, *66*, 1972-1975.
- Spagna, G.; Pifferi, P.G. Purification and separation of oenocyanin anthocyanins on sulphoxyethylcellulose. *Food Chem.* **1992**, *44*, 185-188.
- Kantz, K.; Singleton, V.L. Isolation and determination of polymeric polyphenols using Sephadex LH-20 and analysis of grape tissue extracts. *Am. J. Enol. Vitic.* **1990**, *41*, 223-228.
- Jeffrey, D.W.; Mercurio, M.D.; Herderich, M.J.; Hayasaka, Y.; Smith, P.A. Rapid isolation of red wine polymeric polyphenols by solid-phase extraction. *J. Agric. Food Chem.* **2008**, *56*, 2571-2580.
- Kammerer, D.; Kljusuric, J.G.; Carle, R.; Schieber, A. Recovery of anthocyanins from grape pomace extracts (*Vitis vinifera* L. cv. Cabernet Mitos) using a polymeric adsorber resin. *Eur. Food Res. Technol.* **2005**, *220*, 431-437.
- Lin, R.I.; Hilton, B.W. Purification of commercial grape pigment. *J. Food Sci.* **1980**, *45*, 297-306.
- Saunders, C.C.; Stites, W.E. An electrophoretic mobility shift assay for methionine sulfoxide in proteins. *Anal. Biochem.* **2012**, *421*, 767-769.

- Oliveira, J.; Alinho da Silva, M.; Parola, A.J.; Mateus, N.; Bras, N.F.; Ramos, M.J.; de Freitas, V. Structural characterization of a A-type linked trimeric anthocyanin derived pigment occurring in a young Port wine. *Food Chem.* **2013**, *141*, 1987-1996.
- Kennedy, J.A.; Waterhouse, A.L. Analysis of pigmented high molecular-mass grape phenolics using ion-pair, normal-phase high-performance liquid chromatography. *J. Chromat. A.* **2000**, *866*, 25-34.
- Khanal, R.C.; Howard, L.R.; Prior, R.L. Procyanidin content of grape seed and pomace and total anthocyanin content of grape pomace as affected by extrusion processing. *J. Food Sci.* **2009**, *74*, H174-H182.
- Wilkes, K.; Howard, L.R.; Brownmiller, C.; Prior, R.L. Changes in chokeberry (*Aronia melanocarpa* L.) polyphenols during juice processing and storage. *J. Agric. Food Chem.* **2014**, *62*, 4018-4025.
- Oliveira, J.; Bras, N.F.; Alinho da Silva, M.; Mateus, N.; Parola, A.J.; de Freitas, V. Grape anthocyanin oligomerization: A putative mechanism for red color stabilization? *Phytochem.* **2014**, *105*, 178-185.

Figures

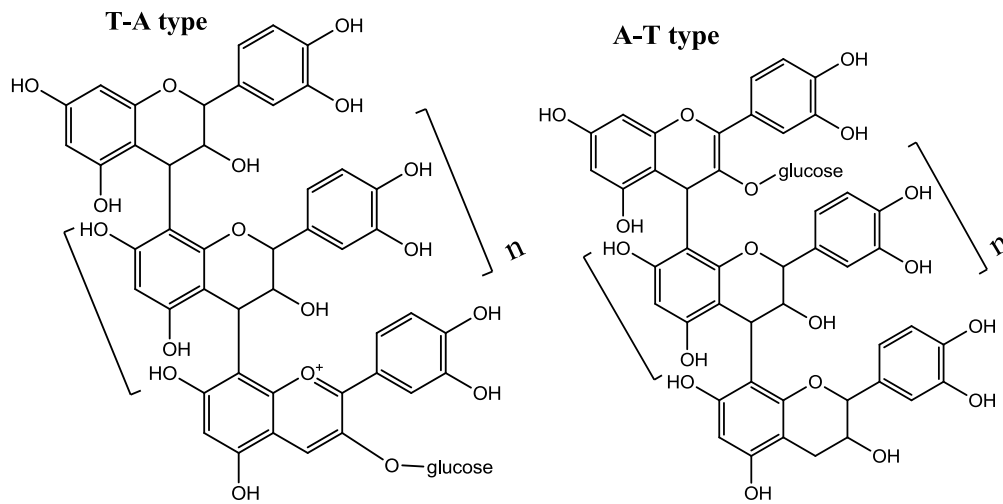


Figure 1: Polymeric Pigment Structures (adapted from Hayasaka and Kennedy 2003)

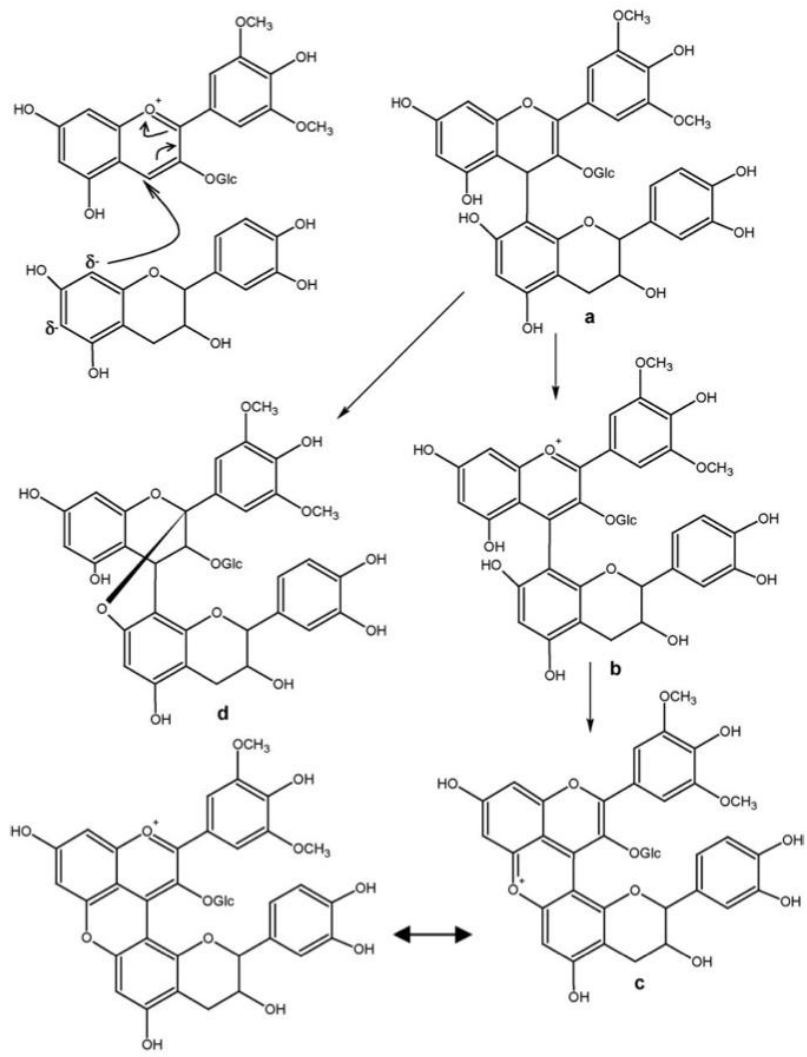


Figure 2: Direct anthocyanin-flavanol reactions and structure of A-F adducts. (a) Flavene, (b) flavylium cation, (c) xanthylium cation, and (d) A(-O-)F (A-type) dimer (Duenas et al. 2006).

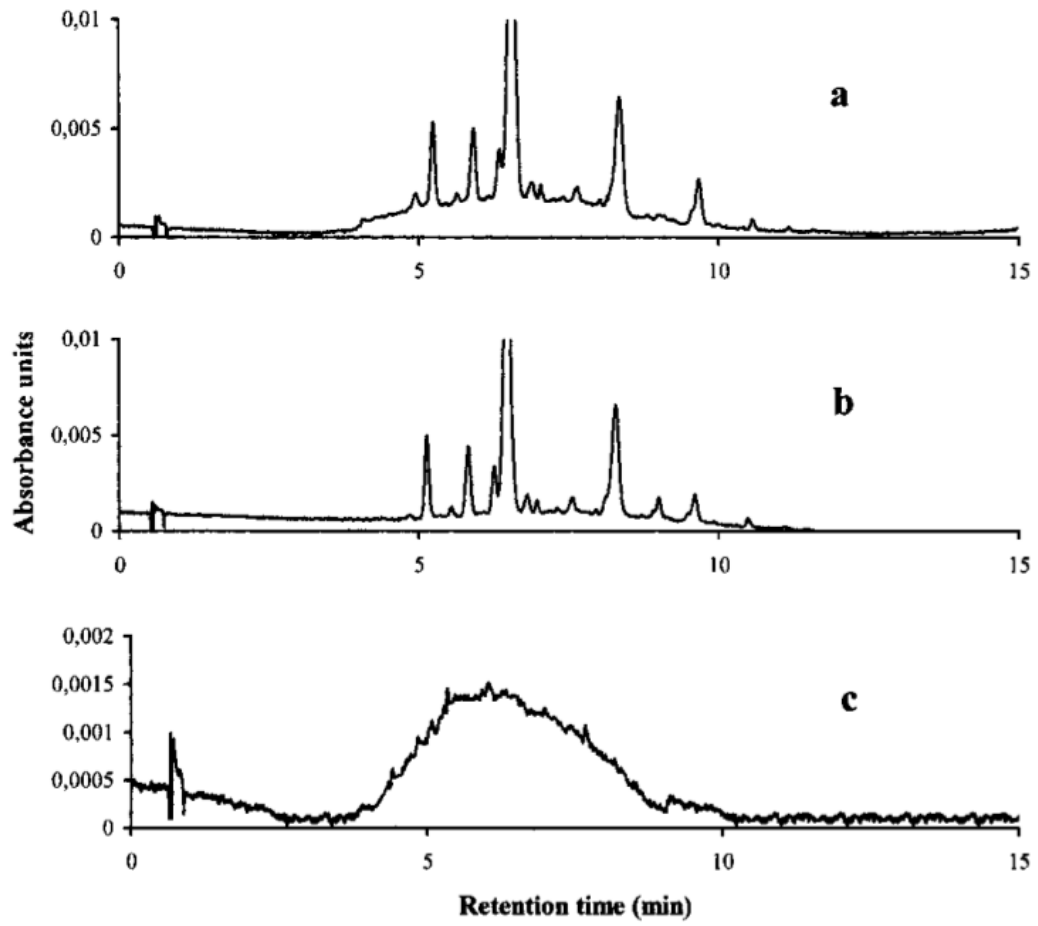


Figure 3: Chromatogram recorded on Nucleosil C18 column at 520 nm of (a) fraction 1 and its (b) organic and (c) aqueous phase after iso-amyl alcohol extraction (Remy et al. 2000).

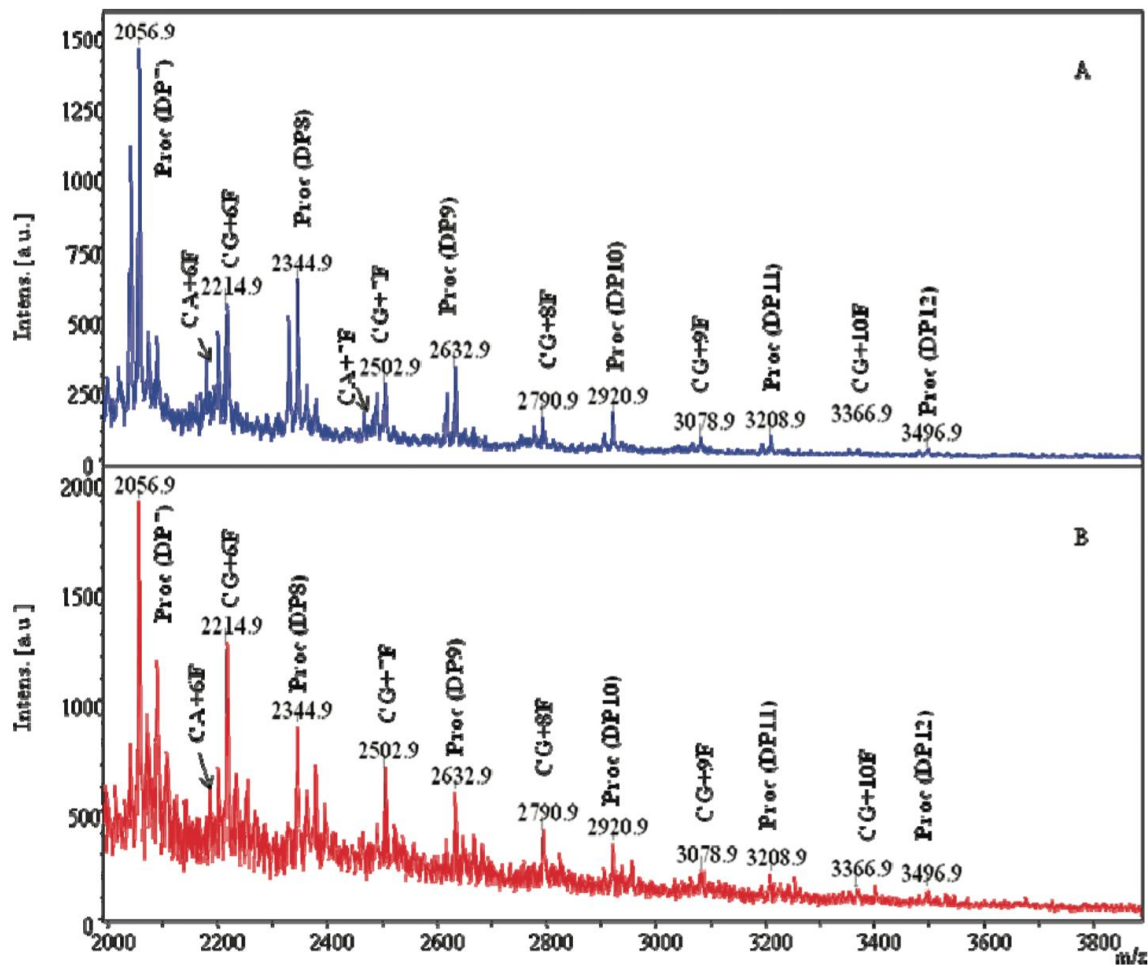


Figure 4: MALDI-TOF mass spectrum (m/z 2000-3850) of (A) pasteurized and (B) aged juice in reflection mode showing the $[M - H + K]^+$ of cyanidin-3-galactoside plus 6 flavan-3-ol units (m/z 2214.9) to cyanidin-3-galactoside plus 10 flavan-3-ol units (m/z 3366.9) and procyanidin series ranging from DP7 (m/z 2056.9) to DP12 (m/z 3496.9). CA= cyanidin-3-arbinoside; CG=cyanidin-3-galactoside; F= flavan-3-ol (Howard et al. 2012).

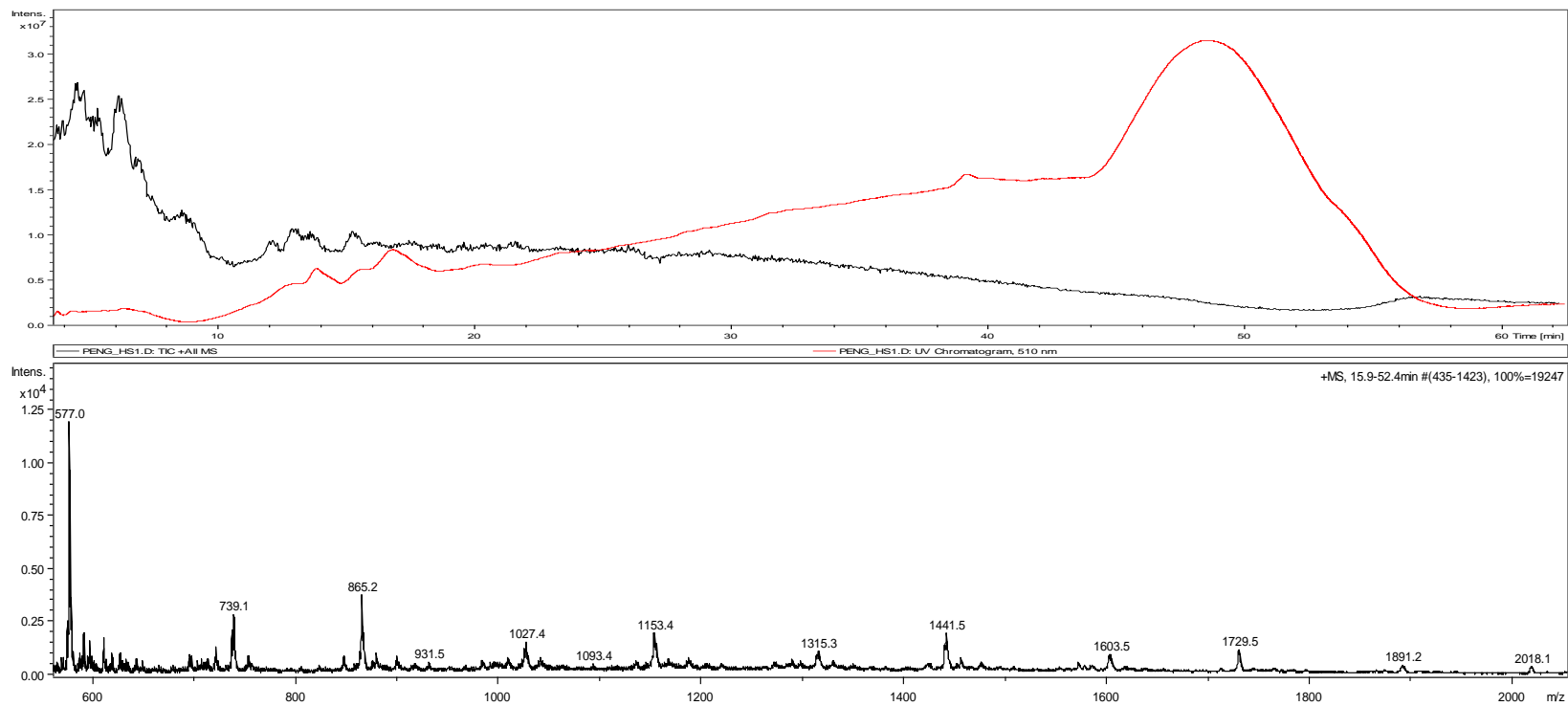


Figure 5: Chromatogram of aged chokeberry juice on divinylbenzene HPLC column with detection at 510 nm. The UV trace is in red and MS trace is in black. (top); Spectrum of procyanidins and polymeric pigments eluting throughout this chromatogram (bottom).

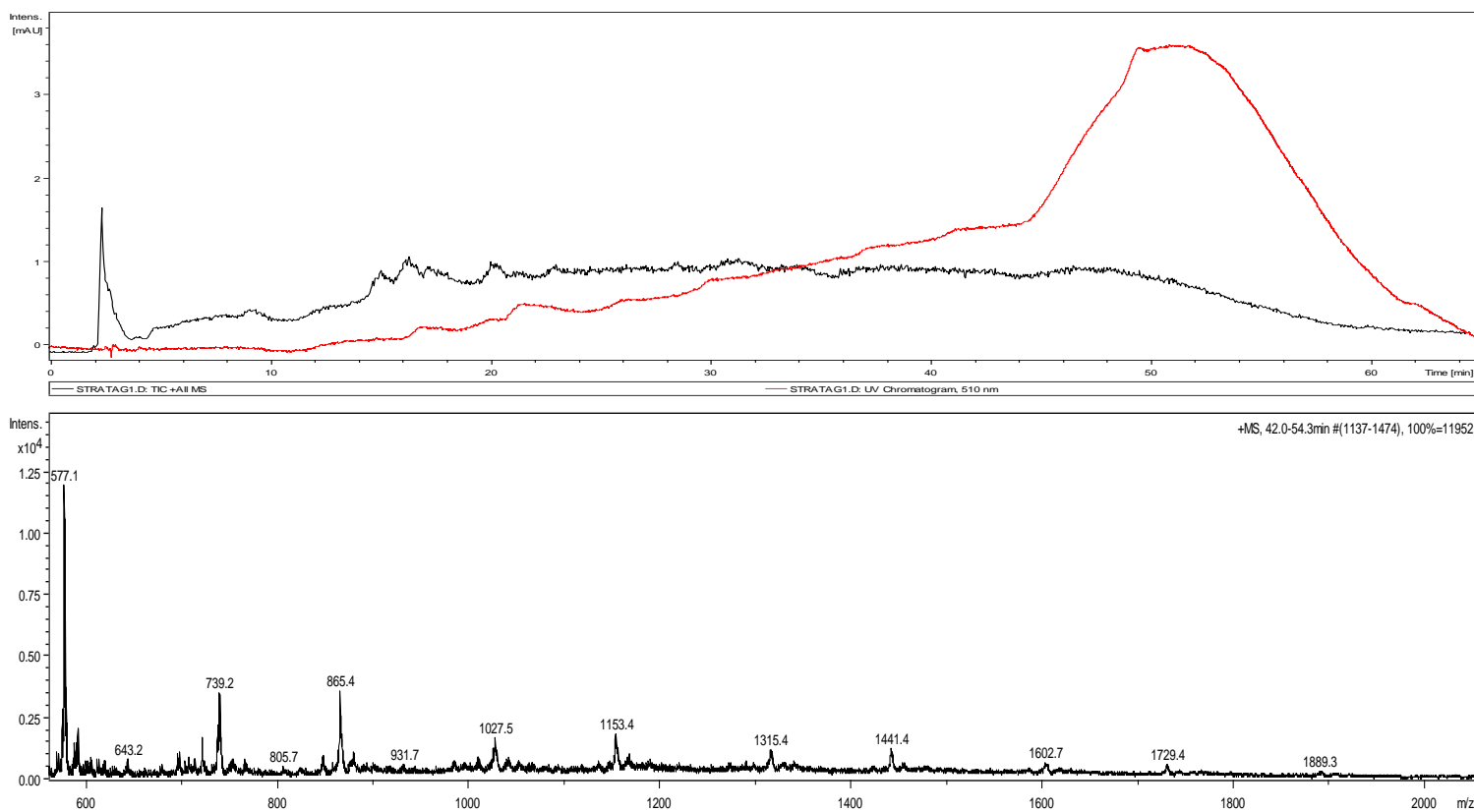


Figure 6: Chromatogram of aged chokeberry juice on divinylbenzene column after Strata-XC ion exchange solid phase extraction. The UV trace is in red and MS trace is in black. (top); Spectrum of procyanidins and polymeric pigments eluting in this chromatogram (bottom).

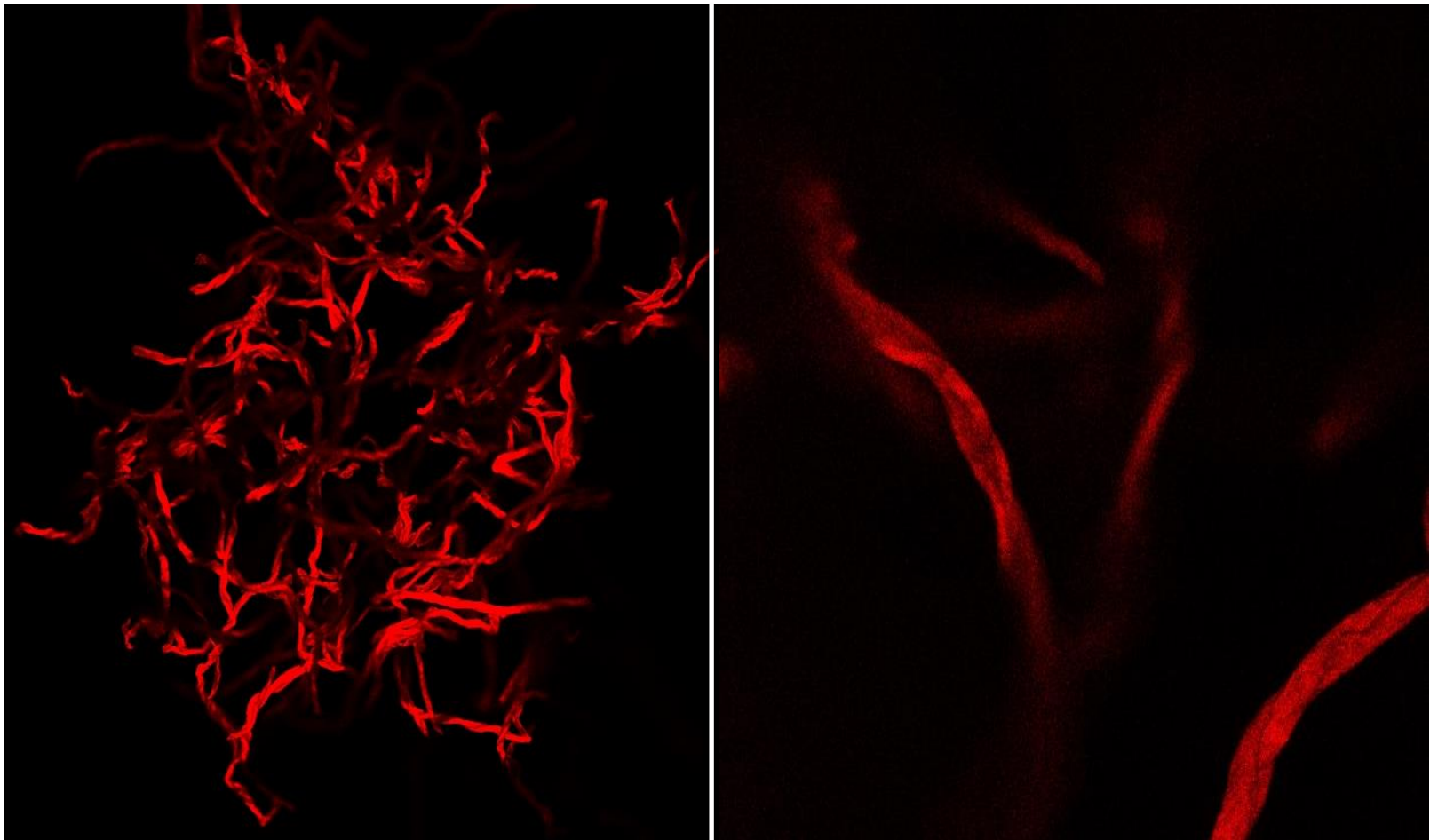


Figure 7: Confocal laser scanning microscope false-colored image of sulfoxyethyl cellulose after application of three year old chokeberry juice (left). Further magnification (right).

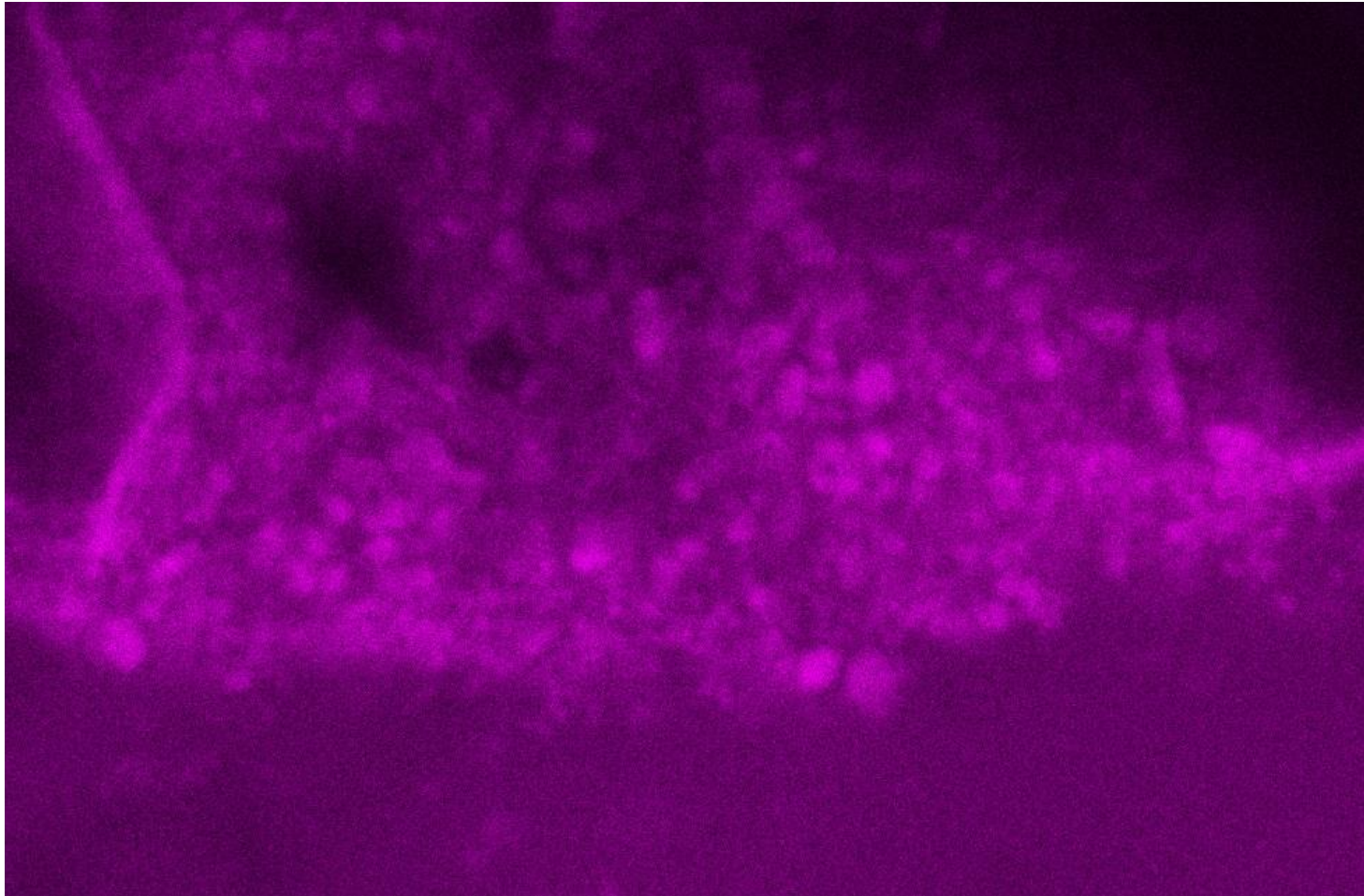
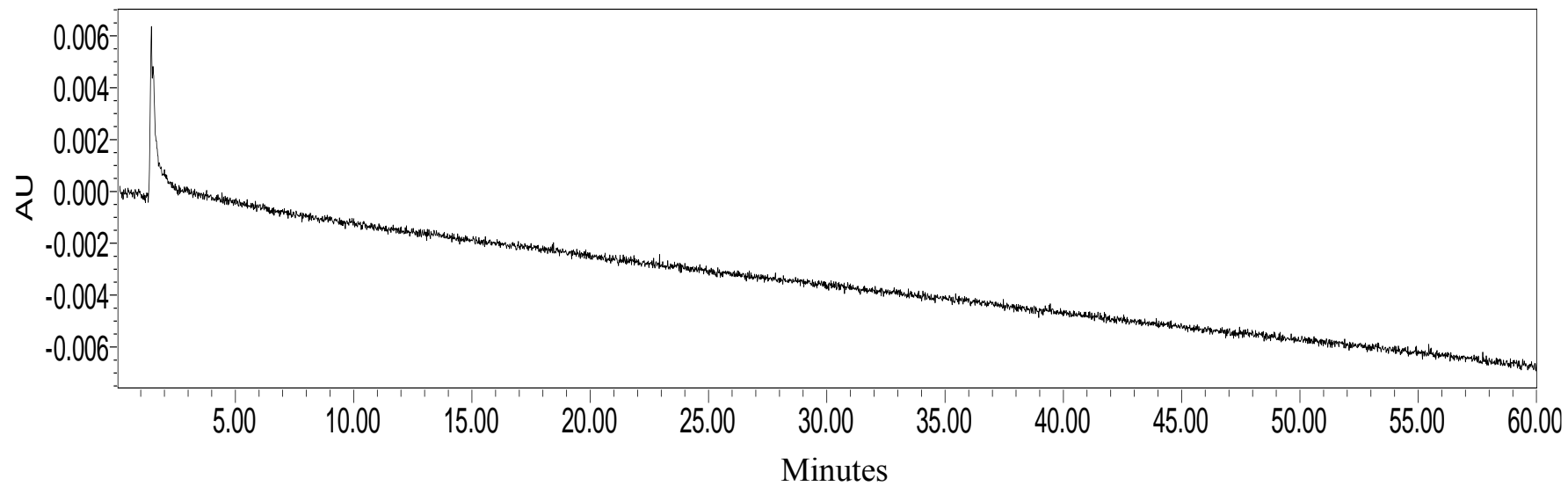


Figure 8: Confocal laser scanning microscope false-colored image of juice residue from a three year old chokeberry juice.



16

Figure 9: Chromatogram of aged chokeberry juice on Waters S5 SCX column with a gradient elution of water and 20 mM ammonium phosphate in methanol with detection at 510 nm.

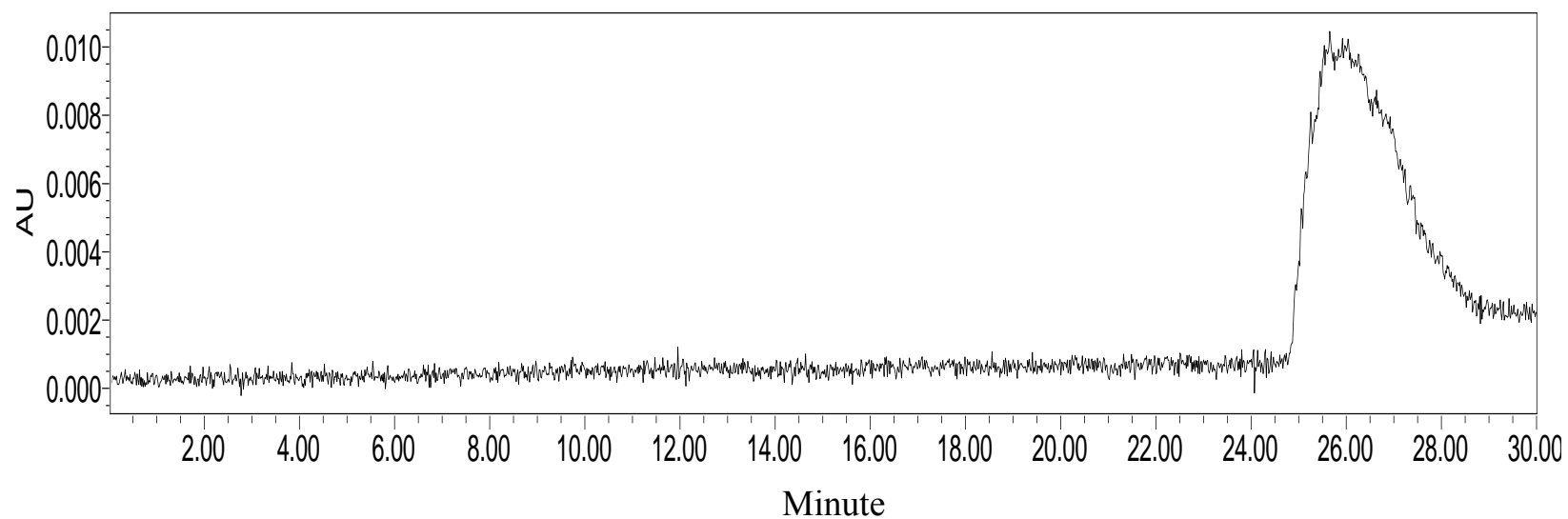
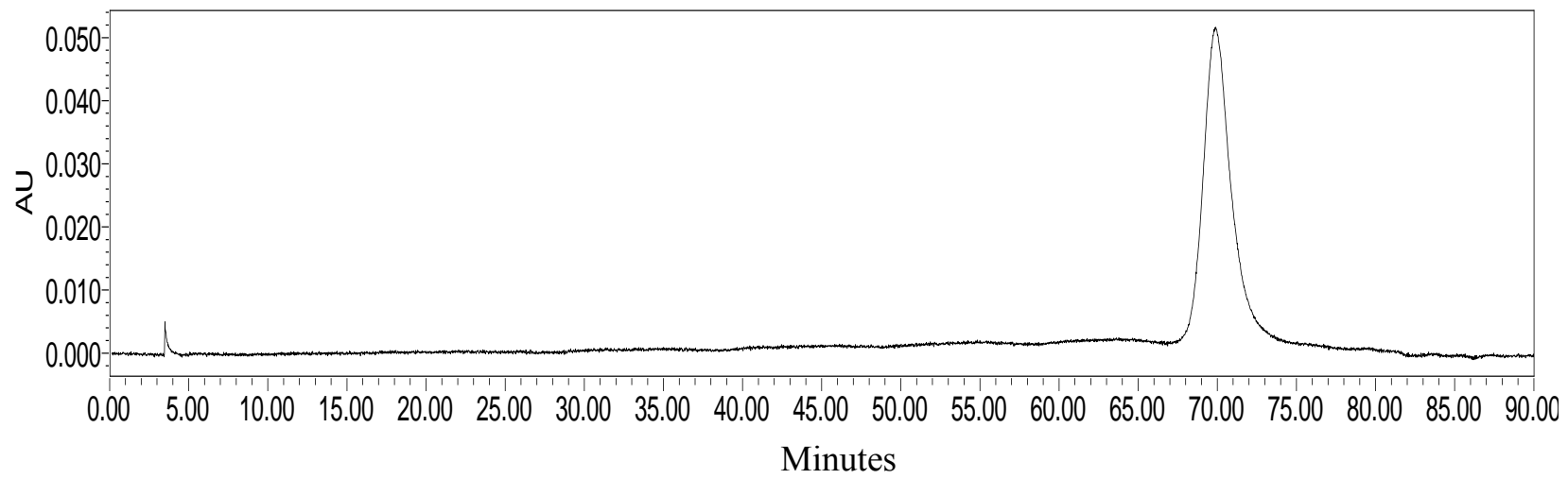


Figure 10: Chromatogram of aged chokeberry juice on Waters S5 SCX column with a gradient elution of water and 20 mM ammonium phosphate in acetonitrile with detection at 510 nm.



93

Figure 11: Chromatogram of collected fraction of PACs and PPs from Peng et al. 2002 method using a Waters Symmetry C₁₈ column at 510 nm.

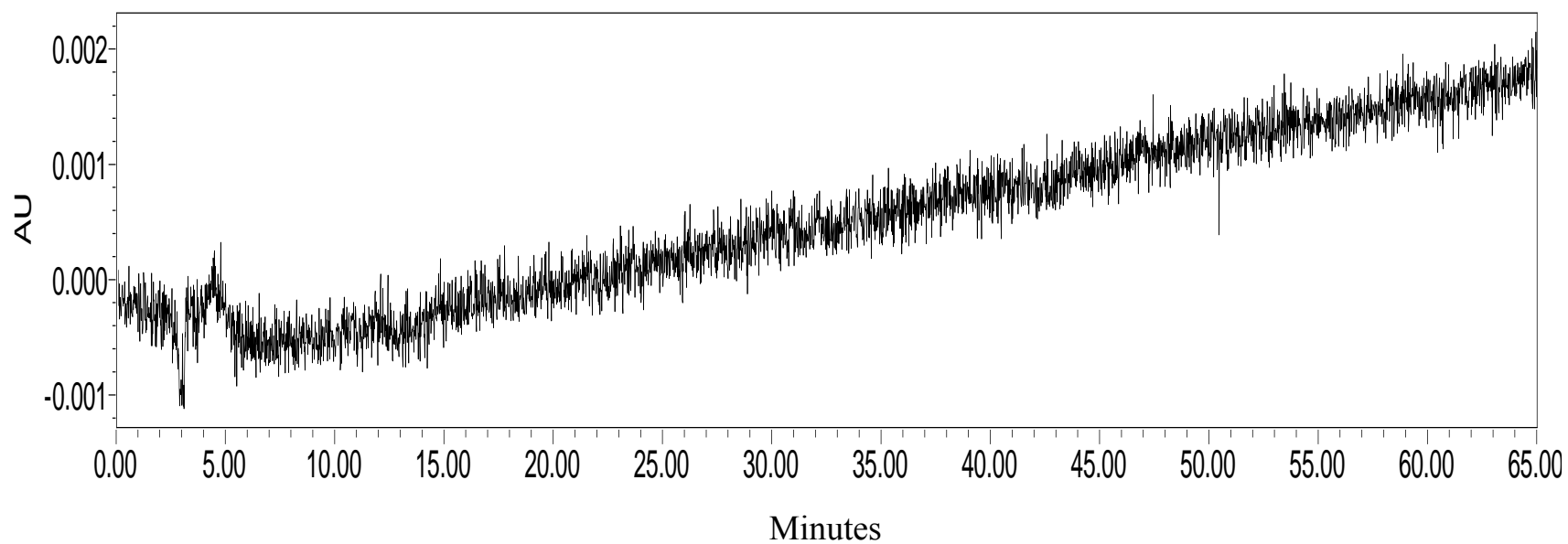
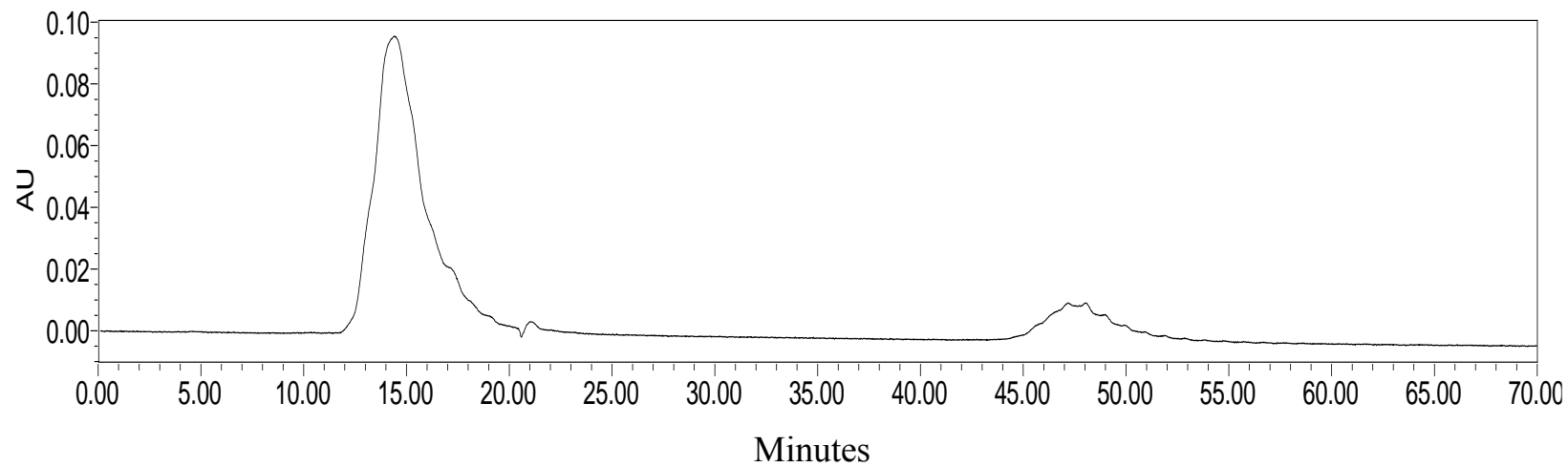


Figure 12: Chromatogram of collected fraction of PACs and PPs from Peng et al. 2002 method using a Waters Symmetry C₁₈ column with heptanesulfonic acid in the mobile phase at 510 nm.



95 Figure 13: Chromatogram of the acetonitrile fraction (F2) of HLB SPE column using a Waters Symmetry C₁₈ column at 510 nm.

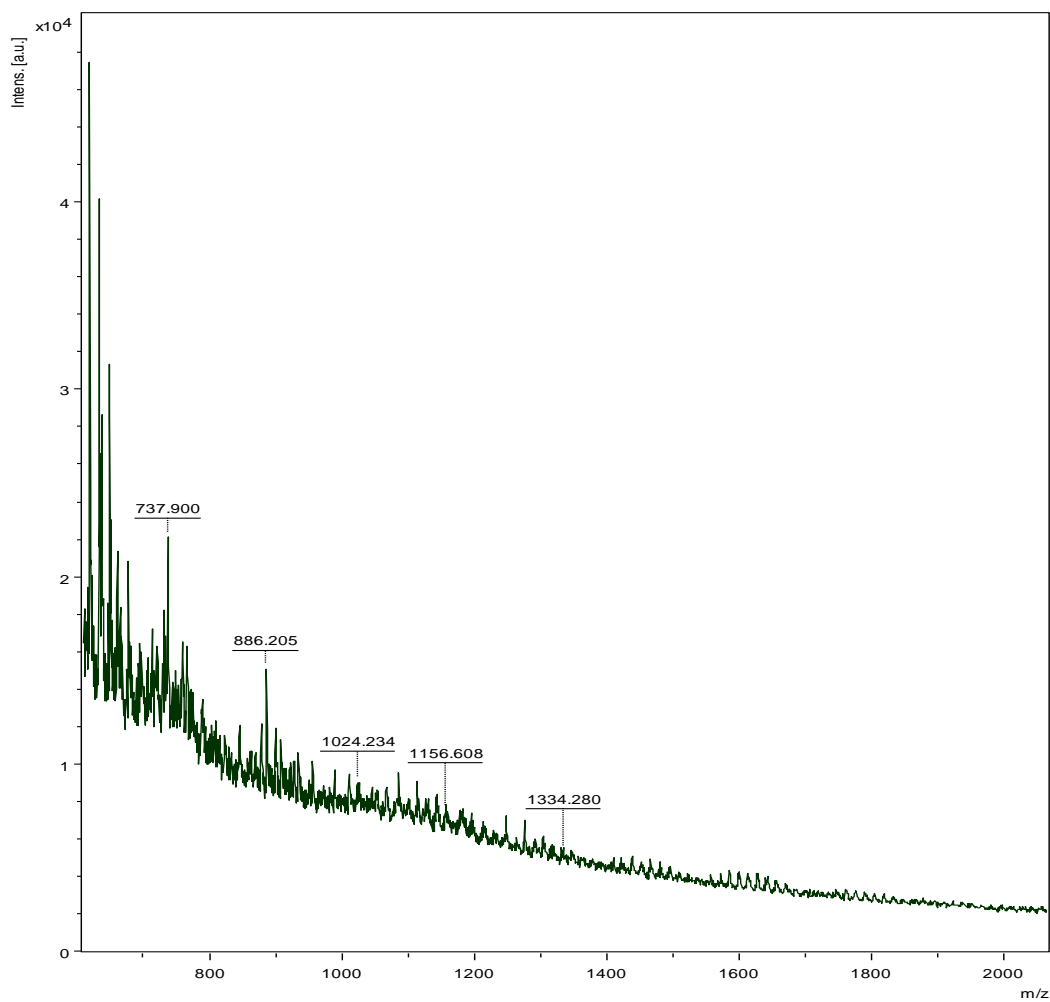


Figure 14: MALDI-TOF mass spectrum of fraction two (F2) of aged chokeberry juice after HLB solid phase extraction.

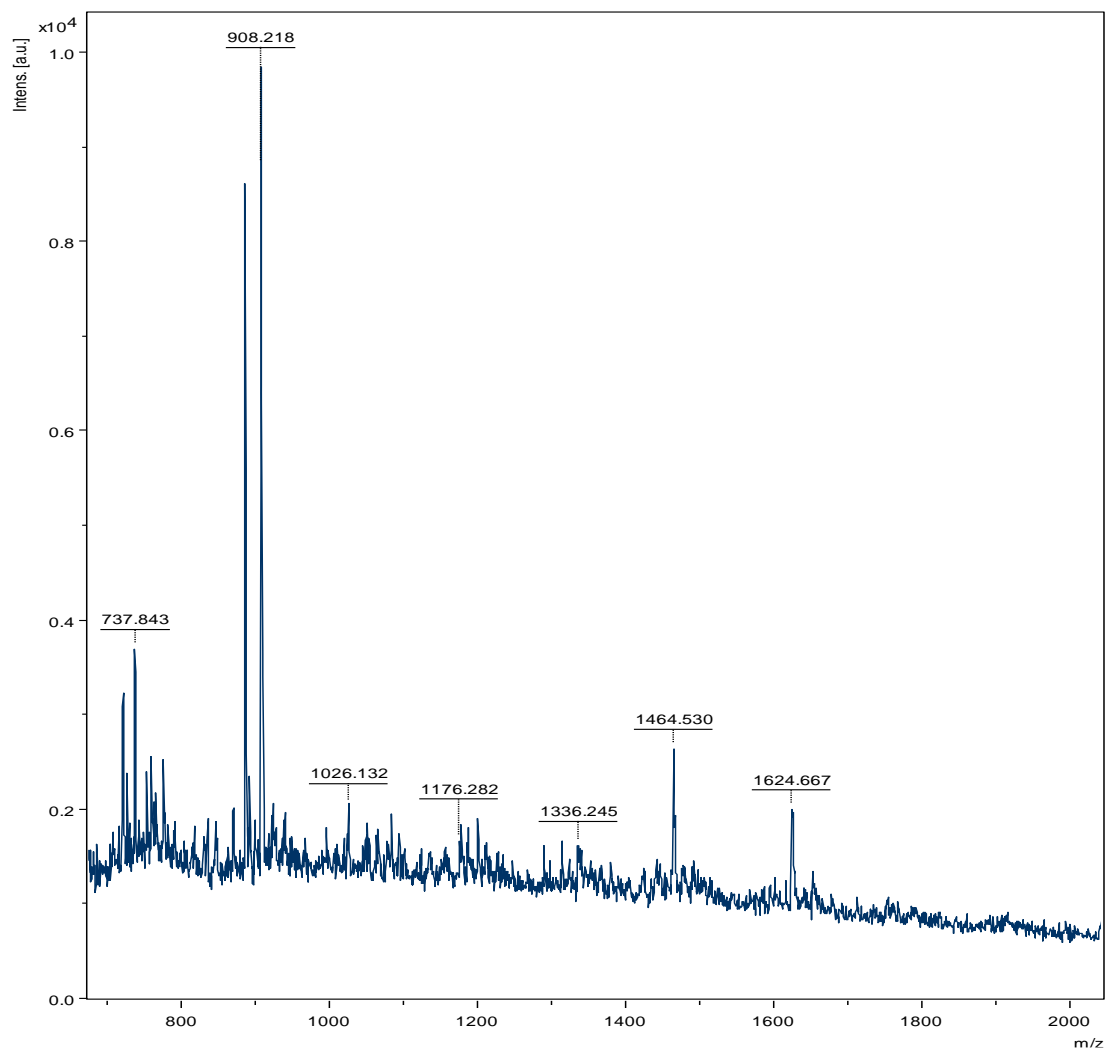


Figure 15: MALDI-TOF mass spectrum of fraction three (F3) of aged chokeberry juice after HLB solid phase extraction.

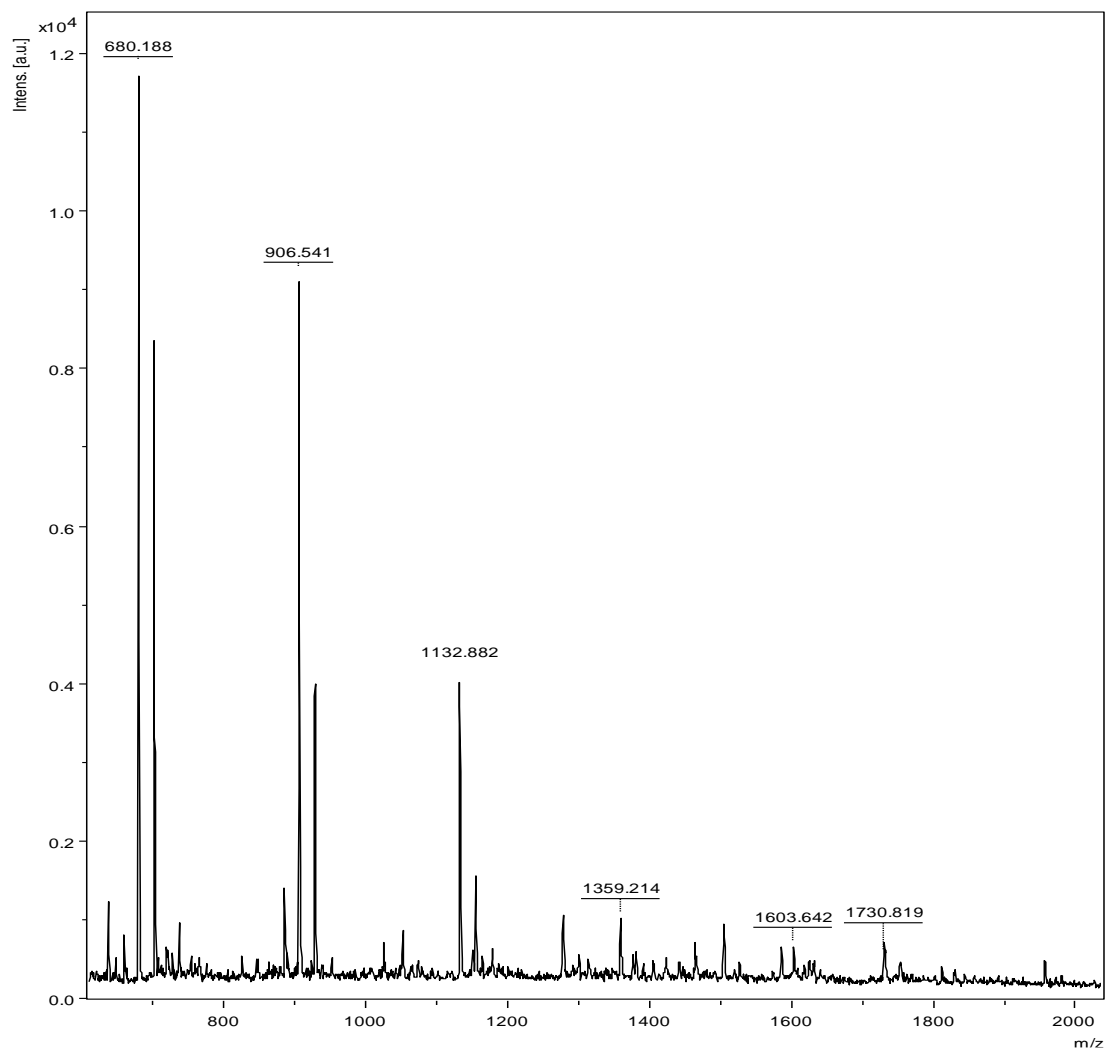


Figure 16: MALDI-TOF mass spectrum of fraction four (F4) of aged chokeberry juice after HLB solid phase extraction.

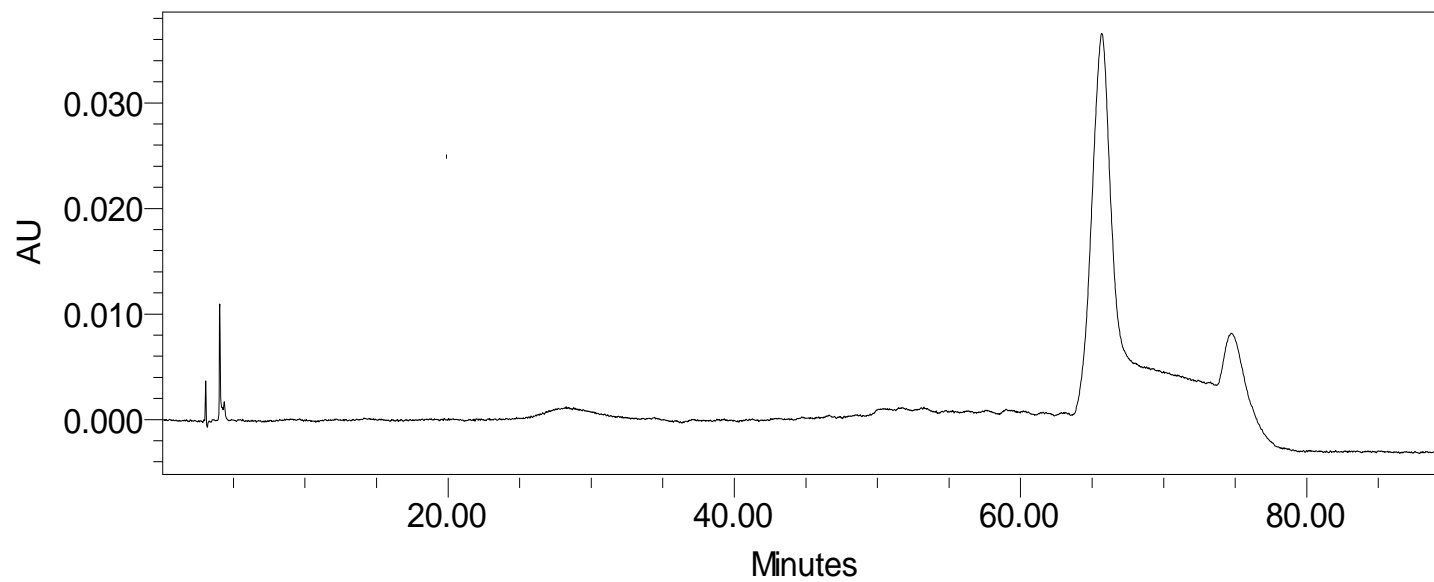


Figure 17: Chromatogram of aged chokeberry juice after Sephadex LH-20 solid phase extraction on diol HPLC column with detection at 510 nm.

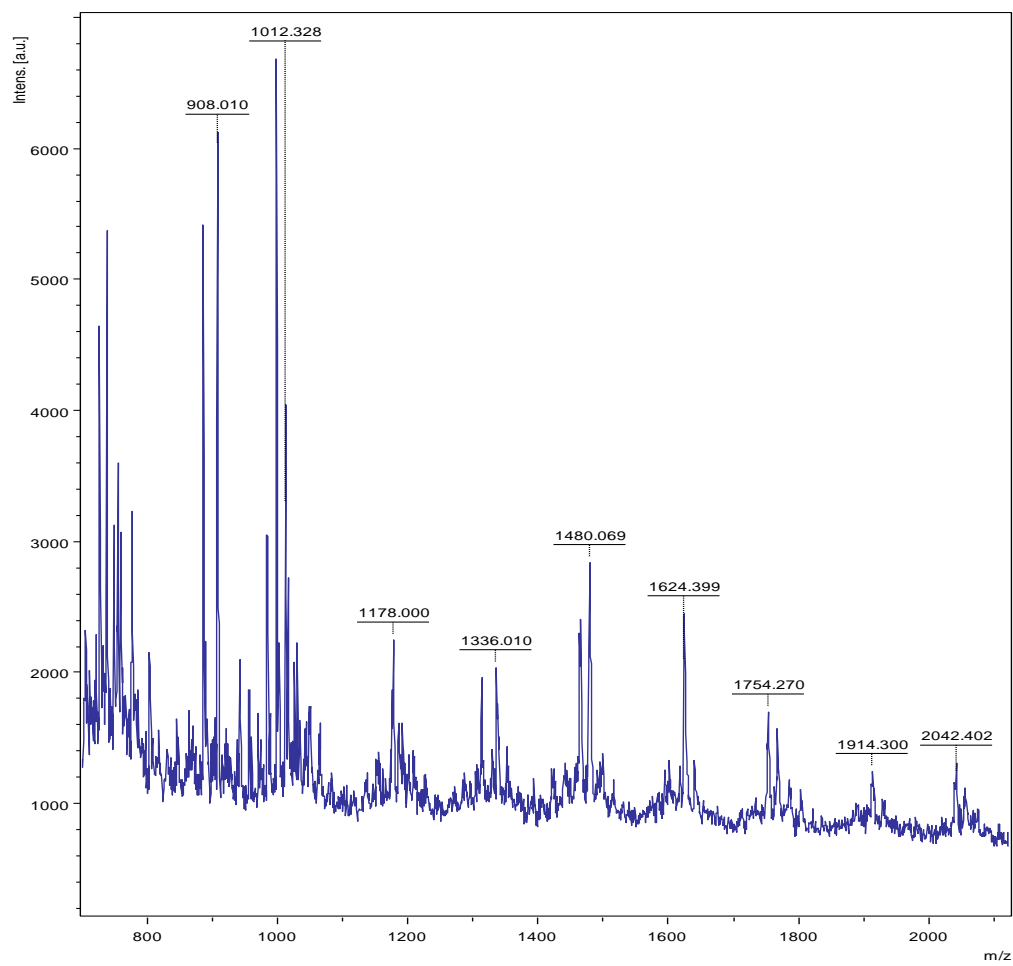


Figure 18. MALDI-TOF mass spectrum of the collected fraction from a diol column of aged chokeberry juice after LH-20 solid phase extraction.

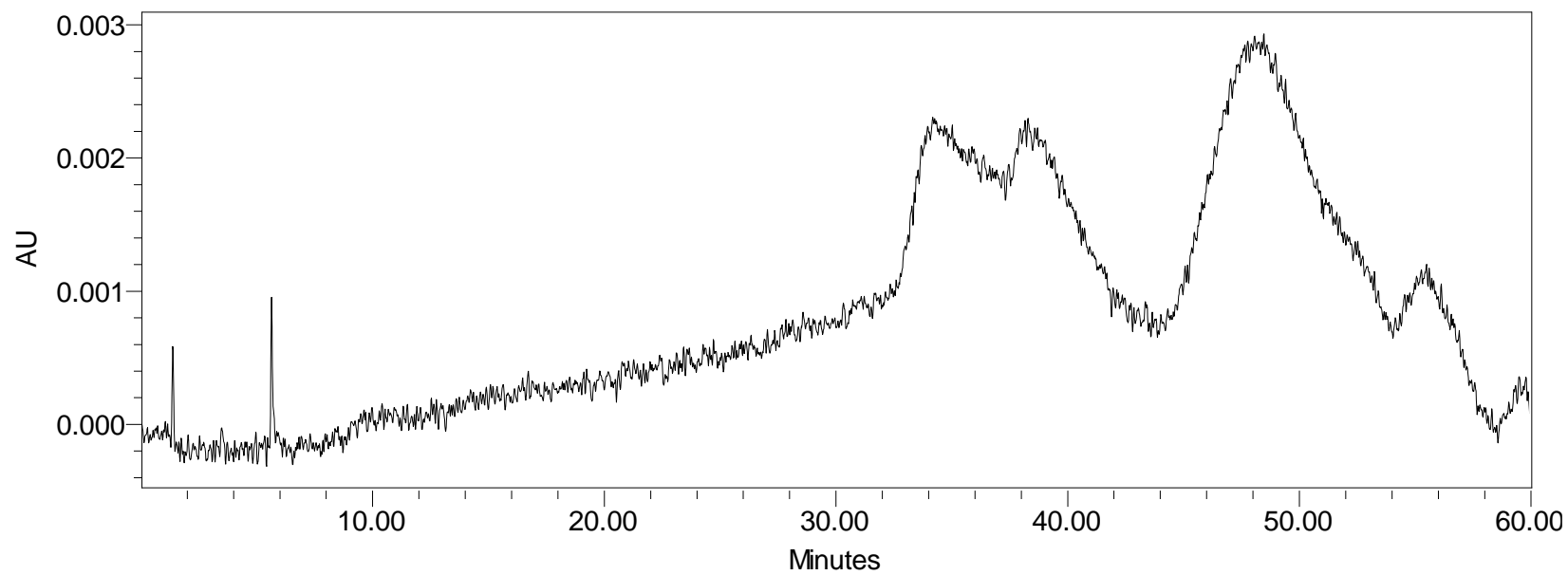


Figure 19: Chromatogram of sulfoxyethyl cellulose SPE eluent on Develosil diol column at 510 nm.

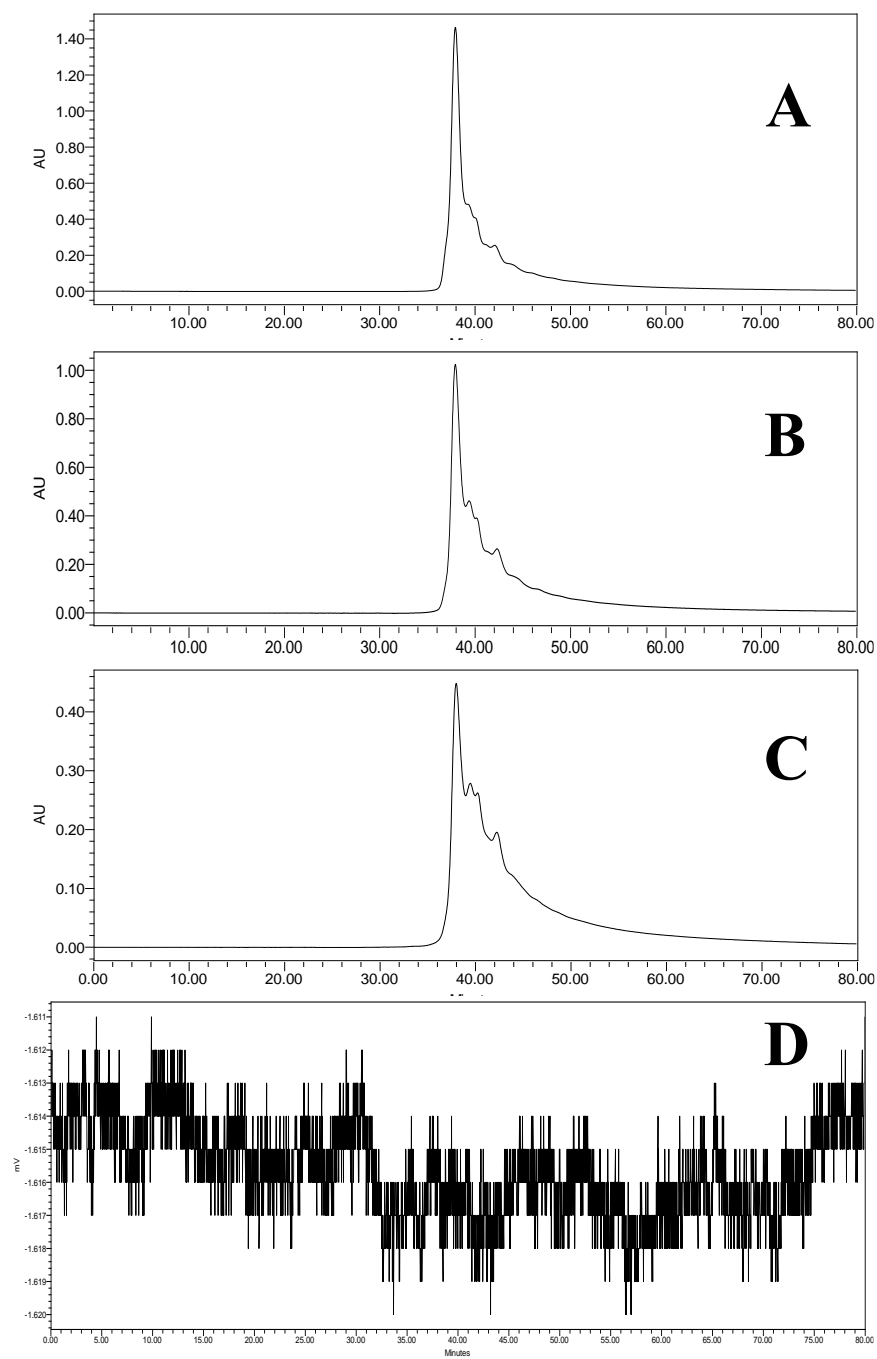


Figure 20: Chromatogram of chokeberry juice on TSKgel size exclusion HPLC column. Pasteurized juice at 510 nm (A), 1 month aged juice at 510 nm (B), 6 month aged juice at 510 nm (C), and fluorescence signal of average juice sample (D).

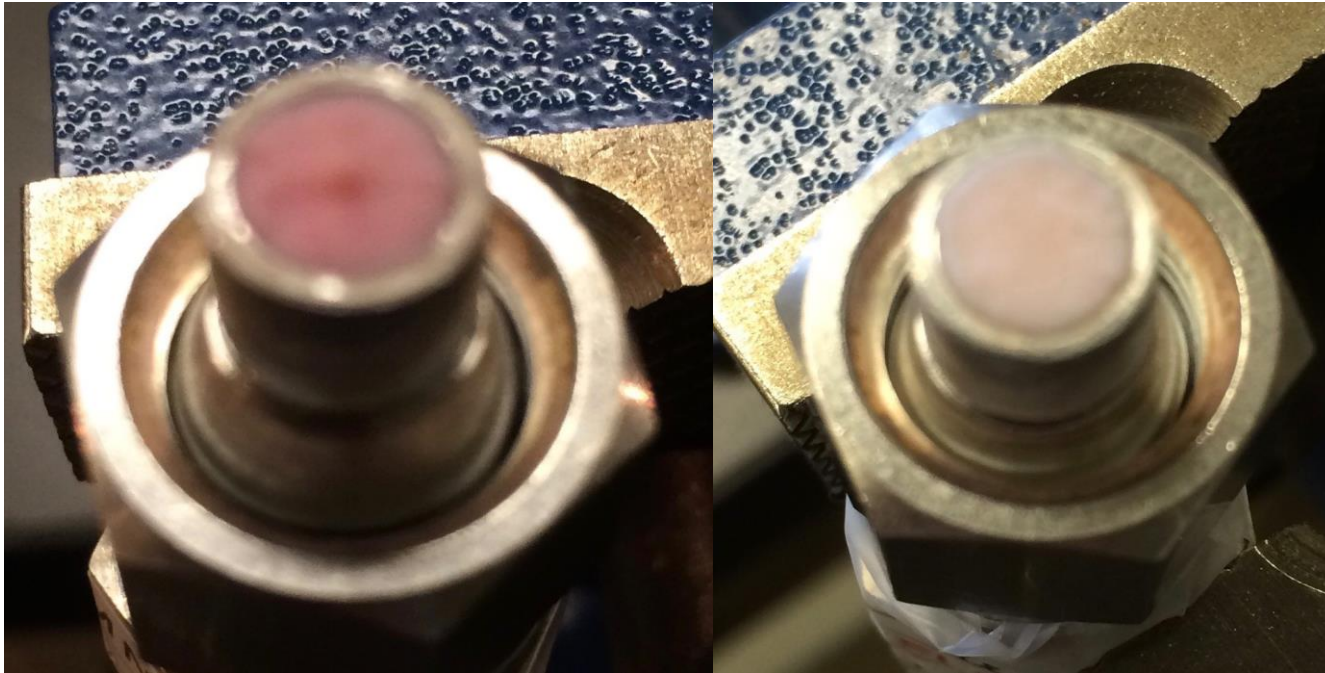


Figure 21: Photograph of TSKgel column inlet before and after reversed flow cleaning.

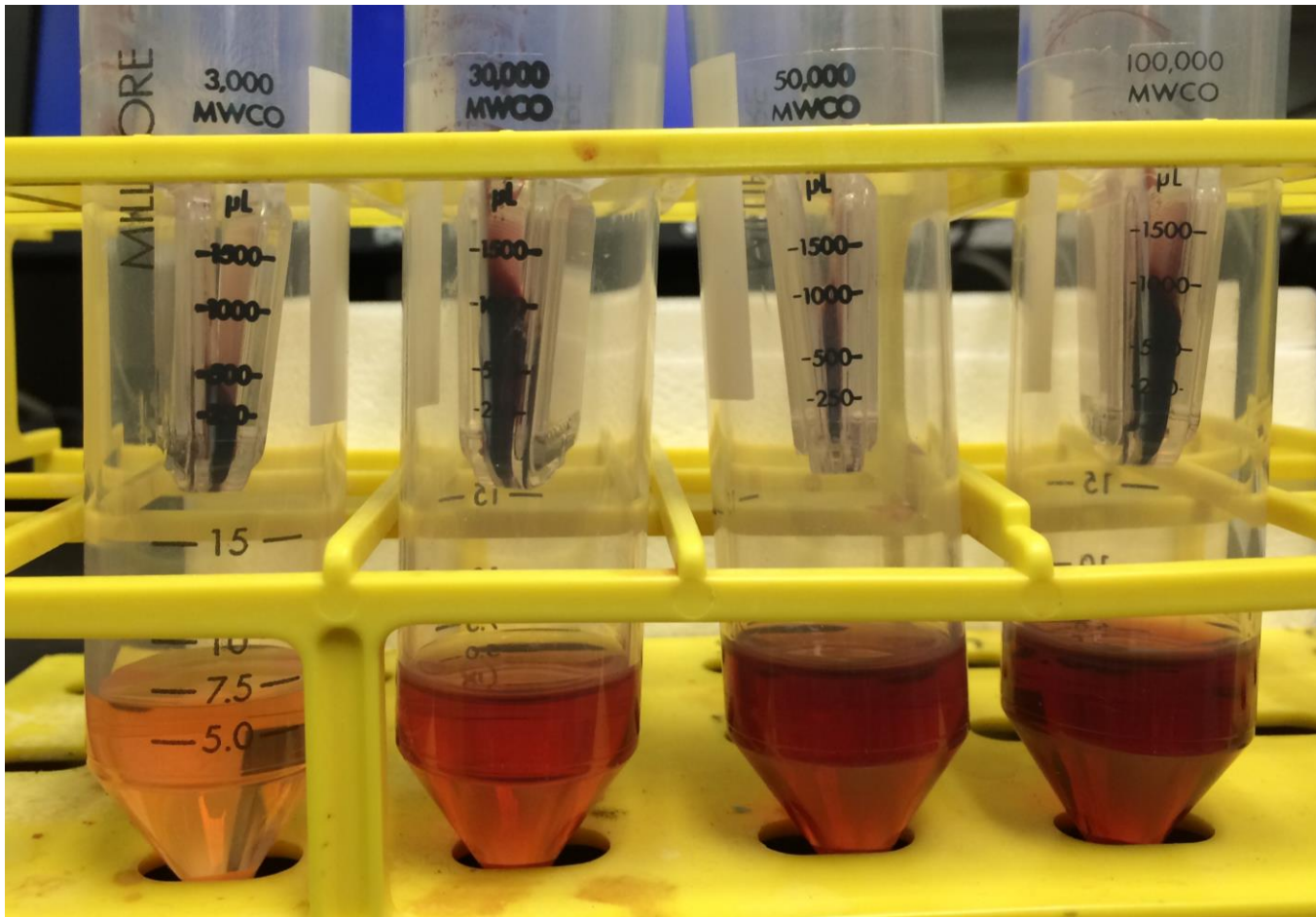


Figure 22: Photograph of molecular weight cutoff filters of 3,000, 30,000, 50,000, and 100,000 after centrifugation of aged chokeberry juice.

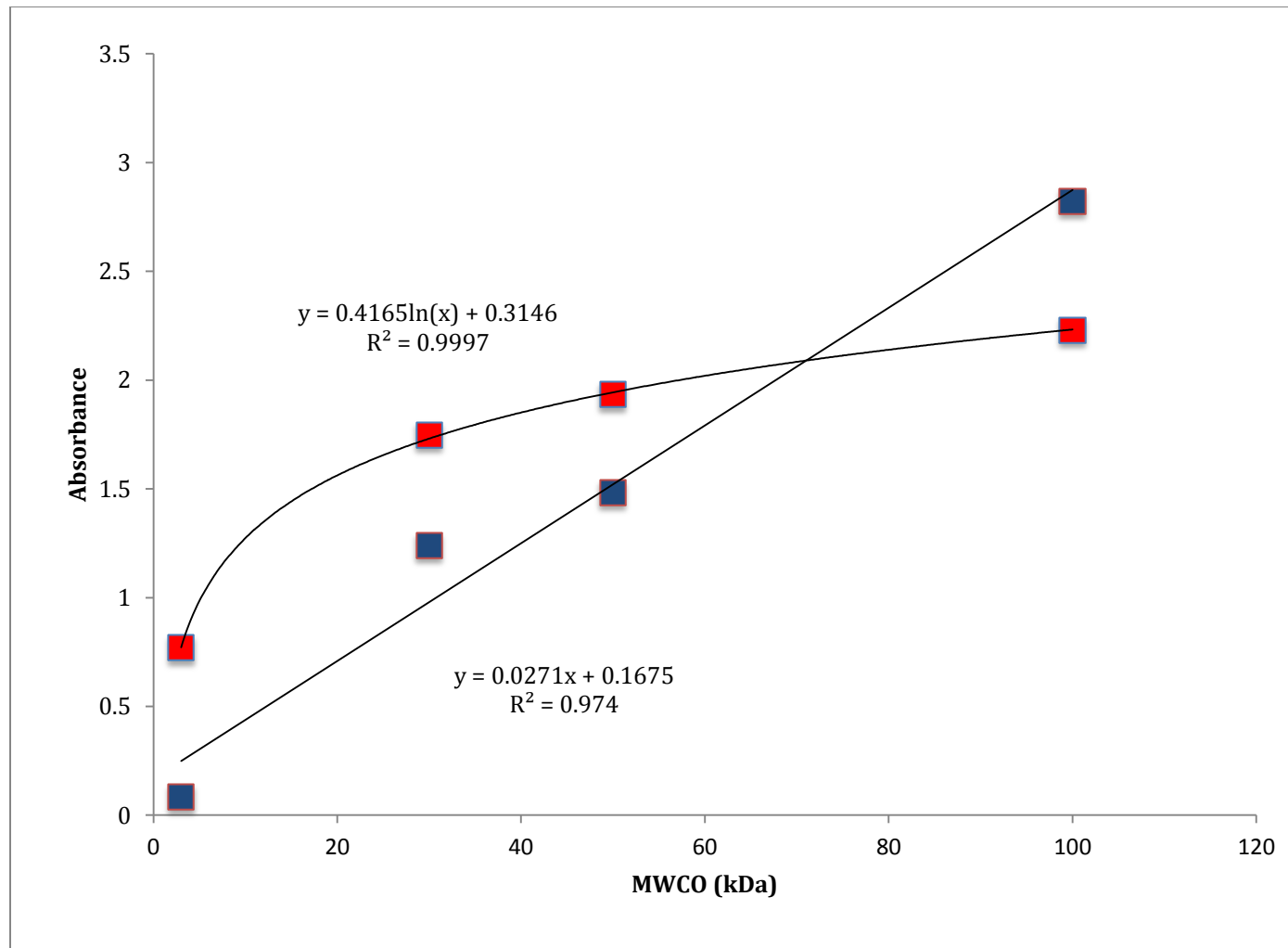


Figure 23: Absorbance (510 nm) of molecular weight cutoff filters of aged chokeberry juice (blue) and pasteurized chokeberry juice (red).

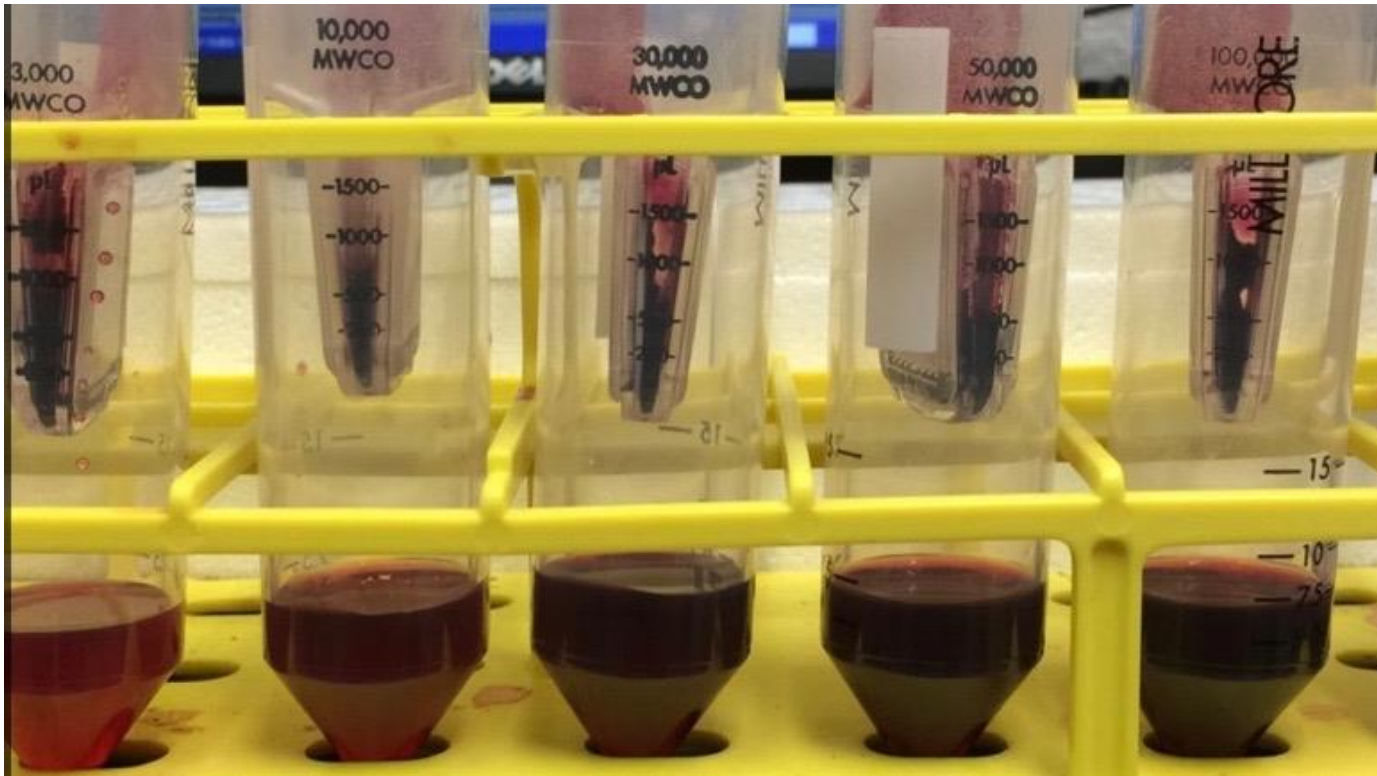


Figure 24: Photograph of molecular weight cutoff filters of 3,000, 10,000, 30,000, 50,000, and 100,000 after centrifugation of pasteurized chokeberry juice.

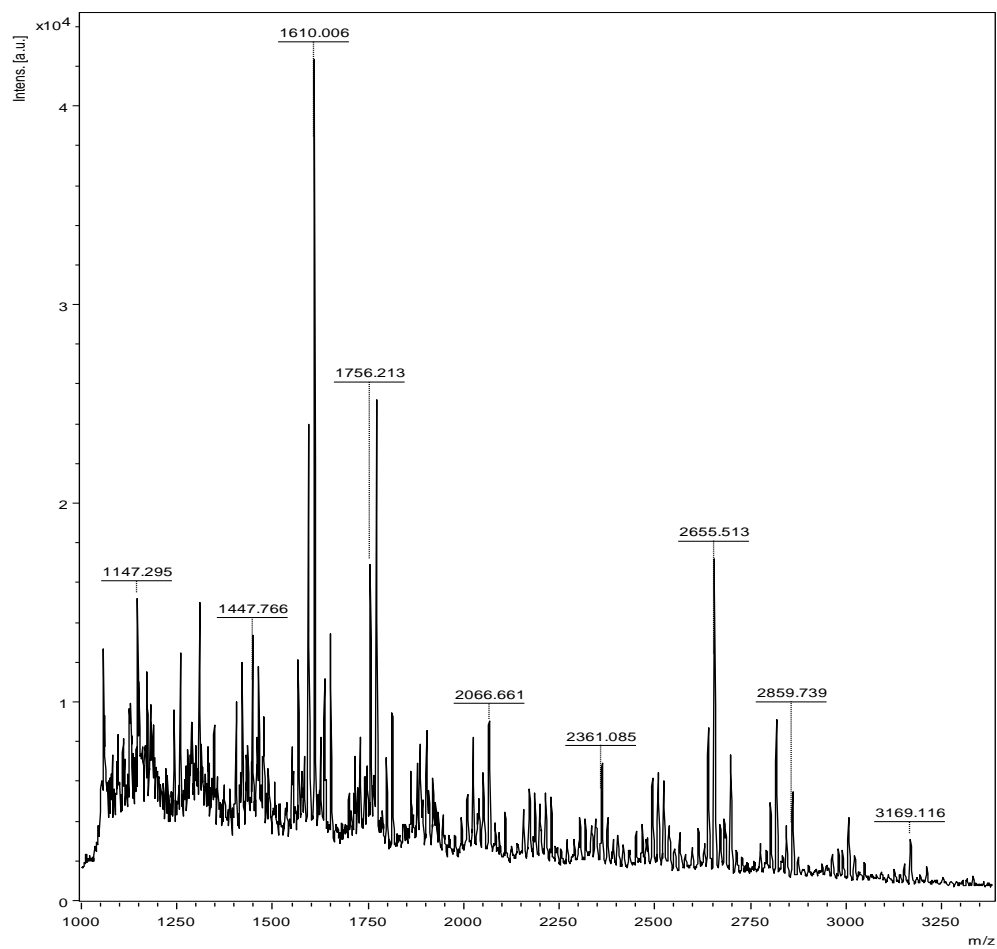


Figure 25: MALDI-TOF mass spectrum of 30,000-50,000 Dalton molecular weight cutoff filters of aged chokeberry juice.

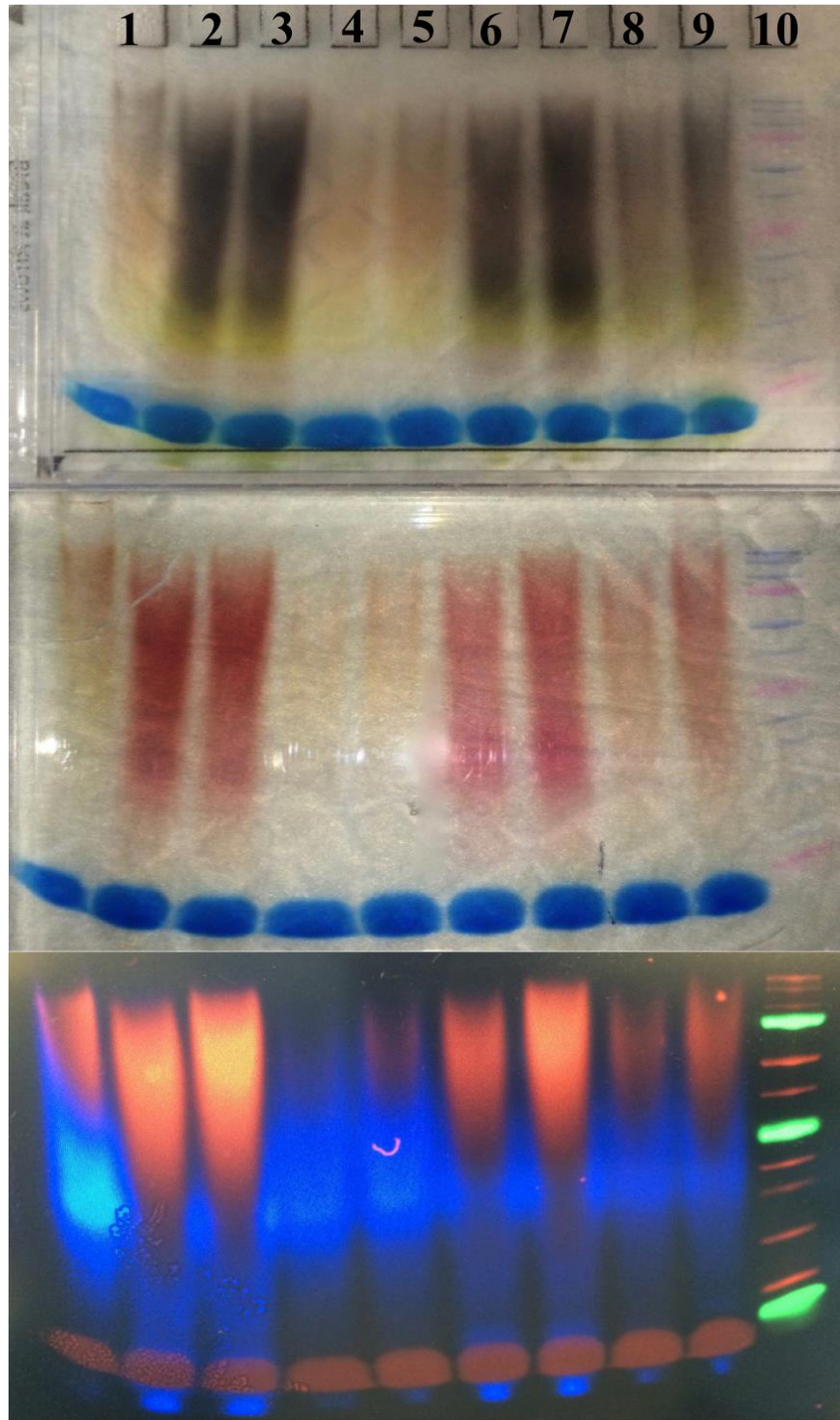


Figure 26: Polyacrylamide gel electrophoresis of chokeberry juice at running pH 8.3 (top), acidified to pH 2 (middle), Fluoro RGB scan (bottom). Lane 1: 3 year aged juice, lanes 2-5: 6 months aged juice after MWCO filters: 0-50 kDa (2), 0-100 kDa (3), 10-30 kDa (4), 30-50 kDa (5), lanes 6-9: pasteurized juice after MWCO filters: 0-50 kDa (6), 0-100 kDa (7), 10-30 kDa (8), 30-50 kDa (9), lane 10: protein standard.

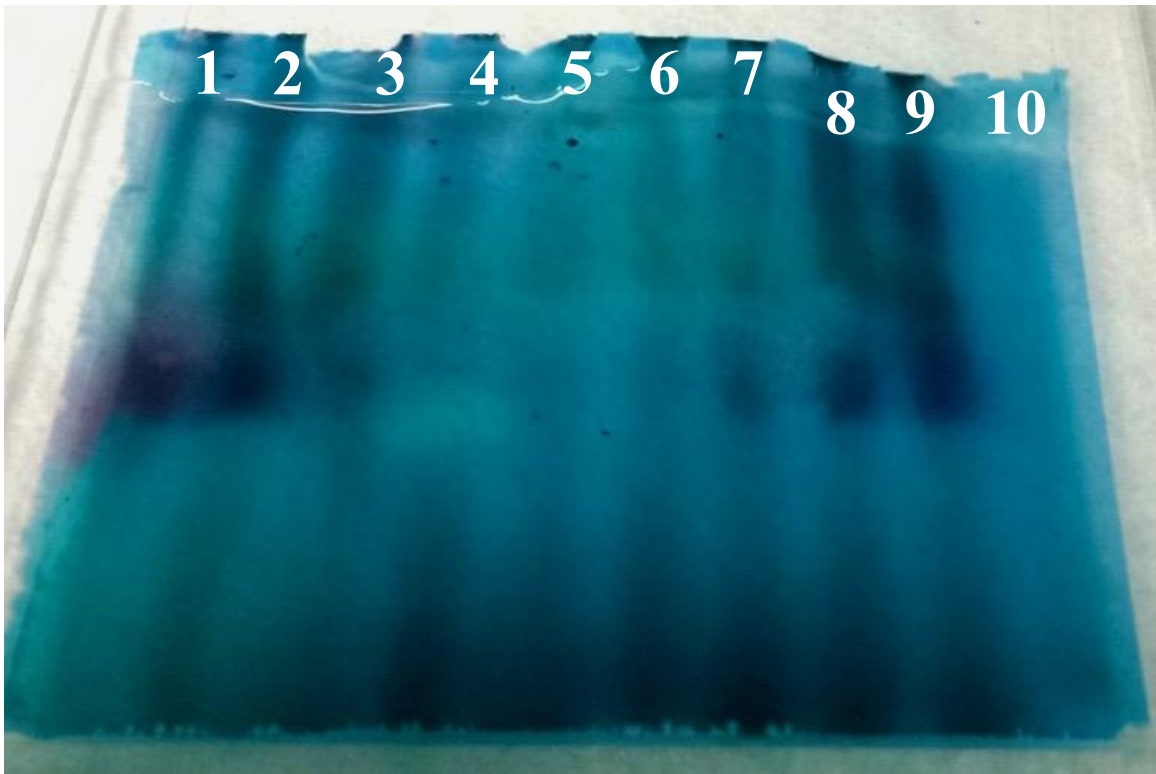


Figure 27: Low pH polyacrylamide gel electrophoresis of chokeberry juice. Lane 1: unpasteurized juice after C18 SepPak, lane 2: unpasteurized juice, lane 3: pasteurized juice after C18 SepPak, lane 4: pasteurized juice, lane 5: 6 months aged juice after C18 SepPak, lane 6: 6 months aged juice, lane 7: pasteurized juice after MWCO filter 0-50 kDa, lane 8: pasteurized juice after MWCO filter 0-100 kDa, lane 9: 6 months aged juice after MWCO filter 0-50 kDa, lane 10: protein standard.

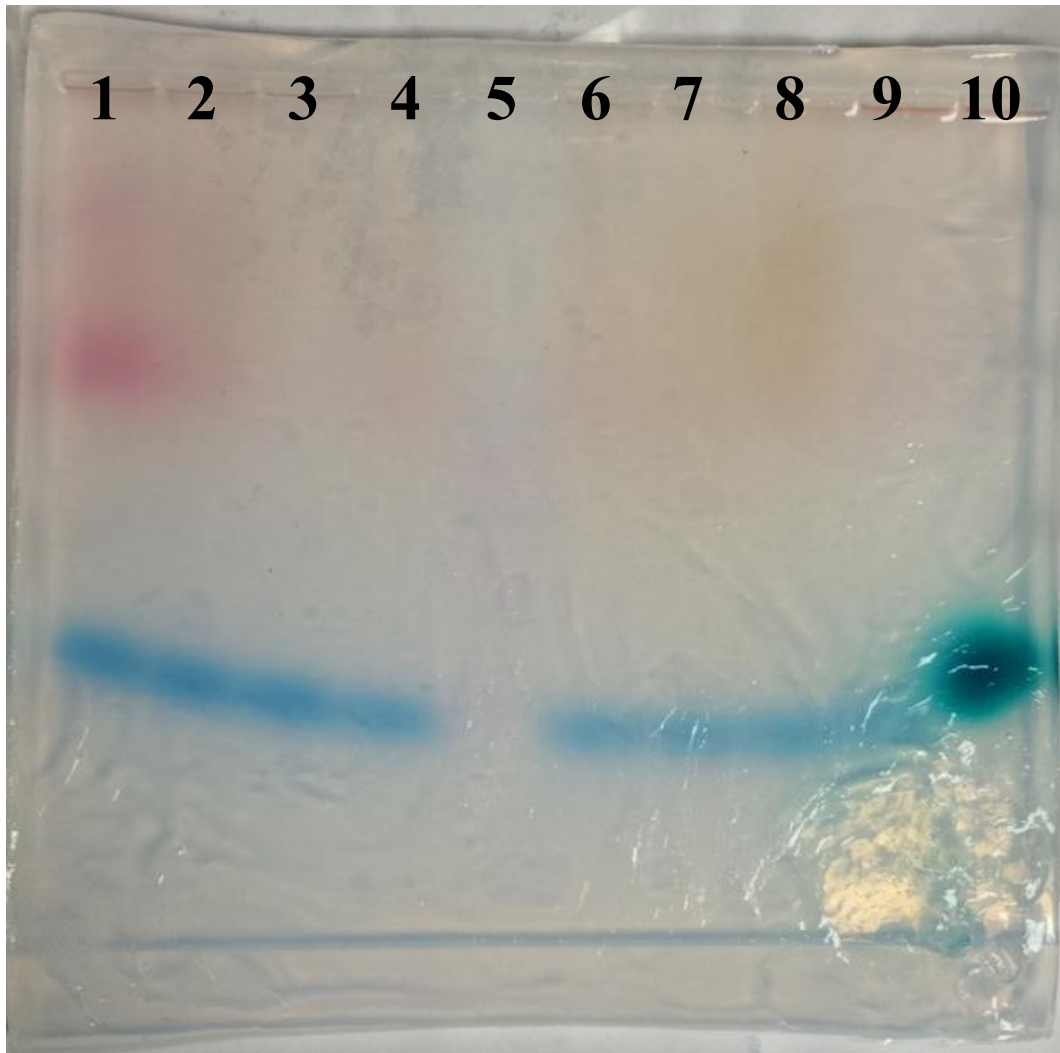


Figure 28: Agarose gel electrophoresis of chokeberry juice. Lane 1: unpasteurized juice after C18 SepPak, lane 2: pasteurized juice after C18 SepPak, lane 3: 6 months aged juice after C18 SepPak, lane 4: pasteurized juice after MWCO filter 0-50 kDa, lane 5: protein standard, lane 6: pasteurized juice after MWCO filter 0-100 kDa, lane 7: 6 months aged juice after MWCO filter 0-50 kDa, lane 8: 6 months aged juice after MWCO filter 0-100 kDa, lane 9: unpasteurized juice, lane 10: pasteurized juice.

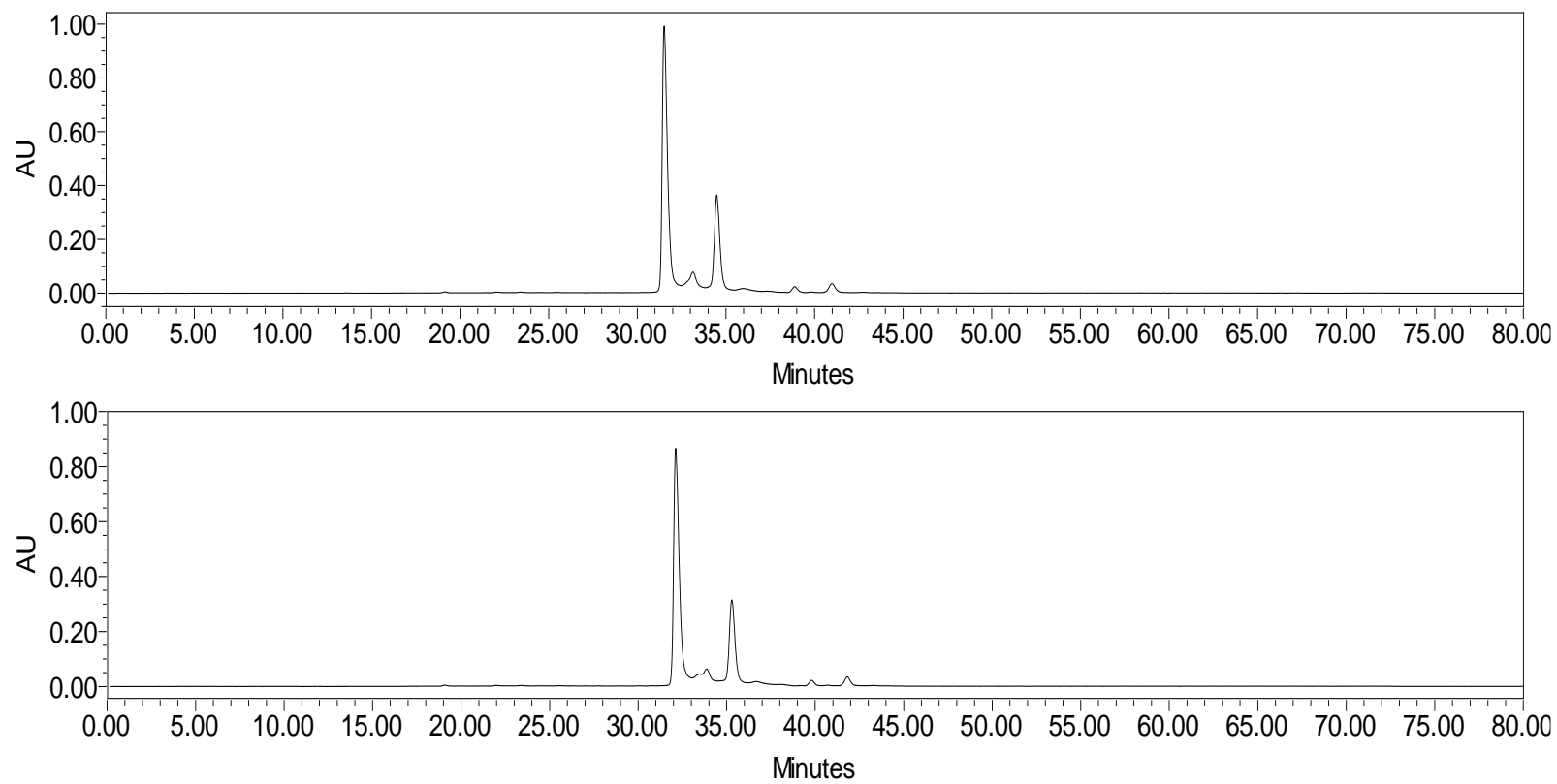


Figure 29: Fresh chokeberry juice chromatograms at 510 nm before (top) and after (bottom) ultrasonication for 60 minutes.

CHAPTER 4. Ascorbic acid-catalyzed degradation of cyanidin-3-glucoside: Proposed mechanism and identification of a novel hydroxylated product

Nathan B. Stebbins¹, Luke R. Howard^{*1}, Ronald L. Prior¹, Cindi Brownmiller¹, Rohana Liyanage², Jackson O. Lay², Xiaoyu Yang³, Steven Yue Qian³

¹University of Arkansas, Department of Food Science, Fayetteville, Arkansas 72704, USA

²University of Arkansas Statewide Mass Spectrometry Facility, Fayetteville, Arkansas 72701, USA

³North Dakota State University, Department of Pharmaceutical Science, Fargo, North Dakota 58108, USA

Corresponding author: Dr. Luke Howard, Department of Food Science, University of Arkansas, 2650 N. Young Avenue, Fayetteville, AR 72704, USA. Tel.: 1 479 575 2978; Fax: 479 575 6936; E-mail: lukeh@uark.edu

This manuscript is published in *J. Berry Res.* **2016**, *6*, 175-187.

Abstract

BACKGROUND: Many brightly colored fruits and vegetables owe their pigmentation and beneficial health effects to anthocyanins. Unfortunately, anthocyanins in the presence of ascorbic acid are readily degraded over juice processing and storage, which adversely affects color stability and potential health benefits.

OBJECTIVE: This project focused on the effect of ascorbic acid as a catalyst in anthocyanin degradation.

METHODS: The project involved searching for novel pigmented compounds in a simple model system composed of the most common anthocyanin cyanidin-3-*O*- β -glucoside and ascorbic acid, and a second model system consisting of blackberry extract supplemented with ascorbic acid. Degradation products were identified by HPLC-PDA and HPLC-MS. ESR was used to monitor hydroxyl radical formation in the model systems.

RESULTS: Over 72 hours at ambient temperature, 67% of cyanidin-3-glucoside was lost in the model system during which time an unknown pigmented compound was formed. The unknown compound was also formed in a more complex model system consisting of blackberry extract and ascorbic acid. HPLC with PDA monitoring at 510 nm was used to detect a novel compound and LC-ESI-MS³ allowed a proposed structure to be built based on the fragmentation patterns. The unknown structure formed via oxidation of cyanidin 3-glucoside by ascorbic acid was identified as 6-hydroxy-cyanidin-3-glucoside. Production of hydroxyl radical in the base and blackberry model systems was confirmed by ESR.

CONCLUSIONS: We propose that the pigmented compound is formed from hydroxyl radicals via the Haber-Weiss reaction. The addition of food grade hydroxyl radical scavengers to juices may be a viable treatment to prevent ascorbic acid catalyzed degradation of anthocyanins.

Keywords: Anthocyanin, ascorbic acid, blackberry, cyanidin-3-glucoside, degradation product, hydroxyl radical, tandem mass spectrometry

Introduction

The vibrant blue, red, and purple colors of berries and many other fruits are due to anthocyanins. In addition to serving as pigments, anthocyanins are thought to afford protection against chronic diseases through antioxidant, anti-inflammatory, and anti-cancer activities [1]. Fresh berry consumption is limited by seasonal availability and short shelf life. Therefore, many berries are processed and consumed in shelf stable products such as juices, jellies, and jams. Unfortunately, anthocyanins are susceptible to degradation during berry processing and storage of processed products at ambient temperature [2]. Anthocyanin losses have been attributed to many factors including exposure to heat, oxygen, enzymes, metals, and ascorbic acid [3-6].

Oxidation by secondary oxidizing agents, such as hydroxyl radicals and superoxide, are thought to be contributing factors to color deterioration [7].

Many studies report that anthocyanins and the color of processed berry products are unstable in the presence of ascorbic acid [8-11]. Two different mechanisms have been proposed for ascorbic acid (AA) catalyzed degradation of anthocyanins. The first involves a condensation reaction between anthocyanins and other components, such as ascorbic or organic acids [3, 8], and the second involves a radical mechanism leading to cleavage of the anthocyanin into phenolic acids [11, 12]. Much of the research related to structural changes in anthocyanins has been conducted on wine. Pyranoanthocyanins, which are anthocyanin conjugates with an additional pyran ring between C-4 and the 5-OH have been identified in several studies [13-15]. Pyranoanthocyanins can be formed from reactions between anthocyanins and fermentation products, such as acetaldehyde, pyruvic and acetoacetic acids [13, 16], as well as hydroxycinnamic acids [17, 18]. These compounds, which are consistent with the condensation product hypothesis proposed by Jurd [8] appear more pH stable [19] and have been detected in wine stored for several years [20]. Other than pyranoanthocyanins, polymeric pigments are a potential source of long-term color stability [21]. Polymeric pigments are the condensation product of anthocyanins and flavanols [22] and most often detected by MALDI-TOF-MS [23-25].

The fate of anthocyanins in the presence of AA is unclear. This study was undertaken to identify novel degradation products of anthocyanins formed via AA mediated oxidation using a C3G model system and blackberry model system.

Materials and methods

Materials

Cyanidin-3-*O*- β -glucoside standard (>95%) was purchased from Chromadex (Irvine, CA, USA). HPLC grade methanol was purchased from EMD Millipore (Billerica, MA, USA) and formic acid from Fischer-Scientific (Fair Lawn, NJ, USA). ACS grade L-ascorbic acid was obtained from VWR International (Radnor, PA, USA), Dimethyl sulfoxide (DMSO) was obtained from Sigma-Aldrich (St. Louis, MO, USA). High-purity α -(4-pyridyl-1-oxide)-*N*-tert-butyl nitron (POBN) was purchased from Alexis Biochemicals (San Diego, CA, USA). The University of Arkansas Horticulture department provided frozen blackberries.

Formulation model systems

Formulation of base model system and blackberry model system for HPLC and HPLC/MS analyses

The base model system contained cyanidin-3-*O*- β -glucoside (200 μ g/mL) and ascorbic acid (320 μ g/mL) dissolved in water acidified to pH 3.6 by HCl. Each 4 mL replicate was injected once every 70 minutes based on the HPLC gradient duration over 72 hours. The aqueous blackberry extract was concentrated to 200 μ g/mL C3G and supplemented to contain 320 μ g/mL AA forming the blackberry model system. Duplicates of each system were performed.

Formulation of base model system and blackberry model system for ESR analysis

500 μ L of 200 ppm blackberry extract solution (or 200 ppm C3G solution) was mixed with 5 μ L of AA stock solution (32 mg/mL) to generate 320 ppm (0.32 mg/mL, final concentration) in the sample. In order to trap free radicals generated from the system, 50 mM

POBN and 10 mM DMSO was added to the sample. The system was maintained at room temperature. After mixing the AA, DMSO, POBN and blackberry extract (or C3G), the samples were injected into ESR for analysis.

Anthocyanin analysis

Blackberry extraction

Frozen blackberries (18.74 g) were thawed at room temperature and triple extracted with 20 mL methanol/water/formic acid (60:37:3 v/v/v), followed by 20 mL acetone/water/acetic acid (70:29.5:0.5 v/v/v) using an IKA-T18 Ultra-Turrax (Wilmington, NC, USA) [26]. After filtering through Miracloth (CalBiochem, La Jolla, CA), the combined filtrates were evaporated to dryness in a Speed Vac Plus SC210A (Cambridge Scientific, Cambridge, MA) and brought up into 1 mL acidified water (pH 3.6 via HCl).

Alstroemeria extraction

Dark red *Alstroemeria* flowers (11.09 g) (species and variety unknown) were extracted with 50 mL methanol/water/formic acid (60:37:3) using an IKA-T18 Ultra-Turrax (Wilmington, NC, USA). Samples were injected without further concentration for qualitative analysis and used the following HPLC-PDA and HPLC-ESI-MS³ methodology.

HPLC-PDA analysis of anthocyanins and degradation products

Chromatographic analyses were performed using dual Waters 515 pumps, 717plus autosampler, and a Waters 996 photodiode array detector (Milford, MA, USA). A Waters Symmetry C₁₈ column (4.6 x 250 mm; 5µm) separated the analytes using a 1.2 mL/min flow rate

with 5% formic acid in water (Solvent A) and methanol (Solvent B). The elution began with 5% B and rose to 15% B in 10 min, from 15% to 35% B in 35 min, from 35% to 100% B in 5 min, followed by an isocratic wash for 10 min at 100% B, then re-equilibration of the column with 5% B for 10 min. UV-visible spectra were monitored from 200-700 nm and peak areas were recorded at 510 nm.

HPLC-electrospray ionization tandem mass spectrometry (LC-ESI-MSⁿ) analysis of degradation products

LC-ESI-MSⁿ analysis was conducted using an HP 1000 series HPLC and a Bruker Esquire 2000 quadrupole ion trap mass spectrometer. Samples from both model system and blackberry extracts were separated using a Waters Symmetry (4.6 x 250 mm; 5 μ m) column and gradient as described above. The mass spectrometry analysis was performed in both positive and negative ion modes under the following conditions: capillary voltage at 4 kV with polarity [+] for negative ion mode and [-] for positive ion mode analysis, nebulizer gas pressure 32 psi, dry gas flow 12 L/min, and skim voltage at 53.7 V and again polarity switched for respective mode. Ions were isolated and fragmented in quadrupole ion trap with excitation amplitude of 1.2 volts.

Direct infusion electrospray ionization ion cyclotron resonance (ICR) mass spectrometry analysis of degradation product

Bruker ApexOe 9.4 T ion cyclotron resonance mass spectrometer was used in its positive ion mode by infusing the sample using syringe pump operating at 180 μ l/hr. Capillary voltage at 4.4 kV, spray shield voltage at 3.8 kV with polarity [-], nebulizer gas pressure at 1.2 L/min, dry gas flow at 4.4 L/min with dry gas temperature at 200 °C conditions were used during the

analysis. The settings favor both low and high molecular weight trapping conditions in the ICR cell.

Electron spin resolution (ESR) analysis

Electron spin resonance analyses were operated on a Bruker Elexsys spectrometer at 9.76 GHz and room temperature. ESR settings were modulation frequency, 100 kHz; modulation amplitude, 1.0 G; microwave power, 20 mW; receiver gain, 2.5×10^5 ; sweep width, 70 G; and time constant, 0.65 s.

Results and discussion

Unknown formation in base model and blackberry systems

Cyanidin-3-O- β -glucoside was selected for study in the model system since it is the most common anthocyanin in blackberries [27] and in nature [28]. The ascorbic acid:anthocyanin ratio used in the model system is similar to that found in strawberries [29, 30].

To search for potential degradation products of anthocyanins, the base model system containing C3G and AA was scanned for emerging peaks at 510 nm. One salient peak appeared to increase as soon as one hour after addition of AA to the base model system. The unknown peak continued to increase in area for approximately 30 hours before quickly falling to near zero area under the curve by 72 hours. Compound 1 had a λ_{max} of 500.6 nm; therefore Fig. 2 displays the PDA signals of Compound 1 and C3G at 500 nm at 30 hrs. Compound 1 demonstrated greater hydrophilicity than C3G eluting about 10 minutes earlier than C3G. The same peak in the blackberry system also had an earlier retention time and lower λ_{max} than C3G, but had nearly a 10-fold drop in peak area. The greater number of polyphenolic, radical-scavenging analytes in

the blackberry system likely quenched the reaction mechanism resulting in protracted formation and lower production of Compound 1.

The dramatic effect of AA on the degradation of C3G is featured in Fig. 4. In the C3G control, the peak area remains nearly constant over 70 hours, while the addition of AA resulted in a rapid decrease in C3G peak area. This agrees with the findings of other researchers that anthocyanins are readily degraded in the presence of AA [10, 11].

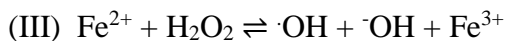
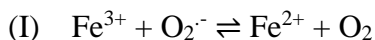
Structural elucidation of compound 1

Tandem mass spectrometry yielded beneficial data toward structural elucidation, as seen in Table 1 and Fig. 5. Electrospray and tandem mass spectrometry are excellent tools for anthocyanin identification [31]. Comparing spectra of C3G and Compound 1, it was clear that Compound 1 had an m/z value 16 amu greater than C3G. We suspect Compound 1 to contain an additional hydroxyl group on one of the unsubstituted carbons. Compound 1 eluted earlier than C3G, which demonstrates increased hydrophilicity, strengthening the argument for an additional hydroxyl group. Anthocyanins often form polymers with a C4 \Rightarrow C8 linkage, but sometimes feature a C4 \Rightarrow C6 [32]. The dearth of reactivity at C6 in polymers is likely due to steric hindrance, which is not an issue in the hydroxyl addition. A related compound is 6-hydroxycyanidin-3-rutinoside, which is found in *Alstroemeria* flowers and described as less stable than cyanidin [33]. An extract of dark red *Alstroemeria* flowers was analyzed with tandem mass spectrometry and compared to the MS³ of Compound 1 (Fig. 5). Although *Alstroemeria* contains a rutinoside, the sugar is fragmented by tandem mass spectrometry allowing a direct comparison between the aglycone: 6-hydroxycyanidin. Therefore we propose that Compound 1 is 6-hydroxy-cyanidin-3-O- β -glucoside (Fig. 1). This is further validated by the observed peak at m/z

465.1030 by high resolution mass data for Compound 1 in the base model system. Mass error of 0.5 ppm between observed and expected mass (465.1028) lead to possible elemental composition as the targeted compound elemental composition, C₂₁H₂₁O₁₂. The search for the elemental composition was done by making no assumptions for the presence or absence of any elements.

Proposed mechanism responsible for the formation of compound 1

Ascorbic acid can have varied effects on anthocyanin content. It has been reported that AA can reduce enzymatic degradation of anthocyanins in grape juice [34]. Alternatively, AA could produce hydrogen peroxide that would bleach anthocyanins [35-37]. Regardless of the presence of oxygen or nitrogen, AA had a significant effect on anthocyanin degradation [3]. This finding led to an agreement with Jurd [8] that a condensation reaction occurred between the anthocyanin and AA, which broke the conjugation and resulted in a loss of color. However, Jurd's condensation reaction mechanism includes a pentavalent carbon in the final product. The current research did not detect a condensation product between AA and C3G. In the absence of AA, a nitrogen flush had a small protective effect on anthocyanin retention compared to an oxygen rich environment [3], demonstrating a greater effect of AA than oxygen.



Hydrogen peroxide formed via the Haber-Weiss reaction (Eq. 1-3) [38] of AA and iron or copper is the likely catalyst in forming Compound 1 from C3G [39]. There is very little iron and copper

in the water used in the model system, but it may be enough to initiate the Haber-Weiss reaction. Although iron is a more efficient catalyst than copper [36], the model system contains more copper. Martell found that extremely low levels (0.7 μM) of copper still exhibited catalytic activity and led to hydroxyl radical production [40]. The water used in the model and blackberry systems contained 0.2 μM copper, which is a comparable concentration. Several researchers have studied the degradation kinetics of anthocyanin by H_2O_2 [41-44], but none reported the presence of Compound 1. Additionally, Tsuda et al. used a strong radical initiator in a model system with C3G, which resulted in the formation of protocatechuic acid and 4,6-dihydroxy-2-*O*- β -glucosyl-3-oxo-2,3-dihydrobenzofuran [45]. However, neither of these compounds were detected at 280 nm in our model systems.

Figure 6 depicts our proposed mechanism of formation for Compound 1 involving the hydroxyl radical from hydrogen peroxide. Since Compound 1's λ_{max} is 500.6 nm, it must retain conjugation throughout the π system and the mechanism must agree with the preservation of conjugation. The hydroxyl radical likely attacks C-6 because that follows an *ortho*-addition between two hydroxyl groups on C-5 and C-7. Hydroxyl radical *ortho*-additions had the highest rate constants and lowest activation energy compared to *meta*- and *para*-additions to aromatic compounds [46]. There is potential for the hydroxyl group to add to C-8, but we do not see any peak separation or splitting via HPLC indicating a majority, if not the entire reaction proceeds to C-6 or the two positional isomers elute simultaneously. The instability of Compound 1 could be caused by the increase in *o*-quinone formation since the additional hydroxyl group allows *o*-quinone formation with either C-5 & C-6 or C-6 & C-7. Given the similarity in structure between C3G and Compound 1, their molar absorptivity constants would be similar and allow comparison of their peak areas. In the model system, the area at Compound 1's C_{max} is $7.56 \pm$

0.53 % of the area of C3G's degradation at that time. The blackberry system had even less of a conversion of C3G to Compound 1 with $1.03 \pm 0.22\%$ of the area converted. The low transformation rate is indicative of a radical mechanism.

Confirmation of hydroxyl radical in the formation of compound 1

To confirm the presence of hydroxyl radical, electron spin resonance (ESR) was used to analyze the base model system and blackberry model system supplemented with AA. Due to the low stability of HO[•] spin adduct, the reaction between dimethyl sulfoxide (DMSO) and HO[•] has been used to enhance the spin trapping detection of HO[•] [47]. This method detects the methyl radical ([•]CH₃) generated from the reaction of DMSO and HO[•] instead of directly trapping HO[•]. In Fig. 7, the ESR spectrum we see in 5) showed the signals of [•]CH₃ indicating HO[•] is formed from the system containing blackberry extract, ascorbic acid, POBN, and DMSO. The signals we see in 6) are stronger than those in 5) mainly due to the use of pure compound C3G. The generation of HO[•] from the reaction of blackberry extract and ascorbic acid support our proposed mechanism.

Conclusions

The addition of AA led to an increased rate of degradation of C3G in a model system based on the AA:C3G ratio found in strawberries. The degradation products of C3G were monitored for red colored compounds and the proposed structure of 6-hydroxy-cyanidin-3-glucoside was detected and described based on tandem mass spectrometric results. The role of hydroxyl radical in formation of the novel compound was confirmed by ESR analysis. The peak area of the degradation product accounted for less than 8% of the area of C3G degraded over time. Additional research is needed to identify other degradation products of anthocyanins

catalyzed by ascorbic acid and to determine if hydroxylation of other polyphenols occurs via AA catalyzed oxidation. The addition of food grade hydroxyl radical scavengers to berry juices may be a viable treatment to prevent ascorbic acid catalyzed degradation of anthocyanins.

References

- [1] Pojer E, Mattivi F, Johnson D, Stockley CS. The case for anthocyanin consumption to promote human health: A review. *Comp. Rev. Food Sci. Food Safety*. 2013, 12:483-508.
- [2] Patras A, Brunton NP, O'Donnell C, Tiwari BK. Effect of thermal processing on anthocyanin stability in foods; mechanisms and kinetics of degradation. *Trends Food Sci & Tech*. 2010, 21:3-11.
- [3] Poeschl L, Langston MS, Wrolstad RE. Color degradation in an ascorbic acid-anthocyanin-flavanol model system. *J. Food Sci*. 1981, 46(4):1218-1222.
- [4] Kader F, Irmouli M, Nicholas JP, Metche M. Involvement of blueberry peroxidase in the mechanisms of anthocyanin degradation of blueberry juice. *J. Food Sci*. 2002, 67(3):910-915.
- [5] Li H, Guo A, Wang H. Mechanisms of oxidative browning of wine. *Food Chem*. 2008, 108(1):1-13.
- [6] Wilkes K, Howard LR, Brownmiller C, Prior RL. Changes in chokeberry (*Aronia melanocarpa* L.) polyphenols during juice processing and storage. *J. Agric. Food Chem*. 2014, 62(18):4018-4025.
- [7] Tiwari BK, O'Donnell CP, Cullen PJ. Effect of non thermal processing technologies on the anthocyanin content of fruit juices. *Trends Food Sci. & Tech*. 2009, 20(3):137-145.
- [8] Jurd L. Some advances in the chemistry of anthocyanin-type plant pigments. In: Chichester CO. Ed. *The chemistry of plant pigments*. New York: Academic Press; 1972, 123-142.
- [9] Bradshaw MP, Barril C, Clark AC, Prenzler PD, Scollary GR. Ascorbic acid: A review of its chemistry and reactivity in relation to a wine environment. *Crit. Rev. Food Sci. Nutr*. 2011, 51(6): 479-498.
- [10] Brenes CH, Del Pozo-Insfran D, Talcott ST. Stability of copigmented anthocyanins and ascorbic acid in a grape juice model system. *J. Agric. Food Chem*. 2005, 53(1): 49-56.
- [11] Garcia-Viguera C, Bridle P. Influence of structure on color stability of anthocyanins and flavylium salts with ascorbic acid. *Food Chem*. 1999, 64(1): 21-26.
- [12] Iacobucci GA, Sweeny JG. The chemistry of anthocyanins and related flavylium salts. *Tetrahedron*. 1983, 39(19): 3005-3038.
- [13] Bakker J, Timberlake CF. Isolation, identification, and some characterization of new color-stable anthocyanins occurring in some red wines. *J. Agric. Food Chem*. 1997, 45(1):35-43.
- [14] Fulcrand H, Cameira dos Santos PJ, Sarni-Manchado P, Chaynier V, Favre-Bonvin J. Structure of new anthocyanin-derived wine pigments. *J. Chem. Soc., Perkin Trans. 1*(7):735-739.

- [15] He J, Santos-Buelga C, Mateus N, de Freitas V. Isolation and quantification of oligomeric pyranoanthocyanin-flavanol pigments from red wines by combination of column chromatographic techniques. *J. Chromato A.* 2006, 1134:215-225.
- [16] Blanco-Vega D, Lopez-Bellido FJ, Alia-Robledo JM, Hermosin-Guiterrez I. HPLC-DAD-ESI-MS/MS characterization of pyranoanthocyanin pigments formed in model wine. *J. Agric. Food Chem.* 2011, 59(17): 9523-9531.
- [17] Rein MJ, Ollilainen V, Vahermo M, Yli-Kauhaluoma J, Heinonen M. Identification of novel pyranoanthocyanins in berry juices. *Eur. Food Res. Technol.* 2005, 220(3):239-244.
- [18] Hillebrand S, Schwarz M, Winterhalter P. Characterization of anthocyanins and pyranoanthocyanins from blood orange [*Citrus sinensis* (L.) Osbeck] juice. *J. Agric. Food Chem.* 2004, 52(24):7331-7338.
- [19] Asenstorfer RE, Hayasaka Y, Jones GP. Isolation and structures of oligomeric wine pigments by bisulfite-mediated ion-exchange chromatography. *J. Agric. Food Chem.* 2001, 49(12):5957-5963.
- [20] Monagas M, Gomez-Cordoves C, Bartolome B. Evolution of polyphenols in red wines from *Vitis vinifera* L. during aging in the bottle. *Eur. Food Res. Technol.* 2005, 220(3):607-614.
- [21] Somers TC. The polymeric nature of wine pigments. *Phytochem.* 1971, 10(9):2175-2186.
- [22] Remy S, Fulcrand H, Labarbe B, Cheynier V, Moutounet M. First confirmation in red wine of product resulting from direct anthocyanin-tannin reactions. *J. Sci. Food Agric.* 2000, 80(6):745-751.
- [23] Reed JD, Krueger CG, Vestling MM. MALDI-TOF mass spectrometry of oligomeric food polyphenols. *Phytochem.* 2005, 66(18):2248-2263.
- [24] Krueger CG, Vestling MM, Reed JD. Matrix-assisted laser desorption/ionization time-of-flight mass spectrometry of heteropolyflavan-3-ols and glucosylated heteropolyflavans in sorghum [*Sorghum bicolor* (L.) Moench]. *J. Agric. Food Chem.* 2003, 51(3):538-543.
- [25] Howard LR, Prior RL, Liyanage R, Lay JO. Processing and storage effect on berry polyphenols: challenges and implications for bioactive properties. *J. Agric. Food Chem.* 2012, 60(27):6678-6693.
- [26] Hager TJ, Howard LR, Prior RL. Processing and storage effects on monomeric anthocyanins, percent polymeric color, and antioxidant capacity of processed blackberry products. *J. Agric. Food Chem.* 2008, 56(3):689-695.
- [27] Veberic R, Stampar F, Schmitzer V, Cunja V, Zupan A, Koron D, Mikulic-Petkocsek M. Changes in the contents of anthocyanins and other compounds in blackberry fruits due to freezing and long-term frozen storage. *J. Agric. Food Chem.* 2014, 62(29):6926-6935.

- [28] Francis FJ. Food Colorants: Anthocyanins. *Crit Rev in Food Sci. Nutr.* 1989, 28(4):273-314.
- [29] United States Department of Agriculture- Agricultural Research Service. National nutrient database for standard reference release 27.
- [30] Aaby K, Mazur S, Nes A, Skrede G. Phenolic compounds in strawberry (*Fragaria x ananassa* Duch.) fruits: Composition in 27 cultivars and changes during ripening. *Food Chem.* 2012, 132(1):96-97.
- [31] Giusti MM, Rodriguez-Saona LE, Griffin D, Wrolstad RE. Electrospray and tandem mass spectrometry as tools for anthocyanin characterization. *J. Agric. Food Chem.* 1999, 47(11):4657-4664.
- [32] Kelm MA, Johnson JC, Robbins RJ, Hammerstone JF, Schmitz HH. High-performance liquid chromatography separation and purification of cacao (*Theobroma cacao* L.) procyanidins according to degree of polymerization using diol stationary phase. *J. Agric. Food Chem.* 2006, 54(5):1571-1576.
- [33] Saito N, Yokoi M, Yamaji M, Honda T. Anthocyanidin glycosides from the flowers of *Alstroemeria*. *Phytochem.* 1985, 24(9):2125-2126.
- [34] Talcott ST, Brenes CH, Pires DM, Del Pozo-Insfran D. Phytochemical stability and color retention of copigmented and processed muscadine grape juice. *J. Agric. Food Chem.* 2003, 51(4):957-963.
- [35] Davidek J, Velisek J, Pokorny J. Chemical changes during food processing. Amsterdam: Elsevier 1990. p.448.
- [36] Taqui Khan MM, Martell AE. Metal ion and metal chelate catalyzed oxidation of ascorbic acid by molecular oxygen. I. Cupric and ferric ion catalyzed oxidation. *J. Am. Chem. Soc.* 1967, 89(16):4176-4185.
- [37] Zhao MJ, Jung L. Kinetics of the competitive degradation of deoxyribose and other molecules by hydroxyl radicals produced by the fenton reaction in the presence of ascorbic acid. *Free. Rad. Res.* 1995, 23(3):229-243.
- [38] Graf E, Mahoney JR, Bryant RG, Eaton JW. Iron-catalyzed hydroxyl radical formation. Stringent requirement for free iron coordination site. *J. Biol. Chem.* 1984, 259(6):3620-3624.
- [39] Mahoney JR, Graf E. Role of alpha-tocopherol, ascorbic acid, citric acid and EDTA as oxidants in model systems. *J. Food Sci.* 1986, 51(5):1293-1296.
- [40] Martell AE. Chelates of ascorbic acid: Formation and catalytic properties. In: *Ascorbic acid: Chemistry, metabolism, and uses.* 1982, p. 153-178. DOI:10.1021/ba-1982-0200.ch007

- [41] Ozkan M, Yemenicioglu A, Asefi N, Cemeroglu B. Degradation kinetics of anthocyanins from sour cherry, pomegranate, and strawberry juices by hydrogen peroxide. *Food Chem Tox.* 2002, 67(2):525-529.
- [42] Iversen CK. Black currant nectar: effect of processing and storage on anthocyanin and ascorbic acid content. *J. Food Sci.* 1999, 64(1):37-41.
- [43] Lopez-Serrano M, Ros Barcelo A. H₂O₂-mediated pigment decay in strawberry as a model system for studying color alterations in processed plant foods. *J. Agric. Food Chem.* 1999, 47(3):824-827.
- [44] Sondheimer E, Kertesz ZI. The kinetics of the oxidation of strawberry anthocyanin by hydrogen peroxide. *Food Res.* 1952, 17(1):288-298.
- [45] Tsuda T, Ohshima K, Kawakishi S, Osawa T. Oxidation products of cyanidin-3-O- β -glucoside with a free radical initiator. *Lipids.* 1996, 31(12):1259-1263.
- [46] Kiliç M, Koçtürk G, Nevim S, Çınar Z. A model for prediction of product distributions for the reactions of phenol derivatives with hydroxyl radicals. *Chemosphere.* 2007, 69(9):1396-1408.
- [47] Qian SY, Kadiiska MB, Guo Q, Mason RP. A novel protocol to identify and quantify all spin trapped free radicals from in vitro/in vivo interaction of HO \cdot and DMSO: LC/ESR, LC/MS, and dual spin trapping combinations. *Free Rad. Biol. Med.* 2005, 38(1):125-135.

Figure captions

Figure 1. Cyanidin-3-glucoside and proposed structure of Compound 1.

Figure 2. HPLC chromatogram (500 nm) of Compound 1 and C3G at 30 hours in the base model system.

Figure 3. Time course of Compound 1 formation in base (□) and blackberry (O) model systems.

Figure 4. Time course of C3G control (□) and in base model system with ascorbic acid (O).

Figure 5. HPLC/MS³ analysis of C3G (A), Compound 1 (B), and 6-hydroxycyanidin (C)

Figure 6. Proposed mechanism of formation of Compound 1.

Figure 7. ESR spectra from the complete blackberry extract-ascorbic acid system. The reaction mixture contained 200 ppm blackberry extract (BE) solution (or 200 ppm C3G solution), 320 ppm ascorbic acid, 50 mM POBN, and 10 mM DMSO. 1) ESR spectrum of the reaction excluding ascorbic acid. No ESR signals were detected. 2) ESR spectrum of the reaction excluding POBN. No ESR signals were detected. 3) ESR spectrum of the reaction excluding DMSO. No ESR signals were detected. 4) ESR spectrum of the reaction excluding blackberry extract. No ESR signals were detected. 5) ESR spectrum of the complete system reaction. ESR signals were detected from the combination of blackberry extract, ascorbic acid, DMSO, and POBN. 6) ESR spectrum of the complete system reaction replacing blackberry extract with pure C3G. Stronger ESR signals were detected from the combination of C3G, ascorbic acid, DMSO and POBN.

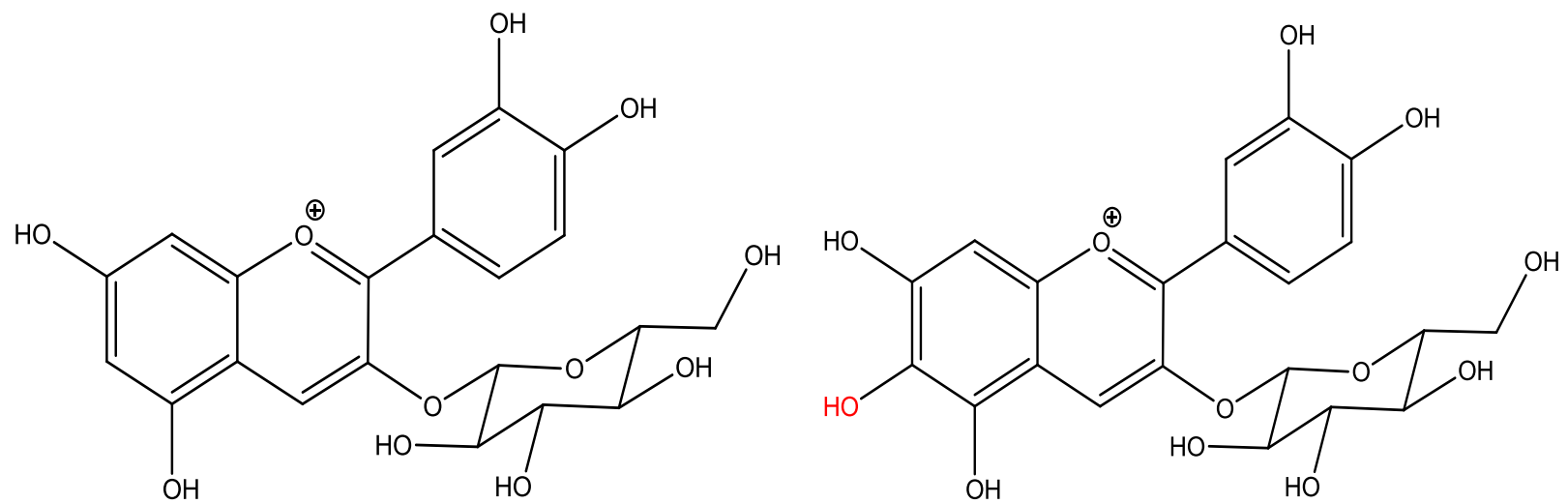


Figure 1

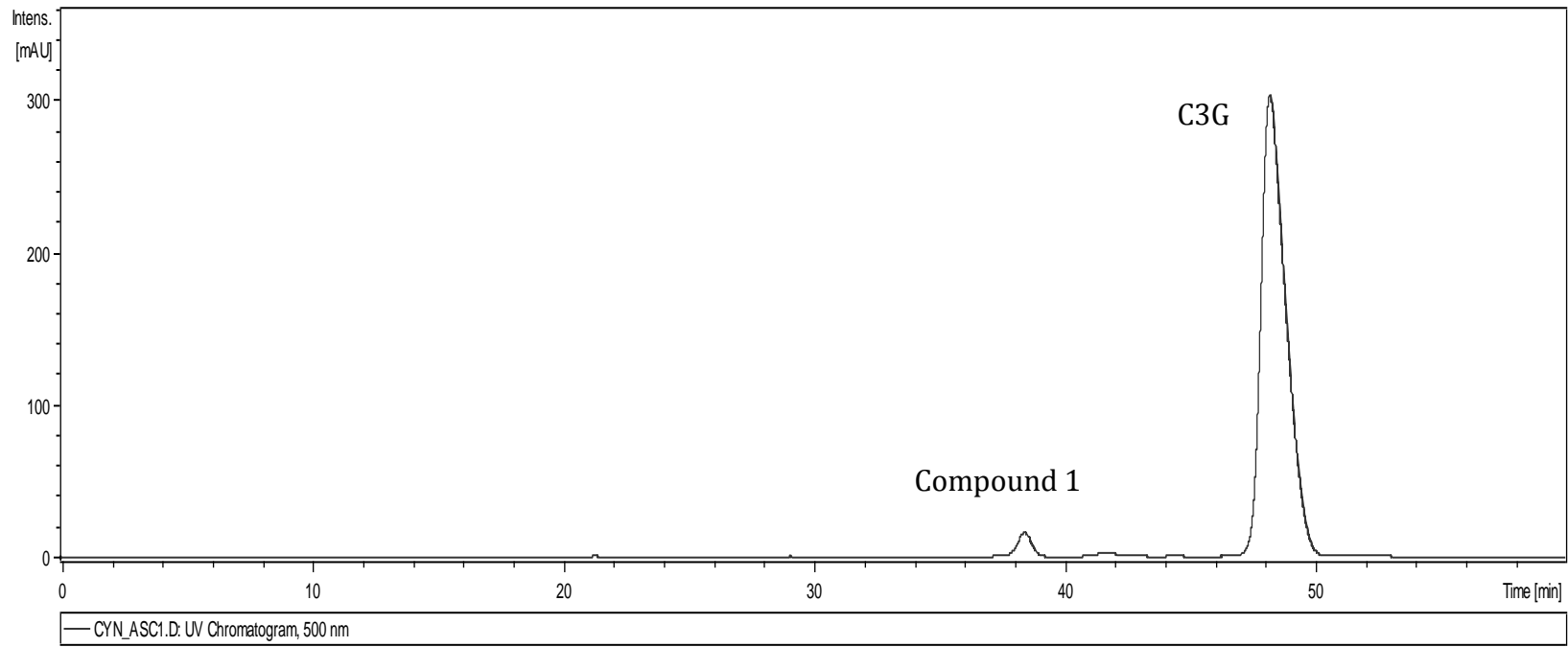


Figure 2

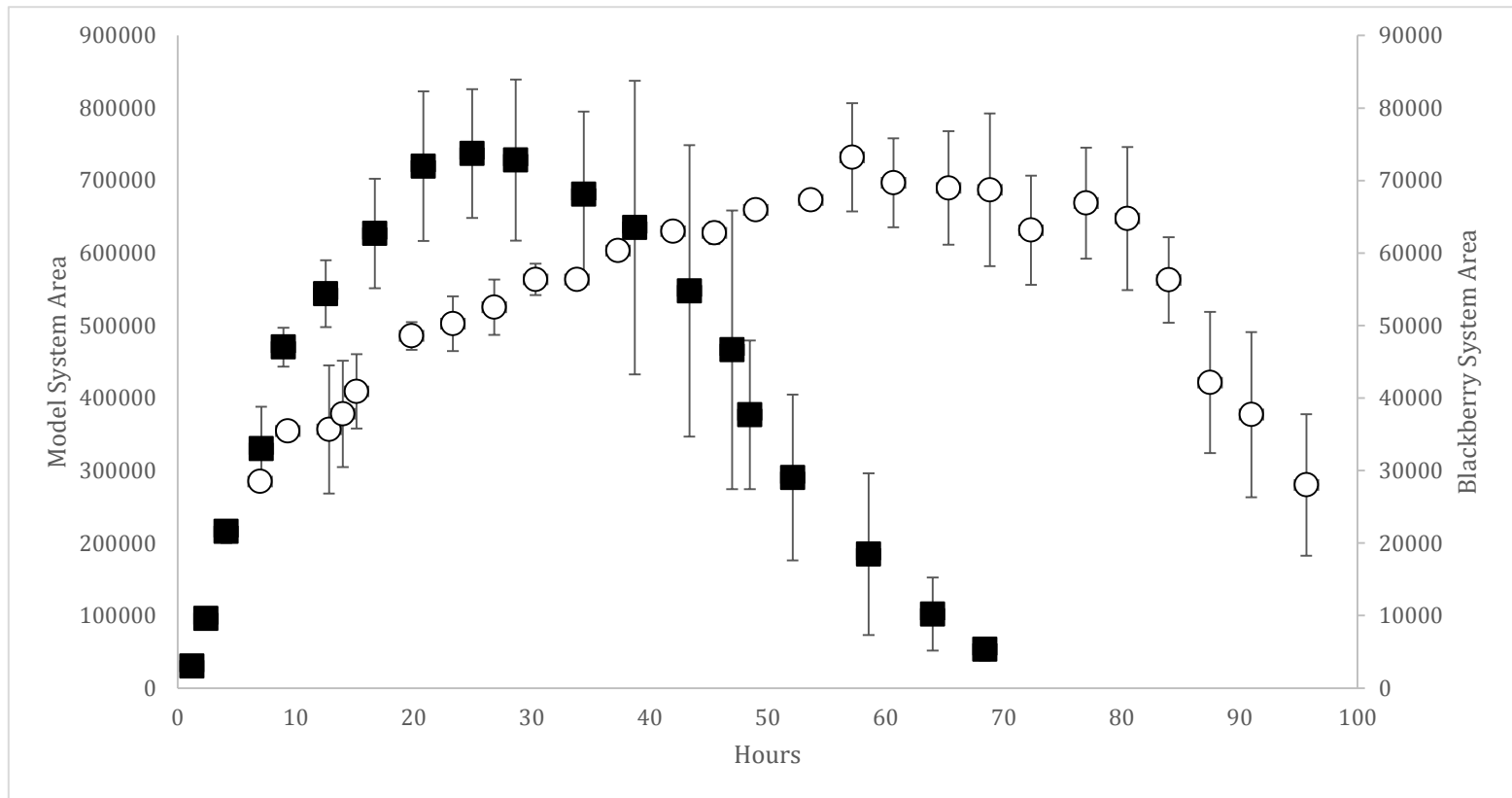


Figure 3

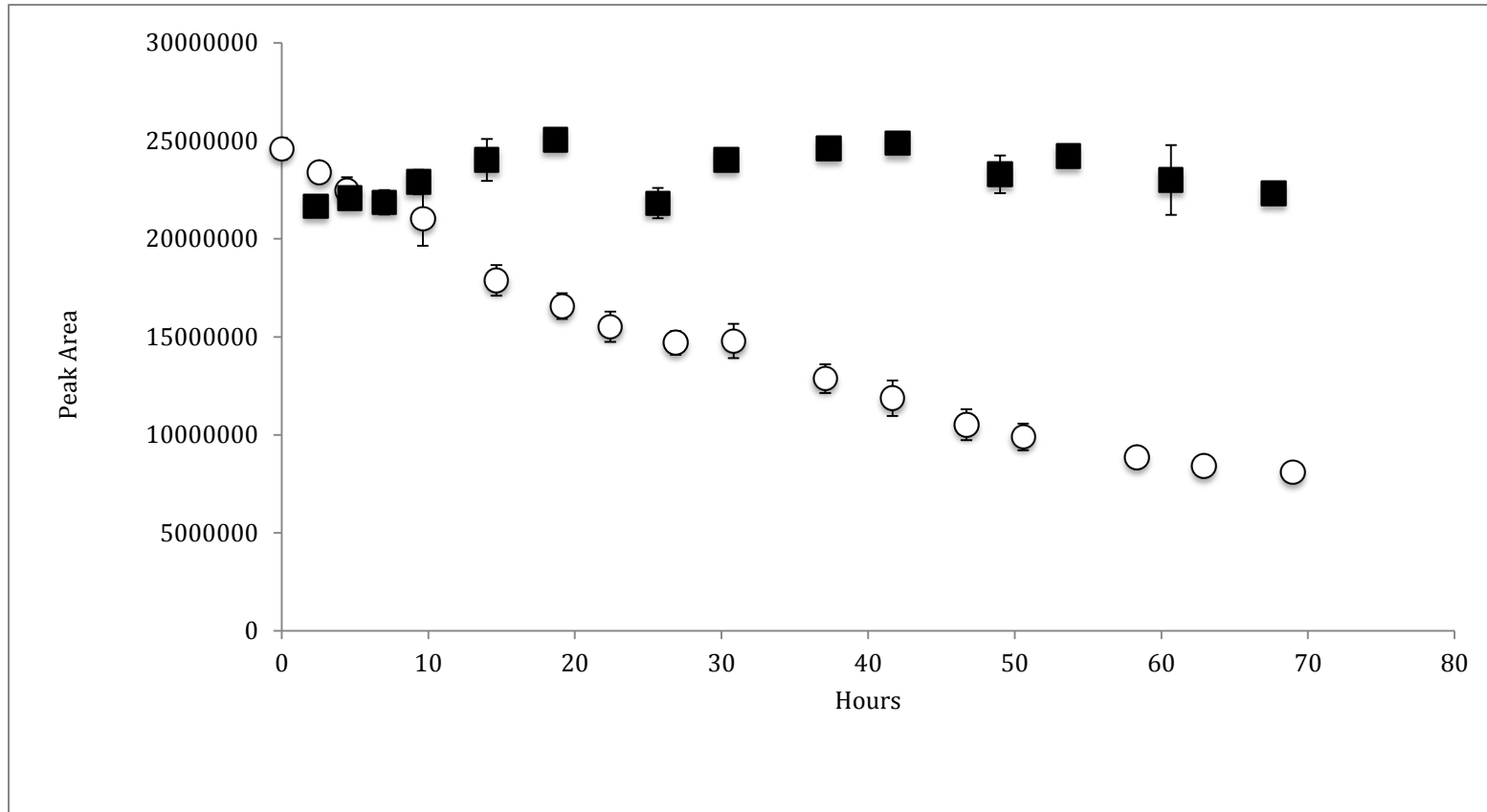


Figure 4

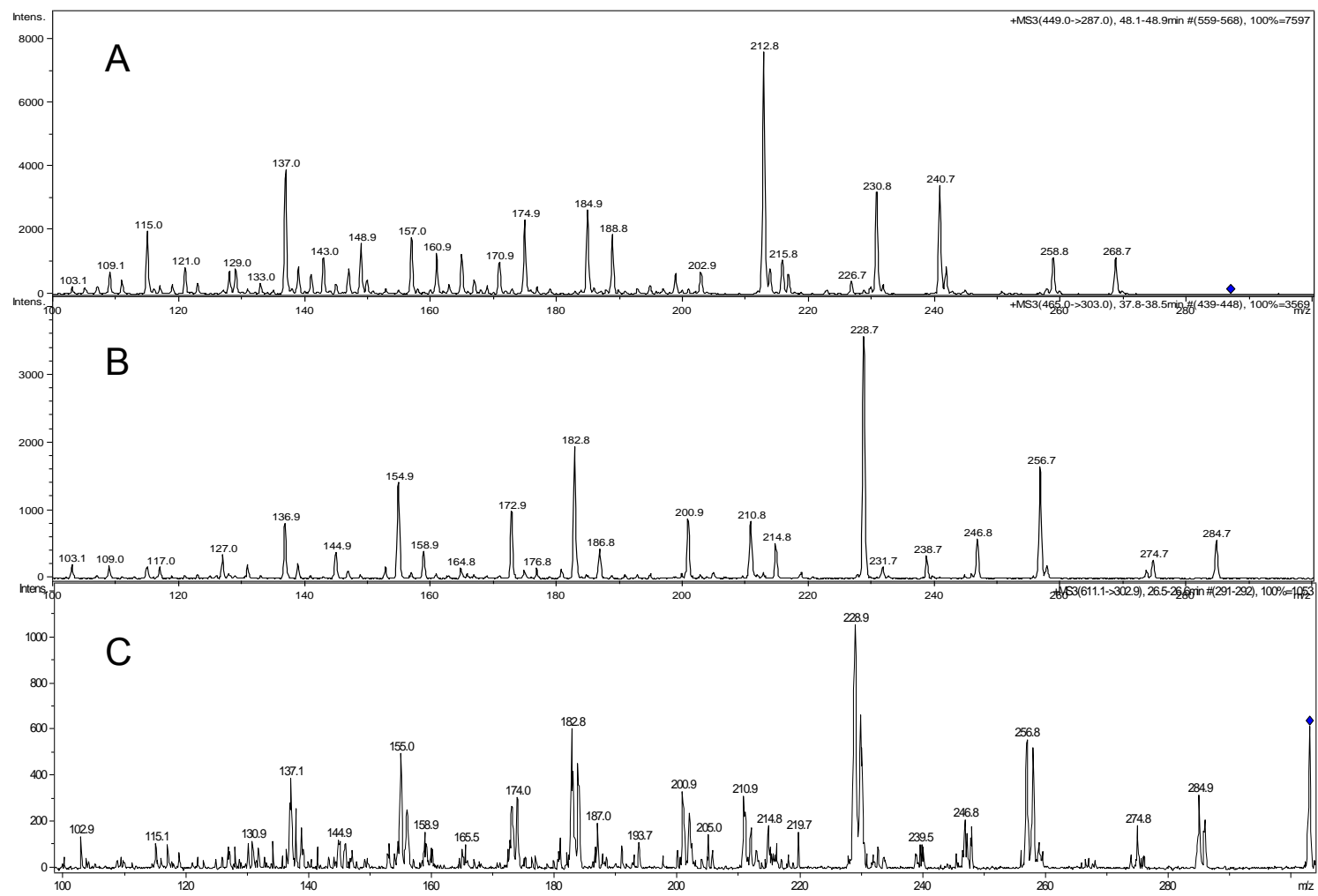


Figure 5

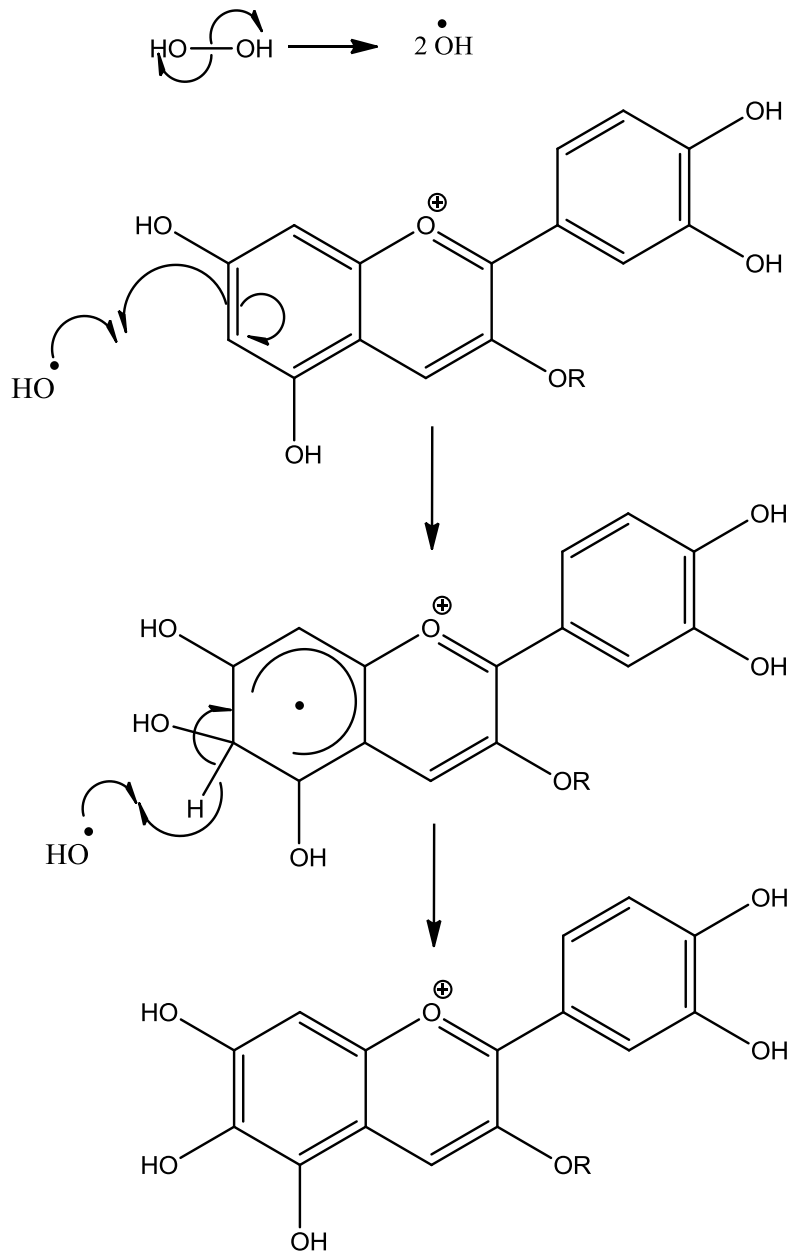


Figure 6

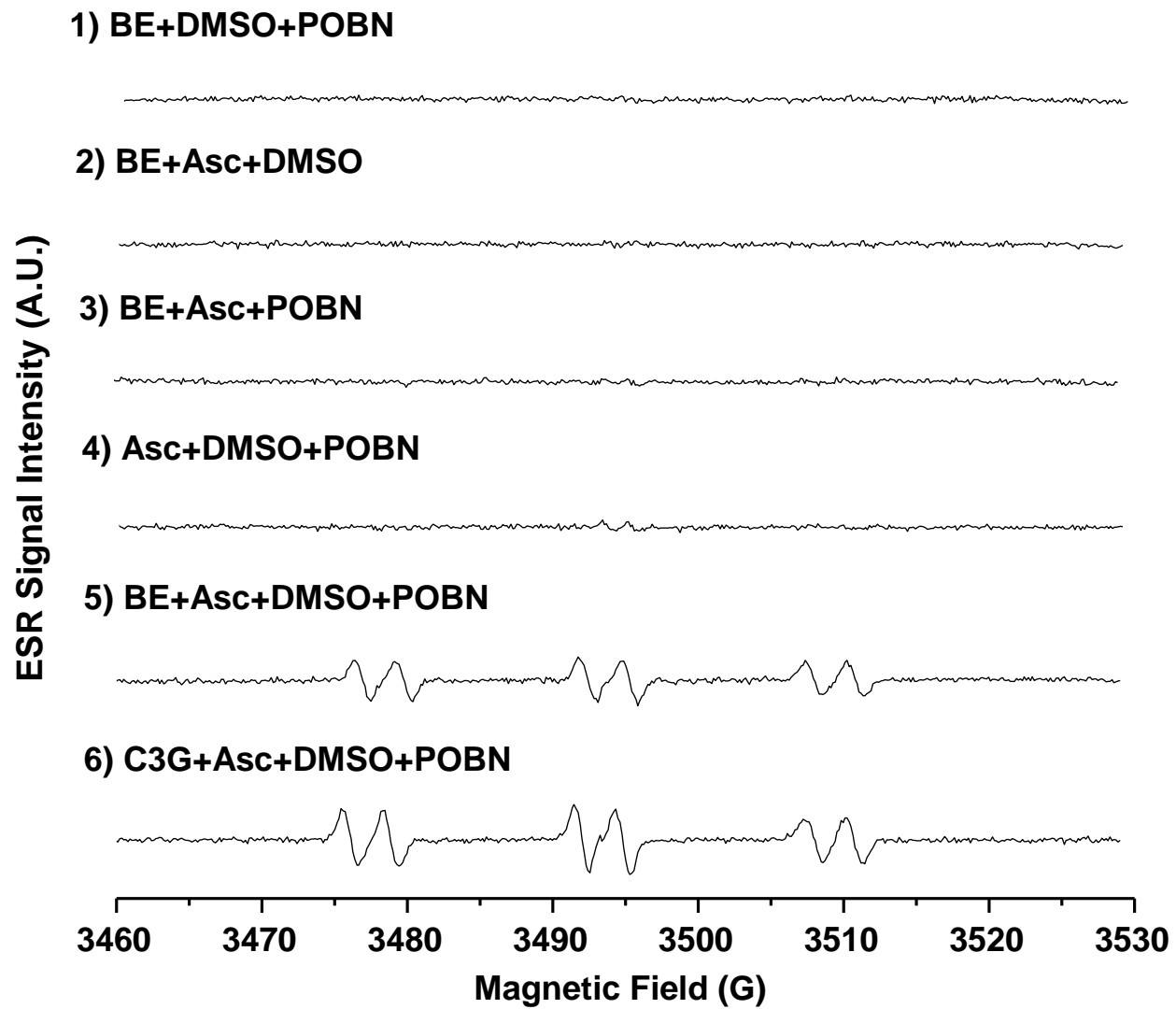


Figure 7

CHAPTER 5. Stabilization of anthocyanins in blackberry juice by glutathione fortification†

Nathan B. Stebbins¹, Luke R. Howard^{*1}, Ronald L. Prior¹, Cindi Brownmiller¹, Andy Mauromoustakos²

¹University of Arkansas, Department of Food Science, Fayetteville, Arkansas 72704, USA

² University of Arkansas, Agricultural Statistics Lab, Fayetteville, AR 72701

Corresponding author: Dr. Luke Howard, Department of Food Science, University of Arkansas, 2650 N. Young Avenue, Fayetteville, AR 72704, USA. Tel.: 1 479 575 2978; Fax: 479 575 6936; E-mail: lukeh@uark.edu

This manuscript is published in *Food Funct.* **2017**, 8, 3459-3468.

Abstract

Blackberry anthocyanins provide a vivid attractive color and antioxidant activity; however, anthocyanins degrade during juice processing and storage. Maintaining high anthocyanin concentrations in berry juices may lead to greater antioxidant and health benefits for the consumer. The objective of this study was to evaluate potential additives to stabilize anthocyanins during storage of blackberry juice. The anthocyanin stabilizing agents; glutathione, galacturonic acid, diethylenetriaminepentaacetic acid and tannic acid were added to blackberry juice at concentration of 500 mg/L. Juices were evaluated over five weeks of accelerated storage at 30°C for anthocyanin, flavonol, and ellagitannin contents by HPLC and percent polymeric color. Glutathione had the greatest protective effect with 11% greater retention (P=0.04) of total anthocyanins and polymeric color was reduced to 25.83% from 33.06% in the control juice receiving no additive following five weeks of storage. Therefore, a second study was performed with glutathione in combination with lipoic and ascorbic acids in an effort to use antioxidant recycling to achieve a synergistic effect. There was no difference in total anthocyanins between glutathione and any of the combinations. There was a similar protective effect of treatments in

total anthocyanins and percent polymeric color during storage, suggesting that the antioxidant recycling system had no protective effect relative to glutathione alone. Anthocyanin degradation was modeled in both studies and the best fit was an exponential decay. The models illustrate how glutathione supplementation provides an additional 1.2 weeks of storage compared to the control, while this time can be approximately doubled based on the elevated temperatures of accelerated storage. There were no notable changes in ellagitannin or flavonol content among additives or over storage. Two flavonols, quercetin-3-glucuronide and quercetin-3-pentosyl-glucuronide, were identified and quantified in blackberries for the first time. Glutathione appears to be a promising blackberry juice additive to protect against anthocyanin degradation during storage.

Keywords: anthocyanin, antioxidant, blackberry, juice, stabilizer, glutathione

†Electronic supplementary information (ESI) available: Figures S1–S10.

Introduction

Blackberries are a popular fruit with high concentrations of antioxidants, particularly anthocyanins and ellagitannins that possess positive health effects.¹⁻³ Fresh berries have limited shelf-life and thus need to be processed into jams, juice, or frozen to limit postharvest losses. Anthocyanin content decreases over processing and storage, which most likely has an adverse effect on health benefits. Various additives have been added to berry juices to stabilize anthocyanins, including β -cyclodextrin,⁴ pectins and other polysaccharides,⁵ and copigments such as phenolic acids.⁶⁻⁷ Cyclodextrin's effectiveness may be due to inclusion of the anthocyanin within the ring shape of the molecule and/or hydrophobic interactions, both of which could restrict the hydration reaction responsible for anthocyanin bleaching.⁴ Pectin can

interact with anthocyanins through ionic and hydrogen bonding potentially limiting the hydration reaction as well.⁸ Galacturonic acid, the monomeric unit of pectin, may protect anthocyanins by electrostatic interactions.⁹ Protection via copigments is frequently described by π - π stacking of phenolic compounds above and below the anthocyanin in a “sandwich” effect.¹⁰

Often very high additive concentrations are needed to limit anthocyanin degradation, therefore a recycling mechanism of multiple additives could be effective at lower concentrations. An antioxidant recycling approach may be advantageous since both enzymatic and non-enzymatic oxidation are reported to play a role in anthocyanin degradation¹¹⁻¹². Antioxidant recycling has been demonstrated in both *in vitro* and *in vivo* cellular systems;¹³ however, to the best of our knowledge this mechanism has not been tested in a juice product. Combinations of glutathione, lipoic acid, ascorbic acid, and vitamin E have been linked in recycling mechanisms.¹⁴⁻¹⁷ Recycling mechanisms involve equilibria between each component in an effort to keep all antioxidants active for greater periods of time. The concentration of each component in the system must be balanced in order to prevent a pro-oxidant environment.¹⁸ The objective of this study was to evaluate the effect of stabilizing agents with different mechanistic tactics on blackberry juice color and an antioxidant recycling mechanism on anthocyanin, flavonol, and ellagitannin content in blackberry juice over accelerated storage.

Materials and methods

Materials

Cyanidin-3-O-glucoside was obtained from Chromadex (Irvine, CA, USA), whereas other standards: ellagic acid, ascorbic acid, lipoic acid, glutathione, galacturonic acid, diethylenetriaminepentaacetic acid (DTPA), tannic acid, potassium metabisulfite were purchased

from Sigma Aldrich (St. Louis, MO, USA). HPLC-grade methanol was purchased from EMD Millipore (Billerica, MA, USA) and formic acid from Fischer-Scientific (Fair Lawn, NJ, USA). Frozen blackberries (Mexican origin) were purchased from a local supermarket.

Juice production

Frozen blackberries were thawed while heating in a steam kettle until boiling and then held for three minutes. The berries were cooled and centrifuged at $9,447 \times g$ for 10 min. Since we were not interested in improving juice yield, no commercial enzyme cocktail was used to macerate cell wall polysaccharides prior to centrifugation. The supernatant was pooled and 500 mg/L of each stabilizing agent was added to the respective volume of blackberry juice. We selected this concentration of stabilizing agents based on the range of maximum concentrations (2-1000 mg/L) allowed by the FDA for the synthetic antioxidants BHA and BHT in foods ¹⁹. Two separate studies were performed. In stage one, the stabilizing agents glutathione, galacturonic acid, tannic acid and diethylenetriaminepentaacetic acid (DTPA) were studied and in stage two glutathione, lipoic acid, ascorbic acid alone and the combinations (500 mg/L of each) of glutathione + lipoic acid and glutathione + lipoic acid + ascorbic acid were studied. A different lot of frozen blackberries was used for each study. Juice samples in triplicate stored in 8 mL glass tubes were pasteurized in a water bath at 90°C for 1.5 min. The pasteurization conditions were comparable to those used in previous studies on blackberry juice ²⁰⁻²². Although we did not measure polyphenol oxidase activity in the juices following processing, we believe the two thermal treatments used during processing were sufficient to inactivate the enzyme. Pasteurized juices were stored in a 30°C oven for accelerated storage until analysis. New samples were removed from the oven each week and analyzed for five weeks.

HPLC-PDA analysis of anthocyanins

Anthocyanin analysis followed the method of Cho et al. 2004.²³ Juice samples were passed through 0.45 µm nylon syringe filters prior to HPLC injection. A Waters HPLC system (Waters Corp., Milford, MA) comprised of dual 515 pumps, a 717plus autosampler, and a 996 photodiode array detector was used for chromatographic analyses. A Waters Symmetry C₁₈ column (4.6 x 250 mm, 5 µm) was used for separation of anthocyanins with a 1 mL/min flow rate and solvent A as 5% formic acid and solvent B as methanol. Elution started with 5% B, increased to 15% B in 10 min, from 15% to 35% in 35 min, then 100% in 5 min, with an isocratic wash at 100% B for 10 min, finishing with 5% B for a 10 min re-equilibration. UV-visible spectra were monitored from 250-600 nm and peak areas were integrated at 510 nm. Anthocyanins were quantified as cyanidin-3-glucoside equivalents using external calibration curves ranging from 1-200 µg/mL.

HPLC-PDA analysis of ellagitannins and flavonols

Ellagitannin and flavonol analysis followed the method of Hager et al. 2008²⁴ using the same HPLC system described above for anthocyanins. Juice samples were passed through 0.45 µm nylon syringe filters prior to HPLC injection. Separation was accomplished on a 250 x 4.6 mm Phenomenex Aqua 5 µm C₁₈ column (Torrance, CA) with solvent A as 2% acetic acid and solvent B as 0.5% acetic acid in water/acetonitrile (1:1 v/v) at 1 mL/min. A gradient was run from 10% to 55% B (0-50 min), from 55% to 100% B (50-60) min, decreasing to 10% B (60-65 min), finishing with a 15 min re-equilibration. UV-visible spectra were monitored from 250-600 nm, with peak areas integrated at 255 nm for ellagitannins and 360 nm for flavonols. Ellagitannins were quantified as ellagic acid equivalents and flavonols were quantified as rutin equivalents using external calibration of authentic standards ranging from 1-100 µg/mL.

HPLC-electrospray ionization tandem mass spectrometry (LC-ESI-MS) analysis of degradation products

LC-ESI-MS analysis was conducted using an HP 1000 series HPLC and a Bruker Esquire 2000 quadrupole ion trap mass spectrometer. Anthocyanins were separated using a Waters Symmetry (250 x 4.6 mm; 5 μ m) column and ellagitannins and flavonols on a Phenomenex Aqua (250 x 4.6 mm; 5 μ m) column with gradients as described above. The mass spectrometry analysis was performed in positive ion mode for anthocyanins and negative ion mode for ellagitannins and flavonols under the following conditions: capillary voltage at 4 kV with polarity [+] for negative ion mode and [-] for positive ion mode analysis, nebulizer gas pressure 32 psi, dry gas flow 12 L/min, and skim voltage at 53.7 V and again polarity switched for respective mode. Ions were isolated and fragmented in quadrupole ion trap with excitation amplitude of 1.2 volts.

Polymeric color analysis

Percent polymeric color was measured according to the method of Giusti and Wrolstad 2001.²⁵ The juice was diluted to have an absorbance reading between 0.5 to 1.0 at 510 nm, detected by an 8452A diode array spectrophotometer (Hewlett-Packard, Palo Alto, CA). A control, unbleached sample was prepared with 0.2 mL of DI water and 2.8 mL of the diluted juice and a bleached sample consisted of 2.8 mL of diluted juice and 0.2 mL of 0.9 M potassium metabisulfite. The samples were allowed to equilibrate for 15 min and absorbance readings were recorded at $\lambda = 420, 510, \text{ and } 700 \text{ nm}$. Color density was calculated from the control sample and polymeric color from the bleached sample using the following formulas:

$$\text{color density} = [(A_{420\text{nm}} - A_{700\text{nm}}) + (A_{510\text{nm}} - A_{700\text{nm}})] \times \text{dilution factor}$$

polymeric color = $[(A_{420\text{nm}} - A_{700\text{nm}}) + (A_{510\text{nm}} - A_{700\text{nm}})] \times \text{dilution factor}$

Percent polymeric color was calculated from the result of these formulas:

% polymeric color = (polymeric color/color density) x 100

Color monitoring

A Konica Minolta Chroma meter CR-400 and data processor DP-400 was used to measure lightness (L), chroma (C), and hue (h) in the L*C*h color scheme (Konica Minolta, Japan). The chroma meter was calibrated with a white tile: $x= 92.41$, $y= 0.3145$, $z= 0.3200$, observer = 2° prior to each use. Color measurements were taken at the end of each five-week study. Juice samples were frozen (-20°C) until the time of analysis.

Statistical Analysis

Three samples stored in different individual tubes per treatment were analyzed and graphed at each storage time using JMP Pro 13. The Fit Model platform in SAS was used to analyze all continuous responses for both experiments with a two factor (Treatments and Storage TIME) factorial design with 5 and 7 Treatments respectively and Time (Week with 6 levels: 0_PAST, 1, 2, 3, 4, and 5 weeks) and their interaction. Due to the highly significant interactions for the most important responses such as the anthocyanins and polymeric color the Treatment*WEEK combination LSmeans (there were few missing values) were sliced and simple effect comparisons among the Treatment LSMEANS for Week5 were performed. Also comparisons among any differences of the interaction LSmeans were assessed using Tukey's HSD test ($\alpha = 0.05$).

Nonlinear regression modeling was performed using the Nonlinear curve fitting platform of JMP Pro 13 to model and compare the decay rates of the Total anthocyanins (and Polymeric Color) of the various treatments for each experiment. Several linear and nonlinear curves were fitted to the data varying for 2-4 parameters and the best fit was in every case the three parameter exponential decay model $a+b*e^{(c*week)}$ (where a was the *asymptote*, b the *scale* and c the *rate*). The analysis provided with ANOM type of comparison of the three individual Treatment nonlinear parameter estimates to their overall mean for each experiment. In addition useful inverse predictions allowed us to estimate and compare the amount of time it will take on average for each treatment in both experiments starting the similar initial amounts of Total anthocyanins to reduce to 1000 mg/L (> 50% of the starting anthocyanins total for each experiment).

All analysis presented in this paper used SAS/Stat ®, Version 9.4 and the Fit Model and Nonlinear univariate platforms of JMP Pro ®, Version 13.1.

Results and discussion

Stabilizer effect on monomeric anthocyanins and percent polymeric color throughout accelerated storage

Following pasteurization, blackberry juice with the addition of DTPA had the highest total anthocyanin content compared to other stabilizing agents in Stage 1 (Fig. 1). Blackberries have 0.62 mg iron and 0.17 mg copper/ 100 g berry.²⁶ It is possible for small quantities of iron or copper to generate hydroxyl radicals that could degrade anthocyanins.²⁷⁻²⁸ DTPA is a strong chelator and likely functions as a protective agent to anthocyanin content by chelating the free iron and copper in the blackberry juice, thus limiting hydroxyl radical formation. Following

pasteurization, the control in Stage 1 had the lowest content of total anthocyanins demonstrating a protective effect by all additives. However in Stage 2, the control and lipoic acid additive had lower contents of total anthocyanins than all other treatments (Fig. 2). All glutathione-containing juices had a protective effect on total anthocyanin content as well as the juice with solely ascorbic acid added. There was no notable pH change with the addition of ascorbic acid or any of the additives. Glutathione and other thiols are reported to protect semi-purified extracts of bilberry and black currant anthocyanins (35-37% concentration) and double their absorption in Caco-2 cells and human plasma. Glutathione is described as having superior functionality to other thiols due to two carboxylic acid moieties. The thiols were postulated to be tightly associated with the anthocyanidin at position 4 or the sugar moiety, which is the basis for thiol stabilization.²⁹ The author included a structure showing a thiol bound to C-4 on delphinidin; however we did not detect any new anthocyanin peaks over the course of storage.

Following five weeks of storage, glutathione treated juices had 13% more anthocyanins than control juices ($p=0.0477$), while all other treatments were similar to the control (Fig. 1). Galacturonic acid was nearly identical to the control (no stabilizing agent added) with regard to total anthocyanin content. Galacturonic acid was chosen for this study because of the potential for anthocyanin stabilization by electrostatic interactions between the molecules.⁹ Co-pigments and self-association are believed to protect anthocyanins from the hydration reaction by excluding water from the vicinity of the flavylium ion.³⁰ Our results indicate galacturonic acid and tannic acid at 500 mg/L concentration had no protective or degradative effect on anthocyanins over five weeks of storage. The structure of tannic acid has a multitude of phenolic moieties that could physically protect the flavylium cation from hydration via a sandwich effect. Previous studies have shown tannic acid's potential to stabilize anthocyanins in other fruit

juices.³¹⁻³³ Other researchers have used tannic acid in a 1:1 ratio to anthocyanin concentration in model system using grape skins with significant stabilizing effects.³³ A copigmentation review of literature using model systems and fruits juice depicted copigment:anthocyanin ratios ranging from 0.1 to 200 with the addition of various copigments, including flavonoids, cinnamic acids, or phenolic acids.⁷ The majority of research used very high ratios that are unrealistic for industrial application.

The changes in the major blackberry anthocyanins, cyanidin-3-glucoside, cyanidin-3-rutinoside, and cyanidin-3-xyloside throughout accelerated storage are shown in Fig. 3 for Stage 1 and Fig. 4 for Stage 2. In Fig. 3, it is clear that glutathione provided the greatest stabilizing effect to each cyanidin glycoside compared to other additives analyzed. Following five weeks of storage glutathione treated juices had 13% and 12% higher levels of cyanidin-3-glucoside and cyanidin-3-rutinoside than the control ($p = 0.05$ and 0.003). Glutathione did not significantly preserve cyanidin-3-xyloside during the final two weeks of storage.

Due to the significant stabilizing effect of glutathione in Stage 1, combinations of glutathione with lipoic acid, and glutathione with both lipoic and ascorbic acids were added at 500 mg/L of each component in an attempt to stabilize anthocyanins via antioxidant recycling in blackberry juice. Control and juice samples containing solely lipoic acid or ascorbic acid were also included in Stage 2. Cyanidin-3-xyloside decreased below the limit of quantification (5 mg/L) following week four and showed a nonlinear decline. As in Stage 1, cyanidin-3-glucoside was the prevalent anthocyanin in blackberry juice, accounting for 92% of total anthocyanins after five weeks of storage, but showed a nonlinear decline over accelerated storage in Stage 2. Following five weeks of storage, all treatment combination with

The percent polymeric color assay measures the ratio of bleachable monomeric anthocyanins to non-bleachable anthocyanins (presumably anthocyanin-tannin polymers) in a sample, which typically negatively correlates with total anthocyanin content. An increase in percent polymeric color could indicate anthocyanin-tannin polymers forming over storage or the same concentration of anthocyanin-tannin polymers accompanied by a decreasing concentration of monomeric anthocyanins. Pyranoanthocyanins are also resistant to bleaching in the presence of SO₂³⁴, but we saw no evidence of these compounds in our HPLC chromatograms. Our findings mirror the anthocyanin quantification by HPLC, indicating a greater likelihood that the percent polymeric color values are caused by a decrease in monomeric anthocyanins and not an increase in anthocyanin-tannin polymers. A strong inverse relationship between percent polymeric color and total anthocyanins was observed in Stage 1 (R²=0.937) and Stage 2 (R²=0.941) indicating that the low amount of anthocyanins remaining following storage are resistant to SO₂ bleaching and may be polymeric compounds.

Stabilizer effect on ellagitannins throughout accelerated storage

The three predominant ellagitannins in blackberries were previously identified using mass spectrometry and two of the compounds have identical *m/z* values: sanguin H-6 and lambertianin A (*m/z* = 1868.7).³⁵ Due to the lack of differentiation among the isomers, these two compound totals were summed in Figs. S1 and S2 for Stage 1 and 2, respectively. Lambertianin C was identified with *m/z* of 1401.1 with doubly charged ion peaks (MW = 2802.2). Collectively, these compounds were fairly stable over accelerated storage of blackberry juice regardless of stabilizer treatment.

After pasteurization, ellagitannin concentration increased slightly (Figs. S1 and S2) and this may be caused by either the depolymerization of larger ellagitannins we detected or the release of bound ellagitannins from soluble cell wall polysaccharides by the thermal treatment. Gancel et al.²² also found an increase in ellagitannin content after pasteurization; however they used blackberry puree and attributed the increase to extraction from seeds. This author performed a second pasteurization on the juice and found a decline in ellagitannins accompanied by an increase in ellagic acid. We found the ellagitannins to be stable over accelerated storage at 30 °C, which is in contrast to the linear decline of lambertianin C and sanguin H6 found at the same temperature in tropical highland blackberry juice storage over 35 days.²²

The concentration of blackberry juice ellagitannins in this study were nearly 10-fold lower than values reported in a previous study using identical HPLC methodology.^{22,35} In the previous studies cv. Apache and tropical highland blackberries were used, while in the present study berries of Mexican origin, likely cv. Tupy, were used so the concentration difference could be due to different cultivars or varying environmental growing conditions. Stage 2 displayed higher total sanguin H-6/lambertianin A levels with nearly 20 mg/L than Stage 1, which only had 8.6 mg/L in the sample with greatest concentration. The lower ellagitannin content found in our juice samples could be caused by a loss of ellagitannins in the pomace since the majority of ellagitannins are found in the seeds.^{24,36}

Stabilizer effect on flavonols throughout accelerated storage

The HPLC profile of flavonols in the blackberry juice is shown in Fig. 5 and includes exclusively quercetin derivatives. The flavonols were identified using mass spectrometry as quercetin-3-rutinoside (peak 1), quercetin-3-pentosyl-glucuronide (peak 2), quercetin-3-

galactoside (peak 3), quercetin-3-glucoside (peak 4), and quercetin-3-glucuronide (peak 5) in Table 1. The sixth peak is also a quercetin moiety based on the mass fragment of m/z 301; however, the substituents were not identified. The mass spectra for each flavonol are depicted in Figs. S5-S10. This is the first evidence in blackberries of quercetin-3-glucuronide (m/z 477, 301), which was previously identified in strawberries,³⁷ northern highbush blueberries,³⁸ and raspberries³⁹ and quercetin-3-pentosyl-glucuronide (m/z 609, 433, 301), which was previously identified in eastern teaberries.⁴⁰

With respect to changes in pasteurization and storage, the quercetin derivatives, regardless of substituent, were stable through the five weeks of storage in Stage 1 (Fig. S3). In Stage 2, fluctuation in concentration occurred between weeks, but remained consistent throughout storage (Fig. S4). None of the additives had a stabilizing effect on flavonol content in Stage 1 or Stage 2. Other researchers found similar stability of quercetin derivatives in blackberry juice stored at temperatures ranging from 5-45 °C, with no effect of temperature on flavonol stability.²² Gancel et al. measured total quercetin derivatives as gallic acid equivalents and reported a concentration of 6.7 mg/L total quercetin derivatives in blackberry juice, while we used rutin equivalents and found 69.7 mg/L total quercetin derivatives in the pasteurized blackberry juice.²²

Changes in blackberry juice color

Color was measured using L^*C^*h and there was a significant increase in lightness values in all samples over accelerated storage in both Stages 1 and 2 (data not shown). This was likely caused by the decline in anthocyanin content measured by HPLC. A similar trend of increasing lightness value was shown in blood orange juice stored over seven weeks at 4.5 °C.⁴¹

Elderberries contain high quantities of cyanidin-3-glucoside, which is comparable to blackberries, and the lightness of elderberry juice and concentrate at pH 3.5 increased significantly after thermal processing at 95 °C.⁴² Anthocyanins are sensitive to elevated temperature; therefore pasteurization must be accomplished quickly. Marchese⁴³ demonstrated fluctuations in anthocyanin content and color change over a range of pasteurization temperatures and times, recommending pasteurization at 80°C.

There were no major changes in hue over storage with all Stage 1 samples averaging 17.20 ± 5.77 , while Stage 2 had an average hue value of 9.54 ± 2.89 . With regard to chroma, tannic acid produced the most notable effect with a significant hyperchromic effect through pasteurization and storage. The same behavior was seen in model systems of pure anthocyanins after addition of tannic acid.⁹ Tannic acid was shown to improve color stability, but not necessarily chroma, in blood orange juice.³¹ Several studies have reported on the degradative effect of ascorbic acid on anthocyanins;^{11, 28,44-45} however, ascorbic acid at 500 mg/L did not significantly affect any color measurements in the present study. After extreme thermal treatment, elderberry juice hue increased from 10.79 to 40.75 and the chroma decreased from 24.77 to 10.61.⁴² The change in chroma is related to a drastic decline in anthocyanins after heating, while the hue change is indicative of more yellow color. These authors compared strawberry, elderberry, and black carrot juice, which are all pigmented due to anthocyanins, finding food matrix critical to color stability.⁴²

Antioxidant recycling and redox potentials

The relative redox potentials of each component in our recycling mechanism allow a comparison of the reduction probability over time. The greater the potential, the greater the

likelihood of that compound being reduced. The anthocyanin profile of blackberries is composed primarily of cyanidin-3-glucoside and is one of the simplest anthocyanin profiles among berries. This allows for easier analysis, especially with redox potentials. At pH 3.5 of blackberry juice, cyanidin-3-glucoside is reported to have a redox potential of 490 mV by differential pulse voltammetry,⁴⁶ which aligns with 584 mV in the aglycone, cyanidin.⁴⁷ Glycosylation lowers redox potential. Other researchers have measured redox potential in blackberries finding 468 mV and 400 mV in Romanian and Croatian blackberries, respectively.^{48,49}

The other components of the antioxidant recycling mechanism in Stage 2 are shown in Fig. 6, where lipoic acid has a redox potential of 1100 mV,⁵⁰ ascorbic acid is 282 mV, and glutathione disulfide is -1500 mV.⁵¹ This illustrates lipoic acid will be the first to be reduced, while glutathione disulfide will be the first to be oxidized. These two compounds can potentially recycle each other and then assist in anthocyanin recycling. Cyanidin-3-glucoside and ascorbic acid will be intermediates in the process due to their median redox potentials. It is thermodynamically favorable to exchange electrons between ascorbic acid/C3G and lipoic acid radical cation in order to regenerate lipoic acid. Ascorbic acid radicals are easily recycled and are “relatively harmless, being neither strongly oxidizing, nor strongly reducing.”⁵¹ The recycling mechanism allows lipoic acid to function as an antioxidant for ROS (reactive oxygen species), but would not recycle any oxidized anthocyanins due to the difference in redox potentials. On the other hand, reduced glutathione has a redox potential of -258 mV⁵² and could serve as the reducing agent for any anthocyanin oxidation in the samples containing glutathione. This is likely why the addition of lipoic acid or lipoic and ascorbic acids did not improve anthocyanin content over storage of blackberry juice more than glutathione alone.

Conclusion

The addition of glutathione to blackberry juice resulted in greater retention of anthocyanins over accelerated storage compared to other stabilizing agents. Color was not visibly different over the course of storage, but lightness values increased presumably in response to anthocyanin degradation. Glutathione in combination with lipoic acid and ascorbic acid was tested to determine if an antioxidant recycling mechanism would reduce the concentration of stabilizing agents needed and stabilize anthocyanins more successfully; however, the combination was not more effective than glutathione alone. Glutathione did not bind to the anthocyanins, so further research is needed to determine the mechanism of stabilization.

References

1. D.X. Hou, Potential mechanisms of cancer chemoprevention by anthocyanins. *Curr. Mol. Med.* 2003, **3**, 149-159.
2. C.A. Rice-Evans, N.J. Miller, Antioxidant activities of flavonoids as bioactive components of food. *Biochem. Soc. Trans.* 1996, **24**, 790-794.
3. L. Kaume, L.R. Howard, L. Devareddy, The blackberry fruit: A review on its composition and chemistry, metabolism and bioavailability, and health benefits. *J. Agric. Food Chem.* 2012, **60**, 5716-5727.
4. L.R. Howard, C. Brownmiller, R.L. Prior, A. Mauromoustakos, Improved stability of chokeberry juice anthocyanins by β -cyclodextrin addition and refrigeration. *J. Agric. Food Chem.* 2013, **61**, 693-699.
5. D.S. Ferreira, A.F. Faria, C.R.F. Grosso, A.Z. Mercadante, Encapsulation of blackberry anthocyanins by thermal gelation of curdlan. *J. Braz. Chem. Soc.* 2009, **20**, 1908-1915.
6. M.J. Rein, M. Heinonen, Stability and enhancement of berry juice color. *J. Agric. Food Chem.* 2004, **52**, 3106-3114.
7. R. Boulton, The copigmentation of anthocyanins and its role in the color of red wine: A critical review. *Am. J. Enol. Vitic.* 2001, **52**, 67-87.
8. A. Fernandes, N.F. Bras, N. Mateus, V. de Freitas, Understanding the molecular mechanism of anthocyanin binding to pectin. *Langmuir*, 2014, **30**, 8516-8527.
9. P. Mazzaracchio, P. Pifferi, M. Kindt, A. Munyaneza, G. Barbiroli, Interactions between anthocyanins and organic food molecules in model systems. *Intl. J. Food Sci. Technol.* 2004, **39**, 53-59.
10. N. Teixeira, L. Cruz, N.F. Bras, N. Mateus, M.J. Ramos, V. de Freitas, Structural features of copigmentation of oenin with different polyphenol copigments. *J. Agric. Food Chem.* 2013, **61**, 6942-6948.
11. M.S. Poesi-Langston, R.E. Wrolstad, Color degradation in an ascorbic acid-anthocyanin-flavanol model system. *J. Food Sci.* 1981, **46**, 1218-1222.
12. A. Patras, N.P. Brunton, C. O'Donnell, B.K. Tiwari. Effect of thermal processing of anthocyanin stability in foods; mechanisms and kinetics of degradation. *Trends Food Sci. Technol.* 2010, **21**, 3-11.

13. R.A. Jacob, G. Sotoudeh, Vitamin C function and status in chronic disease. *Nutr. Clin. Care.* 2002, **5**, 66-74.
14. L. Packer, E.H. Witt, H.J. Tritschler, Alpha-lipoic acid as a biological antioxidant. *Free Rad. Biol. Med.* 1995, **19**, 227-250.
15. V.E. Kagan, Y.Y. Tyurina, Recycling and redox cycling of phenolic antioxidants. *Ann. N.Y. Acad. Sci.* 1998, **854**, 425-434.
16. B.S. Winkler, S.M. Orselli, T.S. Rex, The redox couple between glutathione and ascorbic acid: A chemical and physiological perspective. *Free Rad. Biol. Med.* 1994, **17**, 333-349.
17. K. Rahman, Studies on free radicals, antioxidants, and co-factors. *Clin. Interv. Aging.* 2007, **2**, 219-236.
18. D.C. Liebler, D.S. Kling, D.J. Reed, Antioxidant protection of phospholipid bilayers by α -tocopherol. *J. Biol. Chem.* 1986, **261**, 12114-12119.
19. FDA Food for Human Consumption 21 CFR § 172.110 and 172.115. (2016)
20. G. Azofeifa, S. Quesada, A.M. Pérez, F. Vaillant, A. Michel. Pasteurization of blackberry juice preserves polyphenol-dependent inhibition for lipid peroxidation and intracellular radicals. *J. Food Comp. Anal.* 2015, **42**, 56-62.
21. M. Kopjar, K. Jakšić, V. Piližota. Influence of sugars and chlorogenic acid addition on anthocyanin content, antioxidant activity and color of blackberry juice during storage. *J. Food Proc. Pres.* 2012, **36**, 545-552.
22. A. Gancel, A. Feneuil, O. Acosta, A.M. Perez, F. Vaillant. Impact of industrial processing and storage on major polyphenols and the antioxidant capacity of tropical highland blackberry (*Rubus adenotrichus*). *Food Res. Int.* 2011, **44**, 2243-2251.
23. M.J. Cho, L.R. Howard, R.L. Prior, J.R. Clark, Flavonoid glycosides and antioxidant capacity of various blackberry, blueberry and red grape genotypes determined by high-performance liquid chromatography/mass spectrometry. *J. Sci. Food Agric.* 2004, **84**, 1771-1782.
24. T.J. Hager, L.R. Howard, R. Liyanage, J.O. Lay, R.L. Prior, Ellagitannin composition of blackberry as determined by HPLC-ESI-MS and MALDI-TOF-MS. *J. Agric. Food Chem.* 2008, **56**, 661-669.
25. M.M. Giusti, R.E. Wrolstad, Characterization and measurement of anthocyanins by UV-visible spectroscopy. In *Current Protocols in Food Analytical Chemistry*; R.E. Wrolstad, T.E. Acree, H. An et al, Eds.; Wiley: New York, 2001; pp. F1.2.1-F1.2.9.

26. U.S. Department of Agriculture, USDA National Nutrient Database for Standard Reference, release 28, May 2016. <http://www.ars.usda.gov/>.
27. A.E. Martell, Chelates of ascorbic acid: Formation and catalytic properties. *Advances in Chemistry: Ascorbic acid: Chemistry, metabolism, and uses*. 1982, DOI: 10.1021/ba-1982-0200.ch007, 153-178.
28. N.B. Stebbins, L.R. Howard, R.L. Prior, C. Brownmiller, R. Liyanage, J.O. Lay, X. Yang, S.Y. Qian, Ascorbic acid-catalyzed degradation of cyanidin-3-*O*- β -glucoside: Proposed mechanism and identification of a novel hydroxylated product. *J. Berry Res.* 2016, **6**, 175-187.
29. T. Eidenberger, Stabilized anthocyanin compositions. US Patent 8,623,429, Jan 7, 2014.
30. P. Trouillas, J.C. Sancho-Garcia, V. De Freitas, J. Gierschner, M. Otyepka, O. Dangles, Stabilizing and modulating color by copigmentation: Insight from theory and experiment. *Chem. Rev.* 2016, **116**, 4937-4982.
31. E. Maccarone, A. Maccarrone, P. Rapisarda, Technical note: Colour stabilization of orange fruit juice by tannic acid. *Intl. J. Food Sci. Technol.* 1987, **22**, 159-162.
32. F.O. Bobbio, M.T. Varella, P.A. Bobbio, Effect of light and tannic acid on the stability of anthocyanins in DMSO and in water. *Food Chem.* 1994, **51**, 183-185.
33. L.D. Falcao, C. Gauche, D.M. Barros, E.S. Prudencio, E.F. Gris, E.S. Sant'Anna, P.J. Ogliari, M.T.B. Luiz, Stability of anthocyanins from grape (*Vitis vinifera* L.) skins with tannic acid in a model system. *Ital. J. Food Sci.* 2004, **16**, 323-332.
34. K.A. Bindon, M.G. McCarthy, P.A. Smith. Development of wine colour and non-bleachable pigments during the fermentation and ageing of (*Vitis vinifera* L. cv.) Cabernet Sauvignon wines differing in anthocyanin and tannin concentration. *LWT-Food Sci. Technol.* 2014, **59**, 923-932.
35. T.F. Hager, L.R. Howard, R.L. Prior, Processing and storage effects on the ellagitannin composition of processed blackberry products. *J. Agric. Food Chem.* 2010, **58**, 11749-11754.
36. T. Siriwoharn, R.E. Wrolstad, Polyphenolic composition of Marion and Evergreen blackberries. *J. Food Sci.* 2004, **69**, 233-240.
37. K. Aaby, S. Mazur, A. Nes, G. Skrede, Phenolic compounds in strawberry (*Fragaria x ananassa* Duch.) fruits: Composition in 27 cultivars and changes during ripening. *Food Chem.* 2012, **132**, 86-97.
38. M.J. Cho, L.R. Howard, R.L. Prior, J.R. Clark, Flavonol glycosides and antioxidant capacity of various blackberry and blueberry genotypes determined by high-performance liquid chromatography/mass spectrometry. *J. Sci. Food Agric.* 2005, **85**, 2149-2158.

39. M. Mikulic-Petkovsek, A. Slatnar, F. Stampar, R. Veberic, HPLC-MSⁿ identification and quantification of flavonol glycosides in 28 wild and cultivated berry species. *Food Chem.* 2012, **135**, 2138-2146.
40. P. Michel, A. Dobrowolska, A. Kicel, A. Owczarek, A. Bazytko, S. Granica, J.P. Piwowarski, M.A. Olszewska, Polyphenolic profile, antioxidant and anti-inflammatory activity of eastern teaberry (*Gaultheria procumbens* L.) leaf extracts. *Molec.* 2014, **19**, 20498-20520.
41. M.H. Choi, G.H. Kim, H.S. Lee, Effects of ascorbic acid retention on juice color and pigment stability in blood orange (*Citrus sinensis*) juice during refrigerated storage. *Food Res. Int.* 2002, **35**, 753-759.
42. E. Sadilova, F.C. Stintzing, D.R. Kammerer, R. Carle, Matrix dependent impact of sugar and ascorbic acid addition on color and anthocyanin stability of black carrot, elderberry and strawberry single strength and concentrate juices upon thermal treatment. *Food Res. Int.* 2009, **42**, 1023-1033.
43. D. Marchese, Citrus consumers trend in Europe. New tastes sensation: The blood orange juice case. In *Citrus processing short course proceedings*. 1995, 19-39. University of Florida, Gainesville, FL.
44. P. Markakis, Stability of anthocyanins in foods. In *Anthocyanins as food colorants*. **1982**, 163-180. New York: Academic Press.
45. L. Jurd, Some advances in the chemistry of anthocyanin-type plant pigments. In Chichester CO. Ed. *The chemistry of plant pigments*. 1972, 123-142. New York: Academic Press.
46. P. Janeiro, A.M.O. Brett, Redox behavior of anthocyanins present in *Vitis vinifera* L. *Electroanal.* 2007, **17**, 1779-1786.
47. M. Andoni, M. Medeleanu, M. Stefanut, A. Cata, I. Ienascu, C. Tanasie, R. Pop, Theoretical determination of the redox electrode potential of cyanidin. *J. Serb. Chem. Soc.* 2016, **81**, 177-186.
48. A. Cata, M.N. Stefanut, R. Pop, C. Tanasie, C. Mosoarca, A.D. Zamfir, Evaluation of antioxidant activities of some small fruits containing anthocyanins using electrochemical and chemical methods. *Croat. Chem. Acta.* 2016, **89**, 37-48.
49. S. Komorsky-Lovric, I. Novak, Abrasive stripping square-wave voltammetry of blackberry, raspberry, strawberry, pomegranate, and sweet and blue potatoes. *J. Food Sci.* 2011, **76**, 916-920.
50. C. Lu, Y. Liu, Interactions of lipoic acid radical cations with vitamin C and E analogue and hydroxycinnamic acid derivatives. *Arch. Biochem. Biophys.* 2002, **406**, 78-84.

51. G.R. Buettner, The pecking order of free radicals and antioxidants: Lipid peroxidation, α -tocopherol, and ascorbate. *Arch. Biochem. Biophys.* 1993, **300**, 535-543.

52. W.G. Kirlin, J. Cai, S.A. Thompson, D. Diaz, T.J. Kavanagh, D.P. Jones, Glutathione redox potential in response to differentiation and enzyme inducers. *Free Rad. Biol. Med.* 1999, **27**, 1208-1218.

Tables

Table 1: Flavonol identification depicted in Figure 5.

Peak	Tentative identification	<i>m/z</i>	
		M ⁺	Fragments
1	Quercetin-3-rutinoside	609	301
2	Quercetin-3-pentosyl-glucuronide	609	433, 301
3	Quercetin-3-galactoside	463	301
4	Quercetin-3-glucoside	463	301
5	Quercetin-3-glucuronide	477	301
6	Unidentified	505	465, 301

Table 2: Three parameter exponential decay model

Stage	Variable	AICc	BIC	SSE	MSE	RMSE	R-Square
1	Total ACY	1044.559	1076.821	417873.66	5646.941	75.146	0.972
1	% Polymeric Color	328.596	360.859	134.077	1.811	1.346	0.973
2	Total ACY	12380.013	1280.337	390633.281	4340.369	65.881	0.987
2	% Polymeric Color	443.907	486.231	250.307	2.781	1.667	0.967

Table 3: Goodness of fit measures for the fitted three parameter exponential decay model

Stage	Treatment	Total ACY	Percent polymeric color
1	Control	$888 + 1220e^{(-0.48*\text{week})}$	$47 - 38e^{(-0.20*\text{week})}$
1	Glutathione	$512 + 1662e^{(-0.20*\text{week})}$	$102 - 92e^{(-0.04*\text{week})}$
1	DTPA	$898 + 1344e^{(-0.47*\text{week})}$	$34 - 25e^{(-0.30*\text{week})}$
1	Galacturonic Acid	$770 + 1387e^{(-0.42*\text{week})}$	$49 - 40e^{(-0.16*\text{week})}$
1	Tannic Acid	$819 + 1371e^{(-0.46*\text{week})}$	$62 - 52e^{(-0.12*\text{week})}$
2	Control	$557 + 1569e^{(-0.45*\text{week})}$	$51 - 26e^{(-0.47*\text{week})}$
2	Glutathione	$745 + 1627e^{(-0.45*\text{week})}$	$42 - 22e^{(-0.67*\text{week})}$
2	Glutathione + Lipoic	$691 + 1757e^{(-0.45*\text{week})}$	$47 - 26e^{(-0.37*\text{week})}$
2	GLA	$759 + 1670e^{(-0.49*\text{week})}$	$43 - 20e^{(-0.40*\text{week})}$
2	Lipoic Acid	$664 + 1540e^{(-0.50*\text{week})}$	$49 - 26e^{(-0.49*\text{week})}$
2	Ascorbic Acid	$631 + 1708e^{(-0.68*\text{week})}$	$53 - 30e^{(-0.40*\text{week})}$

Table 4: Inverse prediction of total anthocyanin retention based on nonlinear regression model

Stage	Treatment	Specified Total ACY (mg/L)	Predicted week	Std error	Lower 95%	Upper 95%
1	Control	1000	5.04	0.66	3.75	6.33
1	Glutathione	1000	6.21	0.69	4.87	7.56
1	DTPA	1000	5.46	0.82	3.85	7.06
1	Galacturonic acid	1000	4.28	0.28	3.73	4.82
1	Tannic acid	1000	4.4	0.35	3.71	5.09
2	Control	1000	2.84	0.1	2.64	3.04
2	Glutathione	1000	4.09	0.19	3.72	4.47
2	Glutathione + Lipoic	1000	3.86	0.15	3.57	4.15
2	GLA	1000	3.95	0.18	3.6	4.31
2	Lipoic acid	1000	3.04	0.11	2.81	3.26
2	Ascorbic acid	1000	2.25	0.09	2.08	2.42

Figure captions

Figure 1. Total anthocyanin concentrations in blackberry juice fortified with stabilizing agents through pasteurization and accelerated storage in Stage 1 (LSmeans Treatment*Time \pm one standard error based on the fitted model).

Figure 2. Three parameter exponential decay model of total anthocyanins in Stage 1.

Figure 3. Total anthocyanin concentrations in blackberry juice fortified with stabilizing agents through pasteurization and accelerated storage in Stage 2 (LSmeans Treatment*Time \pm one standard error based on the fitted model).

Figure 4. Three parameter exponential decay model of total anthocyanins in Stage 2.

Figure 5. Individual anthocyanin concentrations in blackberry juice fortified with stabilizing agents over accelerated storage in Stage 1 (LSmeans Treatment*Time \pm one standard error based on the fitted model).

Figure 6. Individual anthocyanin concentrations in blackberry juice fortified with stabilizing agents over accelerated storage in Stage 2 (LSmeans Treatment*Time \pm one standard error based on the fitted model).

Figure 7. HPLC chromatogram (360 nm) of flavonols in blackberry juice

Figure 8. Proposed antioxidant recycling mechanism (adapted from Lu & Liu 2002)

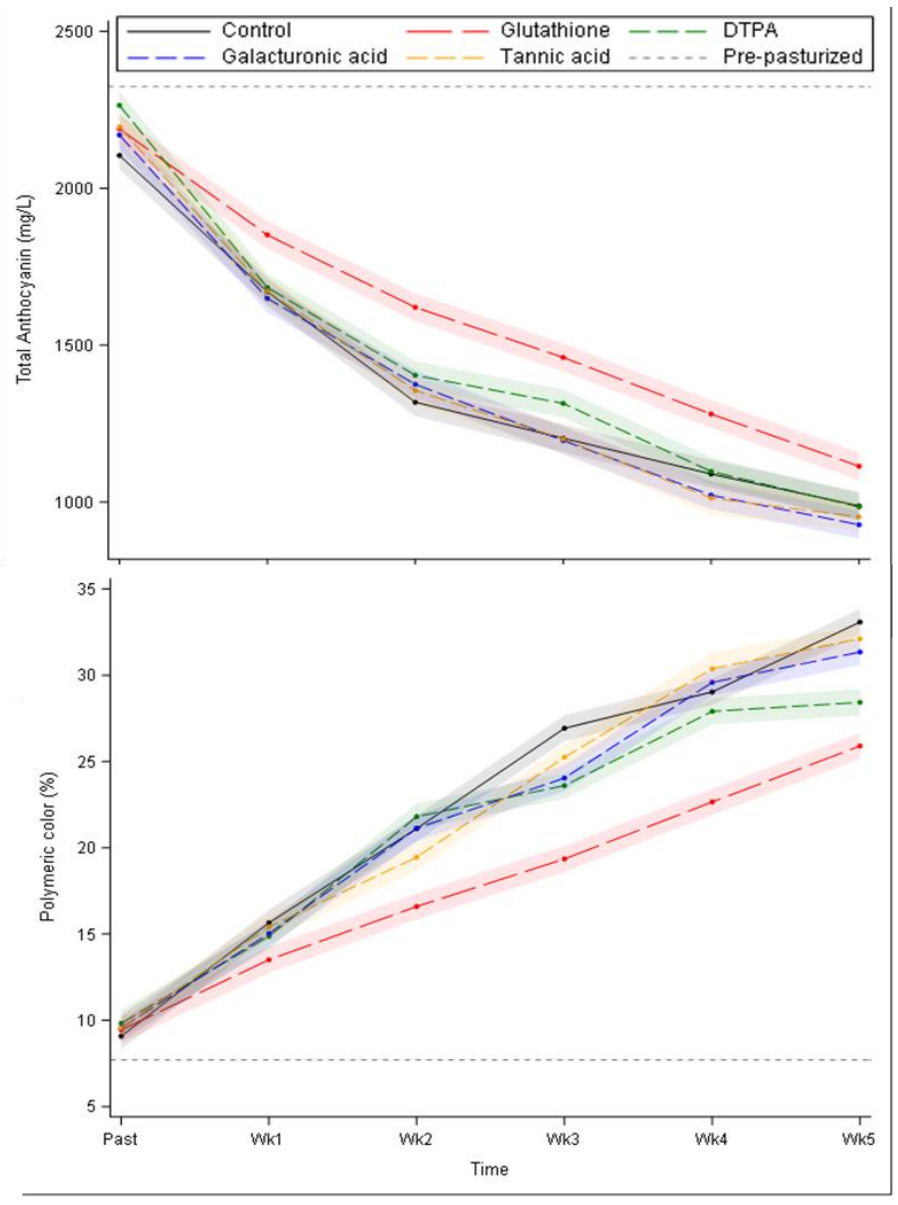


Figure 1

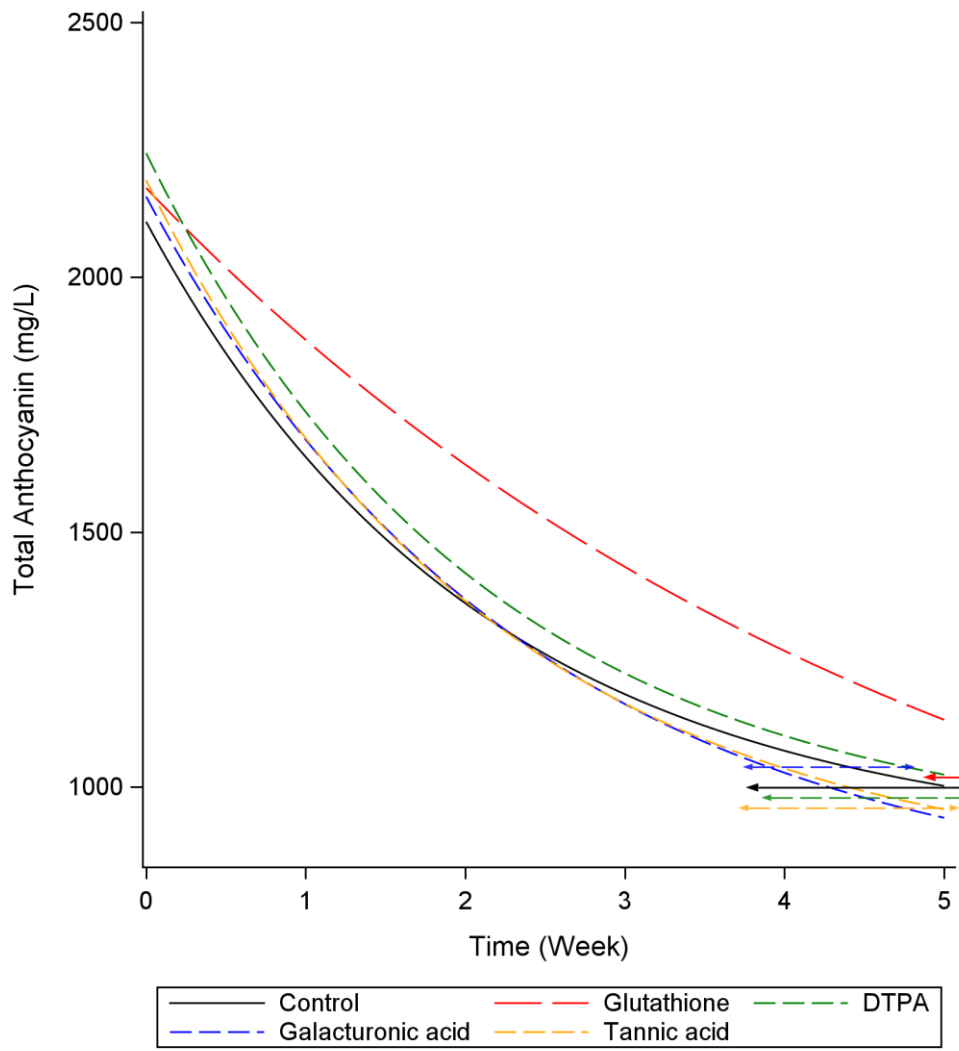


Figure 2

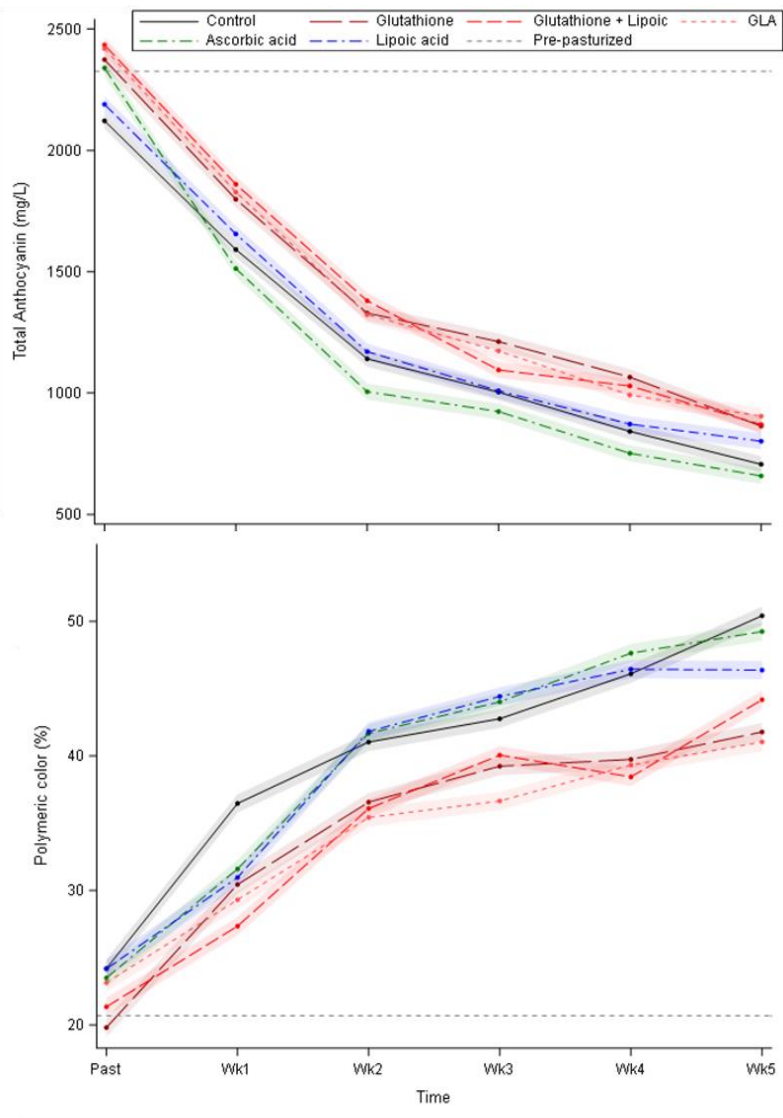


Figure 3

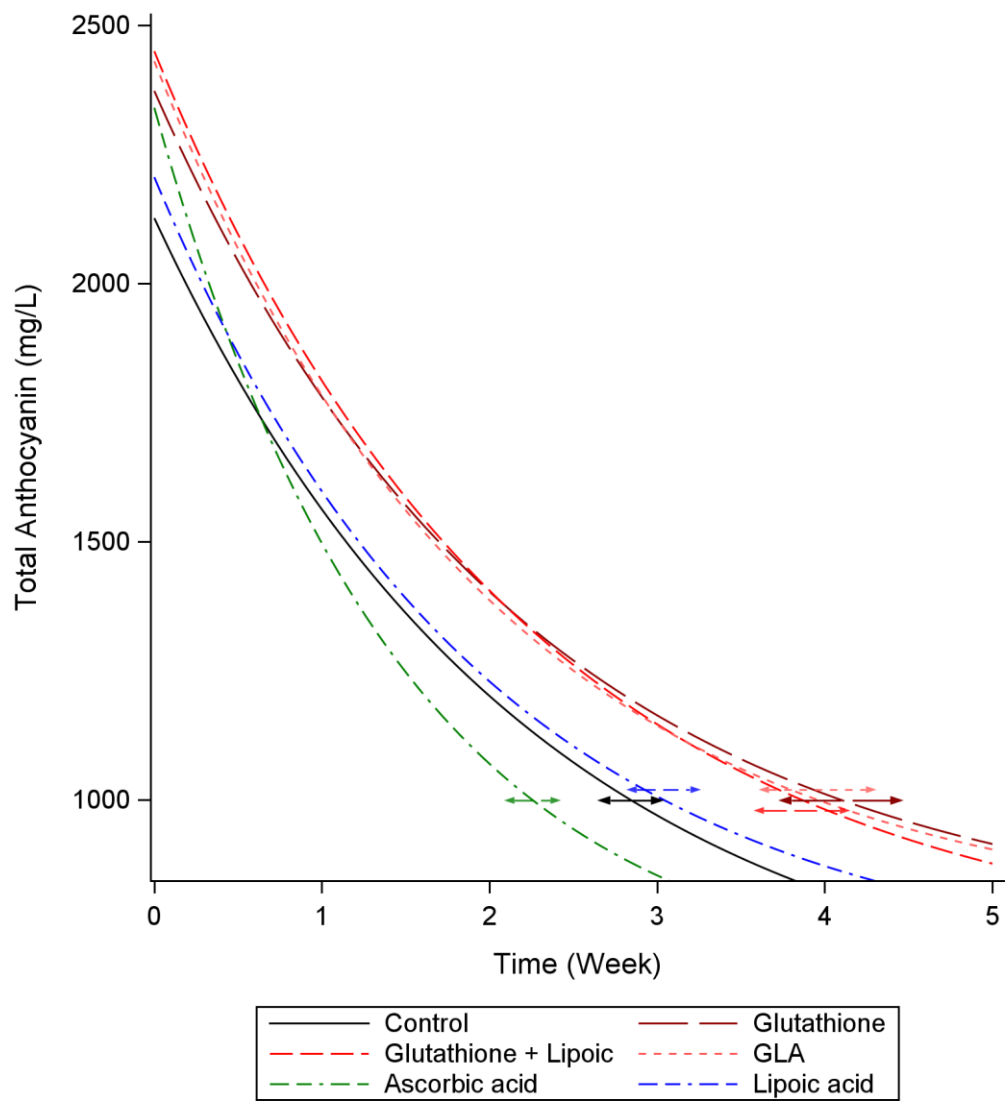


Figure 4

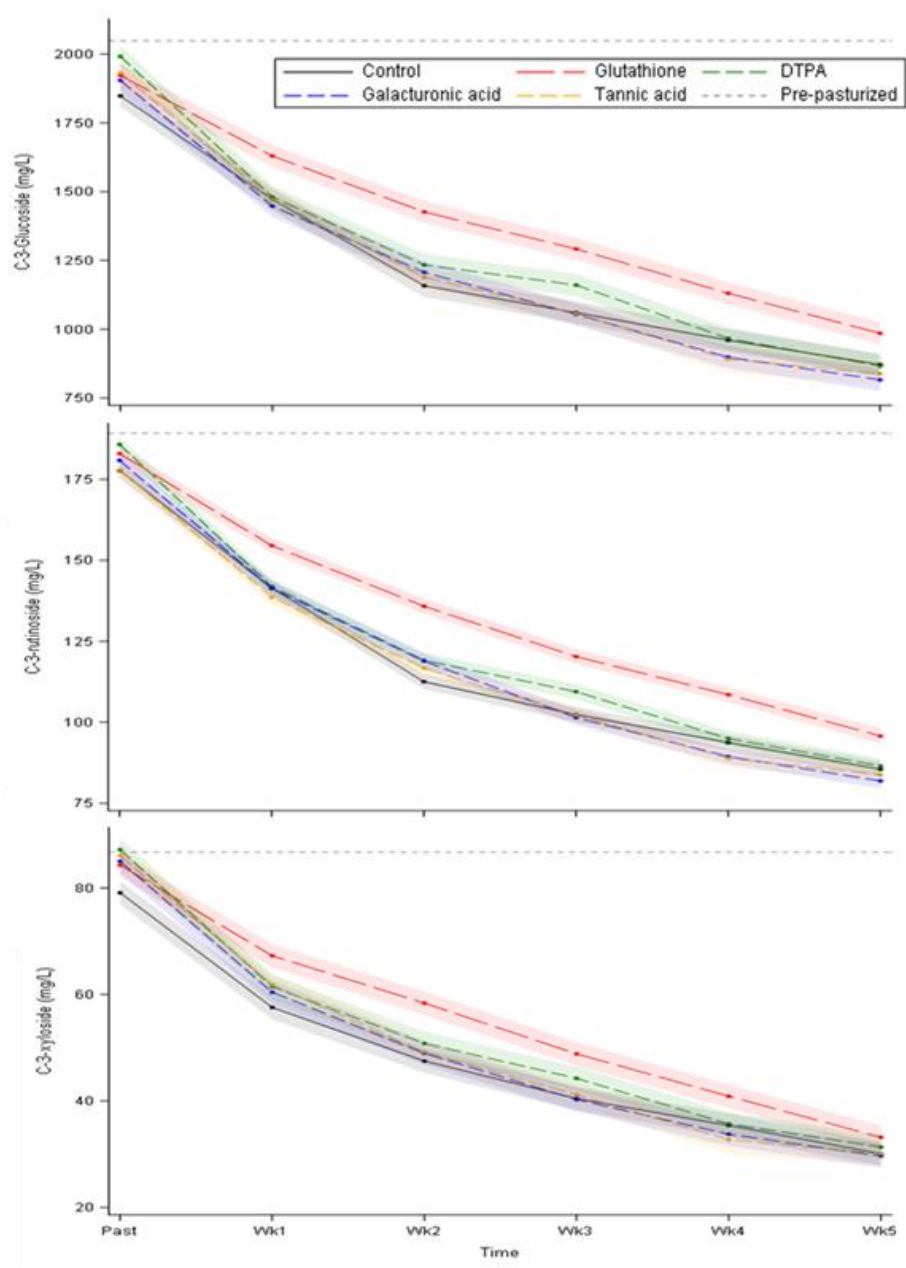


Figure 5

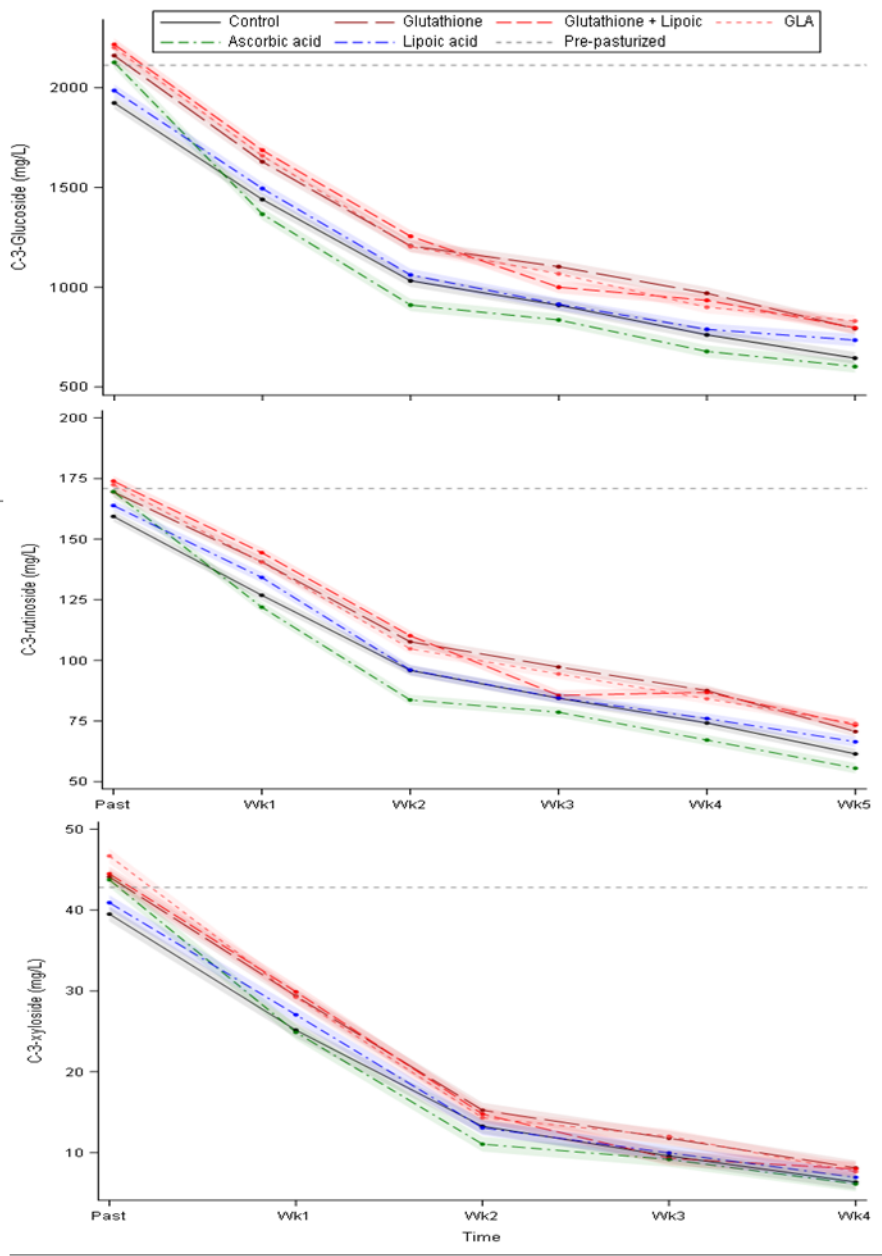


Figure 6

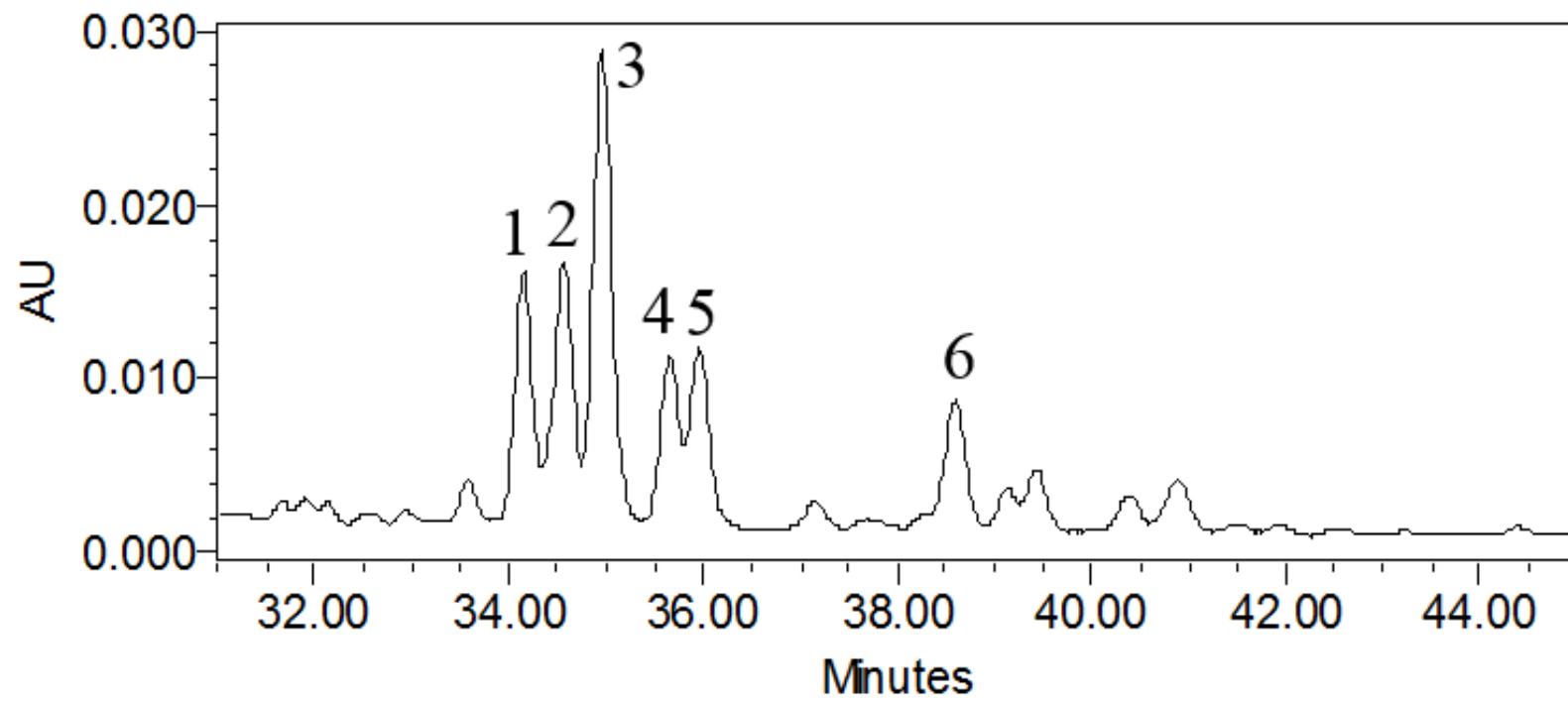


Figure 7

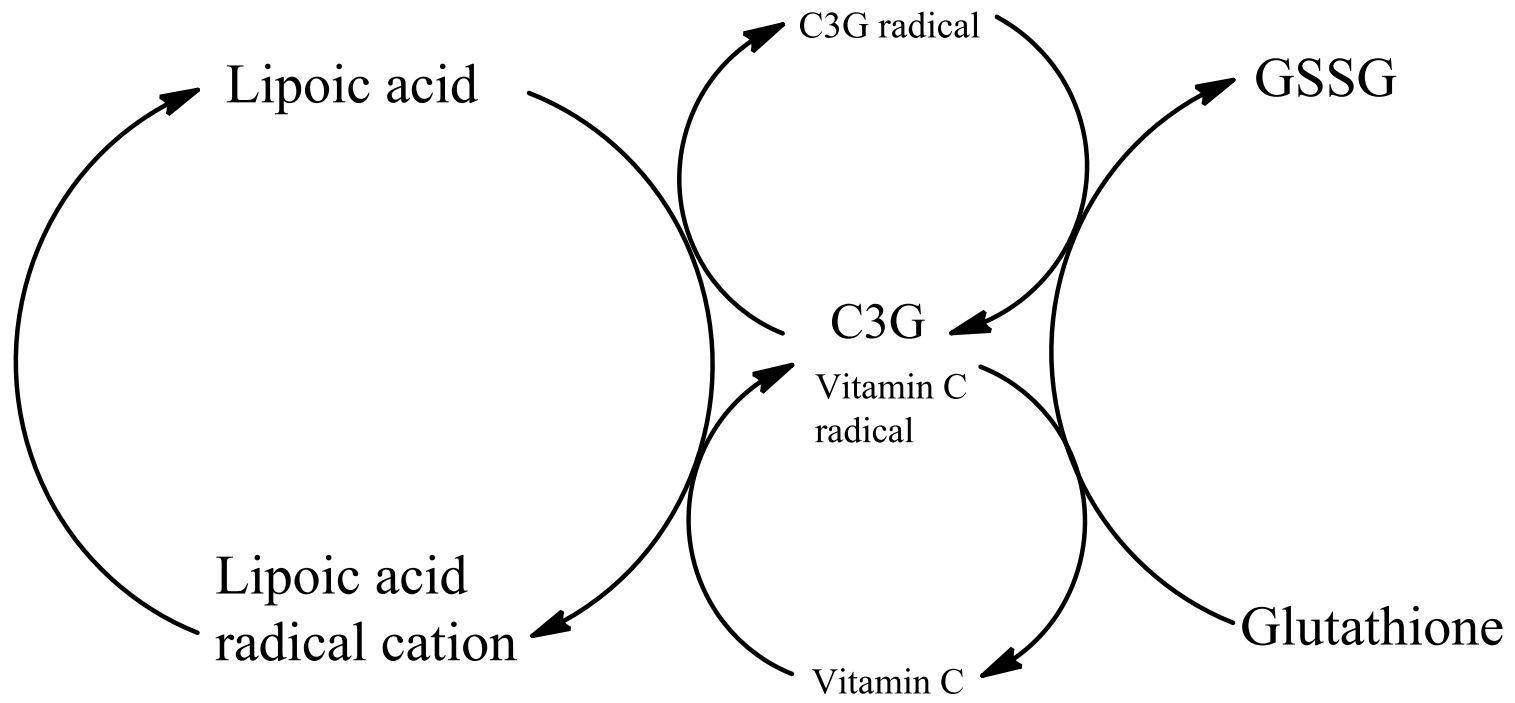


Figure 8

Appendix: Supplementary table:

Table S1: Inverse prediction of percent polymeric color based on nonlinear regression model

Stage	Treatment	Specified Percent Polymeric Color (%)	Predicted week	Std error	Lower 95%	Upper 95%
1	Control	25	2.76	0.11	2.56	2.97
1	Glutathione	25	4.75	0.20	4.35	5.14
1	DTPA	25	3.23	0.14	2.95	3.50
1	Galacturonic acid	25	3.02	0.11	2.80	3.24
1	Tannic acid	25	3.01	0.11	2.80	3.22
2	Control	40	1.83	0.12	1.59	2.07
2	Glutathione	40	3.55	0.35	2.85	4.24
2	Glutathione + Lipoic	40	3.49	0.18	3.14	3.85
2	GLA	40	4.36	0.42	3.53	5.19
2	Lipoic acid	40	2.02	0.13	1.77	2.27
2	Ascorbic acid	40	2.01	0.11	1.78	2.23

Supplementary figures:

Figure S1. Three parameter exponential decay model of percent polymeric color in Stage 1.

Figure S2. Three parameter exponential decay model of percent polymeric color in Stage 2.

Figure S3. Anom plots of predicted week and growth rate of total anthocyanins and percent polymeric color in Stage 1.

Figure S4. Anom plots of predicted week and growth rate of total anthocyanins and percent polymeric color in Stage 2.

Figure S5. Ellagitannin concentrations in blackberry juice fortified with stabilizing agents over accelerated storage in Stage 1 (LSmeans Treatment*Time \pm one standard error based on the fitted model).

Figure S6. Ellagitannin concentrations in blackberry juice fortified with stabilizing agents over accelerated storage in Stage 2 (LSmeans Treatment*Time \pm one standard error based on the fitted model).

Figure S7. Flavonol concentrations in blackberry juice fortified with stabilizing agents over accelerated storage in Stage 1 (LSmeans Treatment*Time \pm one standard error based on the fitted model).

Figure S8. Flavonol concentrations in blackberry juice fortified with stabilizing agents over accelerated storage in Stage 2 (LSmeans Treatment*Time \pm one standard error based on the fitted model).

Figure S9. Mass spectra of quercetin-3-rutinoside in negative mode.

Figure S10. Mass spectra of quercetin-3-pentosyl-glucuronide in negative mode.

Figure S11. Mass spectra of quercetin-3-galactoside in negative mode.

Figure S12. Mass spectra of quercetin-3-glucoside in negative mode.

Figure S13. Mass spectra of quercetin-3-glucuronide in negative mode.

Figure S14. Mass spectra of unidentified blackberry flavonol in negative mode.

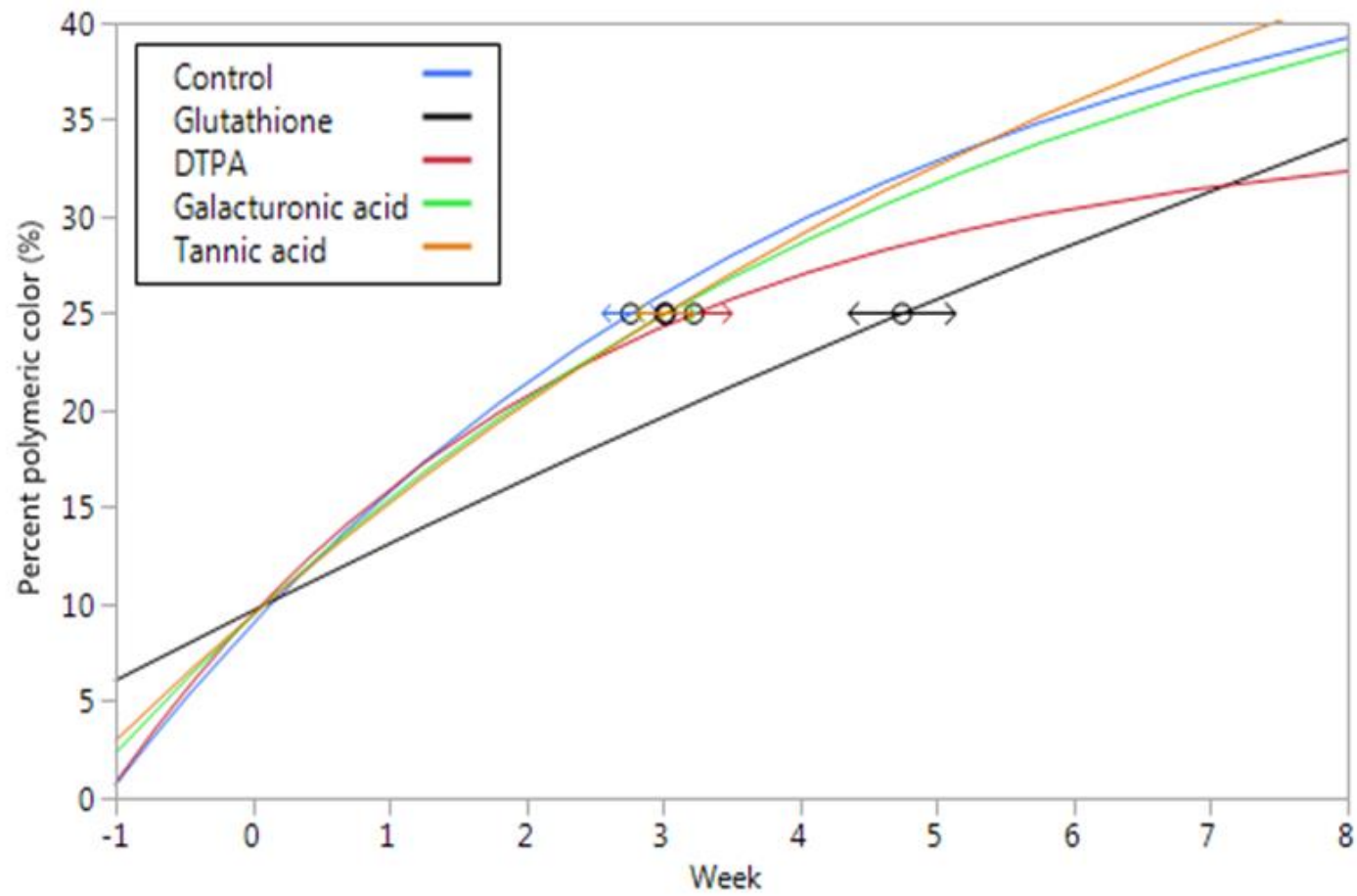


Figure S1

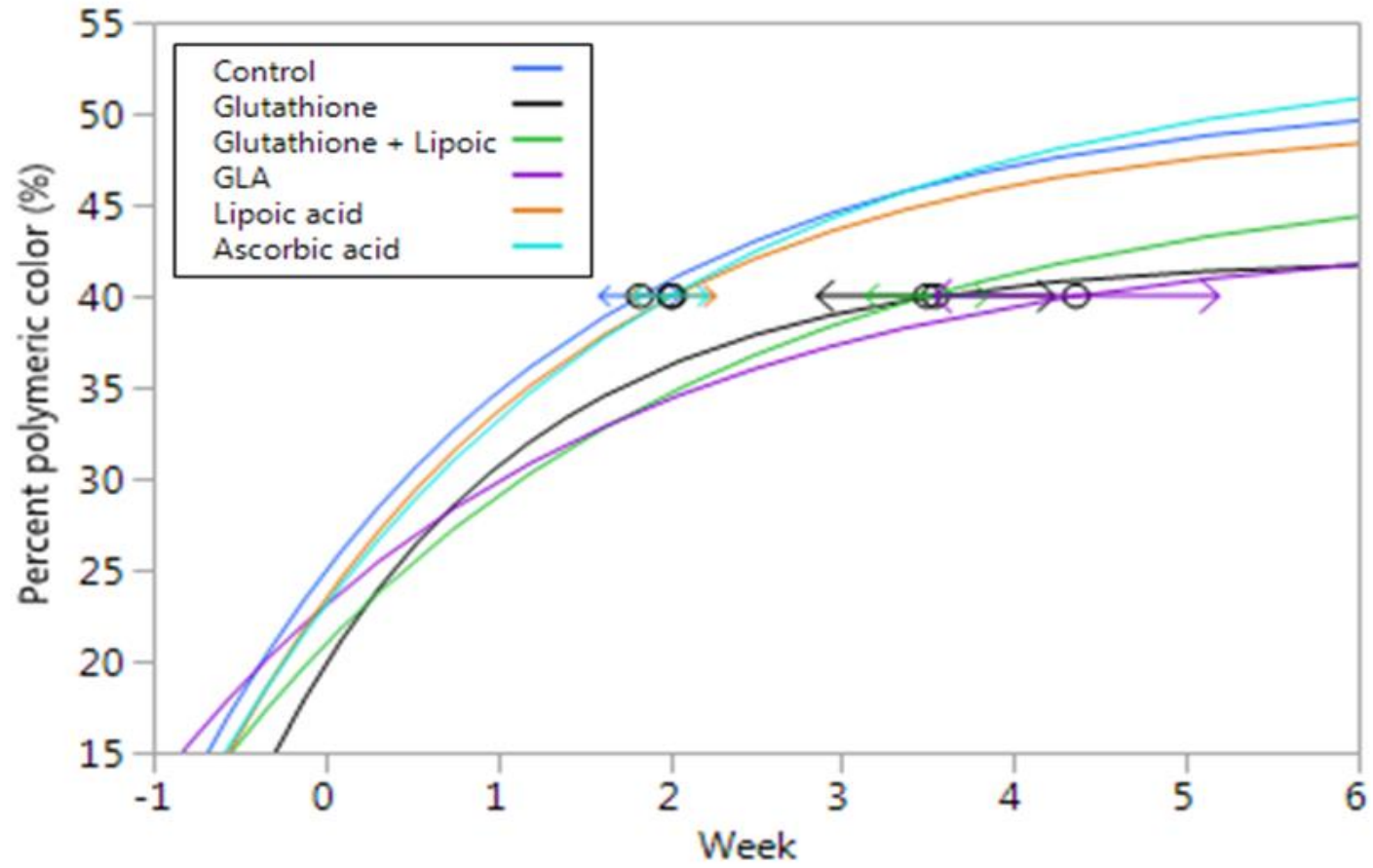


Figure S2

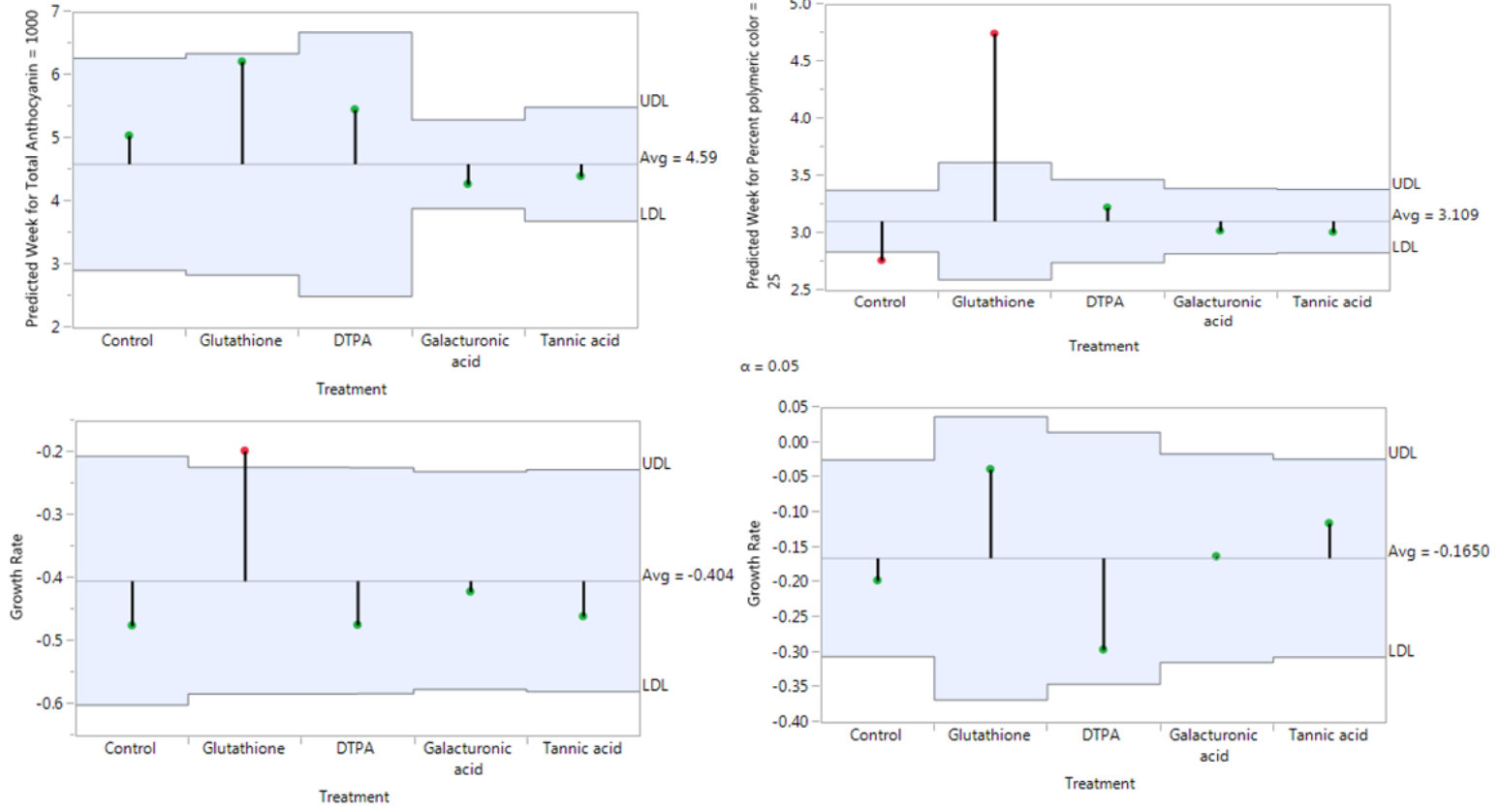


Figure S3

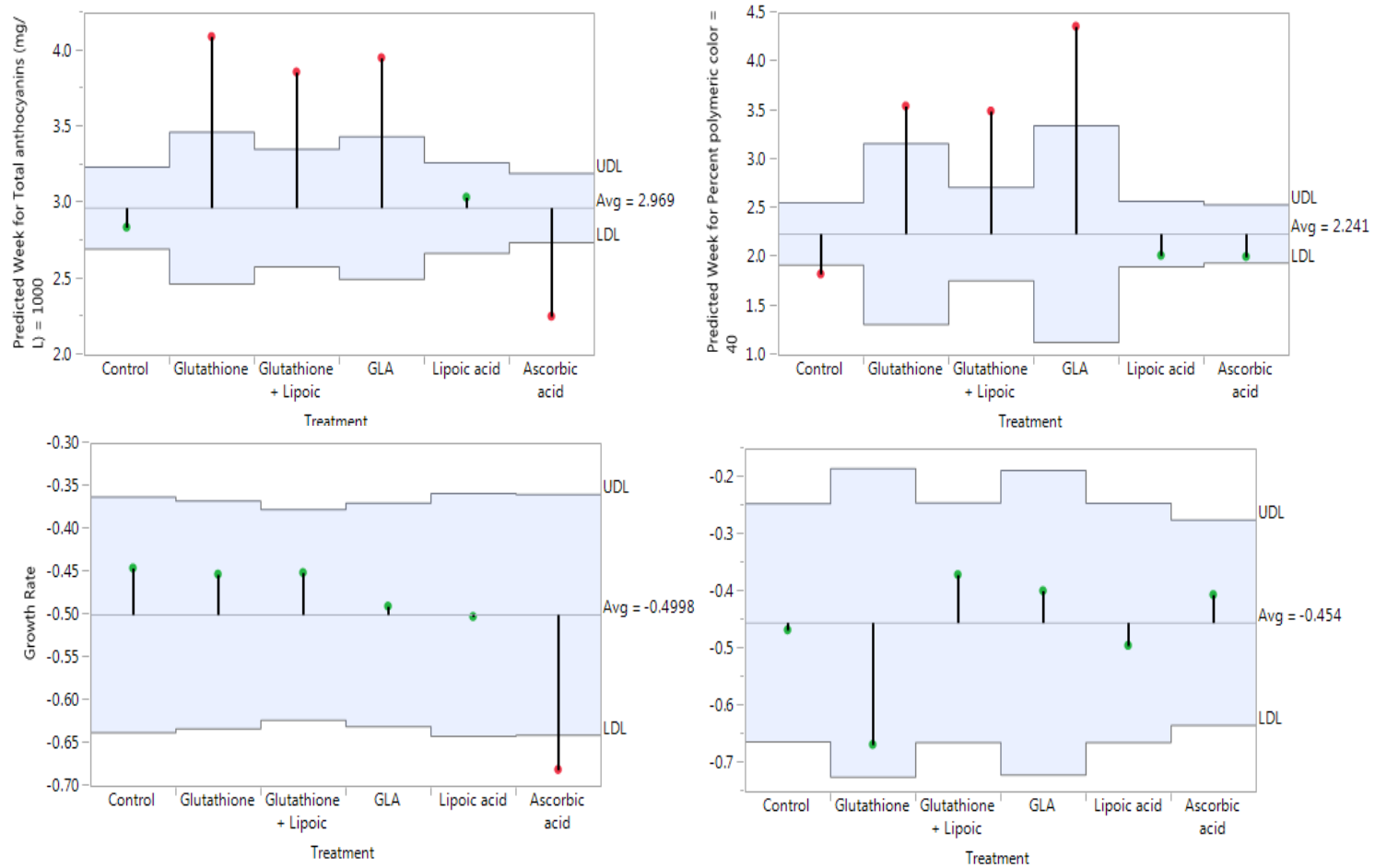


Figure S4

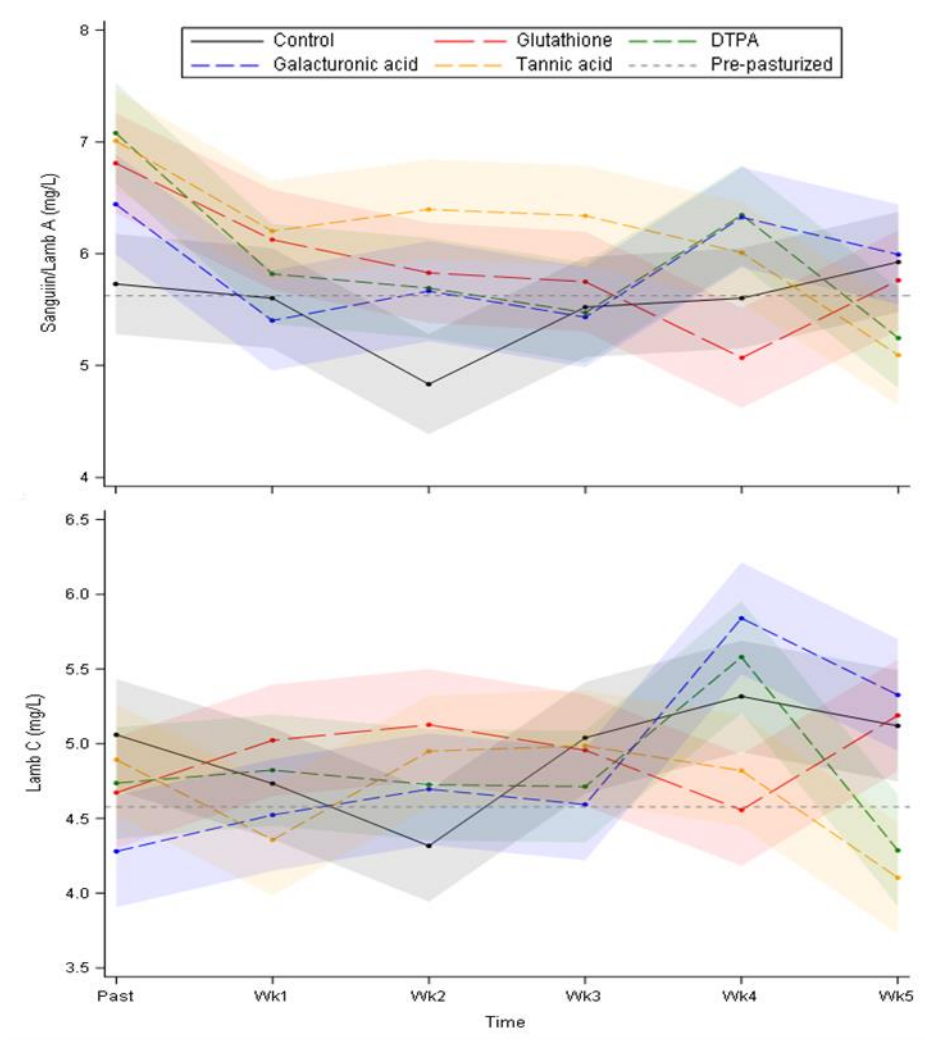


Figure S5

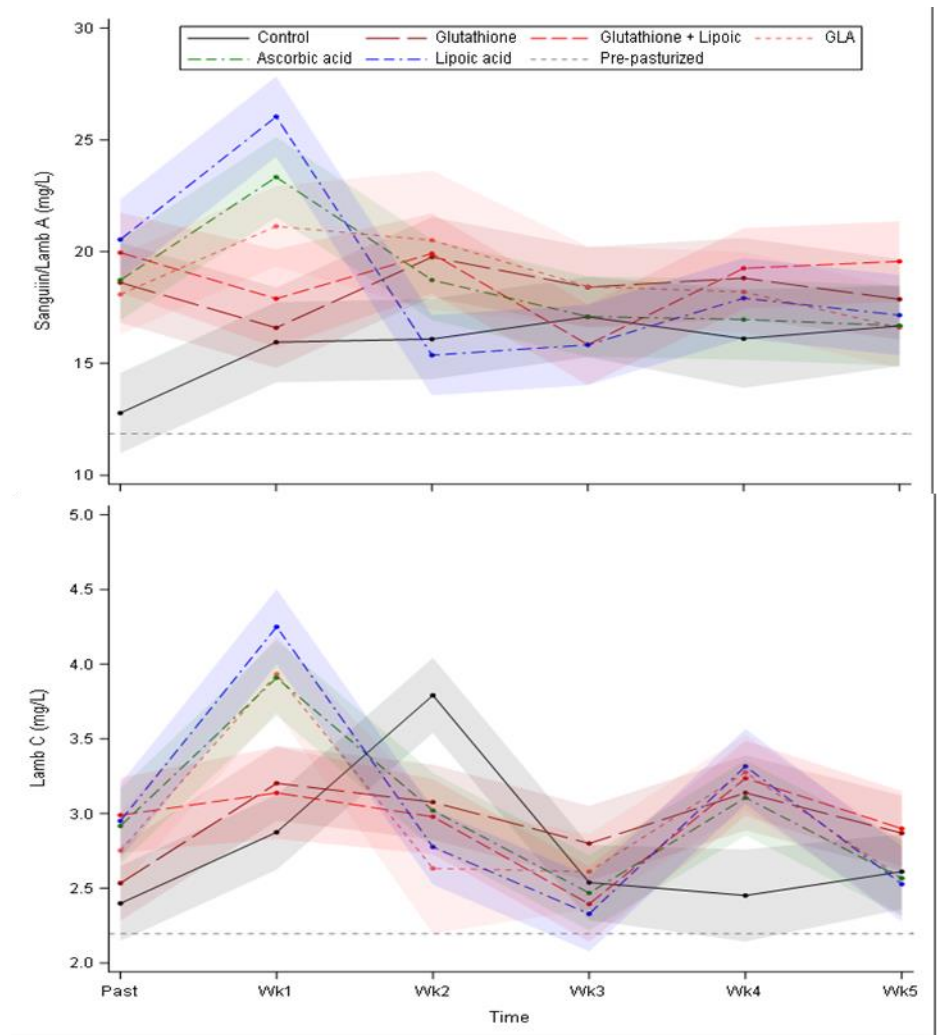


Figure S6

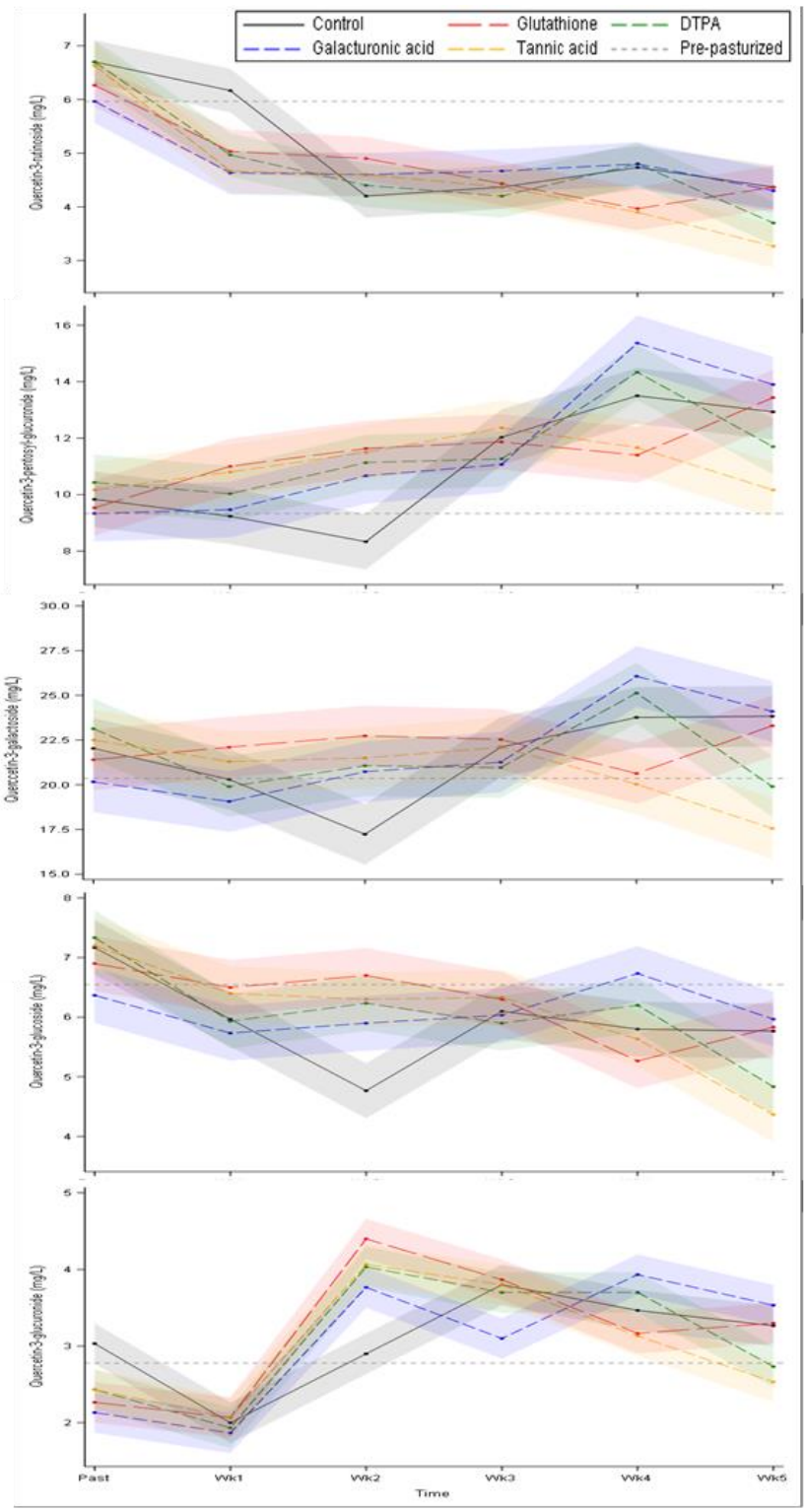


Figure S7

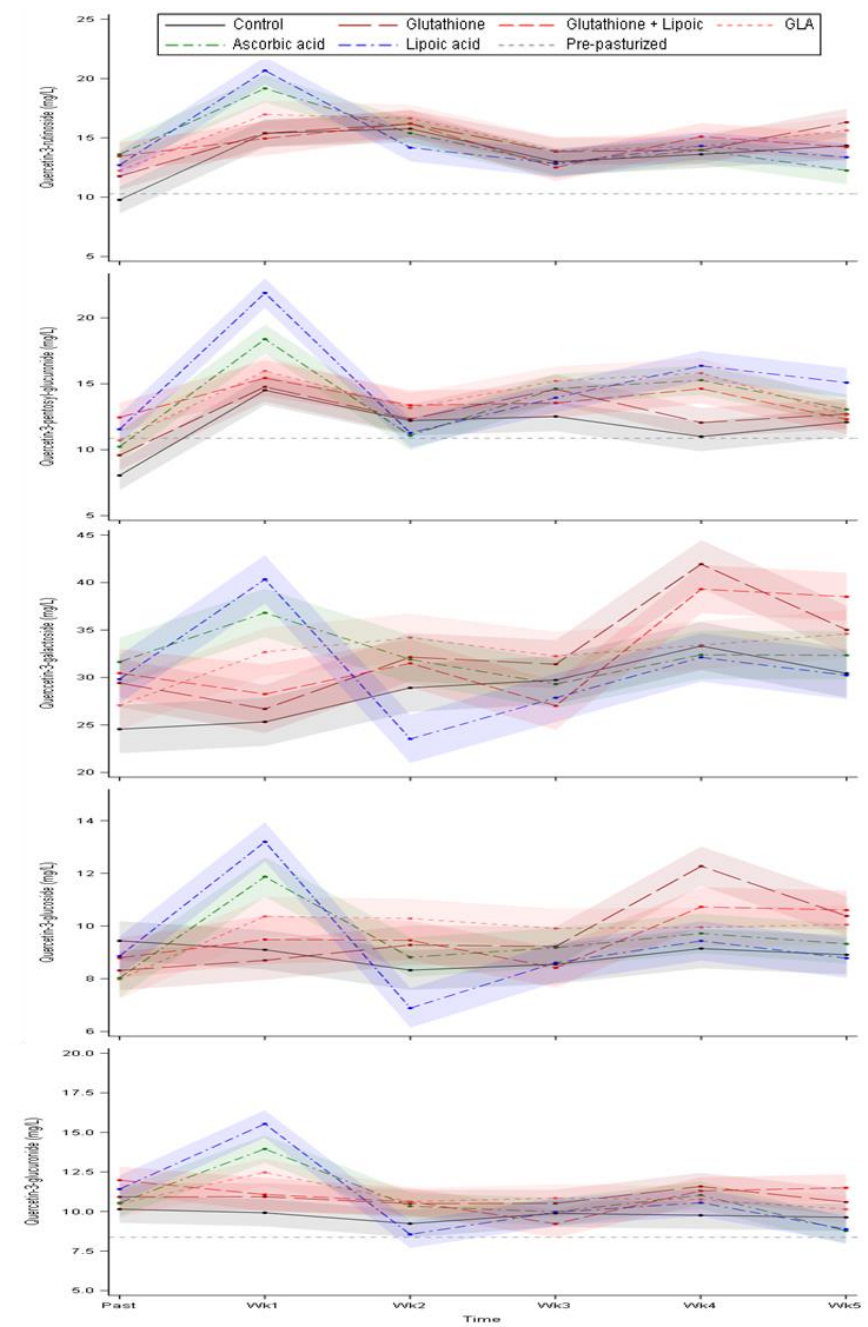


Figure S8

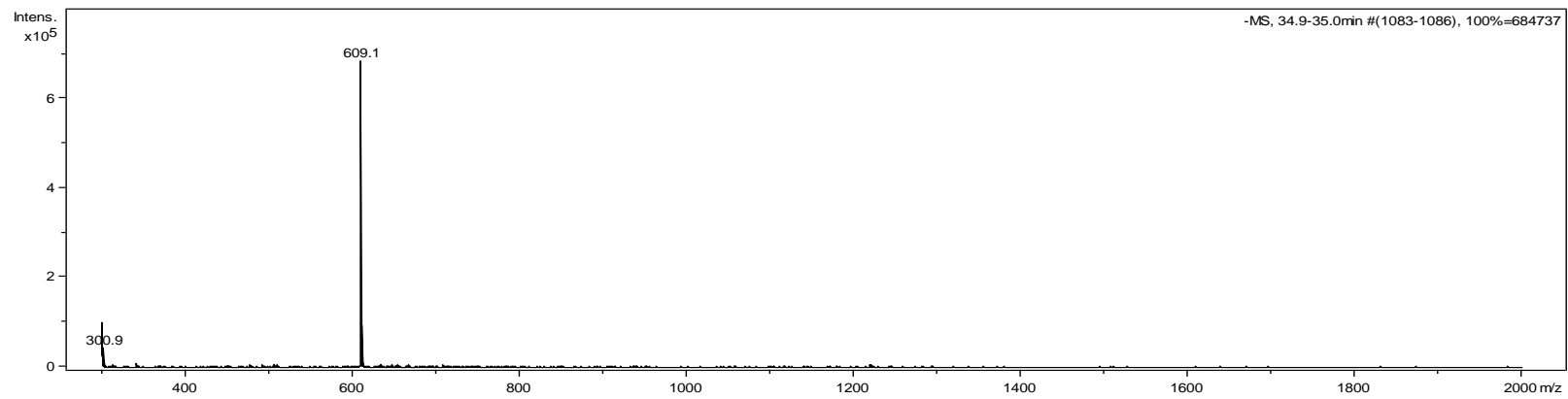


Figure S9

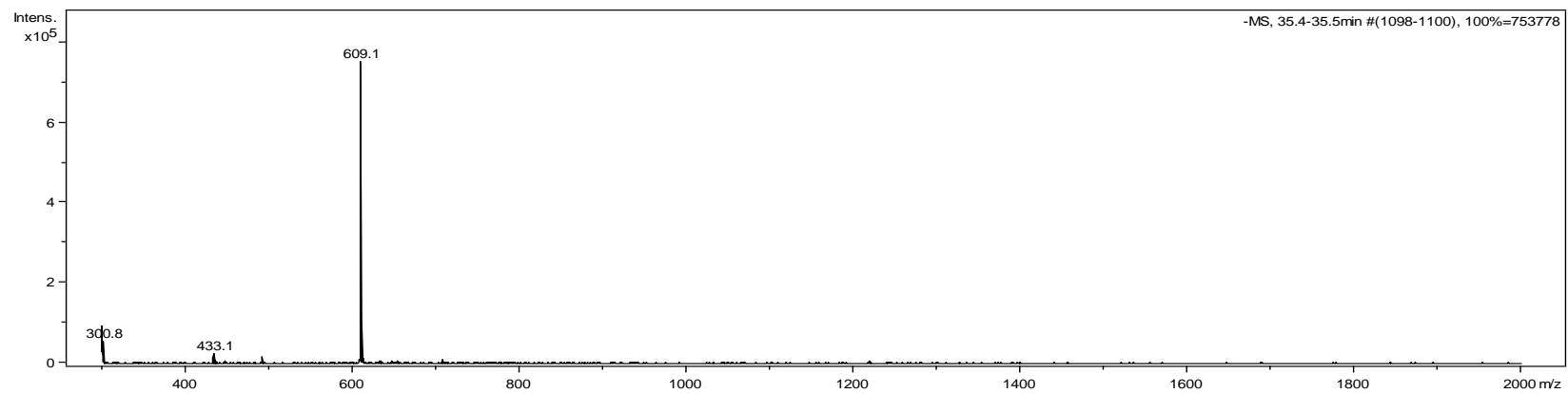


Figure S10

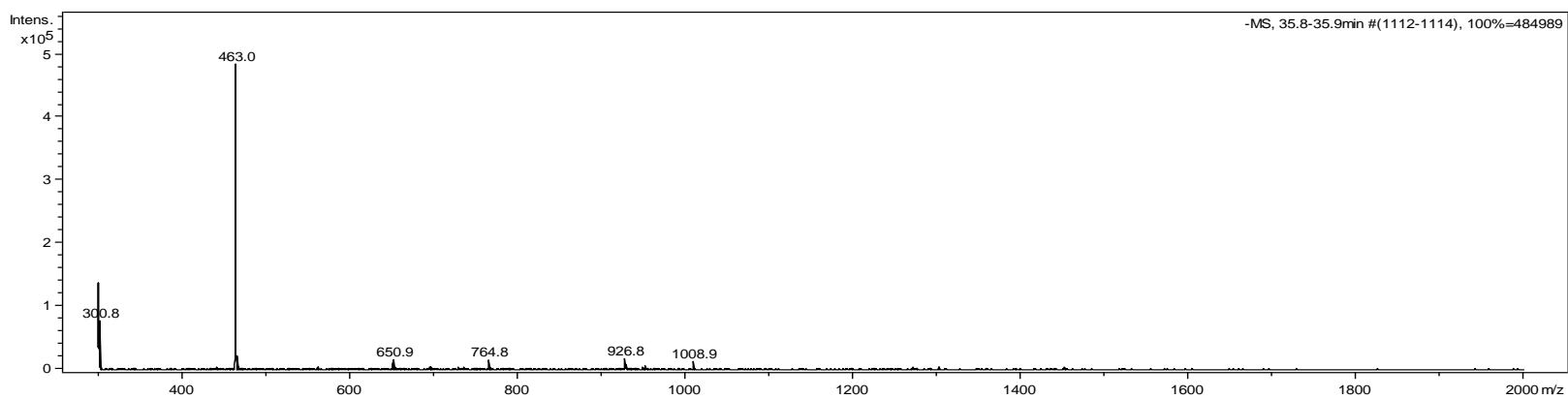


Figure S11

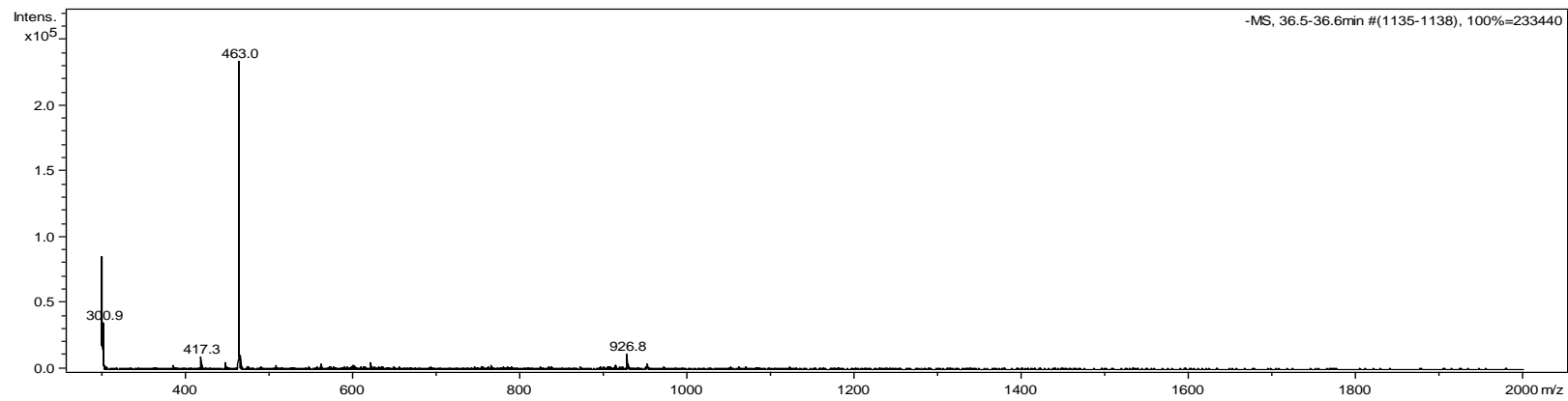


Figure S12

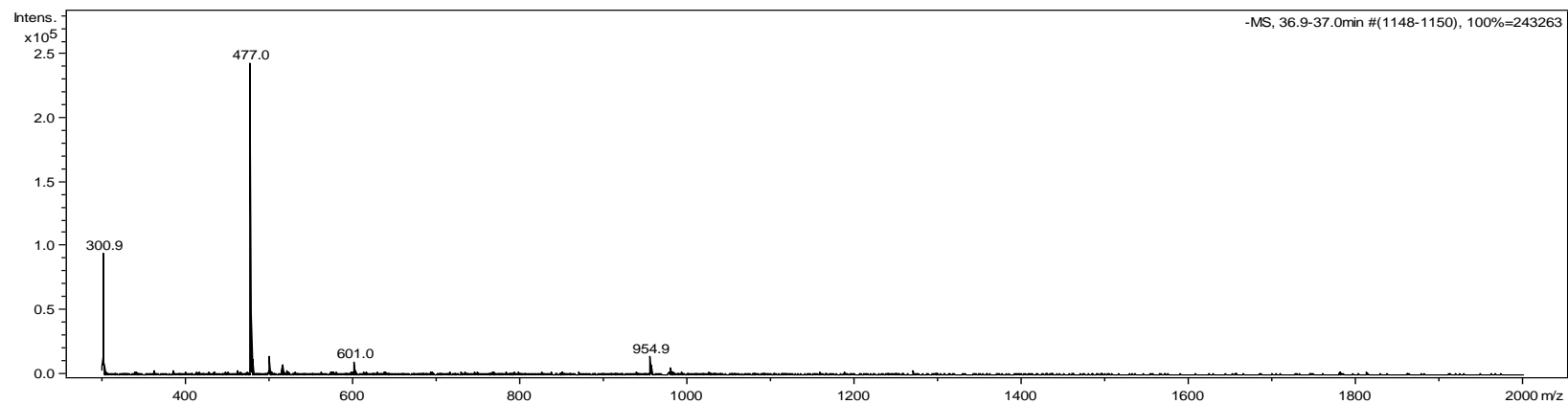


Figure S13

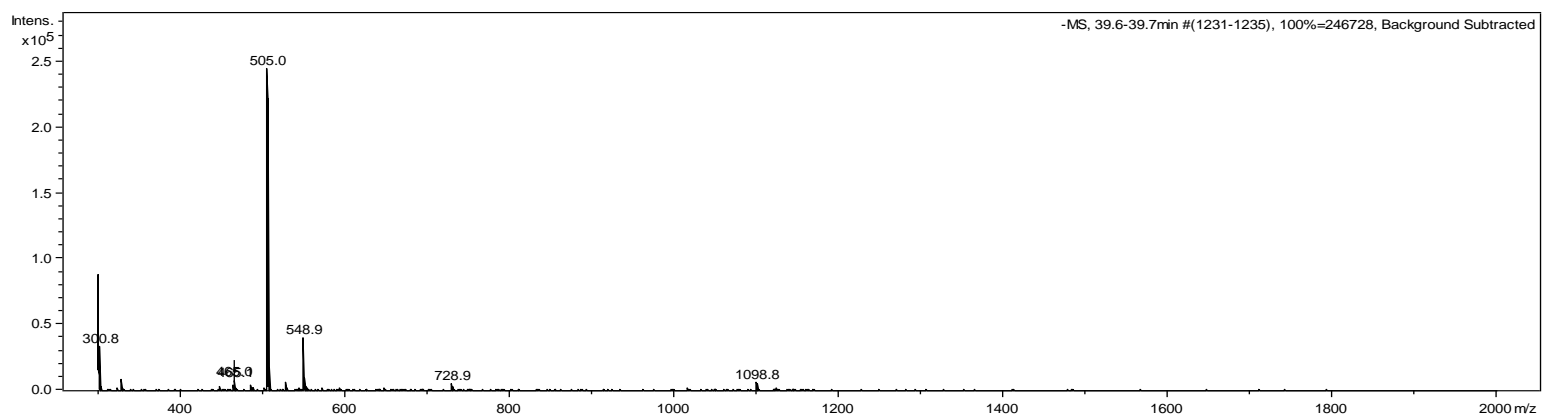


Figure S14

CHAPTER 6. Formation, mass spectrometric identification, and color stability of acetaldehyde-catalyzed condensation of red radish (*Raphanus sativus*) anthocyanins and (+)-catechin

Nathan B. Stebbins¹, Luke R. Howard^{*1}, Ronald L. Prior¹, Cindi Brownmiller¹

¹University of Arkansas, Department of Food Science, Fayetteville, Arkansas 72704, USA

Corresponding author: Dr. Luke Howard, Department of Food Science, University of Arkansas, 2650 N. Young Avenue, Fayetteville, AR 72704, USA. Tel.: 1 479 575 2978; Fax: 479 575 6936; E-mail: lukeh@uark.edu

Abstract

There is great demand to replace artificial colors with natural alternatives. However, many natural colorants face issues with solubility, off flavors, and poor stability to pH, temperature, light and ascorbic acid. Anthocyanins are a class of pigments found in many fruits and vegetables that are water-soluble and range from red to purple. Red radish anthocyanins are particularly stable due to acylation of anthocyanin with organic and phenolic acid moieties. We combined radish anthocyanins with acetaldehyde and catechin in a model system to form ethyl-bridged dimers that retain color. After incubation at ambient temperature for one week the reaction mixture with acetaldehyde and catechin turned from bright red to a vivid purple color. The newly formed compounds were identified with LC-ESI-MS. Color stability was monitored over six months with CIEL*a*b* and anthocyanin stability was evaluated by HPLC. Next, radishes were fermented by *Zymomonas mobilis*, which are known as high acetaldehyde producing bacteria. Natural sources of catechin were used to replace the catechin standard, but the same purple color did not appear with the addition of cranberry, grape seed, cocoa, fava beans, blueberry pomace, muscadine grape pomace, or tea extracts. The ethyl-bridged radish anthocyanins possess excellent color stability and could serve as natural colorants to synthetic food additives.

Keywords: anthocyanin, acetaldehyde, radish, catechin, natural color

Introduction

Anthocyanins are an obvious candidate to replace artificial dyes in the food industry, but these natural colorants currently have stability issues. There is a need for stable natural colorants to satisfy consumer demands, especially in beverages, because some believe artificial dyes may impose negative health effects, such as ADHD (Feingold 1976). Using anthocyanins from natural sources allows a cleaner product label and removal of E number/artificial colorants from the label. Some sources of anthocyanins include berries, red cabbage, eggplant, and radishes. Adding one of these to a label can deliver the appeal of an ingredient over an additive (Stintzing and Carle 2004).

In the presence of anthocyanins and flavanols, like catechin or procyanidins, acetaldehyde can act as a polymerization agent by reacting at carbon-8 in red wines (Timberlake 1976). The reaction of anthocyanins, acetaldehyde, and flavanols has been well documented in wine, but has not been studied extensively in other fruits and vegetables. Authors have found yellow xanthylium ion compounds formed in wine, but the more significant products were violet. Others have found reddish-blue enantiomers of malvidin-3-glucoside (the main anthocyanin in wine) with an ethyl linkage to procyanidin B2 catalyzed by acetaldehyde (Francia-Aricha 1997). Violet compounds were also noted in this study. Acetaldehyde is formed through fermentation and also through oxidation of ethanol. This volatile compound can react with flavanols to form ethyl-bridged flavanol polymers that correlate with wine age (Drinkine et al. 2007), indicating the slow rate of this reaction. By reacting at carbon-4 instead of carbon-8, acetaldehyde can combine with anthocyanins to form pyranoanthocyanins that are highly stable compounds, but found in low concentrations in wine (Morata et al. 2007).

Acylated anthocyanins possess greater color stability than non-acylated anthocyanins (Cevallos-Casals et al. 2004, Eiro et al. 2002, Malien-Aubert et al. 2001) and the acylated anthocyanins from radishes are a suitable replacement for FD&C Red No. 40 (Giusti et al. 1996). Both Red No. 40 and Blue No. 1 are frequently used in dark blue and purple beverages. In an effort to further enhance the stability of acylated ACYs and replace both FD&C Red No. 40 and Blue No. 1, the objective of this study was to naturally create and identify a novel acylated anthocyanin with a stable violet color from red radishes in the presence of acetaldehyde and catechin.

Materials and methods

Materials

Cyanidin-3-O-glucoside was obtained from Chromadex (Irvine, CA, USA). Acetaldehyde, (*O*-2,3,4,5,6-(pentafluorobenzyl) hydroxylamine hydrochloride (PFBHA), glucose, yeast extract, dipotassium phosphate, and catechin were purchased from Sigma Aldrich (St. Louis, MO, USA). HPLC-grade methanol was purchased from EMD Millipore (Billerica, MA, USA) and formic acid from Fischer-Scientific (Fair Lawn, NJ, USA). *Zymomonas mobilis* strain ATCC 31821 was purchased from American Type Culture Collection (Manassas, VA). Radishes, Hershey's special dark cocoa powder, Dagoba cocoa powder, fresh blueberries, cranberry sauce, Lipton green tea, and fava beans were purchased from a local supermarket. MegaNatural gold grape seed extract was obtained from Polyphenolics (Madera, CA).

Extraction of polyphenolics and formulation of model systems

Radishes were hand peeled and the anthocyanin-containing skins were extracted with methanol/water/ formic acid (60:37:3 v/v/v) and acetone/water/acetic acid (70:29.5:0.5 v/v/v) using a Euro Turrax Tissuemizer (Tekmar-Dohrman Corp., Mason, OH). Natural sources of catechin: cranberry, grape seed, cocoa, fava beans, blueberry pomace, muscadine grape pomace, and tea were extracted in a similar manner using acetone/water/acetic acid (70:29.5:0.5 v/v/v). Extracts were filtered using Miracloth (Calbiochem, LaJolla, CA) and concentrated using a Buchi rotary evaporator at 35 °C. Catechin sources were diluted for model systems to 500 mg/L catechin equivalents. Radish extracts were diluted to match the absorbance and color properties of Red No. 40 in sports beverages. The samples contained either the radish extract alone (control), or 70 mM acetaldehyde (RA), 70 mM acetaldehyde and 1.7 mM catechin (RAC) or catechin equivalents in water acidified to pH 3.5 by HCl. Triplicates samples of 5 mL each were repeatedly measured over storage for six months. The natural sources of catechin were added in 500 mg/L equivalents of catechin.

Color monitoring

A Konica Minolta Chroma meter CR-400 and data processor DP-400 was used to measure lightness (L), chroma (C), and hue (h) in the L*C*h color scheme (Konica Minolta, Japan). The chroma meter was calibrated with a white tile: $x = 92.41$, $y = 0.3145$, $z = 0.3200$, observer = 2° prior to each use. Color measurements were taken using five mL of sample with repeated measures at specified time intervals.

HPLC-PDA analysis of anthocyanins

Anthocyanin analysis followed the method of Cho et al. 2004. Radish samples were passed through 0.45 μm nylon syringe filters prior to HPLC injection. A Waters HPLC system (Waters Corp., Milford, MA) comprised of dual 515 pumps, a 717plus autosampler, and a 996 photodiode array detector was used for chromatographic analyses. A Waters Symmetry C₁₈ column (4.6 x 250 mm, 5 μm) was used for separation of anthocyanins with a 1 mL/min flow rate and solvent A as 5% formic acid and solvent B as methanol. Elution started with 15% B, increased to 60% B in 60 min, from 60% to 100% in 2 min, with an isocratic wash at 100% B for 10 min, finishing with 15% B for a 10 min re-equilibration. UV-visible spectra were monitored from 250-600 nm and peak areas were integrated at 510 nm. Anthocyanins were quantified as cyanidin-3-glucoside equivalents using external calibration curves ranging from 1-200 $\mu\text{g/mL}$.

After Sephadex LH-20 purification, the one month aged RAC sample was fractionated from the Waters Symmetry HPLC column. Fractions were collected every minute, evaporated to dryness, then dissolved in a small volume of methanol and used for MALDI-TOF-MS analysis.

HPLC-electrospray ionization tandem mass spectrometry (LC-ESI-MS) analysis of degradation products

LC-ESI-MS analysis was conducted using an HP 1000 series HPLC and a Bruker Esquire 2000 quadrupole ion trap mass spectrometer. Radish samples were separated using a Waters Symmetry (250 x 4.6 mm; 5 μm) column with gradients as described above. The mass spectrometry analysis was performed in positive ion mode under the following conditions: capillary voltage at 4 kV with polarity [-] for positive ion mode analysis, nebulizer gas pressure 32 psi, dry gas flow 12 L/min, and skim voltage at 53.7 V. Ions were isolated and fragmented in quadrupole ion trap with excitation amplitude of 1.2 volts.

Sephadex LH-20 solid phase extraction

Methodology followed Kantz et al. 1990 with some alterations. Triplicate samples were purified and concentrated using Sephadex LH-20 and stored for one month, four months, and one year. Samples were loaded on separate columns of 4 g Sephadex LH-20, which were hydrated overnight in DI water. Samples were loaded onto columns atop the vacuum manifold, allowed to absorb onto the stationary phase, then washed with 30% methanol to remove sugars and small phenolic molecules, which included some monomeric anthocyanins. Next, 70% acetone was used to elute polymeric phenols that were then dried using a SpeedVac concentrator and suspended in 70% acetone for further analysis. LH-20 columns can be reconditioned for immediate reuse by washing with several bed volumes of 30% methanol, then DI water. No changes in chromatographic properties were observed after 8-10 separation cycles.

Matrix assisted laser desorption ionization-time of flight (MALDI-TOF) analysis

Radish samples and a peptide standard were mixed with 1 M dihydroxybenzoic acid (DHB) matrix in methanol in an equal ratio and 1 μ L was spotted onto a stainless steel MALDI plate. Analysis was conducted using a Bruker Reflex III MALDI-TOF-MS (Billerica, MA) equipped with a 337 nm N₂ laser. BrukerDaltonics peptide standard consisting of angiotensin II, angiotensin I, substance P, bombesin, ACTH clip, and somatostatin was used for time of flight calibration. Data was obtained in positive ion reflectron mode with an accelerating voltage of 25 kV and a reflectron voltage of 28 kV. Peaks were statistically evaluated using BrukerClinProTools software.

On-fiber derivatization headspace solid phase microextraction gas chromatography- mass spectrometry (OFD-HS-SPME-GC-MS) and OFD-HS-SPME-GC-FID analysis of acetaldehyde

PFBHA was used to derivatize acetaldehyde to limit analysis to aldehydes. A carboxen/polydimethylsiloxane SPME fiber was inserted into a 20 mL glass headspace vial with one mL of PFBHA (15 mg/mL) and incubated for 15 min at 50 °C with magnetic stirrer (Wang 2005, Carlton 2007). The SPME fiber loaded with PFBHA was transferred to a vial with 5 mL of sample and incubated for 15 min at 50 °C with magnetic stirrer. The SPME was desorbed for 10 min into a Varian 450-GC connected to a Varian 320-MS triple quadrupole mass spectrometer with an EI ionization source on an Agilent 5% phenyl-methylpolysiloxane column (30 m x 250 μ m x 1 μ m). The injector temperature was 270 °C with a split ratio of 5:1. The column oven started at 25 °C, held for 4 min, and then increased to 280 °C at 10 °C/min with a helium flow of 1.0 mL/min. The transfer line and ionization source temperatures were 270 °C and 200 °C, respectively. The ionization energy was 70 eV with m/z range of 35-350. GC-FID conditions followed the same methodology.

Radish fermentation in bioreactor

Batch fermentations of *Zymomonas mobilis* were carried out in ATCC medium #1341, which consisted of 20 g glucose, 10 g yeast extract, 2 g dipotassium phosphate in one L of deionized water. Inoculations were prepared by transferring a single colony to 5 mL of medium and incubated overnight at 30 °C and shaken at 250 rpm. This seed culture was added to 500 mL of medium in a two L Applikon reactor vessel connected to a Bio console ADI 1025 and Bio controller ADI 1010 at 30 °C with constant agitation at 200 rpm and aeration. 100 g of radish

peels was added to each batch, along with a source of catechin (500 mg/L equivalent).

Acetaldehyde content was measured daily over a week for each sample. After each week, the bioreactor was cleaned and sanitized in preparation for the next sample.

Distillation of *Zymomonas* fermentation and distillate model system formation

A Buchi Rotavapor R-114 at 40 °C was used to vacuum distill the *Zymomonas mobilis* growth for 15 min. under 28 in. Hg. The collected distillate was measured using the OFD-HS-SPME-GC-FID method described above. The model system contained radish extract, 1.7 mM catechin, and 70 mM pure acetaldehyde (RAC) or 70 mM acetaldehyde from the *Zymomonas* distillate (RD1Cat). Triplicate samples were monitored for color and chromatographic changes on days 0, 2, 4, 7, and 14. The next model system used two and five fold higher concentrations of distillate to create samples: RD2Cat and RD5Cat. Again, triplicate samples were monitored for color and chromatographic changes on days 0, 2, 4, 7, and 14.

Statistical Analysis

Triplicate samples were analyzed at each storage time using JMP Pro 13 with data expressed as mean \pm standard error. Differences between means were assessed using Tukey's HSD test ($\alpha = 0.05$).

Results and discussion

Color properties of radish samples

Red radish pigments have comparable color properties to FD&C Red No. 40 and function as a natural replacement in maraschino cherries as described by Giusti et al. (1996). There was

no significant difference in color among L^* , a^* , or b^* between FD&C Red No. 40 (200 ppm) and red radish extract at either 600 and 1200 mg/L at the initial time, but the lightness increased, while the chroma and hue decreased (Giusti 1996). After matching the color properties of Red 40, our radish samples exhibited similar color stability over six months of storage.

In Figure 1, the lightness value increased for all radish samples, which agrees with previous literature using red-fleshed potatoes and red radishes that were stored as juice concentrates at room temperature at pH 3.5 (Rodriguez-Saona 1999). The RAC sample darkened over the first four days of storage and developed a purple hue. Over six months of storage, RAC increased in lightness and visually became a red-purple shade. The lightness of all samples with natural sources of catechin mirrored the lightness of the RA sample. This potentially indicates that the natural sources of catechin contained competing reactants for acetaldehyde, which may decrease the reactivity of acetaldehyde and halt the formation of the anthocyanin-catechin dimer.

After mixing the model system, the chroma values decreased in all samples. However, RAC showed a linear decline and slowest rate of decline compared to the other samples containing acetaldehyde, which quickly declined in the first month, then the rate lessened from months two through six. The radish control initially increased in chroma slightly, then gradually declined below the chroma value of RAC to the level of other acetaldehyde containing samples. This relative stability of the chroma of RAC is an important characteristic of a natural colorant and demonstrates its potential application to the beverage industry.

A sample's hue angle provides a numerical assessment of its color. Similar to the lightness of RAC, the hue quickly decreased in the first month. There was no notable change in the hue of RAC for the remainder of the storage time and this stability is another important

character for a potential natural colorant. The sample containing radish, acetaldehyde, and fava bean extract mirrored the RAC's decrease in hue, but visually did not produce the same purple color because of the difference in lightness and chroma between these two samples. There was no visual difference between RA and other acetaldehyde containing samples.

In agreement with these findings, an increase in lightness and decrease in chroma was shown in red-fleshed potatoes and red radishes at pH 3.5 (Rodriguez-Saona 1999). Surprisingly those radish samples, which were in a juice concentrate, exhibited an increase in hue toward orange/yellow, while our radish control declined in hue over storage and eventually reached a plateau. The yellowing of anthocyanins over storage has been previously recognized (Cevallos 2004).

Identification and quantification of radish anthocyanins and anthocyanin-catechin ethyl-bridged dimers over storage:

Anthocyanins in red radishes were first identified in the 1960's (Harborne 1963, Fuleki 1969) with predominantly pelargonidin forms, while purple radishes are composed mainly of cyanidin derivatives (Hanlon 2011). The major anthocyanins in red radish are pelargonidin-3-sophoroside-5-glucoside (P) with malonic acid and either ferulic (PFM) or *p*-coumaric acid (PCM) moieties, while the two secondary anthocyanins are P with either ferulic or *p*-coumaric acid (Giusti 1996). These anthocyanins were initially characterized on a divinylbenzene HPLC column; however, our newly formed dimeric compounds were better separated on a C18 column, as they co-eluted on a divinylbenzene column. The C18 column resulted in co-elution of the two major radish anthocyanins (PFM and PCM), so neither column was faultless. In Figure 2, the wide peak at 41 min. contains both PFM and PCM, which are subtly differentiated by their mass

spectrometric signals at the front and tail edges of the peak. These acylating moieties induce a bathochromic shift, moving the color toward red-purple depending on the acylation (Dangles 1993) and the stability of these anthocyanins is attributed to the phenolic acids bound to the glycosidic moieties. The sugar groups can act as hinges allowing the acyl groups to protect the flavylium cation from hydrolysis by stacking around the pyrylium ring (Brouillard 1981).

Each of the numbered peaks in Figure 2 relates to an anthocyanin-catechin ethyl-bridged dimer. The first peak is identified from mass spectral fragmentation patterns as P+C and elutes nearly seven minutes after P. This is unusual because the PFM+C and PCM+C elute approximately ten minutes earlier than their respective monomeric anthocyanins. Others have found malvidin-3-glucoside ethyl-bridged to catechin, epicatechin, or procyanidin B2 elute after malvidin-3-glucoside in model systems (Escribano-Bailon 2001, Es-Safi 1999, Dallas 1996). Figure 3 depicts the mass spectra for the two largest anthocyanin-catechin bridged dimers. Comparing Figure 3A and 3B, there is a clear difference of m/z 30 for the two greatest mass peaks, which is the difference between ferulic and coumaric acids. Figure 3A corresponds to peak 1 and the spectra suggests this compound is PCM+C, while Fig. 3B is peak 2 and PFM+C. The aglycone mass peak of m/z 287, which is the m/z of cyanidin, is distinctive because radishes contain pelargonidin, having a m/z of 271. It is unclear where the additional m/z of 16 originates. The proposed structure of PFM+C is shown in Figure 4. We propose the ethyl-bridged catechin is attached to the anthocyanin via C-8, although it is possible to attach at C-6 as well.

The change in concentration and formation of radish anthocyanins and anthocyanin-catechin bridged dimers over storage are pictured in Figure 5. This figure illustrates the combined concentration of the two major anthocyanins in radishes because they co-elute using our method. The maximum concentration of the bridged dimers was approximately 100-fold less

than the starting concentration of the radish anthocyanins. The rapid degradation of anthocyanins in the presence of acetaldehyde has been shown in previous literature; however, malvidin-3-glucoside decayed precipitously in 20 hours (Garcia 1994), opposed to 20 days needed for anthocyanin decay in our model system. This difference is likely caused by the enhanced stability caused by acylation of radish anthocyanins. In the absence of acetaldehyde, the radish control demonstrated greater anthocyanin stability. The formation of the bridged dimers started promptly after mixing the model system. Their maximum concentration was reached four days after mixing, then slowly declined over 20 days of measurement. A similar concentration pattern of bridged dimers was shown using each of the six main anthocyanin monoglucosides (Weber 2014). These anthocyanins reached maximum concentration around 12 hours after mixing, then decreased within 48 hours (Weber 2014). The authors detected and quantified oligomeric compounds from the monoglucosides, which followed a similar concentration profile, just offset six hours.

To examine the oligomeric and polymeric products of the acetaldehyde catalyzed reaction, radish samples were stored for one month, four months, and one year. The time course was purified on Sephadex LH-20 and compounds were separated on a C₁₈ HPLC column. Sephadex LH-20 is a unique sorbent known for purifying polymeric phenolic compounds (Kantz et al. 1991). The chromatogram changed dramatically before (Fig. 2) and after (Fig. 6) Sephadex LH-20 purification. A large hump is featured in Fig. 6 and remains through one year of storage, although the size of the hump decreases over time. The hue is stable through storage so it is puzzling where the source of this stability originates.

Next, mass spectrometry was used to identify the compounds within the polymeric hump. The one month, four month, and one year old RAC samples were analyzed using LC-ESI-MS to

determine if the pigment is stemming from molecules under 2000 Da, a range which encompasses a radish ACY with up to three ethyl bridged catechins. The mass spectra of the two peaks at 42 and 46 minutes emerging from the hump did not produce any identifiable m/z values. In the middle of the hump, the m/z value of 1937.1 (PFM+3C) was detected; however, there was only a single m/z peak without any isotopic peaks, so this is simply a noise peak and should not be considered. Unfortunately, there were no true peaks (with isotopic peaks) over 1500 Da through the chromatographic hump in any of the samples through the year-long storage.

Perhaps the polymeric compounds were larger than 2000 Da and could not be detected by the ESI-MS, so MALDI-TOF-MS was used to seek larger pigmented molecules. Figure 7 displays the spectrum of the one month RAC sample and no m/z values were detected over 1000 Da. Figure 8 and 9 show the MALDI-TOF spectra for the four month and one year old RAC samples, respectively. Once again, these spectra do not contain any m/z values greater than 1000 Da. This result aligns with the ESI-MS data and may indicate the polymeric compounds are too low in concentration. Consequently, the one month aged RAC sample was fractionated by HPLC and samples were collected each minute. The fractions were evaporated to dryness and dissolved in a small volume of methanol for MALDI-TOF analysis with higher concentrations. The majority of the fractions did not detect any m/z values greater than 1000 Da; however, one fraction (Fig. 10) revealed several peaks over 1000 Da. Figure 10 displays the forty-third fraction, which eluted in the middle of the chromatographic hump, with m/z 1133.6 and 1368.6 as two of the primary peaks. None of these masses aligned with radish anthocyanins with any degree of ethyl-bridged catechins and were not identified. The source of the long-term pigment in the radish mixture remains to be identified even though color data is stable over storage.

***Zymomonas mobilis* fermentation:**

Zymomonas mobilis, a high acetaldehyde-producing bacterium, was used to naturally produce acetaldehyde in an effort to form bridged dimers. This bacterium also produced notable quantities of ethanol, which aided anthocyanin extraction from radish peels into the media. Pure catechin and equivalent concentrations of natural sources of catechin were added to radish peels in the growing media to be fermented by *Z. mobilis*. Taking into account the yellow-brown color of the media, the purple hue of the bridged dimers never appeared and HPLC data confirmed this finding. To determine the possible effect of the bacteria on the reaction, the same model system was created using radish extract, pure acetaldehyde, and pure catechin in water and in media and monitored via HPLC for 20 days. The dimers were detected in the water based model system, but not in the media based system. The components of the media must be scavenging the acetaldehyde before it can react with the anthocyanins.

Next, the volatile fraction of *Z. mobilis* growth was collected (in the absence of radish peels and catechin) and the acetaldehyde-containing distillate was used in a model system. *Z. mobilis* produces a maximum concentration of acetaldehyde after 48 hours of growth (Fig. 11) and the fermentation was distilled at this time. The concentration of acetaldehyde declines over the following 48 hours because the glucose content, and thus *Z. mobilis* growth declines. If the medium were restocked with glucose on a daily basis, the acetaldehyde content would remain at its maximum (Roy 2016).

A model system of radish extract, catechin, and *Z. mobilis* distillate (RD1Cat) was prepared with the same concentration of acetaldehyde as previous model systems and monitored over two weeks for color change and HPLC detection of dimeric compounds. Figure 12A shows color data for this model system with the RAC sample reacting to form the purple hue. However

the radish control and RD1Cat were identical and no purple color appeared. Chromatograms (not shown) of the radish control and RD1Cat were indistinguishable and confirm no dimeric ethyl bridged ACYs formed. Although the concentration of acetaldehyde was identical between RAC and RD1Cat samples, it is unclear as to why the dimeric compounds were not formed. A follow-up experiment used higher concentrations of *Z. mobilis* distillate in samples RD2Cat and RD5Cat with two and five times the concentration of acetaldehyde compared to RD1Cat, respectively. The results followed the same pattern as the first distillate model system. Color changes over two weeks of storage is shown in Fig. 12B. The color values are slightly different than the first distillate model system because a different batch of radishes was used. Although the values are not the same, the trend is, which means the higher concentrations of acetaldehyde did not produce a purple pigment and HPLC data confirms the lack of dimeric radish anthocyanins.

Conclusion

To recapitulate, radishes are an inexpensive source of acylated ACYs that can be used in a reaction found in wine production in order to produce dimeric compounds that could serve as natural colorants to replace synthetic colors in foods and beverages. This is the first evidence of tailoring the acetaldehyde-catalyzed reaction in an acylated ACY source. Radish extract combined with pure acetaldehyde and catechin produce dimeric compounds with stable red-purple color. *Zymomonas mobilis* was used to naturally produce acetaldehyde in a fermentation with radishes and natural sources of catechin; however, the dimeric compounds were not formed. This reaction can be expanded to other acylated ACY sources in an effort to produce natural colorants for the food and beverage industries. The ethyl-bridged ACYs have a remarkably stable

hue over six months of ambient storage and can serve as a replacement for artificial color additives.

References

- Feingold, B.F. Hyperkinesis and learning disabilities linked to the ingestion of artificial food colors and flavors. *J. Learn Disabil.* **1976**, *9*, 551-559.
- Stintzing, F.C.; Carle, R. Functional properties of anthocyanins and betalains in plants, food, and in human nutrition. *Trends Food Sci. Technol.* **2004**, *15*, 19-38.
- Timberlake, C.F.; Bridle, P. Interactions between anthocyanins, phenolic compounds, and acetaldehyde and their significance in red wines. *Am. J. Enol. Vitic.* **1976**, *27*, 97-105.
- Francia-Aricha, E.M.; Guerra, M.T.; Rivas-Gonzalo, J.C.; Santos-Buelga, C. New anthocyanin pigments formed after condensation with flavanols. *J. Agric. Food Chem.* **1997**, *45*, 2262-2266.
- Drinkine, J.; Lopes, P.; Kennedy, J.A.; Teissedre, P.; Saucier, C. Ethylidene-bridged flavan-3-ols in red wine and correlation with wine age. *J. Agric. Food Chem.* **2007**, *55*, 6292-6299.
- Morata, A.; Calderón, F.; González, M.C.; Gómez-Cordovés, M.C.; Suárez, J.A. Formation of the highly stable pyranoanthocyanins (vitisins A and B) in red wines by the addition of pyruvic acid and acetaldehyde. *Food Chem.* **2007**, *100*, 1144-1152.
- Cevallos-Casals, B.A.; Cisneros-Zevallos, L. Stability of anthocyanin-based aqueous extracts of Andean purple corn and red-fleshed sweet potato compared to synthetic and natural colorants. *Food Chem.* **2004**, *86*, 69-77.
- Eiro, M.J.; Heinonen, M.A. Anthocyanin color behavior and stability during storage: Effect of intermolecular copigmentation. *J. Agric. Food Chem.* **2002**, *50*, 7461-7466.
- Malien-Aubert, C.; Dangles, O.; Amiot, M.J. Color stability of commercial anthocyanin-based extracts in relation to the phenolic composition. Protective effects by intra- and intermolecular copigmentation. *J. Agric. Food Chem.* **2001**, *49*, 170-176.
- Giusti, M.M.; Wrolstad, R.E. Radish anthocyanin extract as a natural colorant for maraschino cherries. *J. Food Sci.* **1996**, *61*, 688-694.
- Cho, M.J.; Howard, L.R.; Prior, R.L.; Clark, J.R. Flavonoid glycosides and antioxidant capacity of various blackberry, blueberry, and red grape genotypes determined by high-performance liquid chromatography/mass spectrometry. *J. Sci. Food Agric.* **2004**, *84*, 1771-1782.
- Kantz, K.; Singleton, V.L. Isolation and determination of polymeric polyphenols using Sephadex LH-20 and analysis of grape tissue extracts. *Am. J. Enol. Vitic.* **1990**, *41*, 223-228.

- Wang, Q.; O'Reilly, J.; Pawliszyn, J. Determination of low-molecular mass aldehydes by automated headspace solid-phase microextraction with in-fibre derivatisation. *J. Chromatogr. A*. **2005**, *1071*, 147-154.
- Carlton, W.K.; Gump, B.; Fugelsang, K.; Hasson, A.S. Monitoring acetaldehyde concentrations during micro-oxygenation of red wine by headspace solid-phase microextraction with on-fiber derivatization. *J. Agric. Food Chem.* **2007**, *55*, 5620-5625.
- Rodriguez-Saona, L.E.; Giusti, M.M.; Wrolstad, R.E. Color and pigment stability of red radish and red-fleshed potato anthocyanins in juice model systems. *J. Food Sci.* **1999**, *64*, 451-456.
- Harborne, J.B. . Plant polyphenols IX: the glycosidic pattern of anthocyanin pigments. *Phytochem.* **1963**, *2*, 85-97.
- Fuleki, T. The anthocyanins of strawberry, rhubarb, radish, and onion. *J. Food Sci.* **1969**, *34*, 365-369.
- Hanlon, P.R.; Barnes, D.M. Phytochemical composition and biological activity of 8 varieties of radish (*Raphanus sativus* L.) sprouts and mature taproots. *J. Food Sci.* **2011**, *76*, C185-C192.
- Dangles, O.; Saito, N.; Brouillard, R. Anthocyanin intramolecular copigment effect. *Phytochem.* **1993**, *34*, 119-124.
- Brouillard, R. Origin of the exceptional colour stability of *Zebrina* anthocyanin. *Phytochem.* **1981**, *20*, 143-145.
- Escribano-Bailon, T.; Alvarez-Garcia, M.; Rivas-Gonzalo, J.C.; Heredia, F.J.; Santos-Buelga, C. Color and stability of pigments derived from the acetaldehyde-mediated condensation between malvidin-3-*O*-glucoside and (+)-catechin. *J. Agric. Food Chem.* **2001**, *49*, 1213-1217.
- Es-Safi, N.; Fulcrand, H.; Cheynier, V.; Moutounet, M. Studies on the acetaldehyde-induced condensation of (-)-epicatechin and malvidin-3-*O*-glucoside in a model solution. *J. Agric. Food Chem.* **1999**, *47*, 2096-2102.
- Dallas, C.; Ricardo0Silva, J.M.; Laureano, O. Products formed in model wine solutions involving anthocyanins, procyanidin B₂, and acetaldehyde. *J. Agric. Food Chem.* **1996**, *44*, 2402-2407.
- Garcia-Viguera, C.; Bridle, P.; Bakker, J. The effect of pH on the formation of coloured compounds in model solutions containing anthocyanins, catechin, and acetaldehyde. *Vitis*, **1994**, *33*, 37-40.
- Weber, F.; Winterhalter, P. Synthesis and structure elucidation of ethylyden-linked anthocyanin-flavan-3-ol oligomers. *Food Res. Intl.* **2014**, *65*, 69-76.

Roy, A.; Mukherjee, R.P.; Howard, L.; Beitle, R. Bio-based extraction and stabilization of anthocyanins. *Biotechnol. Prog.* **2016**, *32*, 601-605.

Figures

Figure 1. Changes in L*a*b* color of radish samples over six months of storage. Bars represent standard error (n=3).

Figure 2. Chromatogram (510 nm) of radish model system with acetaldehyde and catechin (Numbered peaks are anthocyanin-catechin ethyl-bridged compounds).

Figure 3. LC-ESI-MS spectra of PCM+C (A) and PFM+C (B).

Figure 4. Proposed structure of PFM+C.

Figure 5. Changes in anthocyanin content over storage. Bars represent standard error (n=3).

Figure 6. Chromatogram (510 nm) of LH-20 purified radish model system acetaldehyde and catechin samples after one month (A), four months (B), and one year (C) of storage.

Figure 7. MALDI-TOF-MS spectrum of one month aged RAC after Sephadex LH-20 purification.

Figure 8. MALDI-TOF-MS spectrum of four month aged RAC after Sephadex LH-20 purification.

Figure 9. MALDI-TOF-MS spectrum of one year aged RAC after Sephadex LH-20 purification.

Figure 10. MALDI-TOF-MS spectrum of a collected fraction of one month aged RAC after Sephadex LH-20 purification.

Figure 11. Time course of acetaldehyde concentration from *Zymomonas mobilis*. Bars represent standard error (n=3).

Figure 12. Changes in L*a*b* color of radish samples with *Zymomonas* distillate of 70 mM acetaldehyde (A), and two and five times the concentration of distilled-derived acetaldehyde (B). Bars represent standard error (n=3).

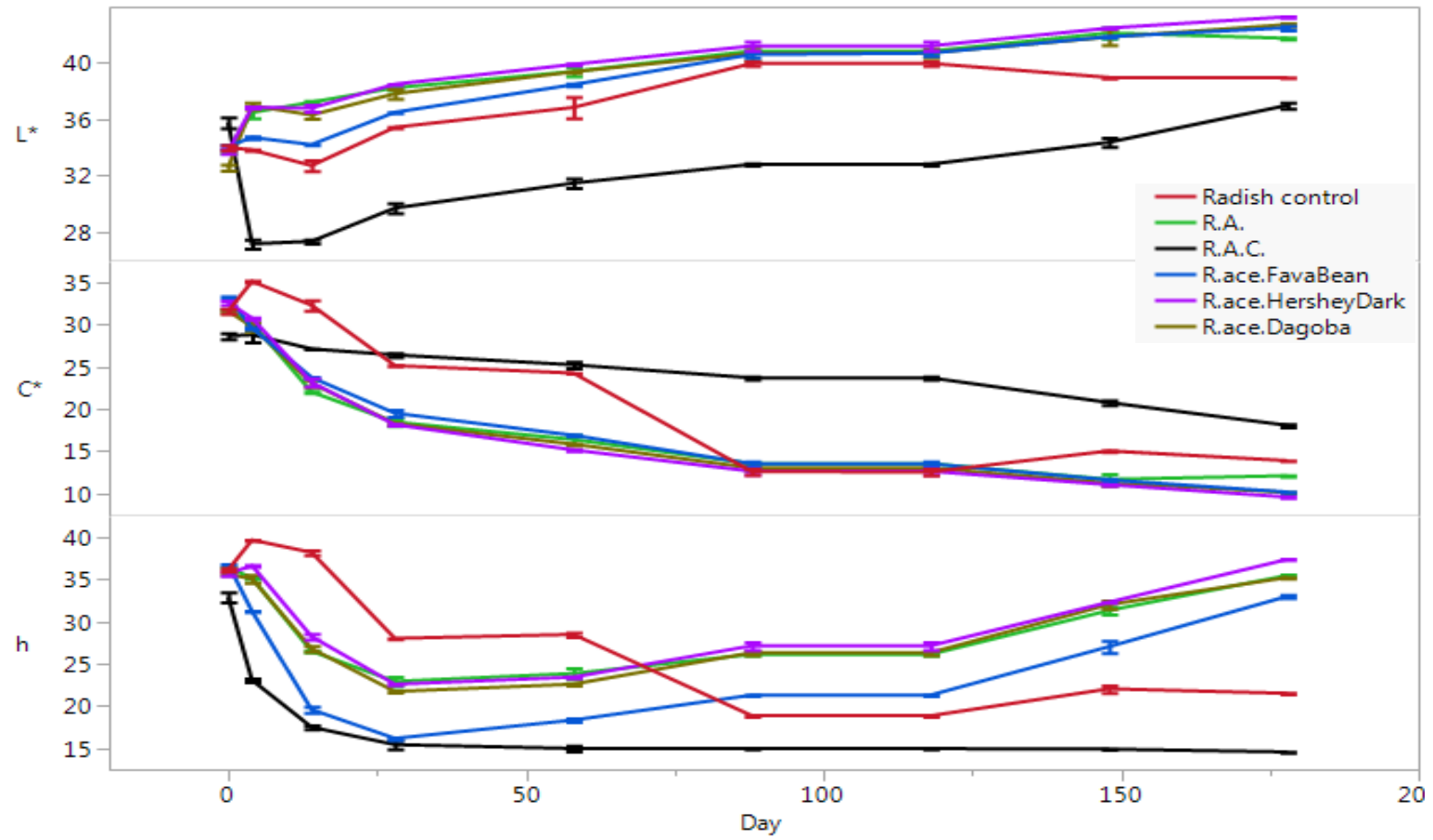


Figure 1

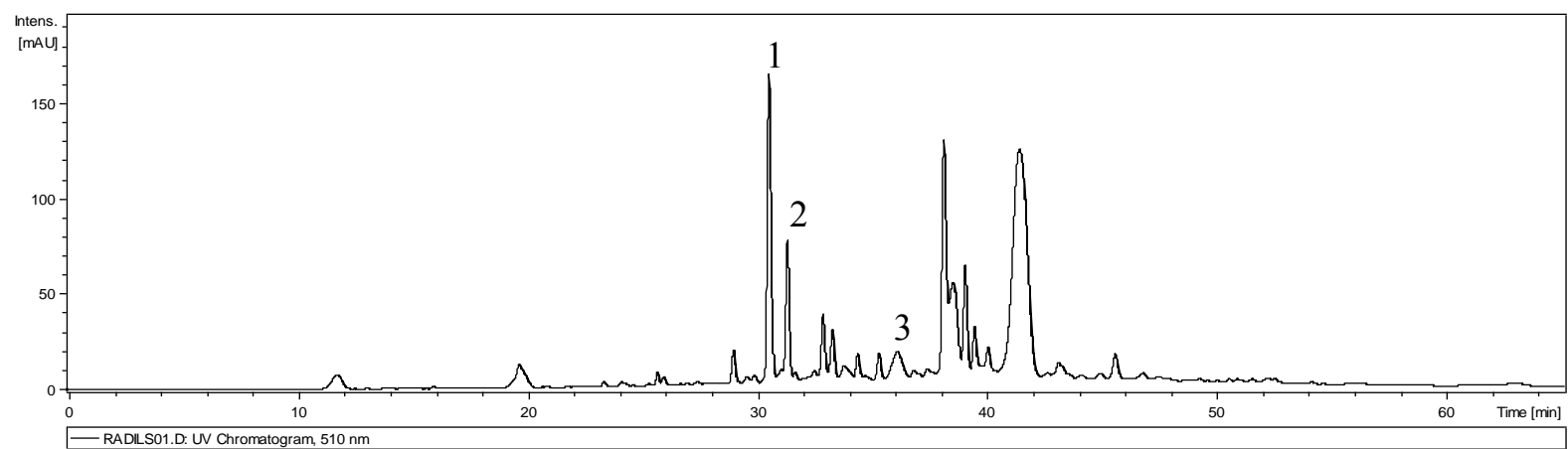


Figure 2

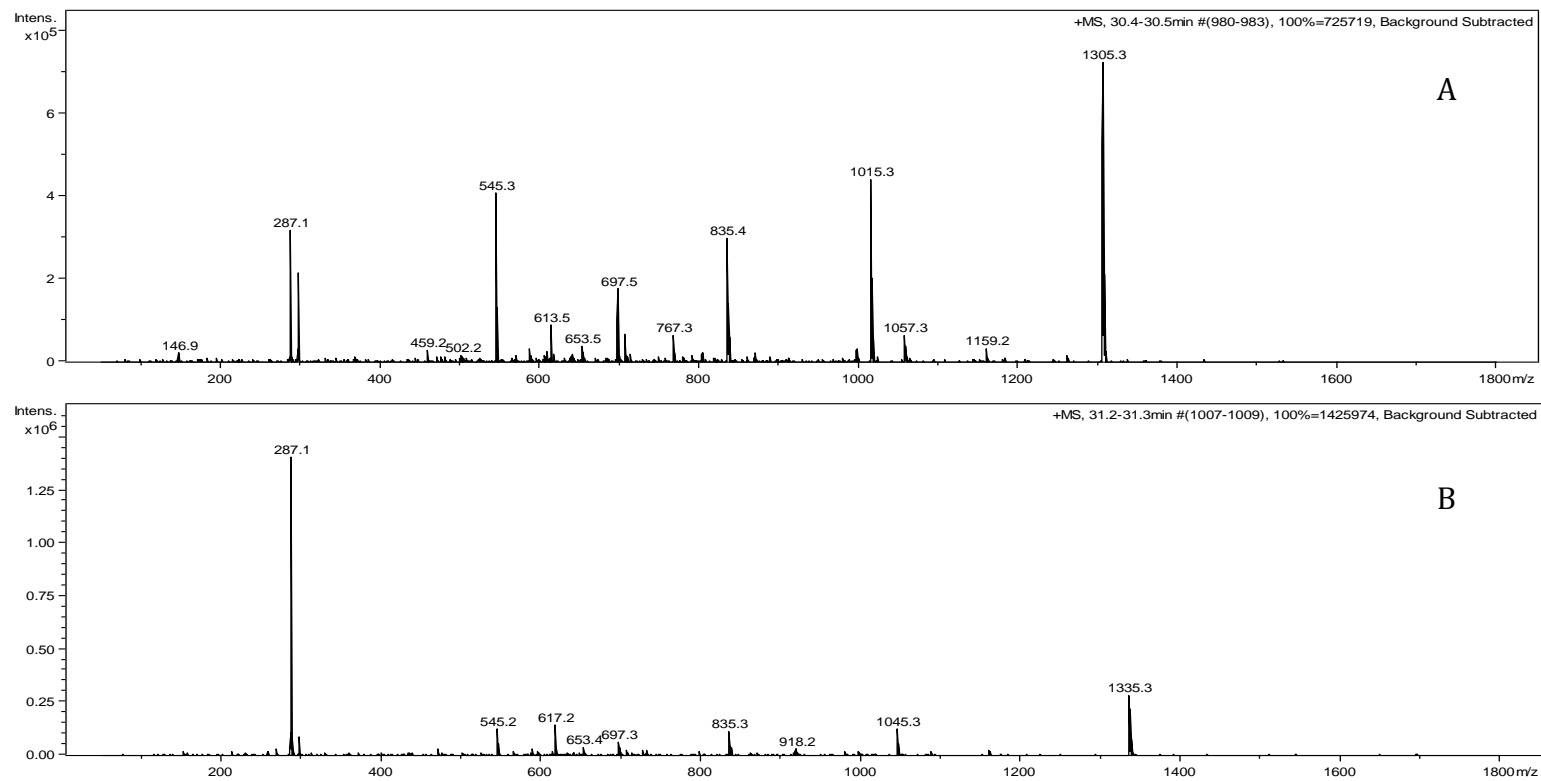


Figure 3

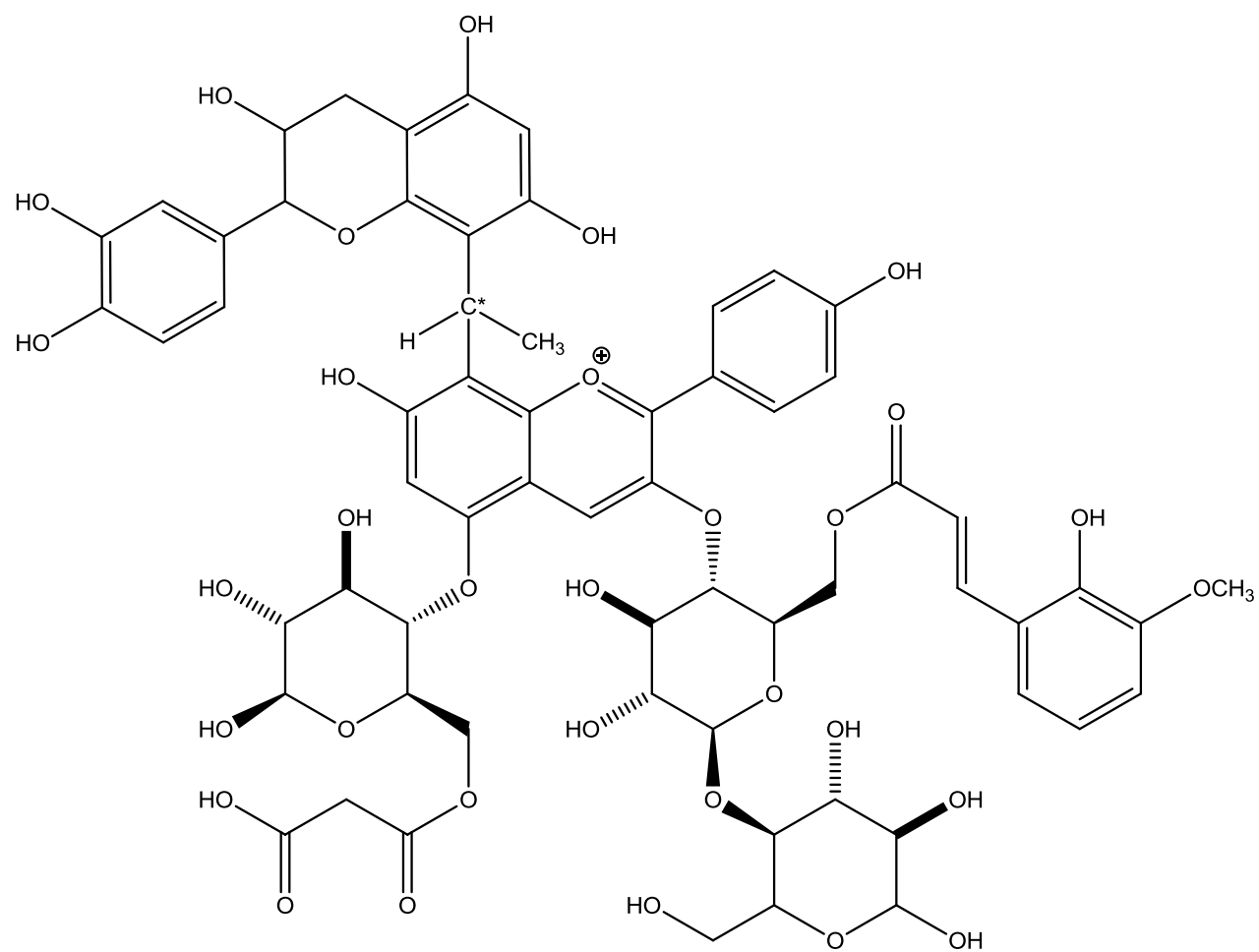


Figure 4

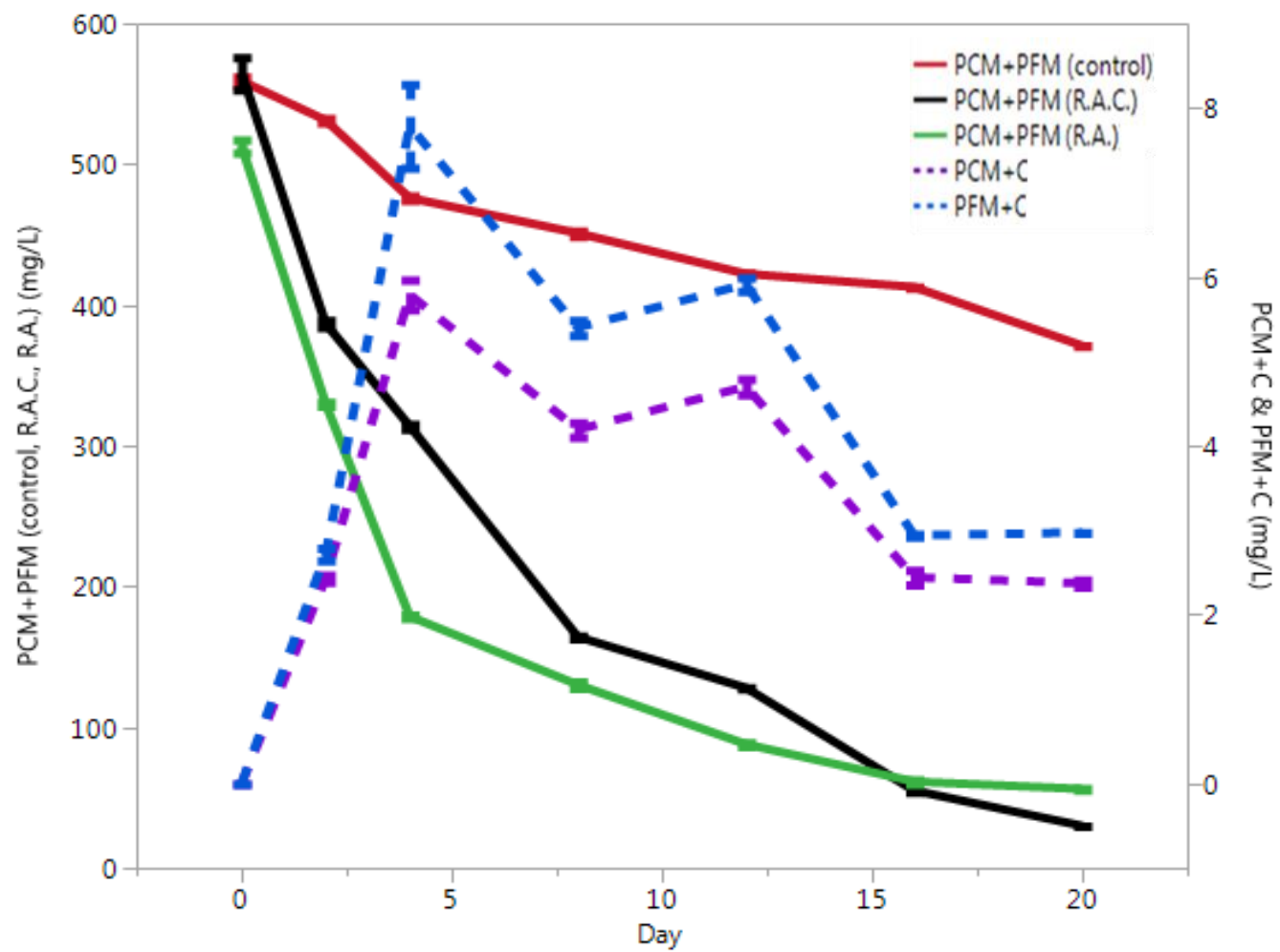


Figure 5

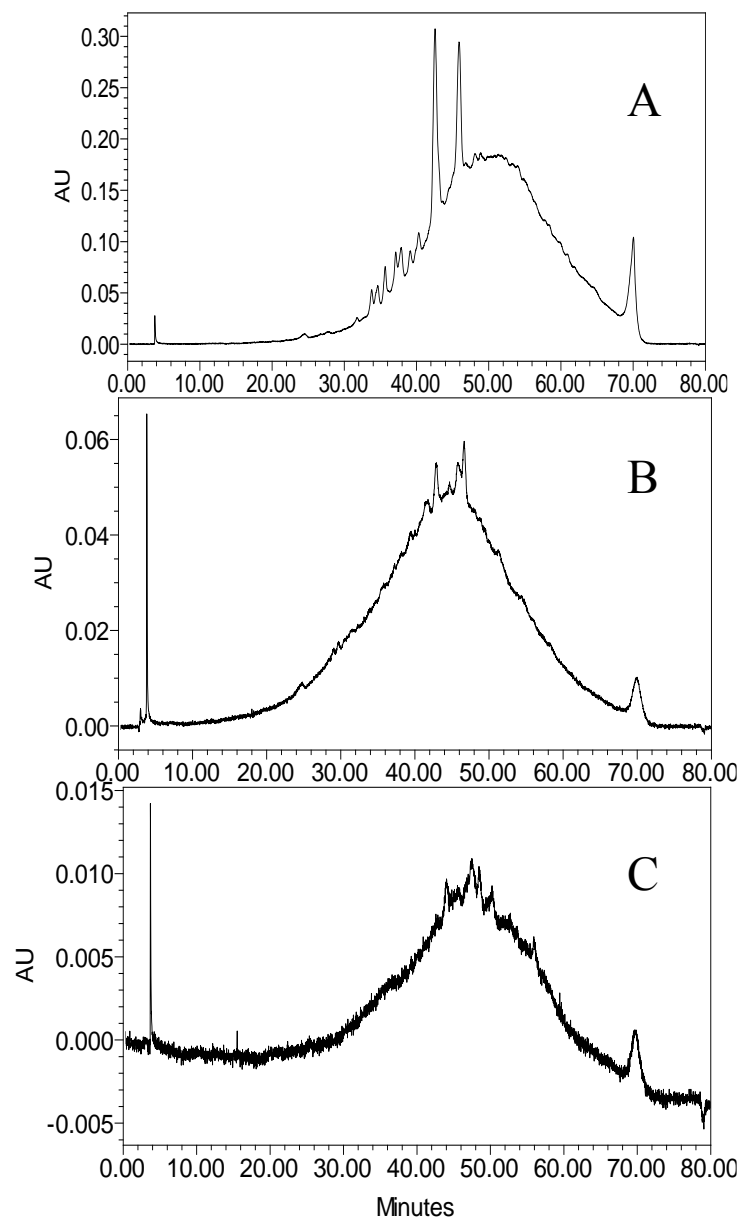


Figure 6

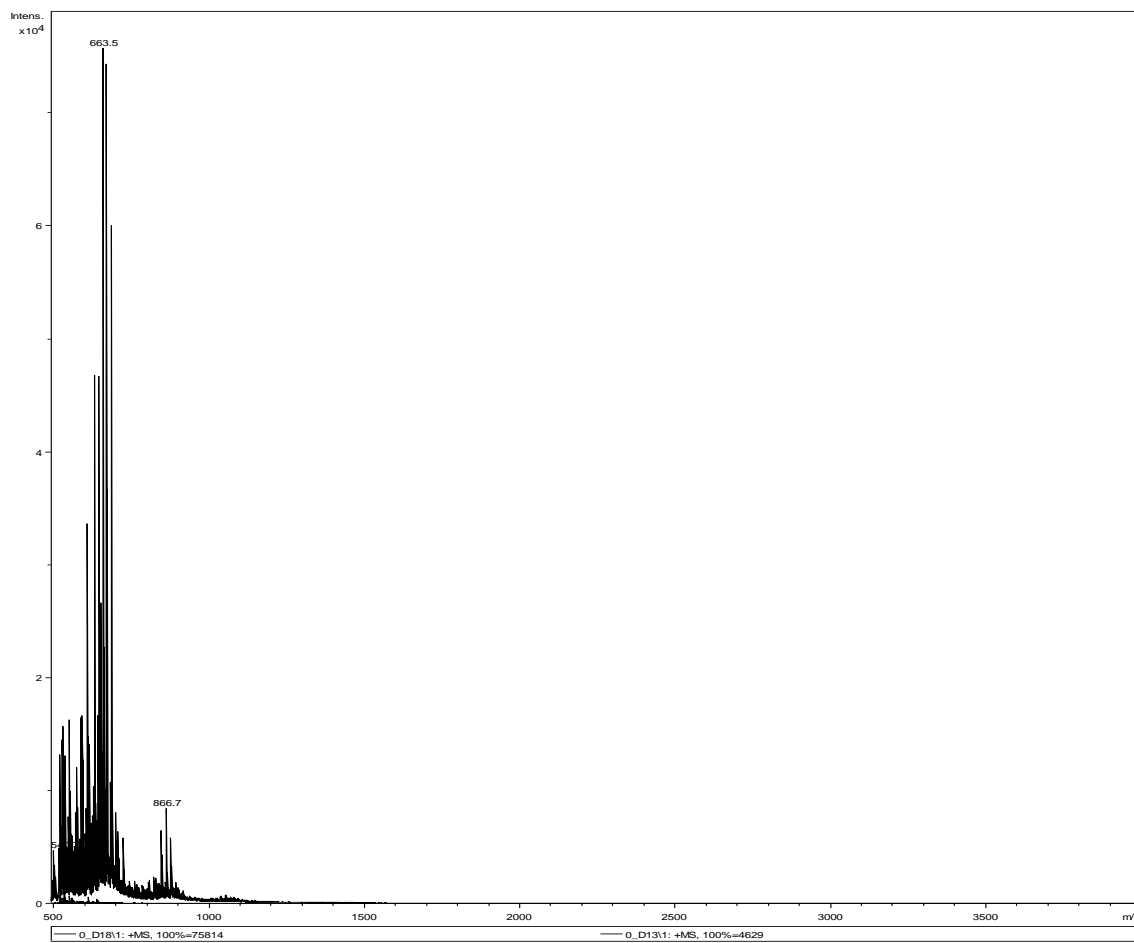


Figure 7

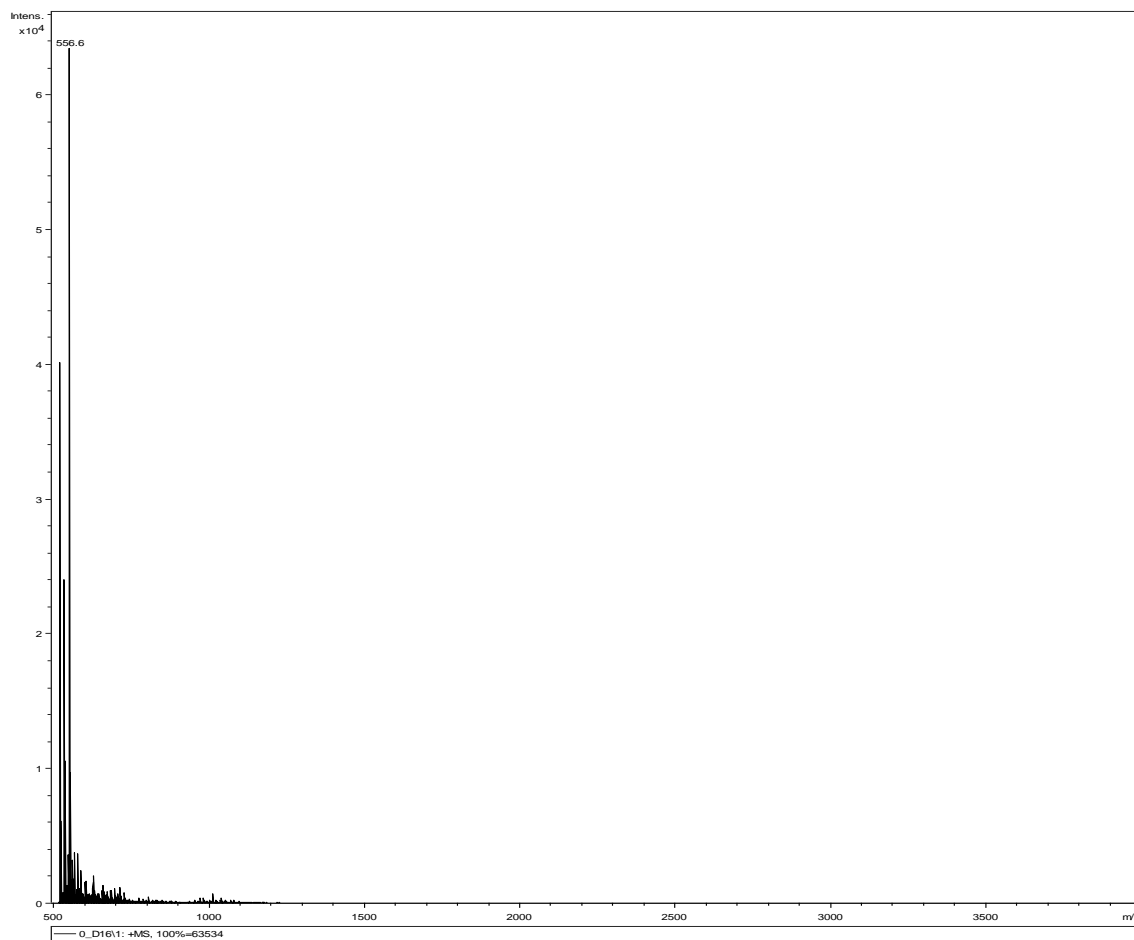


Figure 8

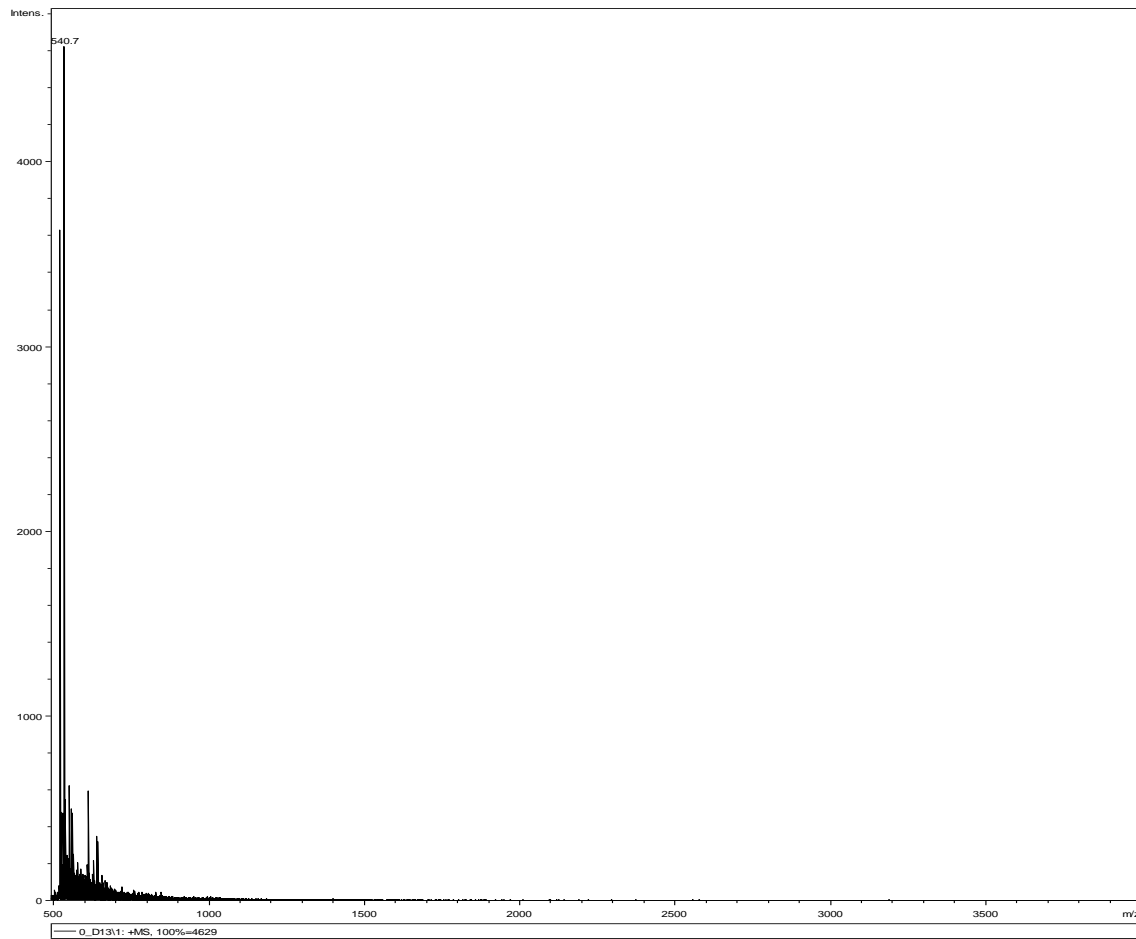


Figure 9

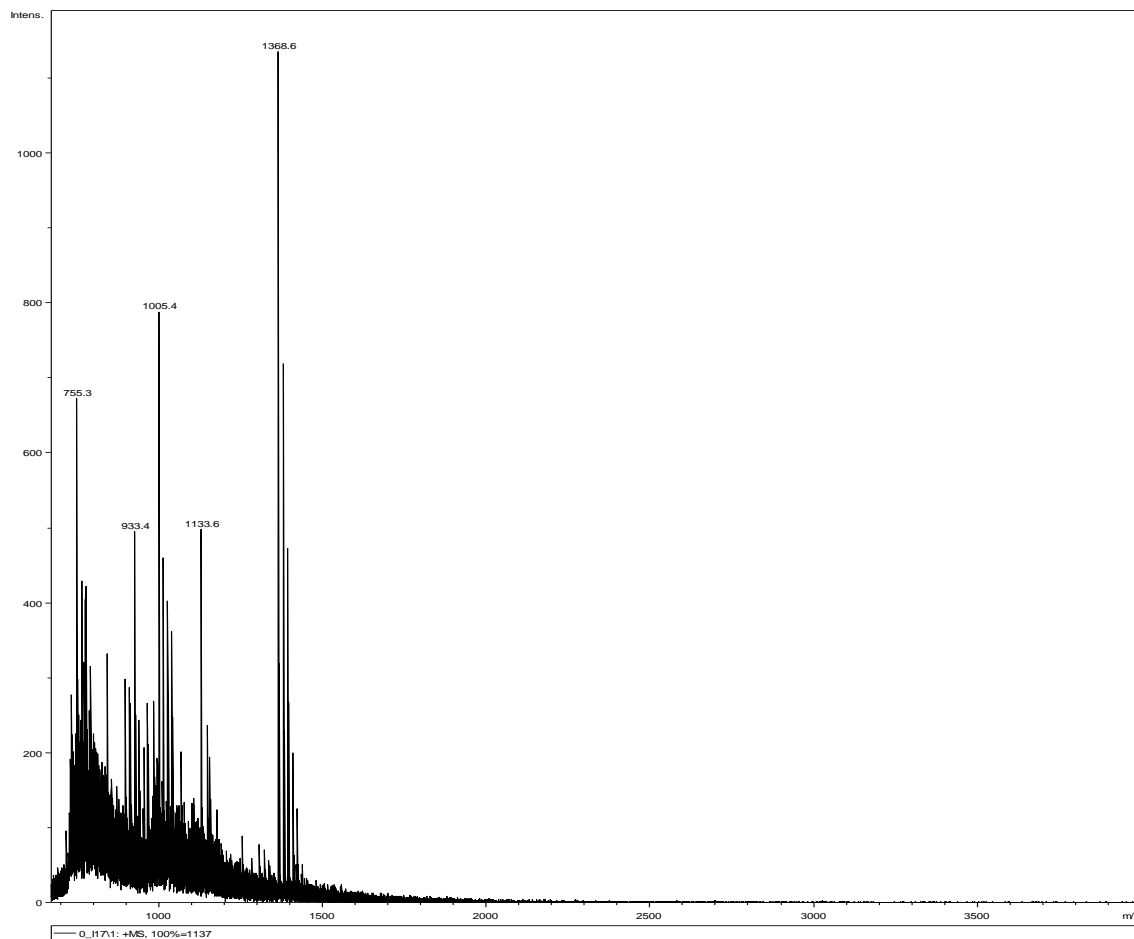


Figure 10

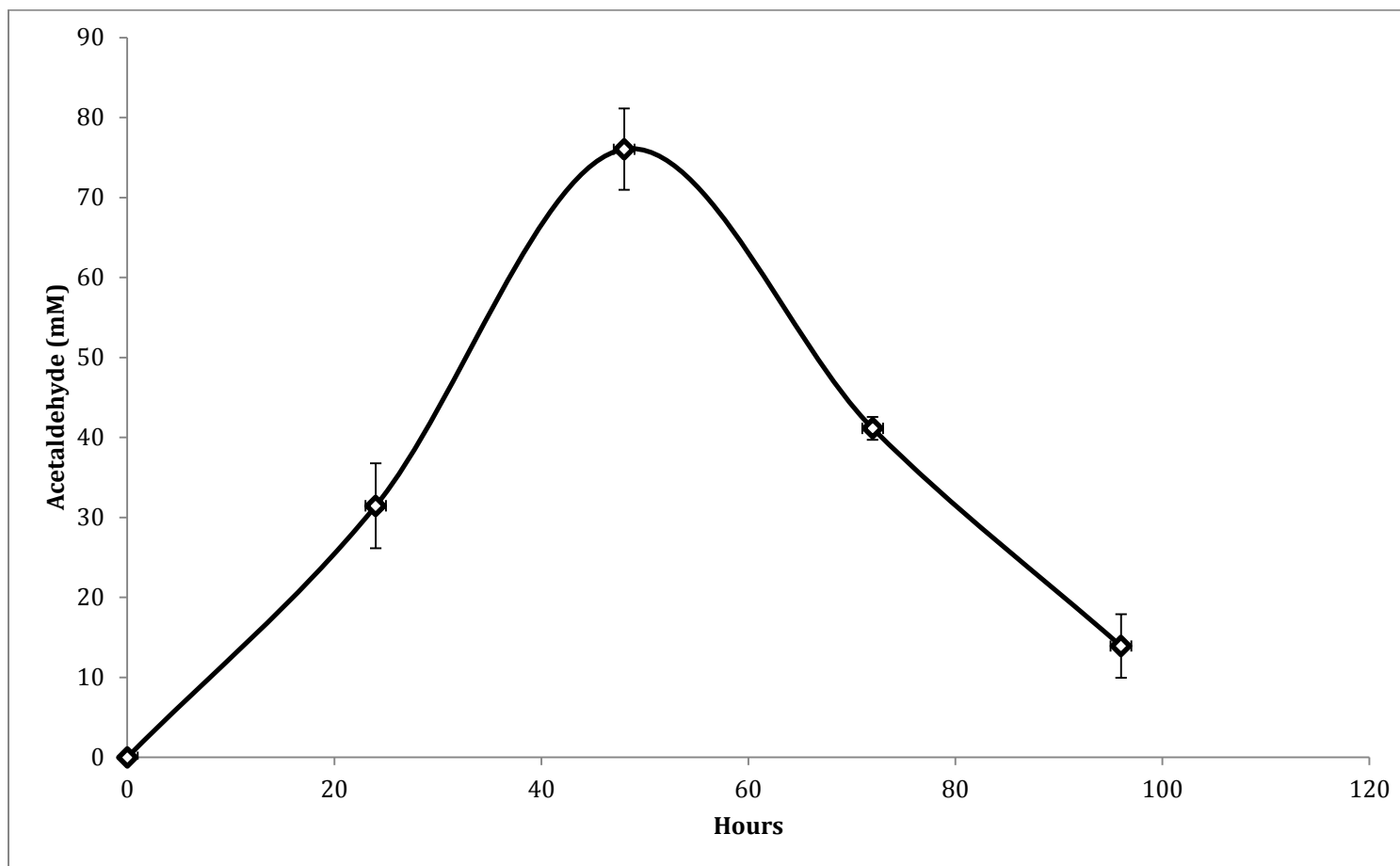


Figure 11

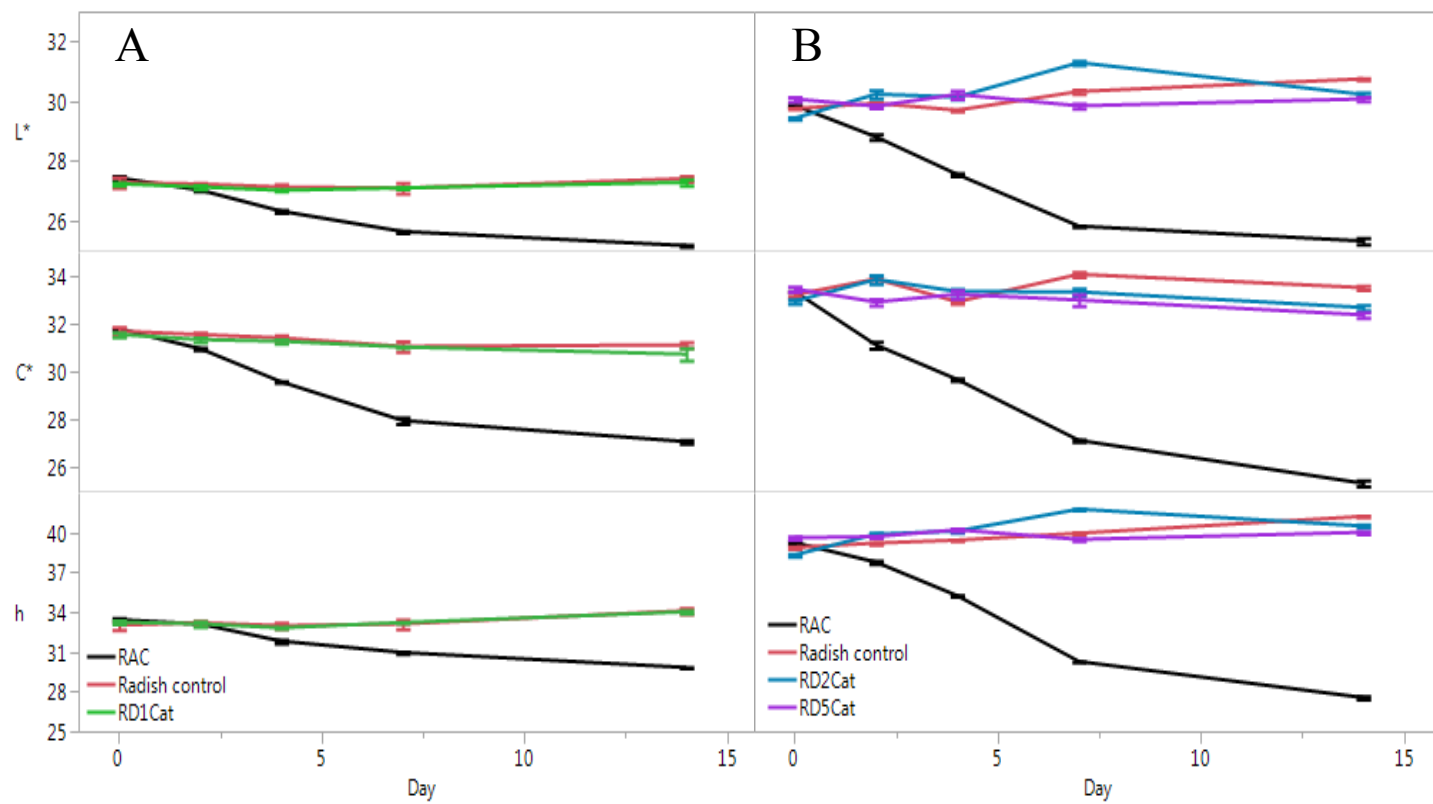


Figure 12

CHAPTER 7. Conclusion

Recent trends show that consumers desire fewer artificial additives in foods and beverages, which translates to natural substitutions on the ingredient list. Artificial colors are one of the most common targets for replacement because appearance is the first assessment of a product. Anthocyanins are water-soluble, pigmented compounds found throughout nature. These vibrant compounds range from orange-red to blue-violet, but do not have the same color stability as the artificial colorants. Anthocyanins degrade in the presence of heat, oxygen, metal ions, ascorbic acid, and other factors that are commonly found in food processing. The long-term fate of anthocyanins is not fully known and this dissertation attempted to advance the understanding of mechanisms responsible for the degradation and stabilization of anthocyanins throughout storage using a plethora of different techniques.

This collection of published and unpublished research details the method development process intended to separate anthocyanin-tannin polymers by degree of polymerization (Chapter 3), clarification of the mechanism of anthocyanin degradation by ascorbic acid (Chapter 4), stabilization of anthocyanins in blackberry juice via glutathione addition (Chapter 5), and preparation of a new natural colorant from an acetaldehyde-catalyzed reaction of radish anthocyanins (Chapter 6).

As anthocyanin concentration decreases over storage, it is believed they combine with tannins (procyanidins) to form large polymers called polymeric pigments (PPs). There is no current method to separate PPs from procyanidins, nor PPs by degree of polymerization and this research attempted many different techniques to create separation. Although PPs are cationic and procyanidins are neutral, ion exchange chromatography did not separate these compounds. One issue that arose was the strong association between the analytes and the stationary phase

indicated by red pigment remaining bound regardless of solvent used on the column. A strong adherence to the column inlet was found in several of the materials evaluated. Chapter 3 discusses the results of numerous forms of chromatography, electrophoresis, and molecular weight filters. A notable finding was a color gradient in a three-year-old chokeberry juice applied to centrifuge filters varying in molecular weight cutoff. The retentate from the 50,000 Da cutoff filter was highly pigmented, and the retentate from the 100,000 Da cutoff filter was even more pigmented. This trend was observed in a fresh chokeberry juice and could indicate the fate of anthocyanins is large molecular weight compounds.

Chapter 4 clarified the mechanism of anthocyanin degradation by ascorbic acid that has been debated for over forty years. Understanding this mechanism is important because of the prevalence of ascorbic acid addition to many anthocyanin-rich juices. In the presence of ascorbic acid, micromolar concentrations of iron or copper catalyze the formation of hydrogen peroxide through the Haber-Weiss reaction. Hydrogen peroxide quickly splits into two hydroxyl radicals, which combine with anthocyanins to form hydroxylated products. The hydroxylated anthocyanin is less stable than the native compound causing an accelerated degradation rate compared to ascorbic acid-free systems. Adding a chelator can bind free metal ions and prevent the Haber-Weiss reaction, thus prolonging anthocyanin content and color.

Chapter 5 evaluated the stabilizing effect of different additives on anthocyanin content in blackberry juice. The additives included glutathione, galacturonic acid, diethylenetriaminepentaacetic acid, and tannic acid, and each had a different mechanistic approach for stabilizing anthocyanins. Glutathione provided the greatest stabilizing effect, so an antioxidant recycling mechanism was applied to blackberry juice. The hypothesis was glutathione could be recycled by lipoic acid and ascorbic acid in order to extend high

anthocyanin content in juice. Although there was no significant difference, the combination of three antioxidants protected anthocyanins by 29%, while glutathione and lipoic acid afforded 24% protection, and glutathione alone had a 23% protective effect over five weeks of accelerated storage at 30 °C compared to control juices. Glutathione appears to be a promising blackberry juice additive to protect against anthocyanin degradation during storage.

Finally, Chapter 6 describes the development a new natural colorant made from radishes using a reaction naturally occurring in wine. Acetaldehyde produced during fermentation can polymerize anthocyanins and catechin in winemaking, so the acetaldehyde-catalyzed reaction was applied to radishes anthocyanins. Radishes contain acylated anthocyanins that are more stable than their monoglucoside counterparts. This was the first synthesis of acylated anthocyanins ethyl-bridged to catechin and the compounds remarkable color stability over six months of storage. The color changed from bright red to vivid purple as acetaldehyde reacted with anthocyanins. The ethyl-bridged dimeric radish anthocyanins possess excellent color stability and could serve as natural alternatives to synthetic food additives.

This dissertation offers an in-depth analysis of factors influencing anthocyanin degradation and stabilization that can hopefully aid future research in this area.